Ammonia-oxidizing archaea in engineered biofiltration systems

by

Laura Sauder

A thesis
presented to the University of Waterloo
in fulfillment of the
thesis requirement for the degree of
Doctor of Philosophy
in
Biology

Waterloo, Ontario, Canada, 2016

Author's Declaration

This thesis consists of material all of which I authored or co-authored: see Statement of Contributions included in the thesis. This is a true copy of the thesis, including any required final revisions, as accepted by my examiners.

I understand that my thesis may be made electronically available to the public.

Statement of Contributions

Chapter 2

Richard Pawliszyn performed sample collection for aquarium biofilters. Andre Masella performed the sequence clustering and Josh Neufeld prepared the NMDS figure (Fig. 2.5).

Chapter 3

Chen-Chi Lo and Karen Davenport performed the described automated genome assembly.

Chapter 4

Francien Peterse performed the lipid extractions and quantification presented in Fig 4.5.

Chapter 5

Jasmin Schwarz performed the microautoradiography presented in Chapter 4 (Figs. 5.5H, 5.15). Mads Albertsen performed the described genome assembly.

Chapter 6

Under my supervisions as a co-op student, Ashley Ross performed the enrichment culture experiments described and prepared figure 6.3.

Abstract

Ammonia is a nitrogenous metabolic waste product that is produced by all animal life. High concentrations of ammonia are toxic to animals and may result in algal blooms and eutrophication in aquatic environments. To prevent negative impacts on animal and environmental health, water treatment systems use biological filters to host populations of nitrifying microorganisms that oxidize ammonia to nitrite and subsequently to nitrate. Ammonia-oxidizing archaea (AOA) outnumber ammonia-oxidizing bacteria (AOB) in many terrestrial and aquatic environments, but few studies have characterized AOA in engineered environments, despite the importance of these systems for ecosystem health. This thesis research examined two types of nitrifying biofiltration systems, including freshwater aquaria and fixed-film reactors from a municipal wastewater treatment plant (WWTP), to investigate the abundance, diversity, activity, and ecology of AOA in freshwater engineered systems.

Although nitrification is the primary function of aquarium biofilters, few studies have investigated the microorganisms responsible for this process in aquaria. Based on quantitative PCR (qPCR) for ammonia monooxygenase (*amoA*) and 16S rRNA genes of *Bacteria* and *Thaumarchaeota*, AOA were numerically dominant in 23 of 27 freshwater biofilters, and contributed all detectable *amoA* genes in 12 of these biofilters. AOA also outnumbered AOB in five of eight sampled marine aquarium biofilters. For freshwater aquaria, the proportion of *amoA* genes from AOA relative to AOB was inversely correlated with ammonia concentration, suggesting an adaptation to low ammonia conditions. Composite clone libraries of AOA *amoA* genes revealed distinct freshwater and saltwater clusters, as well as mixed clusters containing both freshwater and saltwater *amoA* gene sequences.

From one analyzed freshwater aquarium biofilter that demonstrated a high archaeal abundance, AOA representative *Candidatus* Nitrosotenius aquariensis was enriched in laboratory culture. *Ca*. N. aquariensis oxidized ammonia stoichiometrically to nitrite with a concomitant increase in thaumarchaeotal cells. *Ca*. N. aquariensis has a generation time of 34.9 hours, is mesophilic with an optimal growth temperature of 33°C, and can tolerate up to 3 mM NH$_4$Cl. Transmission electron microscopy (TEM) revealed that *Ca*. N. aquariensis

cells are rod-shaped with a diameter of ~0.4 µm and lengths ranging from 0.6-3.6 µm. In addition, these cells possess paracrystalline S-layers and up to five appendages per cell. Phylogenetically, *Ca*. N. aquariensis belongs to the Group I.1a *Thaumarchaeota*, and clusters with environmental sequences from freshwater aquarium biofilters, aquaculture systems, and wastewater treatment plants (WWTPs). The complete genome sequence is 1.70 Mbp, and encodes genes involved in ammonia oxidation, urea hydrolysis, and bicarbonate assimilation. Several genes encoding flagella synthesis and chemotaxis were identified in the genome, as well as genes associated with S-layer production, defense, and protein glycosylation. Incubations of aquarium filter biomass revealed that PTIO is strongly inhibitory of ammonia oxidation, suggesting an *in situ* role for *Ca*. N. aquariensis-like AOA in freshwater aquarium biofilters.

AOA have been detected in WWTPs based on targeted gene sequences, but contributions of AOA to ammonia oxidation in WWTPs remain unclear. In this thesis, ammonia-oxidizing populations in nitrifying rotating biological contactors (RBCs) from a municipal WWTP were investigated. Individual RBC stages are arranged in series, with nitrification at each stage contributing to an ammonia concentration gradient along the flowpath. Quantitative PCR for thaumarchaeotal *amoA* and 16S rRNA genes in RBC biofilm samples demonstrated that AOA abundance increased as ammonia decreased across the RBC flowpath. In addition, a negative correlation (R^2=0.51) existed between ammonia concentration of RBC-associated water samples and the relative abundance of AOA *amoA* genes detected in corresponding biofilm samples. A single AOA population was detected in the RBC biofilms and this phylotype shared low 16S rRNA and *amoA* gene homologies with existing AOA cultures and enrichments.

From RBC biofilm, *Ca*. Nitrosocosmicus exaquare was enriched in laboratory culture. *Ca*. N. exaquare oxidizes ammonia to nitrite stoichiometrically and assimilates bicarbonate, as demonstrated by microautoradiography. The 2.99 Mbp genome of *Ca*. N. exaquare encodes pathways for ammonia oxidation, bicarbonate fixation, and urea transport and hydrolysis. Despite assimilating inorganic carbon, the ammonia-oxidizing activity of *Ca*. N. exaquare is greatly stimulated in enrichment culture by the addition of organic compounds, especially malate and succinate. *Ca*. N. exaquare cells are coccoid and large in comparison to all other cultured AOA, with a diameter of approximately 1-2 µm.

Phylogenetically, *Ca.* N. exaquare belongs to the Group I.1b *Thaumarchaeota*, clustering in the *Nitrososphaera* sister cluster, which includes most other environmental AOA sequences from municipal and industrial WWTPs. Incubations of WWTP biofilm demonstrated partial inhibition of ammonia-oxidizing activity by PTIO, suggesting that *Ca.* N. exaquare-like AOA contribute to nitrification *in situ*. Interestingly, CARD-FISH-microautoradiography revealed no incorporation of bicarbonate by *Ca.* N. exaquare-like AOA in actively nitrifying biofilms, suggesting that these cells may assimilate non-bicarbonate carbon sources.

In natural and engineered environments, differential inhibitors are important for assessing the relative contributions of microbial groups to biogeochemical processes. For example, PTIO is a nitric oxide scavenger used for the specific inhibition of nitrification by AOA. This research investigated four alternative nitric oxide scavengers for their ability to differentially inhibit AOA and AOB in comparison to PTIO. Caffeic acid, curcumin, methylene blue hydrate, and trolox all demonstrated differential inhibition on laboratory cultures of AOA and AOB, providing support for the proposed role of nitric oxide as a key intermediate in the thaumarchaeotal ammonia oxidation pathway.

Overall, this research demonstrated that AOA were abundant in aquarium biofilters and nitrifying RBCs, and that they contributed to ammonia-oxidizing activity in sampled biofilm environments. Niche partitioning of AOA and AOB was observed based on environmental ammonia concentrations, with AOA adapted to low ammonia conditions. Moreover, the enrichment cultures and genome sequences of novel AOA representatives provide insight into the ecophysiology of AOA originating from engineered systems.

Acknowledgements

Table of Contents

List of Figures

List of Tables

List of Abbreviations

Abbreviation	Definition
3HP/4HB	3-hydroypropionate/4-hydroxybutyrate
AAI	Average amino acid identity
ACP	Acyl carrier protein
AMO	Ammonia monooxygenase
amoA	Gene encoding alpha subunit of ammonia monooxygenase
amoB	Gene encoding ammonia monooxygenase subunit B
amoC	Gene encoding ammonia monooxygenase subunit C
Anammox	Anaerobic ammonium oxidation
ANI	Average nucleotide identity
AOA	Ammonia-oxidizing archaea
AOB	Ammonia-oxidizing bacteria
AOP	Ammonia-oxidizing prokaryotes
APCI	Atmospheric pressure channel ionization
ATCC	American Type Culture Collection
ATP	Adenosine triphosphate
ATU	Allylthiourea
BBH	Bi-directional best hits
BDL	Below detection limit
BLAST	Basic local alignment search tool
bp	Base pair
BSA	Bovine serum albumin
CARD	Catalyzed reporter deposition
CCD	Charge-coupled device
CL	Core lipid
CLSM	Confocal laser scanning microscope
Comammox	Complete ammonia oxidation
DAPI	4',6-diamidino-2-phenylindole
DCM	Dichloromethane
DGGE	Denaturing gradient gel electrophoresis
DIC	Dissolved inorganic carbon
DMSO	dimethylsulfoxide
DNA	Deoxyribonucleic acid
DNRA	Dissimilatory nitrate reduction to ammonia
dNTP	Deoxynucleotide triphosphate

dO$_2$	Dissolved oxygen
DOC	Dissolved organic carbon
DOPE	Double labelling of oligonucleotide probes
EHT	Extra high tension
FISH	Fluorescence *in situ* hybridization
FITC	Fluorescein isothiocyanate
FWM	Freshwater media
GDGT	Gycerol dialkyl glycerol tetraether
GTR	General time reversible
HAO	Hydroxylamine oxidoreductase
HCl	Hydrochloric acid
HDT	Hydraulic detention time
HGT	Horizontal gene transfer
HMM	Hidden Markov model
HPLC	High performance liquid chromatography
HRP	Horseradish peroxidase
HWCG	Hot water crenarchaeotal group
IFAS	Integrated fixed-film activated sludge
IPL	Intact polar lipid
kbp	Kilo basepairs
KEGG	Kyoto Encyclopedia of Genes and Genomes
K_m	Half saturation constant
MAR	Microautoradiography
MBH	Methylene blue hydrate
MCP	Methyl-accepting chemotaxis protein
MeOH	Methanol
ML	Mixed liquor
MT	methyltransferase
nd	Not determined
NEDD	N-(1-naphthyl)ethylenediamine dihydrochloride
NE	Northeast
nir	Nitrite reductase gene
NMDS	Non-metric multidimensional scaling
NO	Nitric oxide
NOB	Nitrite-oxidizing bacteria
nor	Nitric oxide reductase gene
NOR	Nitric oxide reductase
nr	Not reported

NW	Northwest
NxOR	Nitroxyl oxidoreductase
ORF	Open reading frame
PBS	Phosphate buffered saline
PCR	Polymerase chain reaction
PEG	Polyethylene glycol
PFA	Paraformaldehyde
PHA	Polyhydroxyalkanoate
PKS	Polyketide synthase
PQQ	Pyrroloquinoline quinone
PROmer	Protein maximum unique matching subsequence
PTFE	Polytetrafluoroethylene
PTIO	2-Phenyl-4,4,5,5-tetramethylimidazoline-1-oxyl-3-oxide
PVC	Polyvinyl chloride
qPCR	Quantitative polymerase chain reaction
RAS	Recirculating aquaculture system
RBC	Rotating biological contactor
RM	Restriction-modification
ROS	Reactive oxygen species
rRNA	Ribosomal RNA
SAGMA	South African gold mine archaea
SAT	Soil aquifer treatment
SdcS	Sodium-dependent dicarboxylate symporter
SE	Southeast
SEM	Scanning electron microscopy
SULF	Sulfanilamide
S-layer	Surface layer
SW	Southwest
TCA	Tricarboxylic acid
TEM	Transmission electron microscopy
ThAOA	Thermophilic AOA
TOC	Total organic carbon
Trolox	6-hydroxy-2,5,7,8-tetramethylchroman-2-carboxylic acid
WWTP	Wastewater treatment plant
YE	Yeast extract

Chapter 1

Introduction and literature review

1.1 Nitrification and the nitrogen cycle

As the fourth most abundant element in biomass and a component of proteins and nucleic acids, nitrogen is a critical component for the structures and biochemical reactions of life. In fact, nitrogen is so central to life on Earth that it has been suggested that we "follow the nitrogen" as a reliable bio-signature when searching for extraterrestrial life (Capone *et al.*, 2006). The Earth's atmosphere is composed of approximately 78% nitrogen, which exists in the form of dinitrogen gas (N_2) and represents the largest nitrogen pool on the planet (Francis *et al.*, 2007). In addition to comprising a critical component of biomass, nitrogen can form single, double, or triple bonds, and exists in a wide variety of chemical forms and oxidation states, making nitrogenous compounds useful to microorganisms as both electron donors and acceptors.

Although abundant, dinitrogen is bound by a strong triple bond, is not biologically active, and must be fixed before it is biologically available. Using nitrogenase enzymes, microorganisms fix N_2 into ammonia (NH_3), which can be assimilated in biomass (Figure 1.1). Physical processes (*e.g.,* lightning) can also result in nitrogen fixation, and these processes may have been important in the production of bioavailable nitrogen in early Earth conditions (Stein and Klotz, 2016). Alternatively, N_2 can be fixed artificially by the Haber-Bosch process, which is primarily used to produce ammonia-rich fertilizers and is now responsible for the majority of nitrogen fixed globally.

Ammonia produced by nitrogen fixation (or by subsequent biomass degradation or waste excretion) can be used as an electron donor for ammonia-oxidizing microorganisms, which convert it to nitrite (NO_2^-). Nitrite can be further oxidized to nitrate (NO_3^-) by nitrite-oxidizing bacteria (NOB). The overall process of oxidation of ammonia to nitrate is known as nitrification. Nitrate can be assimilated by plants into biomass (after reduction to ammonia), or may be used as an electron acceptor in a variety of anaerobic processes. For example, nitrate can be used as an electron acceptor in denitrification, a stepwise reduction

that ultimately yields N_2, which is returned to the atmosphere. Nitrate may also be used for dissimilatory nitrate reduction to ammonia (DNRA), or can be converted to nitrite, which is used as an electron acceptor in anaerobic ammonium oxidation (anammox). Anammox is unique because it uses a nitrogenous compound as both an electron acceptor (NO_2^-) and an electron donor (NH_4^+), and represents a relatively recent addition to known nitrogen cycling processes (Mulder *et al.*, 1995; van de Graaf *et al.*, 1995).
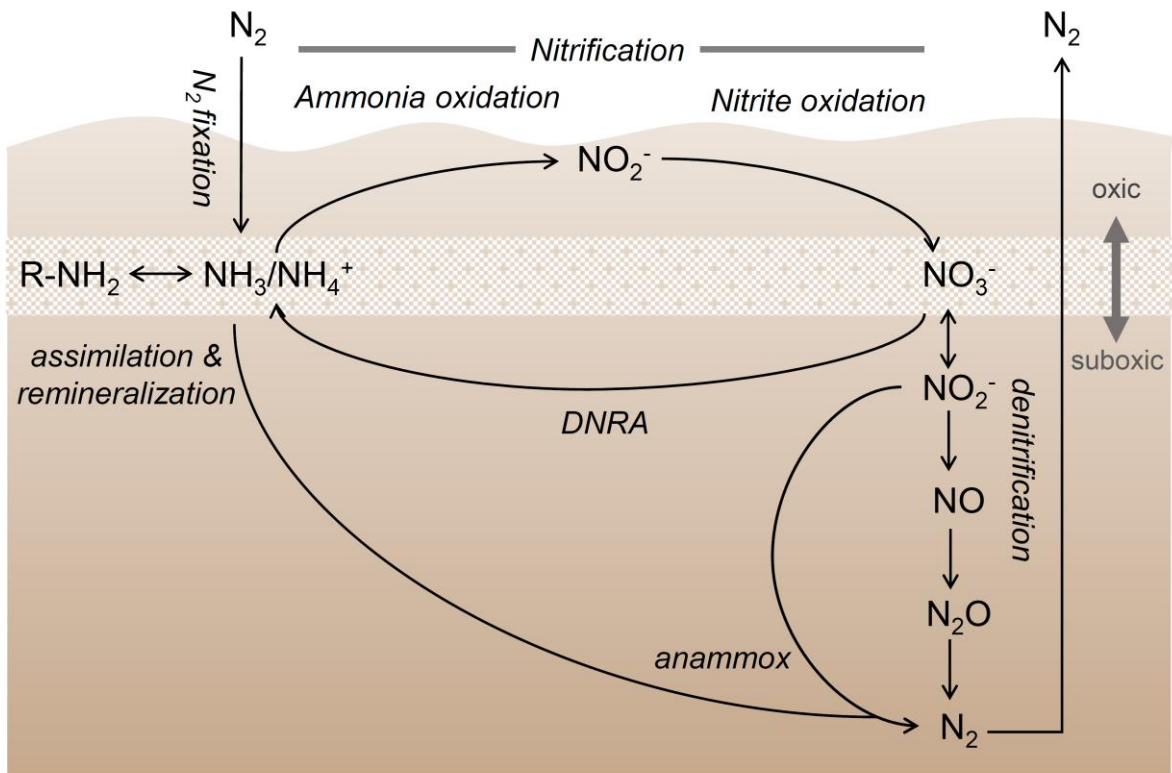
Figure 1.1 The nitrogen cycle in a biofilm environment (modified from Francis *et al*., 2005). Nitrification is comprised of ammonia oxidation and nitrite oxidation, both of which are aerobic processes. DNRA refers to dissimilatory nitrate reduction to ammonia, and R-NH$_2$ represents biomass. For clarity, not all known nitrogen cycle processes are depicted.

Ammonia is a nutrient that is assimilated into biomass by microorganisms and plants. However, at high concentrations, ammonia can be toxic to both micro- and macroorganisms. In addition, excess ammonia can result in negative environmental effects in aquatic ecosystems, such as algal blooms and oxygen depletion. Nitrification is an important process because it produces nitrate, which does not have an associated oxygen demand and is less

toxic to aquatic organisms than ammonia or nitrite. In addition, production of oxidized nitrogenous compounds is critical for closing the nitrogen cycle and returning N_2 to the atmosphere. However, nitrification can also have negative environmental impacts, including contributions to greenhouse gases such as nitrous oxide (Santoro *et al.*, 2011; Löscher *et al.*, 2012) and increased nitrate leaching from agricultural fields, resulting in pollution of surface and groundwater.

Aerobic oxidation of ammonia by members of the *Bacteria* was first discovered over a century ago (Winogradsky, 1890) and has long been viewed as a process that is obligately aerobic, chemolithoautotrophic, and mediated only by a few groups within the *Proteobacteria*. In fact, ammonia-oxidizing bacteria (AOB) have been called "a model system" for microbial ecology because of their ability to use ammonia as a sole energy source and their monophyletic nature (Kowalchuk and Stephen, 2001). In contrast, denitrification is heterotrophic, anaerobic, and is widespread across greater than 50 genera, distributed among all domains of life (Zumft, 1997; Risgaard-Petersen *et al.*, 2006; Francis *et al.*, 2007).

The understanding that AOB are the sole contributors to ammonia oxidation was first challenged by a metagenomic study of the Sargasso Sea. This pioneering research discovered an archaeal-associated scaffold containing a homologue of a bacterial ammonia monooxygenase gene (Venter *et al.*, 2004), suggesting that members of the *Archaea* could oxidize ammonia. In another metagenomic study, a soil fosmid clone was obtained that contained both archaeal ribosomal rRNA genes as well as genes encoding ammonia monooxygenase subunits (Treusch *et al.*, 2005), which supported the hypothesis that some archaea are capable of ammonia oxidation. The existence of ammonia-oxidizing archaea (AOA) was confirmed when the first ammonia-oxidizing archaeon, *Nitrosopumilus maritimus* SCM1, was isolated in pure culture from marine aquarium gravel (Könneke *et al.*, 2005). *N. maritimus* grows chemolithoautotrophically using ammonia as a sole source of energy and bicarbonate as a sole source of carbon. Paradigms of bacterial nitrification continue to be challenged with studies indicating that AOA are ubiquitous and outnumber AOB by orders of magnitude in a variety of environments, including soils (Leininger *et al.*, 2006), oceans (Wuchter *et al.*, 2006; Beman *et al.*, 2008; De Corte *et al.*, 2009), estuarine

sediments (Beman and Francis, 2006), and hot springs (Zhang *et al.*, 2008). In fact, AOA are estimated to represent the most abundant group of prokaryotes in the ocean (Wuchter *et al.*, 2006; Karner *et al.*, 2001; Herndl *et al.*, 2005), and are major global contributors to both ammonia oxidation and nitrous oxide emissions (Schleper and Nicol, 2010; Stahl and de la Torre, 2012; Santoro and Casciotti, 2011; Löscher *et al.*, 2012). However, there is also evidence that AOB are numerically dominant in some environments, and that AOB may mediate ammonia oxidation in several soils, despite numerical dominance of AOA (Mosier and Francis, 2008; Di *et al.*, 2009; Banning *et al.*, 2015; Sterngren *et al.*, 2015).

Further challenging traditional models of nitrification, completely nitrifying bacteria ("comammox") belonging to the genus *Nitrospira* were discovered recently in a deep oil well and an anaerobic compartment of a trickling filter connected to a recirculating aquaculture system (Daims *et al.*, 2015; van Kessel *et al.*, 2015). The extent to which comammox bacteria contribute to nitrification in natural and engineered environments is currently unknown, but they have been detected in one drinking water treatment plant (Pinto *et al.*, 2016).

1.2 History of the phylum *Thaumarchaeota*

Since the discovery of the *Archaea* and classification of life into three domains (Woese *et al.*, 1978, 1990), these organisms were thought of as extremophiles, especially members of the *Crenarchaeota*, which are thermophilic and often acidophilic. However, in the early 1990s, 16S rRNA gene surveys detected three major lineages of *Archaea* in moderate marine environments (DeLong, 1992; Davis, 1992; DeLong, 1998). Phylogenetic analyses of these groups indicated that two of the detected lineages (Groups II and III) were affiliated within the phylum *Euryarchaeota*, whereas one lineage (Group I) represented a sister taxon to the hyperthermophilic *Crenarchaeota*. Subsequent 16S rRNA gene surveys indicated that the Group I lineage is abundant and widely distributed in environments such as soils (Jurgens *et al.*, 1997; Buckley *et al.*, 1998; Ochsenreiter *et al.*, 2003), freshwater sediments (Macgregor *et al.*, 1997; Schleper *et al.*, 1997), and the open ocean and coastal waters (DeLong *et al.*, 1994; Massana *et al.*, 1997; McInerney *et al.*, 1997; Murray *et al.*, 1998; Karner *et al.*, 2001; Church *et al.*, 2003; Herndl *et al.*, 2005). Because no cultured

representatives of Group I *Archaea* were available, insight into their metabolism and biogeochemical significance was first examined by assessing uptake of radiolabelled carbon substrates. These experiments indicated that these members of the Group I *Archaea* largely incorporated inorganic carbon (Wuchter *et al.*, 2003; Herndl *et al.*, 2005), but could also take up amino acids (Ouverney and Fuhrman, 2000). The discovery of contiguous DNA sequences encoding both archaeal 16S rRNA genes and ammonia monooxygenase-related genes (Treusch *et al.*, 2004; Venter *et al.*, 2004) suggested chemolithoautotrophic ammonia oxidation as a likely metabolism, which was confirmed by the isolation of the ammonia oxidizing archaeon *Nitrosopumilus maritimus* (Könneke *et al.*, 2005).

Early studies of AOA frequently used the term "mesophilic crenarchaeota" to describe Group I *Archaea*. However, analysis of the genome of *Candidatus* Cenarchaeum symbiosum, a Group I archaeal representative and marine sponge symbiont, suggested that Group I *Archaea* represented a new phylum, distinct from the previously recognized *Crenarchaeota* (Hallam *et al.*, 2006; Brochier-Armanet *et al.*, 2011). This new phylum was provisionally named the *Thaumarchaeota*, after "*thaumas*", the Greek word for "wonder". Evidence that supported establishment of this phylum included phylogenetic relationships of 53 concatenated ribosomal proteins (R-proteins), which indicated deep branching of the *Thaumarchaeota* lineage (basal to the split of *Crenarchaeota* and *Euryarchaeota*), and the fact that, despite the designation as "mesophilic crenarchaeota", this lineage actually shared more genes with *Euryarchaeota* than *Crenarchaeota* (Brochier-Armanet *et al.*, 2008). Phylogenetic analyses and comparative genomics of two additional Group I representatives, *Nitrososphaera gargensis* and *Nitrosopumilus maritimus*, supported the *Thaumarchaeota* as a distinct phylum (Spang *et al.*, 2010). The assignment of *Thaumarchaeota* as an independent phylum is further supported by phylogenetic analyses of full-length 16S rRNA gene sequences, a distinct set of information-processing genes, a phylum-specific membrane lipid (*i.e.*, thaumarchaeol), insertions and deletions in specific tRNA synthesis genes, and a unique energy metabolism (Spang *et al*. 2010; Hatzenpichler *et al*., 2012).

Within the *Thaumarchaeota*, several lineages of AOA have been detected (Figure 1.2). The Group I.1a *Thaumarchaeota* contains cultured representatives originating from both marine and freshwater environments, as well as environmental sequences originating from a variety of aquatic habitats. This group is often referred to as the "marine group",

despite the inclusion of freshwater, hotspring, and soil AOA representatives (Blainey *et al.*, 2011; French *et al.*, 2012; Kim *et al.*, 2011; Lebedeva *et al.*, 2013; Jung, Park, *et al.*, 2014). A Group I.1a-associated lineage (previously named the South African Gold Mine Archaea; SAGMA) contains sequences obtained from acidic environments as well as the obligately acidophilic archaeon *Candidatus* Nitrosotalea devanaterra (Lehtovirta-Morley *et al.*, 2011). The Group I.1b thaumarchaeotal clade contains cultured representatives and environmental sequences from soils and is also known as the "soil group" (Schleper *et al.*, 2005). A thermophilic AOA lineage (ThAOA; previously the Hot Water Crenarchaeotic Group III; HWCG III) contains AOA representative *Candidatus* Nitrosocaldus yellowstonii, as well as many environmental sequences originating from hot springs. Several other thaumarchaeotal clades have been identified on the basis of environmental 16S rRNA gene sequences. For example, three deep-branching clades have recently been identified in hot springs of Yellowstone National Park (I.1e, I.1f, I.1g; Beam *et al.*, 2014). Several other clades have been identified based on environmental 16S rRNA gene sequences (*e.g.,* Group I.1c, pSL12, ALOHA, Marine Benthic Group B), but there are currently no genomes nor cultures available for any of these representatives, and the metabolism of these microorganisms remains unclear.

All cultured representatives of the *Thaumarchaeota* generate energy via the oxidation of ammonia to nitrite. However, the view that all members of the phylum are ammonia oxidizers is likely biased because all available cultures have been enriched using ammonia-based media. Although not yet cultivated, it is likely that *Thaumarchaeota* members exist that are not ammonia oxidizers. For example, *amoA* genes have not been detected in association with uncultivated Group I.1c *Thaumarchaeota* (Stieglmeier *et al.*, 2014). Moreover, genome analyses of deep-branching thaumarchaeotal clades (*i.e.,* I.1d, I.1e, and I.1f) from thermal habitats have suggested chemoorganoheterotrophy coupled to a variety of electron acceptors, and have been unable to detect genes associated with ammonia oxidation through targeted PCR-based approaches or metagenomics (Beam *et al.*, 2014).
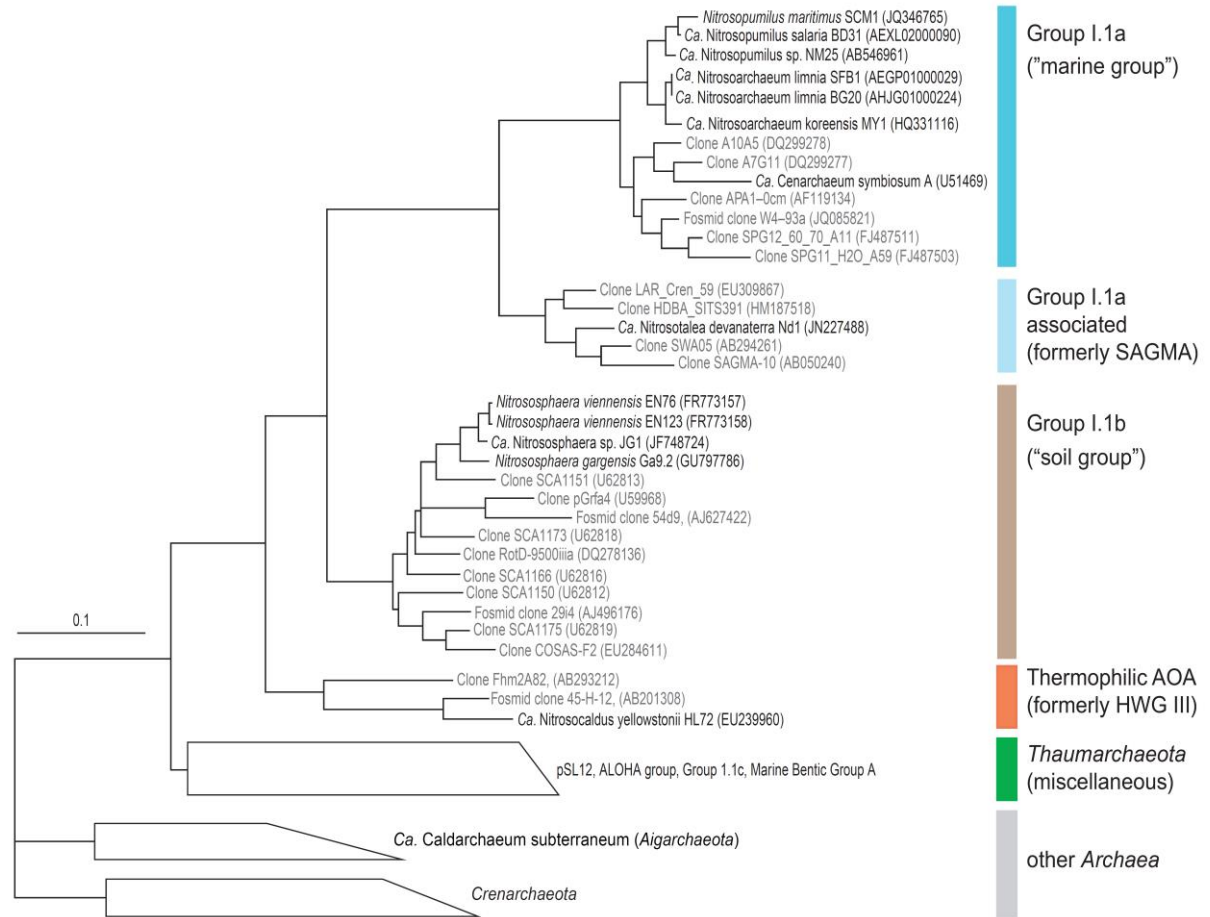
Figure 1.2 Phylogenetic relationships of ammonia-oxidizing archaea based on 16S rRNA gene sequences (modified from Stieglmeier *et al*., 2014). Cultured AOA representatives are indicated with black labels, and environmental sequences are shown in grey. The tree was constructed using the maximum likelihood method using the general time reversible model of sequence evolution. The scale bar represents 10% sequence divergence (i.e. 0.1 nucleotide substitutions per site).

1.3 AOA representatives

Several AOA representatives have been cultivated in the laboratory, providing insight into the metabolism and physiology of the *Thaumarchaeota. Cenarchaeaum symbiosum* was the first *Thaumarchaeota* representative described (Preston *et al.*, 1996). It was enriched in association with a marine sponge, and is a psychrophile with an optimum growth temperature of 10°C. The genome sequence of *C. symbiosum* was critical for establishing the phylum

Thaumarchaeota, and also revealed that this microorganism is an ammonia oxidizer (Hallam *et al.*, 2006). *Nitrosopumilus maritimus* SCM1 belongs to the Group I.1a *Thaumarchaeota* and was obtained in pure culture using marine aquarium gravel as inoculum (Könneke *et al.*, 2005). Several additional Group I.1a *Thaumarchaeota* representatives have since been reported in enrichment culture. For example, *Candidatus* Nitrosoarchaeum limnia strains SFB1 and BG20 have been enriched from an estuary (Blainey *et al.*, 2011; Mosier, Lund *et al.*, 2012), and *Candidatus* Nitrosoarchaeum koreensis MY1 was enriched from an agricultural soil (Jung *et al.*, 2011; Kim *et al.*, 2011). *Candidatus* Nitrosotenuis uzonensis, another Group I.1a representative, was enriched from a hotspring in Russia and is a moderate thermophile, with optimum growth at 46°C (Lebedeva *et al.*, 2013). Additional *Nitrosotenuis* species have since been reported, including *Candidatus* Nitrosotenuis chungbukensis, which was enriched from a deep oligotrophic soil (Jung *et al.*, 2014), and *Candidatus* Nitrosotenuis cloacae, which was enriched from a WWTP (Li, Ding, *et al.*, 2016). A Group I.1a-associated representative, *Candidatus* Nitrosotalea devanaterra, was enriched from an acidic soil and grows in an acidic growth medium (Lehtovirta-Morley *et al.*, 2011). The moderately thermophilic AOA representative *Candidatus* Nitrososphaera gargensis was enriched from a hot spring and was the first reported representative of the Group I.1b *Thaumarchaeota* (Hatzenpichler *et al.*, 2008). Group I.1b representative *Nitrososphaera viennensis* was subsequently isolated from a garden soil (Tourna *et al.*, 2011), and *Candidatus* Nitrososphaera evergladensis was enriched from an agricultural soil (Zhalnina *et al.*, 2014). Recently, a new Group I.1b lineage has been reported with the isolation of *Candidatus* Nitrosocosmicus franklandus from an agricultural soil (Lehtovirta-Morley, Ross, *et al.*, 2016). Thermophilic AOA representative *Candidatus* Nitrosocaldus yellowstonii was enriched from a hot spring in Yellowstone National Park, growing optimally at 72°C (de la Torre *et al.*, 2008). A phylogenetic analysis of publicly available archaeal *amoA* gene sequences has characterized five major AOA clusters, represented by the genera *Nitrosopumilus*, *Nitrosocaldus*, *Nitrosotalea, Nitrososphaera*, and a fifth clade that forms a sister cluster to the *Nitrososphaera* (Pester *et al.*, 2012), which is now represented by the genus *Nitrosocosmicus* (Lehtovirta-Morley, Ross, *et al.*, 2016). Characteristics of several AOA cultures are summarized in Table 1.1.

Table 1.1 Characteristics of selected cultivated ammonia-oxidizing archaea

	Nitrosopumilus maritimus SCM1	*Nitrosoarchaeaum limnia* BG20	*Nitrosoarchaeum koreensis* MY1	*Nitrosotenuis uzonensis* N4	*Nitrosotalea devanaterra* Nd1	*Nitrososphaera gargensis* Ga9-2	*Nitrososphaera viennensis* EN76	*Nitrosocaldus yellowstonii* HL72
affiliation	Group I.1a	Group I.1a	Group I.1a	Group I.1a	Group I.1a-associated	Group I.1b	Group I.1b	Group I.1b
cultivation status	pure culture	enrichment	enrichment	enrichment	enrichment	pure culture	pure culture	enrichment
original habitat	marine aquarium gravel	low salinity estuary sediment	agricultural soil (rhizosphere)	hot spring	acidic agricultural soil	hot spring	garden soil	hot spring sediment
cell morphology	rod	rod	rod	rod	rod	coccoid	irregular coccoid	coccoid
cell size (diameter/length)	0.17-0.22 µm/ 0.5-0.9 µm	0.19-0.27 µm/ 0.55-1 µm	0.3-0.5 µm/ 0.6-1.0 µm	0.2-0.3 µm/ 0.4-1.7 µm	0.32-0.34 µm/ 0.84-0.9 µm	0.87-0.93 µm	0.5-0.8 µm	nr
motility structures	none observed	flagella	nr	flagella	flagella	flagella & pili	flagella & pili	nr
optimal growth temperature (^{o}C)	28	22	25	25	46	46	37	72
growth pH	7.5	7.0-7.2	6.0-8.0	8.0-8.2	4.0-5.0	7.4	7.5	7.0-8.0
NH_4^+ (growth medium)	up to 1 mM	0.5 mM	1 mM	1 mM	0.5 mM	1 mM	2.5 mM	1 mM
inhibitory NH_4^+/ NH_3 conc.	2 mM/18 µM (pH 7.0)	nr	20 mM/145 µM (pH 7.0)	nr	50 mM/9 µM (pH 4.5)	3 mM/67 uM (pH 7)	15 mM/0.57 mM (pH 7.5)	nr
generation time (h)	33	81.6	nr	nr	53	nr	29[a]	30
organic compound response	Stimulated by pyruvate, Inhibited by YE and acetate	nr	nr	nr	No stimulation or inhibition	nr	Stimulated by pyruvate & other carboxylic acids	YE, acetate, and H_2 inhibit growth
urea utilization?	no	no	no	no	no	yes	yes	nr
genome size (Mbp)	1.65	>1.77[b]	>1.61[b]	>1.65[b]	1.81	2.83	2.53	nr
References	Konneke *et al.,* 2005; Walker *et al.,* 2010	Blainey *et al.,* 2011; Mosier *et al.,* 2012	Jung *et al.,* 2011; Kim *et al.,* 2011	Lebedeva *et al.,* 2013	Lehtovirta-Morley *et al.,* 2011, 2016	Hatzenpichler *et al.,* 2008	Tourna *et al.,* 2014; Stieglmeier *et al.,* 2016	de la Torre *et al.,* 2008

nr: not reported, YE: yeast extract, [a] previously reported to be 46 h, [b]unclosed genome: exact size unknown

1.4 AOA ecology

Thaumarchaeota are globally distributed among diverse environments including a wide variety of soils, marine and estuary water columns and sediments, freshwater lakes and rivers, hot springs, subsurface caves, mangrove swamps, human skin, and several engineered environments (for reviews, see Erguder et al., 2009; Schleper and Nicol, 2010; Bouskill et al., 2012; Hatzenpichler, 2012; Zhalnina et al., 2012; Limpiyakorn et al., 2013; Stieglmeier et al., 2014; Bang and Schmitz, 2015). These environments include some not previously thought to be conducive to nitrification, including hot (up to 97°C) and acidic (pH 2.5) environments. In addition to being widely distributed, Thaumarchaeota are often highly abundant: AOA predominate in many soils (Leininger et al., 2006; Stopnisek et al., 2010; Yao et al., 2011; Zhang et al., 2012), and may be the most abundant group of organisms in the ocean (Karner et al., 2001; Herndl et al., 2005; Wuchter et al., 2006). In addition, AOA generally dominate in extreme environments such as Arctic soils (Alves et al., 2013), acidic soils (Nicol et al., 2008; Gubry-Rangin et al., 2010; Lehtovirta-Morley et al., 2011), hydrothermal vents (Wang et al., 2009; Baker et al., 2012), and hot springs (de la Torre et al., 2008; Reigstad et al., 2008; Zhang et al., 2008; Dodsworth et al., 2011).

However, despite a large number studies reporting high AOA abundances, AOB are numerically dominant in some sampled environments, such as the San Francisco Bay Estuary (Mosier and Francis, 2008) and several WWTPs (Park et al., 2006; Wells et al., 2009; Jin et al., 2010; Zhang et al., 2009). In addition, there is evidence that AOB may mediate ammonia oxidation in some soils, despite a numerical dominance of AOA (Mosier and Francis, 2008; Di et al., 2009; Banning et al., 2015; Sterngren et al., 2015). The factors determining whether AOA or AOB dominate a given environment have recently been a topic of intense interest. Several environmental parameters have been suggested to influence the composition of ammonia-oxidizing communities, such as ammonia availability, moisture content, light intensity, oxygen availability, temperature, and pH (Nicol et al., 2008; Erguder et al., 2009; Hatzenpichler, 2012).

High temperatures appear to favour AOA, which dominate geothermal environments such as hot springs and geothermal caves. In addition, one thermophilic (de la Torre et al., 2008) and two moderately thermophilic (Hatzenpichler et al., 2008; Lebedeva et al., 2013) AOA representatives have been grown in laboratory culture. Conversely, AOB are typically absent

10

from very hot environments and, although two moderately thermophilic AOB representatives (optimal growth temperature 50°C) were enriched from the Baikal rift zone (Lebedeva *et al.*, 2005), only mesophilic AOB had been identified prior to that discovery.

Thaumarchaeota are abundant in deep ocean waters (Reinthaler *et al.*, 2005; De Corte *et al.*, 2009; Konstantinidis *et al.*, 2009), which has led to the suggestion that AOA may be adapted to both low light and low oxygen conditions (Nicol *et al.*, 2011). Supporting this suggestion, AOA have also been shown to be more sensitive to light than their AOB counterparts (French *et al.*, 2012; Merbt *et al.*, 2012). In addition, the suggestion that AOA are adapted to low oxygen conditions has been supported by enrichment culture studies (Park *et al.*, 2010), kinetic studies (Jung *et al.*, 2011), and findings that AOA mediate nitrification in oxygen minimum zones of the ocean (Francis *et al.*, 2005; Lam *et al.*, 2007; Lam and Kuypers, 2011; Yan *et al.*, 2012).

Although many physical and chemical parameters may influence the relative abundance and activity of AOA and AOB, environmental ammonia concentration is probably the most widely investigated factor. Kinetic studies of the AOA representatives demonstrate high substrate affinities for ammonia. *N. maritimus* and *N. koreensis* have reported half saturation constants (K_m) of 0.133 µM (Martens-Habbena *et al.*, 2009) and 0.61 µM (Jung *et al.*, 2011) total ammonia, respectively. In comparison, K_m values for AOB are at least 100-fold higher and range from 15-2000 µM (Stehr *et al.*, 1995; Koops and Pommerening-Röser, 2001; Koops *et al.*, 2006; Jung *et al.*, 2011). For example, *Nitrosomonas oligotropha* has reported K_m values that range from 30 to 75 µM total ammonia (Stehr *et al.*, 1995). Studies of soil AOA support this observation by demonstrating that AOB are numerically and metabolically dominant in ammonia-amended soils (Jia and Conrad, 2009; Di *et al.*, 2010; Taylor *et al.*, 2010; Verhamme *et al.*, 2011). As a result of this high substrate affinity and the high relative abundance of AOA in oligotrophic environments, ammonia availability has been suggested to be an important factor in determining niche partitioning of AOA and AOB (Erguder *et al.*, 2009; Schleper, 2010).

1.5 Ammonia oxidation in AOA and AOB

Although AOA and AOB both oxidize ammonia to nitrite, the energy generation pathways used by these groups differ in several ways (for reviews, see Schleper and Nicol, 2010;

11

Stahl and de la Torre, 2012; Hatzenpichler, 2012). In AOB, a membrane-bound ammonia monooxygenase (AMO) catalyzes the oxidation of ammonia to hydroxylamine (NH₂OH), which is further oxidized to nitrite by a heme-rich, periplasmic hydroxylamine oxidoreductase (HAO) (Arp *et al.*, 2002). Hydroxylamine oxidation releases four electrons, two of which are transferred back to AMO to activate the enzyme and initiate ammonia oxidation. The remaining two electrons enter the quinol pool via heme-rich type c cytochromes.

AOA also use an AMO enzyme for ammonia oxidation, although it has low amino acid identity to the bacterial AMO (Pester *et al.*, 2012). Genes encoding all three AMO subunits (*amoA*, *amoB*, *amoC*) are present in all available AOA genomes (Hallam *et al.*, 2006; Walker *et al.*, 2010; Blainey *et al.*, 2011; Park, Kim, Jung, Kim, Cha, Kwon, *et al.*, 2012; Spang *et al.*, 2012; Lebedeva *et al.*, 2013; Stieglmeier, Klingl, *et al.*, 2014; Lehtovirta-Morley, Sayavedra-Soto, *et al.*, 2016; Li, Ding, *et al.*, 2016). However, aside from these AMO-associated genes, AOA lack genes encoding all other elements of the bacterial ammonia oxidation pathway, including homologues of the bacterial HAO and c-type cytochromes. As a result of the missing HAO homologue, an alternate pathway for ammonia oxidation was suggested for AOA, in which nitroxyl (HNO) is the product of the archaeal AMO (Walker *et al.*, 2010; Schleper and Nicol, 2010; Stahl and de la Torre, 2012). In this pathway, HNO would be produced by the AMO, and subsequently oxidized to nitrite by a novel nitroxyl oxidoreductase (NxOR).

Alternatively, it has been suggested that AOA may indeed generate hydroxylamine but use a different enzyme, such as a novel copper-based HAO or cytochrome P460, to generate nitrite and electrons (Walker *et al*., 2010; Kozlowski *et al*., 2016). Indeed, it has now been demonstrated experimentally that *N. maritimus* uses hydroxylamine as an intermediate in ammonia oxidation (Vajrala *et al.*, 2013). Although no HAO has yet been identified in the *N. maritimus* genome, it does contain several multi-copper oxidases, one of which might be involved in nitrite productions (Walker *et al.*, 2010). In addition, AOA encode two conserved redox-active plastocyanin-like proteins, which could be involved in electron transfer from hydroxylamine to the electron transport chain.

Nitric oxide (NO) has been suggested as an intermediate in archaeal ammonia oxidation (Walker *et al.*, 2010). Thaumarchaeotal genes encoding a copper-dependent nitrite reductase have been identified in soils (Treusch *et al.*, 2004; Bartossek *et al.*, 2010) and all available AOA genomes (*e.g.*, Hallam *et al.*, 2006; Walker *et al.*, 2010). Nitrite reductase is used in

denitrification to reduce nitrite to nitric oxide. Indeed, it has been demonstrated that NO is produced during archaeal ammonia oxidation (Martens-Habbena *et al.*, 2015), and that NO scavengers inhibit ammonia oxidation in AOA (Shen *et al.*, 2013; Sauder *et al.*, 2016). In AOA, nitric oxide has been suggested to function as a redox shuttle, which could deliver electrons to the AMO (Walker *et al.*, 2010; Schleper and Nicol, 2010; Stahl and de la Torre, 2012). However, recent evidence suggests that although NO is critical in archaeal ammonia oxidation, it does not act as an electron shuttle, but rather as a co-substrate that reacts with NH_2OH and water to form two molecules of NO_2^-, catalyzed by a novel Cu-containing enzyme (Kozlowski *et al*., 2016). In this scenario, one of the produced NO_2^- molecules would be reduced to NO via nitrite reductase and would be recycled to react with a new molecule of hydoxylamine, leading to near-stoichiometric conversion of ammonia to nitrite.

AOA also produce nitrous oxide (N_2O) during ammonia oxidation (Santoro *et al.*, 2011; Santoro and Casciotti, 2011; Löscher *et al.*, 2012; Jung, Park, *et al.*, 2014; Stieglmeier, Mooshammer, *et al.*, 2014). AOB produce nitrous oxide using a dissimilatory nitric oxide reductase (NOR) in the process of nitrifier denitrification, which increases under low oxygen conditions (Goreau *et al.*, 1980; Frame and Casciotti, 2010; Schleper and Nicol, 2010). However, nitrous oxide production in AOA is independent of oxygen concentration (Stieglmeier, Mooshammer, *et al.*, 2014), and available AOA genomes do not possess a *nor* homologue. A recent study has demonstrated that production of N_2O by *Thaumarchaeaota* is not an enzymatic process, but instead results from an abiotic N-nitrosation reaction of N-oxide intermediates, such as hydroxylamine, NO, or nitroxyl, with media components (Kozlowski *et al*., 2016). This so-called chemodenitrification occurs in anoxic environments in which metal components in medium (such as Fe(II) and reduced trace metals) could act as chemical catalysts for reduction of NO to N_2O, a process which has been suggested to contribute to abiotic N_2) production in reduced environments containing high levels of iron (Samarkin et al., 2010; Kampschreur et al., 2011; Jones et al., 2015). Therefore, although AOA contribute to N_2O production, it is through a different mechanism than that of AOB.

1.6 Carbon metabolism and mixotrophy

All cultivated AOA and AOB grow autotrophically, using ammonia as an energy source to fix inorganic carbon. However, the method of carbon fixation varies between AOA and AOB, with AOB using the Calvin-Benson-Bassham (*i.e.,* Calvin) cycle, and AOA using a modified version of the 3-hydroxypropionate/4-hydroxybutyrate (3HP/4HB) cycle (Berg, 2011 and references therein). Mechanisms of carbon fixation may be of ecological significance because the 3HP/4HP cycle incorporates bicarbonate (HCO_3^-), in contrast to carbon dioxide (CO_2), which is incorporated in the Calvin cycle. Bicarbonate is the predominant carbon species when the pH of an environment is neutral or alkaline, which is typical of marine habitats, and thus may provide an advantage to AOA over their bacterial counterparts in these conditions. In addition, the modified 3HP/4HB cycle used by members of the *Thaumarchaeota* has been shown to be more efficient than any other aerobic carbon assimilation pathway (Könneke *et al.*, 2014), which may contribute to the success of these microorganisms in nutrient poor environments.

Although all cultured members of the *Thaumarchaeota* oxidize ammonia to nitrite and fix inorganic carbon into biomass autotrophically, evidence exists that AOA may have a more complex metabolism, and some representatives may have the capacity for mixotrophic or heterotrophic growth. For example, *Nitrososphaera viennensis* requires pyruvate to achieve optimal growth rates, despite the fact that >90% of the carbon incorporated into its biomass originates from inorganic carbon (Tourna *et al.*, 2011). *N. viennensis* is also stimulated by additional organic carbon sources, including oxaloacetate, α-ketoglutarate, and glyoxlate (Stieglmeier *et al.*, 2014). Even *N. maritimus* is stimulated by the addition of pyruvate (Stahl and de la Torre, 2012) and α-ketoglutaric acid (Qin *et al.*, 2014), despite initial data suggesting inhibition by small amounts of organic carbon, including yeast extract, peptone, and acetate (Könneke *et al.*, 2005). AOA genomes encode components of an oxidative tricarboxylic acid (TCA) cycle, which could be used to convert organic carbon compounds to intermediates for amino acid or cofactor biosynthesis (Schleper and Nicol, 2010). However, a recent study has demonstrated that stimulation of AOA by pyruvate and other alpha-keto acids is the result of chemical (*i.e,.* non-enzymatic) detoxification of hydrogen peroxide (Kim *et al.*, 2016), calling into question the apparent mixotrophic metabolism of some AOA. Nevertheless, evidence suggests that mixotrophy may be an important aspect of AOA metabolism in the environment.

Several environmental studies have shown incorporation of inorganic carbon by *Thaumarchaeota*, as expected from chemolithoautotrophs (Wuchter *et al.*, 2003; Zhang *et al.*, 2010; Pratscher *et al.*, 2011). However, marine archaea have been shown to incorporate amino acids (Ouverney and Fuhrman, 2000; Teira *et al.*, 2004; Herndl *et al.*, 2005), and radiocarbon-based analyses of the membrane lipids demonstrate that pelagic marine archaea include a combination of autotrophs and heterotrophs, or consist of a single population with a mixotrophic metabolism (Ingalls *et al.*, 2006). Several marine AOA strains assimilate fixed organic carbon, with two strains demonstrating obligate mixotrophy (Qin *et al.*, 2014). In addition, several reported AOA genomes contain transporters for a variety of organic carbon compounds, such as acetate, citrate, taurine, and glycerol (Walker *et al.*, 2010; Hallam *et al.*, 2006; Kim *et al.*, 2011; Spang *et al.*, 2012; Lehtovirta-Morley, Ross, *et al.*, 2016; Stieglmeier, Klingl, *et al.*, 2014).

To date, no thaumarchaeotal representatives have been shown to grow heterotrophically. However, the detection of environmental sequences with no associated *amoA* genes (*i.e.,* Group I.1c, I.1d, I.1e, and I.1f *Thaumarchaeota*) suggests that alternative metabolisms exist among the *Thaumarchaeota*. Even among members of *Thaumarchaeota* containing *amoA* genes, there is evidence for metabolisms that are more complex than strict chemolithoautotrophy. For example, in several industrial wastewater treatment plants (WWTPs), detected AOA outnumbered AOB by up to 10,000 fold (Mussman *et al.*, 2011). Although these results could implicate AOA as the dominant ammonia oxidizers, mathematical modelling using ammonia loading rates showed that detected thaumarchaeotal cell numbers were 100- to 1000-fold higher than could be sustained by strict chemolithoautotrophic metabolism. Despite active expression of *amoA* genes, these *Thaumarchaeota* also failed to assimilate bicarbonate in the presence of ammonia. It was therefore suggested that the *Thaumarchaeota* detected in these WWTPs grow heterotrophically using an unknown substrate, or mixotrophically by combining ammonia oxidation with assimilation of a non-bicarbonate compound.

Mixotrophy and heterotrophy have been identified previously in nitrifying microorganisms. Although AOB have been referred to as model chemolithoautotrophs (Kowalchuk and Stephen, 2001), mixotrophy has actually been widely demonstrated. Stimulation of growth and ammonia-oxidizing activity of *Nitrosomonas europaea* by pyruvate has been reported (Clark and Schmidt, 1966), and isotopic labelling studies have provided direct evidence for the incorporation of several organic compounds into *N. europaea*, including

pyruvate, acetate, α-ketoglutarate, succinate, and amino acids (Clark and Schmidt, 1967; Wallace *et al.*, 1970; Martiny and Koops, 1982; Krümmel and Harms, 1982;). Both *N. europaea* and *Nitrosomonas eutropha* are able to grow as chemoorganoheterotrophs under anoxic conditions with pyruvate, lactate, acetate, serine, succinate, α-ketoglutarate, or fructose as substrate and nitrite as terminal electron acceptor (Schmidt, 2009). Furthermore, *N. europaea* can grow as a facultative chemolithoorganoheterotroph, using ammonia for energy, and fructose as a sole source of carbon (Hommes *et al.*, 2003). In addition, although *Nitrospira* spp. are typically thought of as chemolithoautotrophic nitrite oxidizers, recent studies have shown metabolic versatility and demonstrated that several members of the genus *Nitrospira* can use formate (Koch *et al.*, 2015; Gruber-Dorninger *et al.*, 2015), hydrogen (Koch *et al.*, 2014), and ammonia (Daims *et al.*, 2015; van Kessel *et al.*, 2015) as sources of energy.

1.7 AOA in engineered environments

In recent years, a large number of studies have explored the diversity, abundance, and activity of AOA in natural soil, marine, freshwater, estuary, and hot spring environments. However, comparatively few studies have investigated AOA in environments built and used by humans, despite the fact that many engineered systems reduce ammonia loads by promoting nitrification. Engineered systems, such as WWTPs, aquarium filters, aquaculture operations, and groundwater treatment systems utilize biological filters (*i.e.,* biofilters) to host communities of aerobic nitrifying microorganisms that convert ammonia to nitrate. Although nitrate still causes eutrophication, it is generally preferable to ammonia in aquatic environments because it has no direct oxygen demand, it has a relatively low toxicity to aquatic organisms, and it may be further converted to relatively inert nitrogen gas by anaerobic processes. Given the importance of constructed biofilters to humans, engineered environments have been identified as a priority area for AOA research (Hatzenpichler, 2012).

1.7.1 AOA in wastewater treatment systems

Wastewater treatment is critical for human civilization and environmental health. Humans produce large amounts of domestic and commercial waste containing high concentrations of organic carbon and nitrogen. Domestic wastes consist of sewage and grey

water, whereas industrial waste varies widely and may originate from diverse industrial processes such as abattoirs, oil refineries, tanneries, or food processing plants. These wastes contain a variety of compounds that may be toxic or cause eutrophication and must be treated before release into receiving waters. One major objective of WWTPs is to remove nitrogenous ammonia waste, which is toxic to fish and other aquatic organisms, and can result in algal blooms and oxygen depletion. Wastewater treatment processes typically use either fixed-film or suspended growth systems. The most commonly used suspended growth system is an aeration basin, which uses activated sludge to treat wastewater through vigorous mixing and aeration. Alternatively, fixed-film processes use a solid substrate such as polymer, ceramic, or sand as a surface for biofilm attachment. Common examples of fixed-film processes include trickling filters and rotating biological contactors (RBCs), in which the wastewater passes over the media containing the microorganisms. More recently, integrated fixed film-activated sludge (IFAS) systems have been employed, which combine aeration basins with plastic beads as a substrate for biofilm formation, allowing an increase in microbial population densities and improving system performance without expanding the operation footprint (Weerapperuma *et al.*, 2005; Rosso *et al.*, 2011). Despite the importance of nitrifying microorganisms in wastewater treatment, relatively few studies have investigated AOA in WWTPs, and their role in wastewater nitrification remains unclear.

In general, wastewater contains relatively high concentrations of ammonia, which should favour AOB over AOA (Martens-Habbena *et al.*, 2009; Schleper, 2010). Indeed, many studies have reported a dominance of AOB in municipal and industrial WWTPs, with AOA often below detection limits (*e.g.,* Wells *et al.*, 2009; Mussman *et al.*, 2011). Nevertheless, other studies have detected AOA in WWTP in high abundances, in some cases outnumbering AOB (Limpiyakorn *et al.*, 2011; Sauder *et al.*, 2012).

Wastewater AOA were first identified based on archaeal *amoA* genes in DNA extracts from activated sludge of five municipal WWTPs in the U.S.A., and sequencing revealed that the majority of these AOA belonged to the Group I.1b *Thaumarchaeota* (Park *et al.*, 2006). A later study sampled a single municipal WWTP weekly for one year and found that AOA were present in only ~15% of the samples, and were approximately 1000-fold less abundant than AOB (Wells *et al.*, 2009). Several subsequent studies supported these findings and demonstrated numerical dominance of AOB. For example, a survey of 52 industrial and municipal WWTPs in Europe

found that AOB were numerically dominant in all but four WWTPs (Mussman *et al*., 2011). Gao and colleagues (2013) investigated eight full-scale WWTPs in Beijing, and detected both AOA and AOB gene sequences in all plants, but AOB outnumbered AOA in all samples, ranging from 2-fold more abundant to 3 orders of magnitude more abundant. Another analysis of 10 WWTPs found that, although AOA were present at the majority of sites, AOB were numerically dominant in both municipal and industrial WWTPs (Gao *et al.*, 2014). Moreover, in a WWTP treating landfill leachate, AOB outnumbered AOA in three distinct compartments, including an aeration tank, a facultative tank, and a sequential batch reactor (Yapsakli *et al.*, 2011).

Importantly, AOA have been detected in a wide variety of nitrifying WWTPs, including those treating municipal waste and industrial waste from oil refineries, tanneries, fish processing plants, landfill leachate, and coking and dyeing processes (Zhang *et al.*, 2009; Sonthiphand and Limpiyakorn, 2011; Limpiyakorn *et al.*, 2011; Mussman *et al.*, 2011; Oishi, Hirooka, *et al.*, 2012; Sauder *et al.*, 2012; Bai *et al.*, 2012; Reddy *et al.*, 2014; Ding *et al.*, 2015). Several studies have found approximately equal abundances of AOA and AOB (Sonthiphand and Limpiyakorn, 2011; Limpiyakorn *et al.*, 2011; Reddy *et al.*, 2014), while others have found that AOA are numerically dominant in some WWTPs. For example, a survey of six municipal and industrial WWTPs determined that, while both AOA and AOB were present in all samples, AOB were numerically dominant in industrial (coking and dyeing) treatment plants, whereas AOA were more abundant in municipal WWTPs (Bai *et al.*, 2012). The authors suggested that AOB may be less sensitive to the toxic compounds associated with the industrial wastewater operations. In another study, two lab-scale soil aquifer treatment systems were constructed to treat synthetic domestic wastewater and secondary effluent, and AOA outnumbered AOB in both systems based on *amoA* gene abundances (Ding *et al.*, 2015).

Several studies have investigated the influence of ammonia on the relative abundance of AOA and AOB in WWTPs and suggested that ammonia concentrations are an important factor for shaping ammonia-oxidizing communities. For example, quantification of archaeal and bacterial *amoA* in sludge samples showed that incubation with high ammonia concentrations repressed transcription of archaeal, but not bacterial, *amoA* genes (Fukushima *et al.*, 2012). Another study obtained municipal WWTP sludge with approximately equal numbers of AOA and AOB and demonstrated that, upon laboratory incubation with high ammonia concentrations, the AOA abundance declined, whereas the AOB population sizes were stable (Sonthiphand and

Limpiyakorn, 2011). Another study investigated AOA and AOB abundances in activated sludge of three industrial and four municipal WWTPs, and demonstrated that AOA were numerically dominant in WWTPs receiving lower ammonia inputs (Limpiyakorn *et al.*, 2011).

Although ammonia concentrations appear to govern ammonia-oxidizing community composition, additional factors are likely important. For example, one study used a microarray targeting *amoA* genes for samples from an IFAS treatment system, and detected AOA and AOB in all samples tested (Short *et al.*, 2013). In this IFAS system, AOB were numerically dominant in the mixed liquor (ML), but AOA and AOB were present in approximately equal abundance in the media-attached biofilm samples. The authors suggested that AOA may prefer fixed-film processes over suspended processes. However, another study investigating the microbial communities in an IFAS system were unable to detect *Thaumarchaeota* in libraries of prokaryotic 16S rRNA genes obtained from either suspended or fixed-film biomass (Dong *et al.*, 2016). Additional studies have investigated nitrification rates in IFAS reactors and examined microorganisms in both suspended and biofilm biomass, but have only targeted AOB (Veuillet *et al.*, 2014; Malovanyy *et al.*, 2015). Therefore, it remains unclear whether AOA are present in these systems, and whether they are differentially abundant in the suspended versus fixed biomass.

Salinity may also play a role in the nitrifying communities of wastewater treatment systems. For example, a study by Wu and colleagues (2013) of a WWTP with varying salt levels, (due to seawater intrusion) demonstrated that AOA abundance remained relatively constant regardless of salinity level, whereas AOB abundance increased when the salt concentration decreased. Despite consistent overall abundance, community shifts within the AOA were observed. During high salinity conditions, *Nitrosopumilus*-like AOA dominated, whereas Group I.1b *Thaumarchaeota* dominated during low salinity conditions. Another study of membrane bioreactors used to pre-treat seaweater (to prevent biofouling during desalination processes) demonstrated that the archaeal community was dominated by *Nitrosopumilus*-like AOA (Jeong *et al.*, 2016), which have also been detected in other saline attached growth systems (Sakami *et al.*, 2012; Sánchez *et al.*, 2013). In addition, a lab-scale nitrification reactor treating saline wastewater with high nitrogen loading determined that all detected AOA fell within the *Nitrosopumilus* cluster (Ye and Zhang, 2011).

Overall, studies of AOA in freshwater WWTPs have demonstrated low thaumarchaeotal diversity, with most detected sequences belonging to the Group I.1b *Thaumarchaeota* (Limpiyakorn *et al.*, 2011; Zhang *et al.*, 2011; Oishi *et al.*, 2012). Conversely, the majority of AOA sequences obtained from saline nitrification reactors belong to the Group I.1a *Thaumarchaeota*, and cluster closely with *Nitrosopumilus maritimus* and environmental sequences from marine environments (Jin *et al.*, 2010; Ye and Zhang, 2011).

It is worth noting that molecular studies of AOA in WWTPs typically estimate archaeal abundances by qPCR of the *amoA* gene using two published primer sets (Francis *et al.*, 2005; Tourna *et al.*, 2008). However, several studies have documented issues in amplifying *amoA* genes from environmental samples using existing primers (Konstantinidis *et al.*, 2009; Hatzenpichler, 2012; Zhang *et al.*, 2011), which can result in underrepresentation of AOA. Few studies have validated thaumarchaeotal numbers using additional methods (*e.g.,* 16S rRNA qPCR, microscopy), which may result in bias when assessing the relative abundance of AOA and AOB. This may be particularly problematic in non-saline WWTPs where the majority of detected organisms fall into a Group I.1b sister branch of the *Nitrososphaera* (Pester *et al.*, 2012; Limpiyakorn *et al.*, 2013), for which no cultured representatives existed until recently. In addition, although several studies have now quantified AOA and AOB in WWTPs, only one study has attempted to assess the relative contributions of ammonia-oxidizing prokaryotes to ammonia oxidation. Mussman and colleagues (2011) detected *Thaumarchaeota* in high abundance in industrial WWTPs treating oil refinery waste but showed that these organisms were not mediating chemolithoautotrophic ammonia oxidation, despite actively expressing *amoA* genes, a finding which has important implications for the assumption that contributions of AOA and AOB to ammonia oxidation correspond to detection of thaumarchaeotal *amoA* genes. One study has reported the cultivation of an ammonia-oxidizing archaeon from WWTP sludge (Li, Ding, *et al.*, 2016), but it affiliates with the *Nitrosotenuis* cluster, which is not the dominant group detected in saline or freshwater WWTPs. Moreover, AOA may play additional as-yet-unknown roles in wastewater treatment systems, such as the biotransformation of compounds other than ammonia. For example, *Nitrososphaera gargensis* has recently been shown transform the pharmaceuticals mianserin and ranitidine in co-metabolism with ammonia oxidation (Men *et al.*, 2016).

1.7.2 AOA in aquarium biofilters and aquaculture operations

Ammonia is a metabolic waste product excreted by fish and other aquatic organisms. Ammonia toxicity is of particular concern for relatively closed ecosystems, such as aquaculture operations and home aquaria, in which ammonia can accumulate quickly to lethal concentrations in the absence of active nitrification. The unionized form of ammonia (NH_3) is particularly toxic to fish, with chronic stress and disease associated with concentrations exceeding 0.1 mg L^{-1} in aquarium and aquaculture systems (Andrews *et al.*, 1988; Parker, 2002). The average acute toxicities reported for 32 freshwater and 17 marine fish species were 2.79 mg L^{-1} and 1.86 mg L^{-1}, respectively (Randall and Tsui, 2002). In order to convert toxic ammonia to nitrate (NO_3) via nitrite, aquarium biofilters are designed to promote the growth and activity of nitrifying populations due to the high surface area of filter support material (*e.g.*, sponge, ceramic or polymer) and rapid flow rates of aerated water. Despite their importance to fish health and identical function within many industrial biofilters, including aquaculture and wastewater treatment, little is known of the microorganisms catalyzing nitrification in association with aquarium biofilter support material.

Traditionally, ammonia-oxidizing bacteria (AOB), such as *Nitrosomonas* spp., were thought to be solely responsible for the first step of nitrification in both terrestrial and aquatic environments, including aquaria. The use of AOB-containing aquarium supplements is widespread for promoting aquarium nitrification. Indeed, evidence suggests that AOB may play a role in aquarium nitrification. For example, Hovanec and DeLong (1996) used oligonucleotide probes to target bacterial nitrifiers in freshwater and saltwater aquarium biofilter DNA extracts. Although *Nitrosomonas*-like bacteria from the *Betaproteobacteria* were associated with the saltwater aquaria in their study, they only detected AOB in 2 of 38 freshwater aquaria, despite observing vigorous nitrification rates, leading the authors to conclude that an unknown group of organisms was performing ammonia-oxidation in freshwater aquarium biofilters. Subsequent studies determined that *Nitrosomonas* spp. could be enriched from freshwater aquarium biofilters (Burrell *et al.,* 2001), indicating that they may exist in these environments at abundances too low for detection by oligonucleotide probes.

Since the discovery of AOA, several studies have investigated AOA in aquarium biofilters. The first isolated AOA representative, *Nitrosopumilus maritimus* SCM1, was obtained

from sediment of a marine aquarium (Könneke *et al.*, 2005). The *N. maritimus* genome shares high synteny with contigs obtained from the open ocean (Walker *et al.*, 2010), demonstrating that this representative from an aquarium may be an important representative of AOA in natural environments. Urakawa and colleagues (2008) identified the presence of *amoA* genes from AOB and AOA in marine aquarium biofilters from a public aquarium in Japan, including a sunfish tank, a cold water tank, and a coastal fish tank, and suggested that the diversity of AOA and AOB was decreased in low temperature marine aquaria. Additional studies detected AOA in marine and freshwater aquaria, and have provided evidence for the numerical dominance of AOA in freshwater aquarium biofilters (Sauder *et al.*, 2011; Bagchi *et al.*, 2014).

Other studies have examined AOA and AOB in aquaculture systems, which share many characteristics with aquaria. For example, one study found that *Nitrosomonas*-like AOB were numerically dominant over AOA in a marine aquaculture bilfiltration system (Foesel *et al.*, 2008). However, an analysis of the biofiltration systems of a closed marine fish aquaculture system found both AOA and AOB in three biofiltration tanks of varying temperatures (subarctic, temperate, and subtropical), although relative abundance was not assessed (Sakami *et al.*, 2012). Another study found that AOB were more widespread than AOA in shrimp ponds in Thailand (Srithep *et al.*, 2015). Of six sampled ponds, AOB were found in all samples, whereas AOA were only detected in three. Although AOA were not found in all ponds, AOA *amoA* genes were present in high abundance in the two ponds selected for qPCR analysis. The majority of AOA sequences obtained from these shrimp ponds were related to *Nitrosopumilus maritimus* within the Group I.1a *Thaumarchaeota*. Conversely, AOA outnumbered AOB in a zero-discharge shrimp recirculating aquaculture system (RAS) using a multi-stage, nitrifying trickling filter, with three compartments consisting of plastic bioballs, corrugated blocks, or crushed oyster shells (Brown *et al.*, 2013). In all compartments and in sampled tank water, AOA *amoA* genes outnumbered bacterial *amoA* genes by orders of magnitude. Analysis of archaeal *amoA* gene sequences revealed that the detected AOA were also related to *Nitrosopumilus maritimus*.

1.7.3 AOA in drinking water treatment systems

AOA have been detected in a number of nitrifying engineered biofilter environments related to drinking water treatment, including granular activated carbon of drinking water treatment plants (Kasuga *et al.*, 2010), and groundwater treatment systems for drinking water

production (de Vet *et al.*, 2009; van der Wielen *et al.*, 2009; de Vet *et al.*, 2011). An analysis of the biofilm community of a sand filter in a drinking water treatment plant revealed that all detected archaea (up to 7% of the total organisms present) belonged to the phylum *Thaumarchaeota*, and were related to the genus *Nitrosoarchaeum* within the Group I.1a *Thaumarchaeota* (Bai *et al.*, 2013). However, a constructed metagenomic library revealed few *amoA* sequences belonging to AOA, making the overall abundance unclear.

AOA have also been detected in drinking water distribution systems, where nitrifying microorganisms are often considered a nuisance because they accelerate the decomposition of chloramine, which decreases the disinfectant residual. For example, AOA were detected based on archaeal *amoA* genes in two drinking water distribution systems in Ontario, Canada (Scott *et al.*, 2015), and their presence was stable over the course of a nine-month sampling period. In addition, AOA were detected in biofilms of simulated premise plumbing systems for drinking water delivery, using both copper and PVC as pipe materials (Santillana *et al.*, 2016). In these actively nitrifying systems, archaea were detected by fluorescence *in situ* hybridization (FISH) and PCR, and associated gene sequences clustered with the *Nitrosotenuis* cluster, within the I.1a *Thaumarchaeota*.

1.7.4 AOA in compost facilities

In addition to treatment of liquid waste, compost systems are designed to promote decomposition of carbon- and nitrogen-rich solid waste products. Composting is a self-heating process in which microorganisms transform organic wastes in humus-like materials, which can then be used as agricultural fertilizers. AOA related to *Nitrososphaera* have been detected in a cattle manure composting site in Japan (Yamamoto *et al.*, 2010). Although AOB were more abundant after four days of composting, at subsequent sampling points (30 days, 60 days), AOA outnumbered AOB. Another study investigated the abundance of AOA in composts of cow or sheep manure combined with plant waste materials from tropical agriculture (*e.g.,* rice straw, coffee hulls; de Gannes *et al.*, 2012). The results demonstrated that Group I.1b AOA were abundant in all compost samples, and significantly outnumbered detected AOB. In another study, slurries of fermenting cattle manure compost were incubated at various temperatures (37°C, 46°C, or 60°C), and the growth of AOB and AOA was determined by qPCR for bacterial and archaeal *amoA* genes (Oishi, Tada, *et al.*, 2012). Detected AOB increased in abundance at 37°C,

whereas AOA increased in abundance at 46°C, both in conjunction with active ammonia oxidation. When incubated with the nitrification inhibitor allylthiourea (ATU), neither AOA or AOB numbers increased, and no ammonia oxidation occurred. Detected AOA sequences from the seed compost and slurries post-incubation were similar to *Nitrososphaera gargensis*. This study demonstrated that AOA in cattle manure compost can grow using an ammonia-oxidizing metabolism under moderately thermophilic conditions. Given that thermophilic AOA have been cultured and identified in many hot spring environments (de la Torre *et al.*, 2008; Hatzenpichler *et al.*, 2008; Reigstad *et al.*, 2008), the warm environments associated with composting may favour AOA over AOB.

1.7.5 AOA in human-associated environments

In addition to environments designed for treating wastes, members of the *Thaumarchaeota* have been detected on surfaces in built environments, such as space-craft assembly clean rooms (Moissl *et al.*, 2008), hospitals (Moissl-Eichinger, 2011), landfill sites (Im *et al.*, 2011), and door handles (Ross and Neufeld, 2015). Thaumarchaeotal 16S rRNA and *amoA* gene sequences have also been reported on human skin samples through DNA sequencing and FISH (Probst *et al.*, 2013). These sequences clustered phylogenetically within the Group I.1b *Thaumarchaeota*, as a sister taxon to the *Nitrososphaerales*, and were similar to sequences detected in clean rooms, landfill sites, and non-saline WWTPs. Given the sequence similarity between *Thaumarchaeota* detected on skin and those detected in engineered environments, it is possible the skin microbiome plays a role in seeding ammonia-oxidizing archaea into these environments.

1.8 Thesis research outline

As one of the most abundant and ubiquitous groups of microorganisms, the newly discovered *Thaumarchaeota* represent important contributors to global nitrogen cycling and nutrient turnover. In recent years, *Thaumarchaeota* in natural environments have been widely investigated, but little research has assessed these microorganisms in engineered environments. Even when detected, the majority of studies rely solely on the abundance and diversity of *amoA* genes, which provides valuable baseline information but fails to assess several aspects of AOA

activity, ecology, and metabolism. The overall objective of this thesis was to characterize *Thaumarchaeota* in engineered biofilter environments, with a primary focus on two environments: aquarium biofilters in the Waterloo Region, Ontario, and rotating biological contactors (RBCs) of a municipal WWTP in Guelph, Ontario. The thesis research assessed the abundance, diversity, and ecology of AOA in these biofilter environments through targeted molecular analyses and correlation of gene abundances with environmental parameters. This research further investigated AOA from engineered environments by characterizing the key representatives from these samples through laboratory cultivation, genome analyses, and *in situ* activity measurements.

This thesis presents five related studies (chapters 2-6) describing AOA that are associated with engineered environments. Chapter 2 describes a molecular survey assessing the abundance of AOA and AOB and the diversity and ecology of AOA in freshwater and saltwater aquarium biofilters. Chapter 3 describes the cultivation and genome sequence of an AOA representative enriched from an aquarium biofilter, and assesses the relative contributions of AOA and AOB to ammonia oxidation in the original aquarium biofilter. Chapter 4 describes the abundance and diversity of AOA and AOB in a fixed-film, tertiary treatment system of a municipal WWTP (Guelph, Ontario), assessing the relationship between AOA abundance and wastewater ammonia concentration. Chapter 5 details the cultivation and genome sequence of a biofilm-associated AOA representative enriched from nitrification reactors studied in Chapter 4. In addition, Chapter 5 presents nitrification activity data from the RBCs using differential inhibitors of AOA and AOB. Chapter 6 describes the use of these newly cultivated AOA representatives to test novel differential inhibitors of AOA and AOB. Finally, conclusions, significance of the research, and future directions are discussed in Chapter 7.

Chapter 2[1]

Abundance and diversity of ammonia-oxidizing archaea in aquarium biofilters

2.1 Introduction

Ammonia is a nitrogenous metabolic waste product excreted by fish through their gills via passive diffusion (Wilkie, 2002). In closed ecosystems such as home aquaria, ammonia can accumulate to toxic levels. Stress, disease, and death may be associated with concentrations that exceed 0.1 mg L^{-1} in aquarium and aquaculture systems (Parker, 2002; Andrews *et al.*, 1988). However, active nitrification prevents accumulation of ammonia and nitrite through conversion to nitrate. Aquarium biofilters are designed to promote the growth and activity of nitrifying populations and are composed of a high surface area material (*e.g.,* sponge or ceramic), which is oxygenated via flowing water pumped into the filter chamber. Despite their importance to fish health and analogous function within many industrial biofilters, such as aquaculture and wastewater treatment, little is known of the microorganisms catalyzing nitrification in association with aquarium biofilter support material.

Before the discovery of ammonia-oxidizing archaea (AOA), belonging to the newly proposed phylum *Thaumarchaeota* (Brochier-Armanet *et al.*, 2008; Spang *et al.*, 2010), molecular approaches were used to investigate ammonia-oxidizing bacteria (AOB) and nitrite-oxidizing bacteria (NOB) in freshwater and marine aquaria (Hovanec and DeLong, 1996; Hovanec *et al.*, 1998). Oligonucleotide probes were used to target AOB in freshwater and saltwater aquarium biofilter DNA extracts, and although *Nitrosomonas*-like bacteria were associated with all tested saltwater aquaria, these bacteria were not detected in most of the freshwater aquarium samples. Subsequent studies determined that *Nitrosomonas* spp. could indeed be enriched from freshwater aquarium biofilters, leading the authors to suggest their potential involvement in ammonia oxidation under *in situ* conditions (Burrell *et al.*, 2001). Urakawa and colleagues identified both AOA and AOB *amoA* genes in marine aquarium

---

[1] A verion of this chapter has been published as:
Sauder LA, Engel K, Stearns JC, Masella AP, Pawliszyn R, Neufeld JD. (2011). Aquarium nitrification revisited: Thaumarchaeota are the dominant ammonia oxidizers in freshwater aquarium biofilters. PLoS One 6:e23281.

biofilters from a public aquarium in Japan, but did not quantify these groups. In addition, *Nitrosopumilus maritimus* SCM1, the first AOA representative isolated in pure culture, was obtained from a saltwater aquarium (Könneke *et al.*, 2005).

Despite these initial studies, no research has yet investigated the abundance of AOA and AOB in freshwater aquarium biofilters. Based on the ubiquity and high abundance of AOA in natural environments (Francis *et al.*, 2005; Wuchter *et al.*, 2006; Leininger *et al.*, 2006), the inability of Hovanec and DeLong (1996) to detect AOB in freshwater aquaria, and the isolation of the first ammonia-oxidizing archaeon from aquarium substrate (Könneke *et al.*, 2005), we hypothesized that AOA dominate freshwater aquarium biofilters and play an important role in aquarium nitrification. In addition to determining the abundances of AOA and AOB in aquaria, the objectives of this study were to assess the diversity of AOA *amoA* genes in aquaria, and to determine how gene sequences from aquarium AOA clustered with sequences derived from environmental sources and cultured AOA representatives. The results of this study revealed that, based on *amoA* gene abundances, AOA were the dominant putative ammonia oxidizers in the majority of freshwater and saltwater aquaria. These results provide first evidence for the important role of AOA in freshwater aquarium filtration and suggest possible niche adaptation of AOA to conditions associated with freshwater aquarium biofilters.

2.2 Materials and methods

2.2.1 Sampling
Freshwater and saltwater aquarium biofilters were sampled from retail aquarium outlets and homes in Waterloo, Kitchener, and Cambridge (Ontario, Canada). A total of 27 freshwater and 8 marine filters were analyzed in this study. Filter types included sponge, floss, baffle, and live rock, and all filters collected were composed of cotton or synthetic polymeric material (*e.g.,* nylon). Filter samples were collected using flamed forceps and scissors to cut small slices (approximately 1 cm x 1 cm x 3 cm) from sponge material in external aquarium filtration systems. All filter samples were placed into 50 ml sterile tubes and stored on ice until returned to the laboratory within a few hours. Aquarium water samples were collected in 50 ml sterile tubes and stored on ice before being frozen at -80°C. A filter from one aquarium (FW27) was sampled four times over the course of two years to assess temporal stability in AOA/AOB ratios, and

water was sampled several times (over six months and hourly over one day) to assess stability in ammonia concentrations within a given aquarium. The pH was assessed for all water samples with a DELTA 320 pH meter (Mettler Toledo, Columbus, OH). Ammonia concentrations were assessed fluorometrically, according to a previously published method (Holmes *et al.*, 1999) using a TD 700 fluorometer (Turner Designs, Sunnyvale, CA) and calculated from linear standard curves. All ammonia concentrations reported in this chapter (and throughout this thesis) represent total ammonia ($NH_3 + NH_4^+$), unless otherwise specified. Other water chemistry parameters were assessed with a commercial water test kit (Quick Dip Aquarium Multi-Test Kit, Jungle Laboratories Corporation, Cibolo, TX). Sampling was also performed on eight saltwater aquarium filters and two aquarium supplements for comparison. Bacterial supplements (*i.e.*, bottled cell suspensions) are intended to aid in populating newly established aquaria with active nitrifying bacteria, to help ensure that ammonia and nitrite concentrations remain below toxic levels during the initial 1-2 months of aquarium filter colonization. The aquarium supplements included were Cycle (SP1; Rolf C. Hagen Inc., Montreal, Canada), and Bio-Support (SP2; Big Al's Distribution Centre, Niagara Falls, NY).

2.2.2 DNA extraction

A harsh nucleic acid extraction technique (Griffiths *et al.*, 2000) was adapted to extract nucleic acids from sponge filter material that had been cut into small fragments with flame-sterilized scissors. For supplements, 15 ml aliquots were pelleted by centrifugation at 7000 x g for 30 min, then the pellets were suspended in lysis buffer for extraction. The beadbeating extraction was performed according to the published protocol with minor modifications. Nucleic acids were extracted from an approximately equal volume of filter material rather than equivalent weight due to the variation in filter media porosity. To precipitate purified nucleic acids, two volumes of polyethylene glycol (PEG) solution (30% PEG 6000, 1.6 M NaCl) were used in combination with linear polyacrylamide (AppliChem, Darmstadt, Germany) as a co-precipitant to avoid introducing exogenous DNA detected in commercial supplies of glycogen (Bartram *et al.*, 2009). All extracts were separated on a standard 1% agarose gel with Gel Red nucleic acid stain (Biotium, Hayward, CA), visualized with an AlphaImager HP (Alpha Innotech Corporation, Santa Clara, CA) and quantified densitometrically by comparison to dilutions of

known quantities of lamba DNA (New England Biolabs, Pickering, Canada) using AlphaView software (Alpha Innotech Corporation).

2.2.3 Quantitative real-time PCR

Quantification of AOA and AOB *amoA* genes was performed using primers archamoAF and archamoAR (Francis *et al.*, 2005) and amoA-1F and amoA-2R (Rotthauwe *et al.*, 1997), respectively. Thaumarchaeotal and bacterial 16S rRNA genes were quantified using primers 771F and 957R (Ochsenreiter *et al.*, 2003) and 341F and 518R (Muyzer *et al.*, 1993), respectively. All quantitative PCR amplifications were performed in duplicate with a reaction volume of 12.5 µl, which contained 1X iQ SYBR Green Supermix (Bio-Rad, Hercules, CA), 5 pmol of each primer, 5 µg of bovine serum albumin (BSA) and 1 µl of template (at a concentration of 1-10 ng μl^{-1}). Quantitative PCR was performed on a CFX96 system (Bio-Rad). For both thaumarchaeotal and bacterial 16S rRNA genes, PCR conditions were 95°C for 3 min followed by 40 cycles of 95°C for 20 s, 55°C for 30 s and 72°C for 30 s (with a fluorescence plate read following each extension step). For *amoA* genes, the PCR conditions were the same as above, except with an extension time of 1 minute and annealing temperatures of 60°C and 58.5°C for bacterial and thaumarchaeotal *amoA* genes, respectively. For all amplification reactions, melt curves were performed after each run with a temperature range of 65°C to 95°C, with an incremental increase in temperature of 0.5°C.

PCR amplicons were used as qPCR standard template DNA, and were generated using the primers indicated above for their respective genes. Genomic DNA from aquarium FW27 was used to generate standards for thaumarchaeotal and bacterial *amoA* and thaumarchaeotal 16S rRNA genes. Genomic DNA from *Escherichia coli* was used to generate bacterial 16S rRNA gene standards. Standard curves were constructed using serial dilutions of standard template DNA plotted against the cycle threshold (Ct) values for each dilution using CFX Manager Software (Bio-Rad). Amplification efficiencies ranged from 90.6-98.2%, and coefficients of determinations (R^2) ranged from 0.988 to 0.999. Melt curves calculated for each target sequence showed single peaks and all PCR products were verified on a 1% agarose gel.

2.2.4 Denaturing gradient gel electrophoresis (DGGE)

DGGE for AOA *amoA* genes was performed as described previously (Nicol *et al.*, 2008) with minor modifications. Samples were run on 6% acrylamide gels, which provided better resolution than 8% acrylamide gels. AOA *amoA* genes were amplified using primers crenamoA23F and crenamoA616R with thermal cycling as described elsewhere (Tourna *et al.*, 2008). The DGGE system used was a DGGEK-2401 (C.B.S. Scientific Company, Del Mar, CA) using previously described technical modifications (Green *et al.*, 2009). Gels were run for 15 h at 85 V and subsequently stained with SYBR green (Invitrogen, Carlsbad, CA) for 1 h. Gels were scanned using the Typhoon 9400 Variable Mode Imager (GE Healthcare, Piscataway, NJ). Individual DGGE bands were excised, amplified (using the above primers and conditions) and sequenced. From the original gel images, fingerprints were normalized for multi-gel alignment with GelCompar II (Applied Maths, Austin, TX) and a nonmetric multidimensional scaling (NMDS) plot was generated based on Pearson product-moment correlations of background-subtracted densitometric curves.

2.2.5 Clone libraries, ordination, and statistical analyses

PCR amplicons for sequencing were generated using archamoAF and archamoAR, with thermal cycling as described previously (Francis *et al.*, 2005). Composites of freshwater and saltwater samples were produced by pooling equal amounts of PCR products from all freshwater and saltwater samples, respectively. Composite PCR products were ligated into the pGEM-T Easy Vector (Promega, Madison, WI) according to the manufacturer's instructions. Single colonies were picked and grown up in Luria Burtani broth containing ampicillin (100 µg ml^{-1}), followed by a plasmid extraction and Sanger sequencing of inserts with primer M13F. A total of 288 and 96 clones were sequenced for the composite freshwater and saltwater libraries, respectively. Ordination analyses were performed using translated amino acid sequences; DNA sequences derived from both DGGE bands and clone libraries were translated using dna2pep (Wernersson, 2006). After discarding sequences containing stop codons in the amino acid translation, a total of 261 freshwater clones and 84 saltwater clones remained. Reference sequences were obtained from GenBank for environmental clones as well as isolated or enriched AOA representatives. The collection of sequences was aligned using MUSCLE (Edgar, 2004) and the resulting alignment was cropped so that all sequences spanned the same 160 amino acid

region. A distance matrix was produced using protdist (Felenstein, 1989) and scaled by Kruskal's nonmetric multidimensional scaling using the MASS package (Venables and Ripley, 2002). All DNA sequences generated in this study are publicly available in GenBank (accession numbers JN183456-JN183849).

Pearson product-moment correlation coefficients and coefficients of determination were calculated in Excel 2010 (Microsoft, Redmond, WA), and associated *p*-values were calculated using InStat 3.0 (GraphPad Inc, La Jolla, CA). Unpaired *t* tests were utilized to compare means in G+C content between freshwater and saltwater sequences and were conducted in InStat 3.0.

2.3 Results

2.3.1 Aquarium samples

Twenty-seven freshwater and eight saltwater aquarium filter samples were collected from retail and residential locations (Table 2.1). All biofilters sampled in this study were derived from standalone aquaria in homes or offices, or from display tanks in retail outlets, reflecting conditions common to most residential or retail aquaria. In addition to aquarium biofilters, two aquarium supplements were included in the analysis. The aquaria sampled ranged in pH from 7.6 to 9.2 and varied in their fish and live plant composition. The aquaria contained a variety of fish including mixed tropical, goldfish, South American cichlids and African cichlids. Three aquaria had received antibiotic treatment in the previous six months (SW4, SW5, FW8) and several were known to have received doses of bacterial filter supplement when first established (*e.g.*, FW12, FW13, FW19, FW25). Ammonia concentrations (NH_3-N) of aquaria ranged from below detection to approximately 0.5 mg L^{-1}, with the majority of aquaria below 100 µg L^{-1}. In 28 of the 32 aquaria studied, nitrite (NO_2^-) was below detection. As expected, significant positive correlations were observed between ammonia and nitrite concentrations ($r=0.48$, $p<0.05$; Table 2.2) and nitrite and nitrate concentrations ($r=0.52$, $p<0.05$; Table 2.2). Aquaria ranged in size from five gallons to greater than 400 gallons (for large retail show tanks) and approximate fish numbers ranged from zero (in a plant tank; FW3) up to 300 (FW11). Although not a direct measure of fish biomass, the approximate number of fish per gallon was positively correlated with ammonia concentration ($r=0.60$, $p<0.001$; Table 2.2). Water hardness of freshwater aquaria was as low as 25 ppm (in FW12, a breeding tank using softened water), however, the water

31

hardness of 25 of 27 aquaria was >150 ppm. Hardness of saltwater samples could not be determined using the kit utilized. Alkalinity ranged from below detection (*e.g.*, FW24, FW17) to 300 ppm (*e.g.*, SW1, FW3). Neither hardness nor alkalinity correlated significantly with any other water chemistry parameters (Tables 2.2 and 2.3).

Table 2.1 Details of sampled aquaria

ID	Size (gallons)	# of fish	NH$_3$ (µg L^{-1})	pH	NO$_3^-$ (ppm)	NO$_2^-$ (ppm)	Hardness (ppm)	Alkalinity (ppm)	Live plants	Supplement to start filter	Antibiotics in last 6 months?	Filter type	Type of fish
SW1	>100	15	133	8.2	20	0	NA	300	Yes	Unknown	No	Baffle filter	Mixed marine
SW2	>200	10	56	8.3	40	0	NA	40	Yes	Unknown	No	Live Rock	Reef (anemones, tangs)
SW3	>400	12	22	8.6	200	0	NA	300	Yes	Unknown	No	Baffle filter	Moray eel, shark
SW4	30	6	110	8.8	40	0	NA	120	No	Unknown	Yes	Sponge	Clownfish
SW5	110	25	77	8.6	20	0	NA	180	No	Unknown	Yes	Baffle filter	Mixed marine
SW6	300	7	44	8.5	40	0	NA	300	Yes	Unknown	No	Baffle filter	Reef (e.g. anemones)
SW7	150	25	119	8.4	80	0	NA	300	Yes	Unknown	No	Baffle filter	Mixed marine
SW8	110	5	36	8.4	160	0	NA	300	No	Unknown	No	Baffle filter	Mixed marine
FW1	>250	>100	106	8.4	80	0.5	300	120	No	Unknown	No	Baffle filter	Mixed tropical
FW2	>250	>100	10	8.4	40	0	150	80	Yes	Unknown	No	Baffle filter	Mixed tropical
FW3	>100	0	29	8.5	20	0	300	300	Yes	Unknown	No	Baffle filter	Plants only
FW4	110	25	24	8.6	200	0	300	120	No	Unknown	No	Sponge	African cichlids
FW5	110	20	445	7.9	200	2	300	40	No	Unknown	No	Sponge	Mixed tropical
FW6	15	10	164	8.6	20	0	300	300	No	Unknown	No	Floss	South American tropical
FW7	15	7	39	8.0	60	0	300	300	No	Unknown	No	Floss	Live bearers
FW8	15	5	0.9	8.0	20	0	300	180	No	Unknown	Yes	Sponge	Mixed tropical
FW9	22	2	BDL	7.6	40	0	300	180	Yes	Unknown	No	Sponge	Mixed tropical
FW10	22	>150	333	7.9	80	1	300	300	No	Unknown	No	Sponge	Goldfish
FW11	65	300	559	7.7	40	2	300	300	No	Unknown	No	Sponge	Goldfish
FW12	120	100	426	8.1	20	0	25	300	Yes	Yes	No	Sponge	African cichlids
FW13	54	20	16	8.7	20	0	300	300	Yes	Yes	No	Sponge	African cichlids
FW14	110	10	41	8.7	20	0	300	120	No	No	No	Sponge	South American tropical
FW15	40	8	30	8.4	160	0.5	150	300	Yes	Yes	No	Sponge	South American cichlids
FW16	30	4	69	7.9	200	3	150	80	Yes	Yes	No	Sponge	Killifish
FW17	100	12	66	7.9	40	0	150	0	No	No	No	Sponge	Cichlids, Loach, Catfish
FW18	12	5	20	9.2	60	0	75	300	Yes	No	No	Sponge	Corydoras, Killifish
FW19	30	14	7	8.1	120	0	300	80	Yes	Yes	No	Sponge	Mixed tropical
FW20	10	3	17	8.6	40	0	300	180	No	No	No	Sponge	Mixed tropical
FW21	15	15	45	8.3	200	2	300	100	No	No	No	Sponge	Mixed tropical
FW22	30	2	44	7.9	10	0	150	40	Yes	No	No	Sponge	South American cichlids
FW23	75	40	139	8.0	40	0	300	120	Yes	No	No	Sponge	South American cichlids
FW24	25	25	12	8.2	40	0	150	0	Yes	No	No	Sponge	African cichlids
FW25	10	4	20	7.9	10	0	300	180	Yes	Yes	No	Sponge	Mixed tropical
FW26	5	3	11	7.8	10	0	300	120	Yes	No	No	Sponge	Mixed tropical
FW27	110	15	20	8.4	60	0	225	120	No	No	No	Sponge	African cichlids

BDL: below detection limit, NA: not applicable, gDNA: genomic DNA

S: saltwater, F: freshwater

Table 2.2 Pearson correlation coefficients for aquarium chemistry parameters and AOA/AOB abundances for all aquaria

	% AOA *amoA*	% AOB *amoA*	NH_4^+	NO_2^-	NO_3^-	pH	alkalinity	Hardness	fish gallon^{-1}
% AOA *amoA*	--								
% AOB *amoA*	-1.00	--							
NH_4^+	-0.67	0.67	--						
NO_2^-	-0.07	0.07	0.01	--					
NO_3^-	-0.21	0.21	0.48	0.52	--				
pH	-0.31	0.31	-0.34	0.13	-0.35	--			
alkalinity	-0.30	0.30	0.20	-0.03	-0.14	0.28	--		
hardness	NA	NA	NA	NA	NA	NA	NA	--	
fish gallon^{-1}	-0.21	0.21	0.60	-0.04	0.36	-0.31	0.24	NA	--

Legend:
- □ No significance
- ▨ $p < 0.05$
- ▦ $p < 0.001$

NA: not applicable (not data available for hardness in saltwater samples)

Table 2.3 Pearson correlation coefficients for aquarium chemistry parameters and AOA/AOB abundances for freshwater aquaria

	% AOA *amoA*	% AOB *amoA*	NH_4^+	NO_2^-	NO_3^-	pH	alkalinity	Hardness	fish gallon^{-1}
% AOA *amoA*	--								
% AOB *amoA*	-1.00	--							
NH_4^+	-0.88	0.88	--						
NO_2^-	-0.80	0.80	0.78	--					
NO_3^-	-0.46	0.46	0.22	0.54	--				
pH	0.34	-0.34	-0.39	-0.24	0.18	--			
alkalinity	0.08	-0.08	0.24	0.04	-0.34	-0.04	--		
hardness	-0.19	0.19	0.15	0.20	0.23	0.03	0.38	--	
fish gallon^{-1}	-0.30	0.30	0.59	0.41	0.03	-0.25	0.54	0.18	--

Legend:
- □ No significance
- ▨ $p < 0.05$
- ▦ $p < 0.001$

2.3.2 AOA and AOB abundances

Quantitative PCR results demonstrated that thaumarchaeotal *amoA* genes were dominant in 23 of the 27 sampled freshwater filters (Fig. 2.1). For 12 of the freshwater biofilters thaumarchaeotal *amoA* genes represented the entire detected *amoA* gene signal. Interestingly, this included FW13, FW15, FW16, and FW25, aquaria that received bacterial aquarium supplements when first established. For saltwater aquaria, *amoA* genes from both AOA and AOB were detected in all samples, with AOA dominating five of eight samples. For both commercially available aquarium supplements, AOB *amoA* genes were abundant, and both archaeal *amoA* and 16S rRNA genes were below detection limits.

Both bacterial and thaumarchaeotal 16S rRNA genes were detected in all aquarium DNA extracts, but bacterial 16S rRNA genes generally greatly outnumbered thaumarchaeotal 16S rRNA genes (Fig 2.1, Table 2.4). In one aquarium biofilter (FW11), thaumarchaeotal and bacterial 16S rRNA gene copy numbers were approximately equal. For all aquaria, bacterial *amoA* gene copy numbers were at least three orders of magnitude less than bacterial 16S rRNA genes (Table 2.4). In some aquaria (*e.g.*, FW2, FW27, SW4), thaumarchaeotal *amoA* and 16S rRNA gene copy numbers were approximately equal, but in others (*e.g.*, FW11, FW12, SW8), thaumarchaeotal *amoA* gene copies were orders of magnitude less abundant than thaumarchaeotal 16S rRNA genes, which may suggest the presence of *Thaumarchaeota* that do not oxidize ammonia.

Table 2.4 Quantitative PCR data for genomic DNA extracts of sampled aquaria

ID	Archaeal *amoA* Gene copies per ng gDNA	St. dev.	Bacterial *amoA* Gene copies per ng gDNA	St. dev.	Archaeal 16S rRNA Gene copies per ng gDNA	St. dev.	Bacterial 16S rRNA Gene copies per ng gDNA	St. dev.
SW1	710	645	1140	196	163265	3946	610398	381154
SW2	2015	77	821	193	32002	3719	482665	65658
SW3	212	27	63	5.4	3661	102	225042	25758
SW4	34	4	5.0	0.2	44	2.5	165868	5789
SW5	434	92	155	37	292	5.8	369465	40869
SW6	69	23	82	8.0	7588	1204	399543	53000
SW7	1606	117	87	13	4588	154	143187	10529
SW8	337	38	4223	26	164666	34482	350116	18458
FW1	346	5	3.7	0.8	117	4.7	256214	13124
FW2	709	275	BDL	NA	758	168	177265	9905
FW3	38	3	BDL	NA	197	12	95060	4490
FW4	3128	78	BDL	NA	5312	48	208012	5902
FW5	BDL	NA	4.0	1.9	114	24	172519	53070
FW6	119	20	50	8.5	1735	405	302936	80903
FW7	1562	62	BDL	NA	24577	733	214194	14074
FW8	209	33	4.7	0.2	549	12	159612	274
FW9	148	0.4	5.4	0.6	392	38	159475	22177
FW10	1242	114	599	3.3	11426	891	350549	32859
FW11	1800	577	5382	765	433105	42675	413670	13140
FW12	42	0.5	926	18	10870	1066	296657	12395
FW13	376	28	BDL	NA	2281	10	111295	13940
FW14	389	78	BDL	NA	6726	650	257006	41257
FW15	150	24	BDL	NA	1693	54	172204	7170
FW16	230	26	BDL	NA	9321	426	755417	59916
FW17	1261	69	BDL	NA	7342	697	876849	121988
FW18	531	25	BDL	NA	11802	426	172741	2817
FW19	191	24	4.3	0.2	3416	239	52770	7630
FW20	23	2	38	0.4	70	11	165467	3139
FW21	86	13	5.4	0.1	1644	47	147223	7798
FW22	395	17	4.5	1.5	7371	334	172139	15213
FW23	32	14	3.7	0.9	5882	151	241338	134289
FW24	2482	270	6.5	0.4	5078	48	250438	23138
FW25	2160	179	BDL	NA	3944	55	112034	3240
FW26	1138	143	12	4.2	10161	236	210381	2803
FW27	30180	3156	BDL	NA	37536	5094	253781	15544
SP1	BDL	NA	13586	443	BDL	NA	945223	4331
SP2	BDL	NA	43950	17070	BDL	NA	137850	8718

gDNA: genomic DNA, St. dev: standard deviation, BDL: below detection limits, NA: not applicable

SP1: Bio-Support, SP2: Cycle
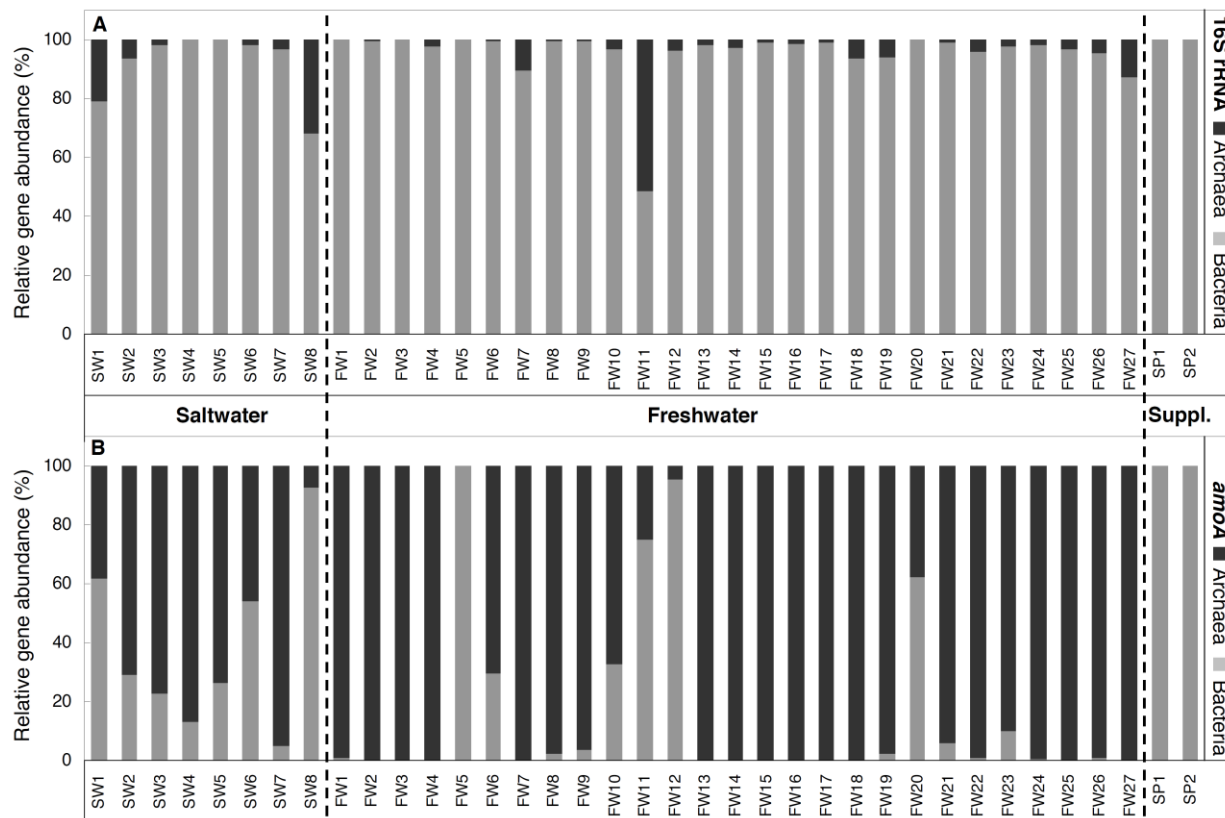
Figure 2.1 Relative gene abundances of bacteria and thaumarchaeota in aquaria. Relative 16S rRNA (A) and *amoA* (B) gene abundances for bacteria and archaea in saltwater (SW1–SW8) and freshwater (FW1–F27) aquaria and in aquarium supplements (SP1, SP2).

This study also examined aspects of water chemistry (Table 2.1) to assess correlations that might provide an explanation for differential *amoA* gene abundances. Regression analyses focused on freshwater aquarium samples (Table 2.3) because these were the primary focus of this study, and because too few saltwater samples were available to yield statistically significant correlations. Correlations were also calculated that included both fresh and saltwater samples (Table 2.2), which yielded similar results to freshwater correlations. For freshwater aquaria, we observed a significant negative correlation between ammonia concentrations and the proportion of *amoA* genes belonging to AOA rather than AOB (r=-0.85, p<0.001, R^2=0.72; Fig. 2.2 and Table 2.3). Low ammonia concentrations were typically associated with high AOA *amoA* gene abundances, although one sample (FW20) had high proportions of AOB *amoA* genes, despite an

37

ammonia concentration of less than 20 µg L^{-1}. In all cases, higher concentrations of ammonia were associated with higher relative abundances of AOB *amoA* genes. No other factors related to water chemistry or aquarium setup (*e.g.,* pH, hardness, alkalinity) yielded significant correlations with *amoA* gene abundances (Tables 2.2, 2.3). Ammonia concentrations in one freshwater aquarium (FW27) fluctuated very little, both on daily and monthly scales (Fig. 2.3A). The high proportion (>85%) of AOA in this filter was also consistent over a two-year sampling period (Fig. 2.3B). Together, these results suggest temporal consistency in individual freshwater aquarium filter environmental conditions and AOA communities.
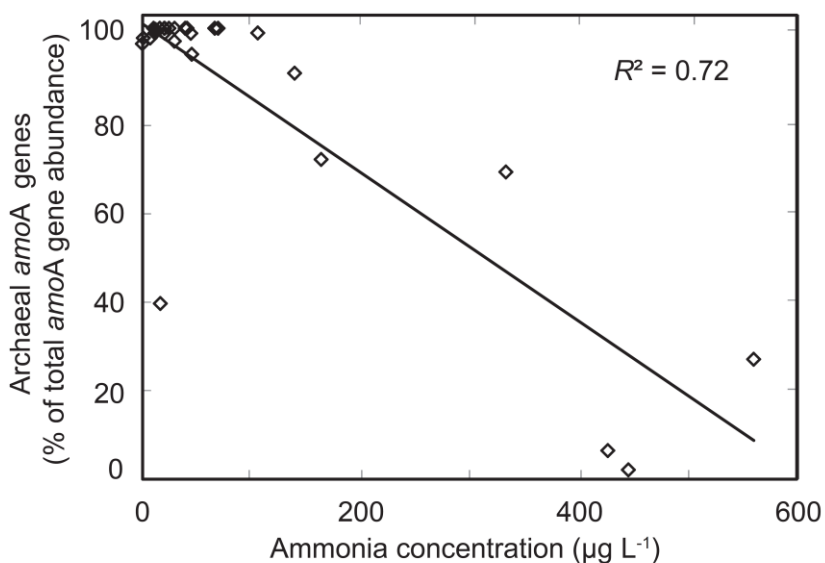
Figure 2.2 Freshwater aquarium ammonia concentrations and relative thaumarchaeotal *amoA* gene abundances. AOA *amoA* gene copies are expressed as a percentage of the total *amoA* gene copies (per ng gDNA). The coefficient of determination (R^2) for the linear regression is 0.72. The associated Pearson correlation coefficient (*r*) is −0.85, with an associated *p*-value of <0.001. See Tables 2.1 and 2.4 for all sample data.
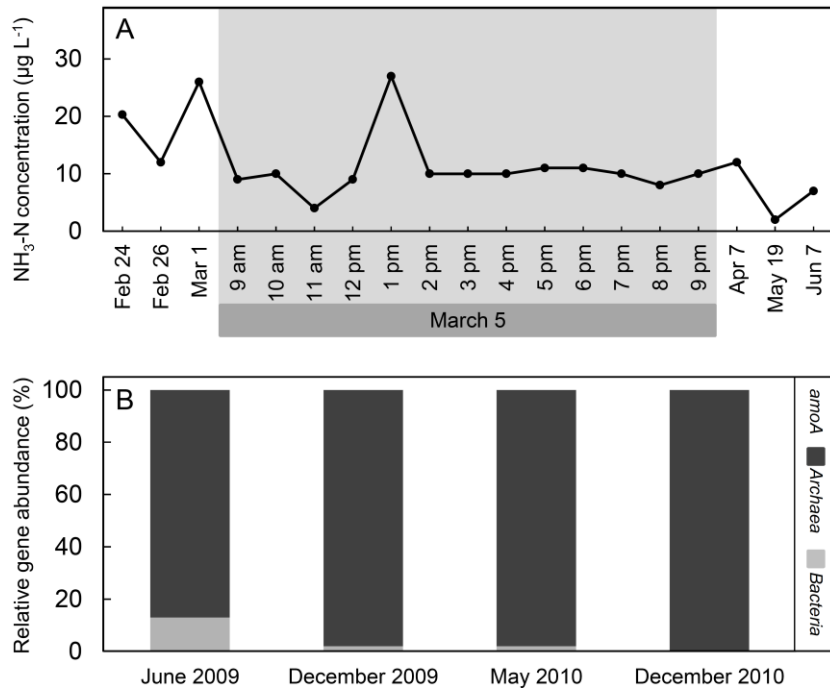
Figure 2.3 Aquarium FW27 temporal patterns. A) Ammonia concentrations over several months, and hourly over a 12 hour period. B) Proportions of AOA (as a percent of AOA *amoA* + AOB *amoA*) in the FW27 sponge filter DNA extract are shown from four time points over the course of two years.

2.3.3 AOA gene diversity

In order to assess the sample-to-sample variability of thaumarchaeotal populations possessing *amoA* genes, all biofilter DNA extracts were analyzed by DGGE. Based on the physical separation of PCR products by sequence heterogeneity and G+C content (Green *et al.*, 2009), the patterns generated by *amoA* gene amplicons varied between samples from very simple with few bands (*e.g.*, FW8, FW20, SW4) to relatively complex with many bands (*e.g.*, FW10, FW15, SW1; Fig. 2.4). DGGE patterns revealed shared bands between aquarium biofilters from the same location (*e.g.*, FW8 and FW9, FW25 and FW26, and SW1 and SW2), indicating that location-specific factors likely influenced the specific composition of AOA. Despite these similarities, distinct clustering of fingerprints was not observed based on location, and many bands were shared between multiple samples from various locations (Fig. 2.4). Based on visual inspection of aligned fingerprints, a shift in G+C content was observed between salt- and freshwater fingerprints, with saltwater bands typically melting at lower denaturant concentrations than the majority of freshwater sequences (Fig. 2.4). This apparent difference in G+C content was supported by sequences from both clone libraries and sequenced DGGE bands. Freshwater *amoA* gene sequences from clone libraries had an average G+C content of 45.4%, versus 43.8% in saltwater clones. Sequences of DGGE bands showed a similar pattern, with average G+C

contents of 45.5% and 44.0% for freshwater and saltwater bands, respectively. Although relatively small (~1.5%), this difference in average G+C content between freshwater and saltwater sequences was statistically significant ($p<0.0001$) for both clones and DGGE sequences, as determined by unpaired t tests. Nonmetric multidimensional scaling (NMDS) using densitometric curves generated from DGGE fingerprints revealed that freshwater and saltwater fingerprints were largely separated in two-dimensional space (Fig. 2.4C). However, some freshwater samples (*e.g*., FW1, FW12, FW15) were intermediate to freshwater and saltwater clusters (Fig. 2.4C). In addition to DGGE, we generated clone libraries of 261 and 84 sequences for freshwater and saltwater composite thaumarchaeotal *amoA* gene PCR amplicons, respectively. Multidimensional scaling of translated and aligned *amoA* gene sequences (from DGGE bands, clone libraries, and reference sequences) revealed four distinct clusters, each of which contained both clones and DGGE band sequences (Fig. 2.5). The first cluster (cluster 1; Fig. 2.5) contained saltwater and freshwater clone library sequences in approximately equal proportions, as well as both saltwater and freshwater DGGE band sequences. The freshwater DGGE band sequences that fell into this cluster were generated from samples which had fingerprints that fell near the periphery of the freshwater cluster, close to saltwater sequences (Fig. 2.4C). Both the second and third cluster (clusters 2 and 3; Fig. 2.5) were dominated by saltwater clone sequences. Cluster 2 was a distinctly saline cluster that contained *amoA* gene sequences from AOA originating from saline environments, including *N. maritimus* and *Cenarchaeum symbiosum* A (Hallam *et al.*, 2006), as well as an environmental clone obtained from a saltwater aquarium biofilter (Urakawa *et al.*, 2008). The majority of saltwater DGGE band sequences also fell into this cluster, including SW2-3, SW1-2, SW8-2 and SW6-2, sequences that represent a band shared across the majority of saltwater fingerprints (Fig. 2.4A). Cluster 3 was variable in composition, and contained both freshwater and saltwater DGGE band sequences. Reference *amoA* gene sequences in this cluster were from soil fosmid 54d9 (Treusch *et al.*, 2005) and hotspring organisms *Nitrososphaera gargensis* (Hatzenpichler *et al.*, 2008) and
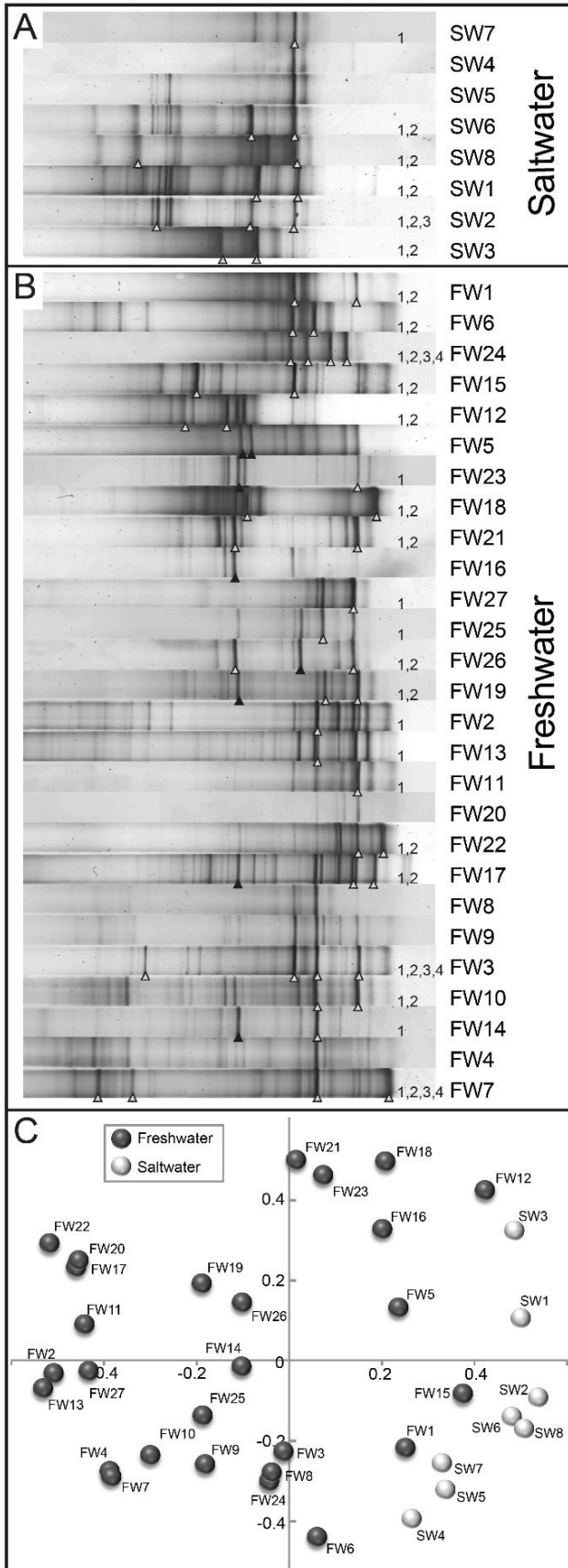
Candidatus Nitrosocaldus yellowstonii (de la Torre *et al.*, 2008). Cluster 4 was a distinct freshwater cluster; it was the largest of the clusters and contained the vast majority of the freshwater clone library and DGGE band sequences generated in this study. This cluster contained all sequences generated from a DGGE band that was shared over approximately half of the freshwater fingerprints (*i.e.*, FW2-4, 6-11, 13, 14, 17, 19, 27; Fig. 2.4B). In addition, reference sequences from a variety of low-salinity environments fall into this cluster, including rivers, lakes, sediments, and wastewater, as well as *Candidatus* Nitrosoarchaeum limnia (Blainey *et al.*, 2011).

Figure 2.4 Denaturing gradient gel electrophoresis of thaumarchaeotal *amoA* genes. Saltwater (A) and freshwater (B) fingerprints have been normalized and aligned. Bands chosen for sequencing are indicated with triangles: white triangles correspond to bands appearing in Figure 2.5. Black triangles represent failed sequencing reactions. Clustering of freshwater and saltwater fingerprints (C) is based on nonmetric multidimensional scaling (NMDS) using Pearson correlations of background-subtracted densitometric curves.

41
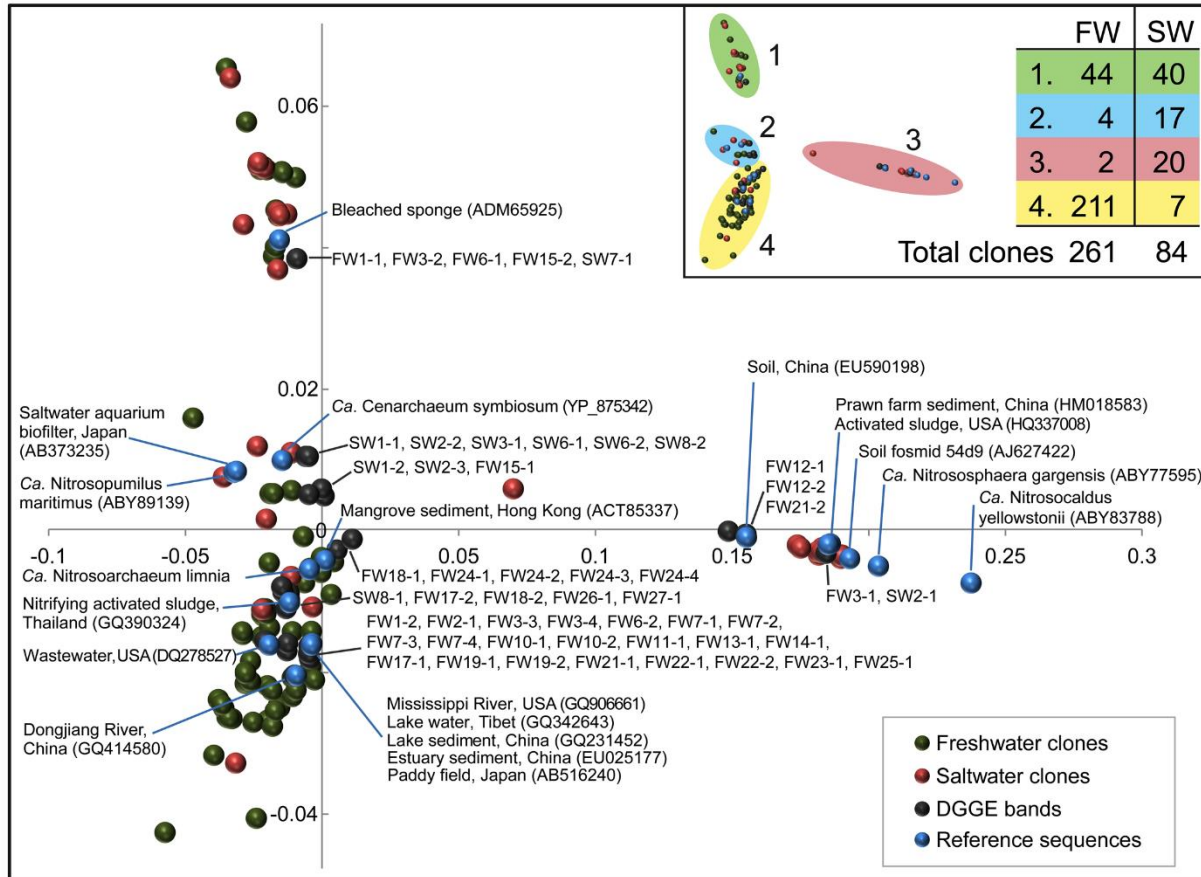
Figure 2.5 NMDS ordination of translated thaumarchaeotal *amoA* gene sequences. Sequences were obtained from clone libraries and DGGE bands derived from freshwater and saltwater aquarium filter samples. The inset panel provides a summary of the number of freshwater and saltwater clone library sequences contained within each cluster. Sequences obtained from DGGE bands correspond to the white triangles in Figure 2.5, and are labelled with sample and band numbers. Selected GenBank sequences from uncultivated clones and reference strains are included for comparison. The sampling environment and GenBank accession numbers for all reference sequences are included within parentheses.

2.4 Discussion

The present study has generated data that challenge decades of common knowledge regarding nitrogen cycling within aquarium filtration systems and solves outstanding questions remaining since *Nitrosomonas* spp. were undetected in freshwater aquaria (Hovanec and DeLong, 1996). From the sampling of 27 standalone freshwater aquaria from homes and retail outlets, the qPCR results revealed a dominant AOA population in the majority of freshwater filters sampled (Fig. 2.1). Indeed, 12 of the aquarium filters were associated only with an AOA *amoA* gene signal, despite using 40 cycles for the PCR. These results are important because they provide the first qualitative evidence that AOA may act alone in catalyzing ammonia oxidation. Though also generally dominated by AOA *amoA*, saltwater aquaria were more variable in the relative abundances of AOA and AOB, with both groups detected in each biofilter. Based on *amoA* gene abundances, the results of this study suggest that AOA are likely to be the primary contributors to nitrification in freshwater aquaria, while both AOA and AOB are likely to contribute to nitrification in saltwater aquaria.

The results of this study also answer longstanding questions related to nitrification in aquarium biofilter environments. For example, the low relative abundance of AOB *amoA* genes (Fig. 2.1) provides an explanation for previous studies that were unable to detect *Nitrosomonas* spp. with gene probes (Hovanec and DeLong, 1996), despite the ability to detect *Nitrosomonas* spp. with PCR primers for most samples (Burrell *et al.*, 2001). Probe hybridization methods have limited detection for genes that represent less than 1% of the total community (Neufeld *et al.*, 2006), whereas the high sensitivity of PCR can allow even a single copy of a gene to be detected. In the present study, relative proportions of AOB in saltwater aquaria were generally greater than in freshwater biofilters (Fig. 2.1), which may explain the ability of both probe hybridization and PCR amplification to detect *Nitrosomonas* spp. in saltwater aquarium biofilters (Hovanec and DeLong, 1996; Burrell *et al.*, 2001; Foesel *et al.*, 2008).

For a variety of genes in *Bacteria*, including both 16S rRNA and *amoA* genes, copy numbers within a cell are variable and often greater than one, and can therefore not be taken as a direct indication of population sizes. Conversely, available genomes from AOA representatives suggest that AOA cells contain one gene copy of each *amoA* and 16S rRNA (Walker *et al.*, 2010; Hallam *et al.*, 2006). Whether all *Thaumarchaeota* possess ammonia monooxygenase genes

43

remains unknown, but thaumarchaeotal 16S rRNA genes have been detected that are up to 100 times more abundant than archaeal *amoA* genes (Agogué *et al.*, 2008), suggesting that some thaumarchaeotal lineages do not gain energy by oxidizing ammonia. Some aquarium biofilters examined in this study (*e.g.*, FW2, FW27, SW4; Fig. 2.1) yielded *amoA* gene copy numbers approximately equal to thaumarchaeotal 16S rRNA copy numbers, implying that all *Thaumarchaeota* present in these aquaria possess *amoA* genes and presumably oxidize ammonia. Interestingly, other aquaria contained 16S rRNA genes that were orders of magnitude higher than AOA *amoA* genes (*e.g.*, FW11, FW12, SW8; Fig. 2.1), and may support the existence of thaumarchaeotal lineages that do not oxidize ammonia. Conversely, this may arise from failure to amplify all AOA lineages due to *amoA* primer bias, which has been reported previously (Konstantinidis *et al.*, 2009; Hatzenpichler, 2012)

AOA *amoA* gene diversity was variable across the filters collected in this study (Fig. 2.4A and B), with DGGE patterns ranging from relatively simple with few bands to complex with greater than ten discernible bands. In addition, many bands were shared across multiple aquarium filters from a variety of locations. Multidimensional scaling of DGGE fingerprints revealed that freshwater and saltwater fingerprints were largely separated in two-dimensional space. However, fingerprints of some freshwater samples were intermediate to major saltwater and freshwater clusters (Fig. 2.4C). DGGE band sequences derived from these intermediate fingerprints fell into a cluster of sequences containing approximately equal proportions of freshwater and saltwater clones (cluster 1, Fig. 2.5). DGGE profiles (Fig. 2.4) suggested a shift in *amoA* gene G+C content between freshwater and saltwater samples, and this was likely a factor in the separation observed. This trend was supported by clone libraries, which indicated that freshwater AOA *amoA* sequences had a higher average G+C content than their marine counterparts. Low G+C content could represent an adaptation of marine AOA to the low temperatures typical of the ocean. Indeed, the genome of marine AOA *N. maritimus* has a G+C content of only 33% (Walker *et al.*, 2010). Multidimensional scaling of thaumarchaeotal *amoA* clone library sequences (Fig. 2.5) revealed that freshwater and saltwater AOA *amoA* gene sequences largely cluster in distinct groups, which supports the separation observed in ordination analysis of DGGE profiles. Clusters were observed that predominantly contained saltwater sequences (*i.e.*, clusters 2 and 3; Fig. 2.5), while one cluster (cluster 1; Fig. 2.5) contained approximately equal proportions of freshwater and saltwater sequences. Based on

multidimensional scaling of both AOA *amoA* DGGE profiles and gene sequences, salinity appears to be a major factor in AOA differentiation. Nonetheless, these results suggest that at least some sequences are similar between environments, an observation that may indicate halotolerance of some AOA. Despite incomplete separation of saltwater and freshwater AOA *amoA* gene sequences, the majority (>80%) of freshwater sequences derived from clone libraries and DGGE bands clustered with sequences derived from a variety of freshwater environments, including lake sediments, wastewater, paddy soil, lakes and rivers (Fig. 2.5). This clustering supports previous evidence for niche adaptation of aquatic freshwater AOA (Herrmann *et al.*, 2008, 2009) and suggests that aquaria might provide valuable microcosms for investigating the ecology of aquatic AOA.

Although thaumarchaeotal *amoA* gene copies may be several thousand fold more abundant than betaproteobacterial *amoA* genes in some marine (Wuchter *et al.*, 2006) and terrestrial (Leininger *et al.*, 2006) environments, the relative contributions of AOA and AOB to environmental ammonia oxidation and the factors that affect their activity remain unclear. The concentration of ammonia may be a major factor affecting bacterial and thaumarchaeotal ammonia oxidation. Recent studies have provided evidence that AOB are the dominant ammonia-oxidizing organisms in ammonia-rich soil and aquatic environments. For example, a recent study used stable-isotope labelled (^{13}C) inorganic carbon and supplemented ammonia in soil to demonstrate that the labelled carbon was assimilated primarily into the nucleic acid of bacterial nitrifiers (Jia and Conrad, 2009). Foesel and colleagues (2008) found that *Nitrosomonas*-like AOB were numerically dominant in a marine aquaculture biofiltration system receiving high-ammonia influent (ranging from 340-1700 µg L^{-1}). Further, the metabolic and numerical dominance of bacterial ammonia oxidizers in the presence of high ammonia concentrations is consistent with a previous study (Burrell *et al.*, 2001) investigating the eventual establishment of bacterial ammonia oxidizer colonization of ammonia-supplemented aquarium biofilters (5-60 mg NH$_3$ L^{-1}).

Predominance of AOA in low ammonia conditions has now been relatively well established in soil environments (Di *et al.*, 2010; Verhamme *et al.*, 2011; Taylor *et al.*, 2010). However, the role of ammonia in regulating ammonia-oxidizing populations in aquatic environments has not yet been well studied. That AOA are better adapted to low ammonia

environments is supported by the present study with aquarium biofilters, where ammonia concentrations are maintained at consistently low concentrations (Table 2.1; Fig. 2.2). The majority of freshwater aquaria with very low ammonia concentrations ($<100 \mu g L^{-1}$) were associated with increased proportions of AOA, and a significant inverse correlation was identified (Fig. 2.2, Table 2.3). For statistical analyses, inclusion of additional samples with intermediate to high ammonia concentrations would have been preferable; however, established and maintained aquaria are typically kept at low ammonia concentrations to ensure fish health, and as a result we were unable to locate additional ammonia-rich aquaria. The results of this study suggest that ammonia concentration in freshwater environments is an important parameter for determining the relative abundance of AOA and AOB. These results are consistent with other studies that have retrieved AOA *amoA* genes from low ammonia aquatic environments and demonstrated corresponding activity (Beman *et al.*, 2008; Reigstad *et al.*, 2008; Herrmann *et al.*, 2011). In addition, growth kinetics of *N. maritimus* demonstrated a half saturation constant (K_m) for ammonia that is substantially lower than for cultured AOB representatives (Martens-Habbena *et al.*, 2009), and similar to the measured ammonia concentrations associated with most of the aquaria sampled in this study (*i.e.*, low $\mu g L^{-1}$ ranges). However, because *N. maritimus* is the only AOA representative for which kinetic studies have been reported, it remains unclear whether all AOA are similarly adapted to oligotrophic conditions and demonstrate high substrate affinities for ammonia. For example, the recently isolated *Nitrososphaera viennensis* tolerates ammonia concentrations of up to 20 mM (Tourna *et al.*, 2011), which is considerably higher than the inhibitory concentrations of 2 to 3 mM that have been reported for *N. maritimus* and *N. gargensis* (Hatzenpichler *et al.*, 2008; Martens-Habbena *et al.*, 2009).

Although the detectable ammonia concentrations in established freshwater aquaria are typically low as a result of biological ammonia oxidation, a preference for high ammonia concentrations by AOB suggests a possible role for their involvement in first establishing an aquarium when ammonia concentrations may approach levels associated with fish toxicity. In addition, ammonia concentration was positively and significantly correlated with the number of fish per gallon of aquarium water (Tables 2.2 and 2.3), suggesting that AOB may also be important for heavily stocked tanks that experience chronic high ammonia concentrations.

This study has identified that AOA are the dominant ammonia oxidizing microorganisms in freshwater aquarium biofilters. Aquarium ammonia concentrations were significantly and inversely correlated with AOA:AOB ratios. Freshwater aquarium AOA *amoA* gene sequences largely clustered with other freshwater-associated sequences. This work provides a foundation for future studies of aquarium nitrification and AOA ecology. Aquaria may serve as valuable microcosms to investigate the factors affecting AOA and AOB dynamics in both natural and engineered aquatic communities, including wastewater treatment systems, aquaculture, lakes, rivers, and oceans.

Chapter 3

Cultivation and characterization of *Candidatus* Nitrosotenuis aquariensis, an ammonia-oxidizing archaeon from a freshwater aquarium biofilter[2]

3.1 Introduction

Nitrification in aquarium systems is a critical process for maintaining fish health by preventing high ammonia and nitrite concentrations in aquarium water. Biological filters are used to promote the growth of nitrifying microorganisms by circulating oxygenated water through solid support materials. Until recently, it has been assumed that ammonia-oxidizing bacteria (AOB) were solely responsible for ammonia oxidation in aquaria. Commercial aquarium supplements are commonly added to aquaria to promote nitrification, and all supplements examined to date contain high proportions of AOB (Sauder *et al.*, 2011; Bagchi *et al.*, 2014). In addition, AOB affiliated with *Nitrosomonas europaea*, *Nitrosospira tenuis*, and *Nitrosomonas marina* lineages have been enriched from aquaculture environments (Burrell *et al.*, 2001). Although this study did not detect AOB in clone libraries prepared from freshwater aquaria, *Nitrosomonas marina*-like AOB were observed at low abundance within aquarium filter biofilm using fluorescence *in situ* hybridization (FISH). Another study failed to detect AOB in 36 of 38 sampled freshwater aquaria using oligonucleotide probes, causing the authors to suggest that an unknown organism must be responsible for ammonia-oxidizing activity *in situ* (Hovanec and DeLong, 1996). Recent evidence demonstrated that ammonia-oxidizing archaea (AOA), not AOB, dominate the majority of freshwater aquarium biofilters, suggesting an important role for AOA in aquarium nitrification (Sauder *et al.*, 2011; Bagchi *et al.*, 2014).

The first reported AOA representative, *Nitrosopumilus maritimus*, was isolated from a marine aquarium (Könneke *et al.*, 2005), and shows high genome similarity to AOA from globally distributed marine metagenomes (Walker *et al.*, 2010). *N. maritimus* has become a model organism for marine AOA, offering insight into AOA ecology and physiology, including

---

[2] A version of this chapter is in preparation for submission to Applied and Environmental Microbiology: Sauder LA, Engel K, Lo, C-C, Chain P, Neufeld JD. Cultivation characterization of *Candidatus* Nitrosotenuis aquariensis, an ammonia-oxidizing archaeon from a freshwater aquarium biofilter. *In preparation.*

the discovery of high substrate affinity for ammonia (Martens-Habbena and Stahl, 2011), sensitivity to light (Merbt *et al.*, 2012), cell division by the Cdv system (Busiek and Margolin, 2011; Pelve *et al.*, 2011; Ng *et al.*, 2013), and demonstration of hydroxylamine (Vajrala *et al.*, 2013) and nitric oxide (Martens-Habbena *et al.*, 2015, Kozlowski *et al.*, 2016) as intermediates in ammonia oxidation. Despite the importance of freshwater ecosystems to human and environmental health, few freshwater AOA representatives exist. *Ca*. Nitrosotenuis uzonensis originates from a freshwater hot spring and is moderately thermophilic (Lebedeva *et al.*, 2013). Within the same lineage, *Ca*. Nitrosotenuis chungbukensis was enriched from a deep horizon soil (Jung, Park, *et al.*, 2014), and *Ca*. Nitrosotenuis cloacae was enriched from a low-salinity WWTP (Li *et al.*, 2016). In addition, *Ca*. Nitrosoarchaeum limnia strains SFB1 and BD20 have been reported in enrichment culture, but these organisms originate from estuarine environments despite the fact that *limnia* means "freshwater".

In this study, we used biomass from an aquarium biofilter that was previously shown to have a high abundance of AOA (FW27; Sauder *et al.*, 2011, Chapter 2) as starting inoculum for enrichment of AOA. We aimed to cultivate and sequence the genome of an AOA representative from this freshwater aquarium to characterize AOA involved in aquarium nitrification and to provide insight into the ecology and metabolism of freshwater AOA.

3.2 Materials and methods

3.2.1 Cultivation

The starting inoculum for the cultivation of *Ca*. N. aquariensis was obtained from a Fluval 404 Canister Filter sponge (Hagen, Baie d'Urfé, QC, Canada) from a previously described freshwater aquarium biofilter that was dominated by AOA (FW27; Sauder *et al.*, 2011, Chapter 2). Biomass was removed from the aquarium filter by squeezing the sponge into aquarium water and creating a biomass suspension, which was then pre-filtered with Whatman paper. To select for AOA, which were expected to be small, the biomass suspension was filtered through a 0.45 µm syringe filter and the filtrate was used as starting inoculum for the enrichment culture. Subsequent inocula for subcultures were also passed through 0.45 µm filters. Cultivation was originally performed using plastic culture flasks with vented 0.22 µm mesh caps (VWR, Rador,

49

PA), using synthetic freshwater medium (FWM) with 0.5 mM NH_4Cl, as described previously (Tourna *et al.*, 2011). Cultures were later transitioned to a minimal growth medium used previously for growth of AOB and AOA (Krümmel and Harms, 1982; Lebedeva *et al.*, 2005; Hatzenpichler *et al.*, 2008). This medium contained (per L): 0.05 g KH_2PO_4, 0.075 g KCl, 0.05 g $MgSO_4 \cdot 7H_2O$, 0.58 g NaCl, and 4 g $CaCO_3$. Calcium carbonate is sparingly soluble and provided inorganic carbon for autotrophic growth, buffering capacity, and physical substrate for biofilm attachment. After autoclaving the basal salts, the medium was supplemented with filter-sterilized NH_4Cl (to 0.5-1 mM), 1 ml selenite-tungstate solution, and 1 ml trace element solution as described previously (Widdel and Bak, 1992; Könneke *et al.*, 2005). The pH of the medium was approximately 8.5 and was not adjusted. Cultures were grown in acid-washed and autoclaved glass bottles with sealed plastic caps, and were incubated at 28-30°C in the dark, without shaking. In addition to size selection by filtration, enrichment of AOA was achieved using several rounds of dilution to extinction and addition of antibiotics, including streptomycin (100 $\mu g\ ml^{-1}$), ampicillin (100 $\mu g\ ml^{-1}$), and nalidixic acid (30 $\mu g\ ml^{-1}$).

3.2.2 Incubations for growth curve, temperature, ammonia inhibition, and growth with urea

Incubations for growth curves were performed in quadruplicate in 100 ml volumes in the media described previously. Actively growing *Ca*. N. aquariensis cells were subcultured into fresh media (1% inoculum) and incubated at 30°C, in the dark, without shaking. Culture samples (2 ml) were removed every two days and pelleted for 10 minutes at 15,000 x g. Supernatants were removed and used for water chemistry analyses and pellets were used for DNA extraction and quantitative polymerase chain reaction (qPCR). All samples were stored at -20°C until processing.

For temperature experiments, actively growing *Ca*. N. aquariensis cultures were subcultured (1%) into fresh medium containing 0.5 mM NH_4Cl (50 ml volumes) and incubated at a variety of growth temperatures. For ammonia inhibition experiments, actively growing *Ca*. N. aquariensis cultures were subcultured (1%) into fresh medium (25 ml volumes). Ammonia was added at concentrations ranging from 0.25 mM to 10 mM, and cultures were incubated at 28°C. For assessing growth on urea, *Ca*. N. aquariensis was subcultured (1% inoculum) in fresh growth medium (50 ml) containing either 0.5 mM NH_4Cl, 0.5 mM urea, or 0.5 mM NH_4Cl and 0.5 mM urea. Sterile controls containing 0.5 mM urea were included to assess the potential for

ammonia production from spontaneous urea breakdown under the incubation conditions, and cultures were incubated at 30°C. For each activity experiment, various conditions were set up on the same day, using the same inoculum and batch of growth medium. All incubations were performed in triplicate unless otherwise indicated. All incubations were performed in the dark and without shaking of the cultures.

3.2.3 DNA extractions and quantitative PCR

DNA extractions for growth curves were performed using the Ultra Clean Microbial DNA Isolation kit (MO BIO, Carlsbad, CA) according to the manufacturer's instructions, except samples were incubated at 60°C prior to beadbeating, and homogenized using a FastPrep 24 beadbeater (MP Biomedical, Santa Ana, CA) for 45 s at 5.5 m s^{-1}. The qPCR was performed in 10 µl reaction volumes containing 5 µl 2X SsoAdvanced Universal SYBR Green Supermix (Bio-Rad, Hercules, CA), 500 nM of each primer, 5 µg of bovine serum albumin, and 1 µl template genomic DNA (containing ~0.1-5 ng ul^{-1}). Primers used for amplification of thaumarchaeotal 16S rRNA genes were 771F and 957R (Ochsenreiter *et al.*, 2003) and for bacterial 16S rRNA genes were 341F and 518R (Muyzer *et al.*, 1993). The qPCR standards for thaumarchaeotal and bacterial 16S rRNA genes were prepared from serial dilutions of amplicons generated using the above primers and quantified fluorometrically using the Qubit 2.0 fluorometer (Thermo Fisher Scientific, Waltam, MA) with the high-sensitivity dsDNA kit. Template DNA for standard amplicons for bacterial and thaumarchaeotal 16S rRNA genes was genomic DNA from *Ca*. N. aquariensis enrichment culture and *Escherichia coli*, respectively. Thermal cycling for qPCR used a two-step protocol, with cycling conditions as follows: 98°C for 2 minutes, 35 cycles of 98°C for 10 seconds, 55°C for 45 seconds, and with a fluorescence plate read after each extension step. For each qPCR run, a melt curve was constructed from 65°C-95°C in 0.5°C increments, held for 2 seconds. The qPCR was performed on a C1000 Thermal Cycler with a CFX96 Real-Time System attachment (Bio-Rad). CFX Manager software (version 1.5.5; Bio-Rad) was used for constructing standard curves and calculating unknown starting gene quantities. Generation time was calculated using the slope of log-transformed thaumarchaeotal 16S rRNA gene copies. Gene copies were used as an approximation of cell numbers, assuming one 16S rRNA gene copy per genome and one genome per cell.

3.2.4 Phylogenetic analyses

       The full-length *amoA* gene sequence from *Ca*. N. aquariensis was compared to cultured AOA representatives and environmental clones. All reference sequences were obtained from GenBank, and nucleotide sequences were aligned with MUSCLE (Edgar, 2004). Using the resulting alignment, an evolutionary history was inferred using the Maximum Likelihood method based on the General Time Reversible model of sequence evolution. The tree with the highest log likelihood is shown. A discrete Gamma distribution was used to model evolutionary rate differences among sites (using five categories), and the rate variation model allowed for some sites to be evolutionarily invariable. The tree is drawn to scale, with branch lengths measured in the number of nucleotide substitutions per site. Bootstrap values were calculated based on 1000 replicates and are indicated above tree branches, representing the number of times the associated taxa clustered together. All phylogenetic analyses were conducted in MEGA6 (Tamura *et al.*, 2013).

3.2.5 Fluorescence microscopy: CARD-FISH and DOPE-FISH

       For all fluorescence microscopy, samples were fixed with 4% formaldehyde at room temperature for three hours. Prior to fluorescence *in situ* hybridization (FISH), all samples were subjected to a standard ethanol series (50%, 80%, 98%; 3 minutes each). Catalyzed reporter deposition (CARD)-FISH was performed as described previously (Ishii *et al.*, 2004; Mussman *et al.*, 2011) with modifications. Briefly, fixed samples were applied to poly-l-lysine coated slides, and embedded in 0.2% agarose. Cells were permeabilized with proteinase K (15 µg ml^{-1} in 0.1 M Tris-0.01 M EDTA) for 10 minutes at room temperature and then incubated in 0.01 M HCl for 20 minutes at room temperature to inactivate the proteinase K. Alternatively, for some samples, cells were permeabilized with 0.1 M HCl at room temperature for 30 seconds. To inactivate endogenous peroxidases, slides were treated with 3% H_2O_2 at room temperature for 10 minutes. Probe Arch915 (Stahl and Amann, 1991; Table A1) was labelled with horseradish peroxidase (HRP) and applied at a concentration of 0.17 ng µl^{-1} in hybridization buffer containing 20% formamide. HRP-labelled probes were hybridized for 2.5 hours at 46°C and then washed in wash buffer (with corresponding stringency) for 15 minutes at 48°C. FITC tyramides and H_2O_2 (0.15%) were added to the amplification buffer and incubated at 46°C for 30 minutes. All samples were counterstained with 4',6-diamidino-2-phenylindole (DAPI; 5 µg ml^{-1}) for

nonspecific DNA staining. In all cases, no probe controls and HRP-labelled nonsense probes were prepared and imaged to ensure signal specificity.

For some samples, double labeling of oligonucleotide probes (DOPE)-FISH for bacteria was performed following CARD-FISH staining for archaea. Following the CARD-FISH procedure, samples were hybridized with EUB I-III probes (Table A1) that were double labeled with Cy3. Probes were hybridized in buffer containing 20% formamide at 46°C for 90 minutes in a humid chamber, then washed for 15 minutes at 48°C in corresponding 20% wash buffer (215 mM NaCl, 20 mM Tris-HCl, 5 mM EDTA). Finally, samples were rinsed with ice cold distilled water and dried using compressed air.

Citifluor AF1 antifadent mountant solution (Citiflour, London, UK) was applied to samples prior to fluorescence microscopy. Samples were visualized and imaged on an inverted Leica TCS SP8 confocal laser-scanning microscope (CLSM). For imaging fluorescein/FITC (green) signals, excitation and emission wavelengths were 492 nm and 520 nm, respectively. For imaging Cy3 (red) signals, excitation and emission wavelengths were 514 nm and 566 nm, respectively. For imaging DAPI signal, excitation and emission wavelengths were 400 nm and 600 nm, respectively. All images were obtained with a 60X glycerol objective for a total magnification of 600X.

3.2.6 Scanning electron microscopy and transmission electron microscopy

For scanning electron microscopy (SEM), a 10-μl sample was obtained from an actively growing culture and applied to a 5 mm x 5 mm silicon wafer (SPI supplies, West Chester, PA) that was attached to an aluminum stub (VWR, Radnor, PA) with conductive carbon tape (VWR) and dried in a fume hood. Cells were imaged without fixation or straining to preserve morphology. Immediately after drying, cells were imaged using a LEO 1550 field-emission scanning electron microscope (Zeiss, Oberkochen, DE). The InLens SE detector was used for high resolution topographic imaging, with an electron high voltage (EHT) of 5.00-7.00 kV, and a working distance of 10.3-10.5 mm.

For transmission electron microscopy (TEM), cells from actively growing *Ca*. N. aquariensis cultures were imaged without fixation. A 5-μl sample was placed onto a 200 mesh copper grid with formvar/carbon coating (Electron Microscopy Sciences, Hatfield, PA). Samples were dried, washed with 0.05 M HEPES buffer to remove media salts, and negatively stained

with 2% uranyl acetate. Imaging was performed using a Tecnai G2 F20 transmission electron microscope (FEI, Hillsboro, OR) operating at 200 kV with a bottom-mount Gatan 4K CCD camera and Digital Micrograph software (Gatan Inc, Pleasanton, CA).

3.2.7 Genome sequencing and assembly

Genomic DNA for metagenomic sequencing was extracted from the *Ca*. N. aquariensis enrichment culture using the Powersoil DNA Isolation Kit (MO BIO Laboratories) according to manufacturer's instructions, with beadbeating performed at 5.5 m s^{-1} for 45 seconds. Enrichment culture samples (6 x 50 ml) were pelleted at 7197 x g for 30 minutes, supernatant discarded, then pellets suspended in bead lysis solution for DNA extraction. Genomic DNA was visualized by standard 1% gel electrophoresis and quantified using a NanoDrop 2000 Spectrophotometer (Thermo Fisher Scientific).

A short-insert, paired-end library was constructed using the NEBNext Ultra DNA Library Prep Kit for Illumina and sequenced with a single index using the Illumina platform (Bennett, 2004) on a MiSeq Sequencing System (Illumina, San Diego, CA) at Los Alamos National Laboratories (LANL). In total, 26,430,800 reads of 251 bases were generated, for a total of 6,634 Mbp. Sequence data were quality trimmed using FAQCs (Lo and Chain, 2014) and assembled with SPAdes v3.5.0 (Bankevich *et al.*, 2012). The assembled contigs were binned using MaxBin v1.4.5 (Wu *et al.*, 2014) to isolate contigs for the genome of interest. Four contigs (contained in one bin) were identified as "*Nitrosopumilus*-like" using EDGE (Li, Lo, *et al.*, 2016). An automatic cutoff threshold of 500 bases was used for identifying contigs of interest, but obtained contigs were much longer, ranging from 180,742-674,865 bases. These four contigs were extended computationally with the quality-trimmed data using PRICE (Ruby *et al.*, 2013), which closed the gap between two of the contigs, leaving three remaining contigs (C1, C2, C3).

3.2.8 Primer walking for gap closure

Following assembly of Illumina reads, primer walking was used to close remaining gaps. Primers were designed from the ends of the extended contigs (see Table A3 for sequences) and PCR and Sanger sequencing was run to close gaps. Because the order and orientation of the contigs was unknown, pairwise PCRs between all primer sets were performed. All PCRs were performed in 20-μl reactions using 1X Phusion high fidelity (HF) buffer, 200 μM dNTPs, 500

nM each primer, 0.5 units Phusion HF polymerase (Thermo Fisher Scientific), and approximately 20 ng of genomic DNA per reaction. Thermal cycling conditions consisted of an initial denaturation time of 98°C for 1 min, followed by 30 cycles of 98°C for 10 s, 62°C for 20 s, and 72°C for 10 minutes, and a final extension of 72°C for 10 minutes. Long extension times were used to amplify up to 20-kb fragments. Annealing temperatures were calculated based on the online Phusion Tm calculator, and the average annealing temperature of all primer pairs was used. Resulting fragments were run on a 0.8% agarose gel agarose gel using the 1 KB Plus DNA Ladder and 1 KB DNA Extension Ladder markers (Thermo Fisher Scientific) to determine reaction specificity, and approximate length of remaining gaps. The three remaining gaps (G1, G2, G3) ranged in size from approximately 5-10 kb. The resulting PCR products were Sanger sequenced in both the forward and reverse direction (see Table A3 for primer sequences). After contigs were extended by one Sanger reaction per end, the contigs were again run through PRICE to determine if it was possible to extend the ends further using a new starting point. This approach closed the smallest gap (G1) and slightly extended a second gap (G2). Primers flanking the remaining gaps were designed, and used for PCR amplification with reaction details and cycling profiles as described above. The resulting PCR products were Sanger sequenced, and the process was repeated iteratively until both remaining gaps (G2, G3) were closed. All primers used for primer walking are outlined in Table A3. Primer design and assembly of overlapping Sanger sequences was performed in Geneious R9 (Biomatter Ltd, Auckland, New Zealand). Upon assembly of the complete genome sequence with closed gaps, a few (<5) nucleotide ambiguities remained where Sanger reads were low quality. The quality-trimmed Illumina sequences were mapped back to the contiguous genome sequence to correct any ambiguities using LANL in-house scripts. The total size of the genome is 1,697,207 bp and the final assembly is covered by 430 Mbp of Illumina draft data which provided an average depth of coverage of 2380X.

3.2.9 Genome annotation and analysis

Genome annotation was completed using two automatic annotation pipelines, including Integrated Microbial Genome/Expert Review (IMG ER; Markowitz *et al*., 2009) and the MicroScope Microbial Genome Annotation & Analysis Platform (MaGe; Vallenet *et al*., 2009). Manual annotations were also performed using MaGe using gene functions predicted by

COGnitor or HMMPfam, or when strong homology existed to proteins in UniProt or SwissProt databases. All annotation history is publicly available on the MicroScope/MaGe platform, and genes with manual annotations include notes indicating the basis of proposed function. If not otherwise indicated, genome analyses, including presence/absence of genes, locus tags, and gene arrangements, are based on annotation in Microscope/MaGe.

The average nucleotide identity (ANI) and average amino acid identity (AAI) of protein coding genes were calculated using online tools (http://enve-omics.ce.gatech.edu/ani/), implementing methods described previously (Goris *et al.*, 2007; Konstantinidis and Tiedje, 2005a; Rodriguez and Konstantinidis, 2016). For ANI values, a window size of 1000 bases with a 200 base step size was used to determine reciprocal best hits (with blastn). A minimum alignment length of 700 bases (70%) was used, and a minimum identity of 70%. For AAI values, protein coding sequences were based on MaGe protein-coding gene predictions. AAIs were calculated based on reciprocal best hits (blastp) with a minimum alignment of 50% and a minimum identity of 20%.

Full genome alignments and dot plots between *Ca*. N. aquariensis and other AOA genomes were generated using Protein MUMmer (PROmer; Kurtz *et al.*, 2004), implemented in IMG ER. Six-frame amino acid translations of input DNA sequences were used to identify matches, and a match length of six amino acids was used. Blue points on the dot plot indicate matches found on parallel strands, and red point indicate matches on antiparallel strands. Analysis of pan, core, and variable genes were performed in MaGe, using the Pan/Core Genome Analysis tool. This tool uses MicroScope gene families (MICFAMs), which are computed using a single linkage clustering algorithm of homologous genes as described by Miele and colleagues (2011). Permissive alignment constraints were applied, including 80% amino-acid alignment coverage and 50% amino-acid identity.

The full genome sequence and associated annotations of *Ca*. N. aquariensis are publically available in IMG ER (ID 78086) and MaGe (#T3JK6F).

3.2.10 Incubations of sponge filter with nitrification inhibitors

To assess *in situ* contributions to ammonia-oxidizing activity, biofilm samples from the sponge filter of FW27 (the biofilter from which *Ca*. N. aquariensis was enriched) were incubated with differential inhibitors. Incubations of sponge biofilter material were set up in both

December 2014 and April 2016. At the first time point, the aquarium had been established for approximately six years. However, soon after this experiment, the fish and filter were moved to a different location; the aquarium was dismantled and out of commission for approximately 10 months. This aquarium was then set up again using the same fish and filter system, and was re-established for approximately eight months prior to the second time point.

For each experiment, biofilm was squeezed from the sponge filter into aquarium water. The resulting slurry was diluted 1:2 in aquarium water and distributed in 25 ml volumes to 125 ml serum bottles with silicone stoppers. At the first time point, flasks were amended with PTIO (200 µM) or no inhibitor. In addition, paraformaldehyde (PFA)-killed biomass controls were included. At the second time point, flasks were amended with PTIO (200 µM), octyne (6 µM; aqueous), acetylene (4 µM; aqueous), or no inhibitor. All incubations were performed in triplicate. All flasks were amended with 0.5 mM NH_4Cl and incubated at 28°C, in the dark, without shaking. Samples were taken from flasks at ~12 hour intervals until ammonia was depleted. Samples were stored at -20°C until processing.

3.2.11 Water chemistry measurements

Nitrite measurements were performed using a colourimetric protocol (Miranda *et al.*, 2001). Briefly, reactions were carried out in clear plastic 96-well plates with 200 µl reaction volumes. Samples were diluted 1:10 in ammonia-free media to a total volume of 100 µl, and then 50 µl of each 2% (w/v) sulfanilamide (SULF) and 0.1% (w/v) N-(1-naphthyl)ethylenediamine dihydrochloride (NEDD) were added. After incubation for 10 minutes at room temperature, absorbance readings were taken at 550 nm with a FilterMax F5 MultiMode Microplate Reader (Molecular Devices). Standards of sodium nitrite ($NaNO_2$) were prepared in the linear range of 3-200 µM. Ammonia measurements were performed using Nessler's reagent as reported previously (Meseguer-Lloret *et al.*, 2002). Briefly, reactions were performed in clear plastic 96-well plates and consisted of 80 µl sample, 80 µl sodium potassium tartrate (17 mM), and 80 µl commercial Nessler's reagent (Ricca Chemical Company, Arlington, TX). Reactions were incubated for 10 minutes at room temperature and read on a spectrophotometric plate reader (see details above) at 450 nm. Standards of NH_4Cl were prepared and measured in the range of 15-1000 µM, and reported ammonia concentrations represent total ammonia ($NH_3 + NH_4^+$). For

both nitrite and ammonia measurements, SoftMax Pro 6.4 (Molecular Devices) was used for plotting standard curves and calculating sample concentrations.

3.3 Results and discussion

3.3.1 Ca. *N. aquariensis enrichment culture*

3.3.1.1 Culture activity

AOA may be important contributors to nitrogen and carbon cycling in freshwater environments, but relatively little research exists regarding AOA in these environments, and few laboratory cultures of freshwater AOA exist. Here we describe the enrichment culture and genome sequence of *Ca*. N. aquariensis, an ammonia-oxidizing archaeon from a freshwater aquarium biofilter. The proposed genus for this organism is based on related AOA representative *Ca*. Nitrosotenuis uzonensis (Lebedeva *et al.*, 2013). The Latin word "*tenuis*" translates to "slender" or "thin", a description which is appropriate for the organism described here. The species name "*aquariensis*" refers to the habitat from which this organism originates.

Ca. N. aquariensis has been growing stably in enrichment culture for over three years, and oxidizes ammonia to nitrite at near stoichiometric values (Fig. 3.1). Following a 1% subculture, an increase in thaumarchaeotal cell numbers (as estimated by 16S rRNA gene copies) was observed concomitantly with nitrite production, providing evidence that growth is based on ammonia oxidation for energy production, and that nitrite production can be used as an approximation of cell growth, at least following a 1% subculture. Similar results have been demonstrated for other AOA, which also oxidize ammonia to nitrite in association with increasing cell numbers (Könneke *et al.*, 2005; Tourna *et al.*, 2011). The generation time of *Ca*. N. aquariensis, estimated based on thaumarchaeotal 16S rRNA gene copies, was 34.9 hours. This generation time is similar that reported previously for *N. maritimus* (33 hours; Könneke *et al.*, 2005), *Ca*. Nitrososphaera yellowstonii (30 hours; de la Torre *et al.*, 2008), and *N. viennensis* (28 hours; Stieglmeier, Klingl, *et al.*, 2014), and shorter than that reported for *Ca*. N. cloacae (70 hours; Li, Ding, *et al.*, 2016), *Ca*. N. limnia (82 hours; Mosier, Lund, *et al.*, 2012) and *Ca*. N. devanaterra (53 hours; Lehtovirta-Morley *et al.*, 2011). However, the growth rate of *N. viennensis* was originally reported to be 46 hours (Tourna *et al.*, 2008), and it is likely that the

reported growth rates do not necessarily reflect the maximum possible growth rates. All reported AOA generation times are within the same order of magnitude, ranging between 1 and 4 days.

Quantitative PCR of bacterial and thaumarchaeotal 16S rRNA gene copies (assuming one 16S rRNA gene copy per bacterial and archaeal cell) demonstrated that the proportion of *Ca*. N. aquariensis in the enrichment culture in this experiment ranged from 96.7-99.9% (Fig. 3.1). DNA extraction and qPCR of *Ca*. N. aquariensis enrichment cultures at several other time points indicated >99% archaeal cells (data not shown), though these measurements were always performed when cultures were in exponential or stationary phase.
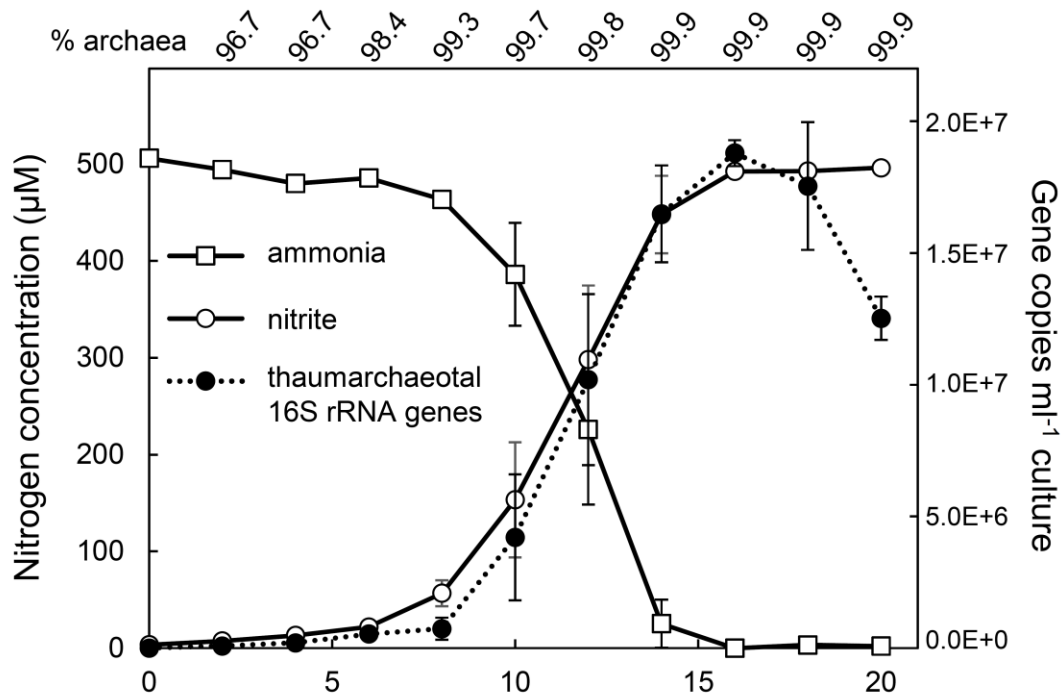
Figure 3.1 Growth and ammonia-oxidizing activity of *Ca*. N. aquariensis. Proportion of archaea (%) shown above graph correspond to the time points below, and values are based on measured thaumarchaeotal and bacterial 16S rRNA gene copies in genomic DNA extracts. Thaumarchaeotal 16S rRNA gene copies represent an approximate number of *Ca*. N. aquariensis cells, assuming one gene copy per genome and one genome per cell. Error bars represent the standard error of the mean for biological quadruplicates. Error bars not seen are contained within the symbols.

Ca. N. aquariensis actively produced nitrite at temperatures ranging from 20°C – 40°C, with an optimal growth temperature of 33°C (Fig. 3.2A), demonstrating that this is a mesophilic AOA representative. None of the tested temperatures completely inhibited nitrite production, although it was substantially slower at the lower (20°C) and upper (40°C) temperatures tested. Although the optimal growth temperature of closely related *Ca*. N. cloacae was only 4°C lower (29°C; Li, Ding, *et al.*, 2016), *Ca*. N. aquariensis appears to be adapted to slightly higher temperatures; the specific growth rate of *Ca*. N. cloacae decreased sharply (by approximately half) at 33°C, and nitrite production was completely inhibited at 37°C, whereas *Ca*. N. aquariensis was not fully inhibited at 40°C. Most reported Group I.1a *Thaumarchaeota* are mesophiles, with optimal growth temperatures ranging from 24–28°C (Könneke *et al.*, 2005; *e.g.*, Blainey *et al.*, 2011; Jung *et al.*, 2011; Mosier, Lund, *et al.*, 2012; Lehtovirta-Morley *et al.*, 2011). *Ca*. N. uzonensis is moderately thermophilic, with an optimal growth temperature of 46°C (Lebedeva *et al.*, 2013). A slightly higher temperature range for *Ca*. N. aquariensis is consistent with its origin from a tropical fish tank (28°C), which is warmer than typical marine and estuarine environments where many other Group I.1a *Thaumarchaeota* originate.

Ca. N. aquariensis activity was fastest when incubated with 0.25-1 mM NH_4Cl, with substantial inhibition observed at 2-3 mM NH_4Cl (Fig 3.2B). Complete inhibition of ammonia-oxidizing activity by *Ca*. N. aquariensis was observed when incubated with 5 mM NH_4Cl. Similarly, the growth rate of closely related *Ca*. N. cloacae was also reduced at 3 mM and completely inhibited at 5 mM NH_4Cl (Li, Ding, *et al.*, 2016). However, because of different medium pH values, the amount of unionized ammonia (NH_3), the putative substrate for the ammonia monooxygenase, varies considerably. At pH 8.5 (*Ca*. N. aquariensis growth medium pH), 3 mM NH_4Cl is equivalent to 0.54 mM NH_3, while it is only equivalent to 0.0071 mM NH3 at pH 6.5 (*Ca*. N. cloacae medium pH). Therefore, *Ca*. N. aquariensis can tolerate higher ammonia concentrations than *Ca*. N. cloacae, which is unexpected given that ammonia concentrations in aquaria typically remain relatively low. Indeed, the measured ammonia concentration in the aquarium from which *Ca*. N. aquariensis originates was previously reported to range between 5-30 µg L^{-1} (0.35-2.14 µM; Sauder *et al.*, 2011, Chapter 2), which is orders of magnitude below the concentration that *Ca*. N. aquariensis can tolerate.

When incubated with 0.5 mM urea as a sole energy source, nitrite production was observed by *Ca*. N. aquariensis, but was slow compared to cultures containing 0.5 mM ammonia

(Fig. 3.2C, D). In cultures containing 0.5 mM NH_4Cl and 0.5 mM urea, more nitrite was produced than with 0.5 mM NH_4Cl only, demonstrating that some of the supplied urea was converted to ammonia and oxidized to nitrite. Accumulation of ammonia was not observed in urea-only conditions (Fig. 3.2D), indicating that any ammonia produced from urea was oxidized rapidly. In addition, sterile controls did not show production of ammonia from urea within the timeframe of this experiment (Fig. 3.2D), indicating that any urea was the result of biological activity rather than physicochemical reactions. Nitrite production from urea appeared to occur only when ammonia was absent or depleted (Fig. 3.2C). This could indicate that although ammonia is a preferred nitrogen source, urease is expressed when ammonia is unavailable. This would be consistent with growth in a fish culture environment, because the vast majority of teleost fish excrete their nitrogenous waste primarily as ammonia (*i.e.*, ammoniotely; Wood, 1993). However, some teleosts excrete the majority of their nitrogenous waste as urea (*i.e.*, ureotely), and some are ammoniotelic in the wild but become predominantly ureotelic when kept in confined environments (Wood, 1993; Walsh and Milligan, 1995). In addition, bacterial decomposition of organic matter can produce urea (Satoh, 1980; Pedersen *et al.*, 1993), so urea could represent a viable alternative energy source in times of ammonia depletion. Many (but not all) AOB are able to use convert urea to ammonia for chemoautotrophic oxidation (Allison and Prosser, 1991; Koops *et al.*, 1991; Kowalchuk and Stephen, 2001; Koper *et al.*, 2004). In addition, some AOA have been shown to grow using urea as a sole source of energy, including *N. viennensis* (Tourna *et al.*, 2011; Stieglmeier, Klingl, *et al.*, 2014) and *Ca*. N. chungbukensis (Jung, Park, *et al.*, 2014). Although the *Ca*. N. aquariensis culture is highly enriched (~99%), it remains possible that remaining heterotrophic bacteria mediated urea degradation. In prokaryotes, ureolysis provides a source of nitrogen for assimilation, and urease expression in bacteria is often regulated based on nitrogen availability (Cussac *et al.*, 1992; Mobley *et al.*, 1995; Cruz-Ramos *et al.*, 1997; Morou-Bermudez and Burne, 2000; Murphy *et al.*, 2011). Therefore, expression of urea transporters and urease genes by heterotrophs would be unlikely under these conditions because excess nitrogen is available in the form of ammonia and/or nitrite, and because organic carbon concentrations would be very low, especially in no-ammonia conditions, when the primary producers are not actively growing.
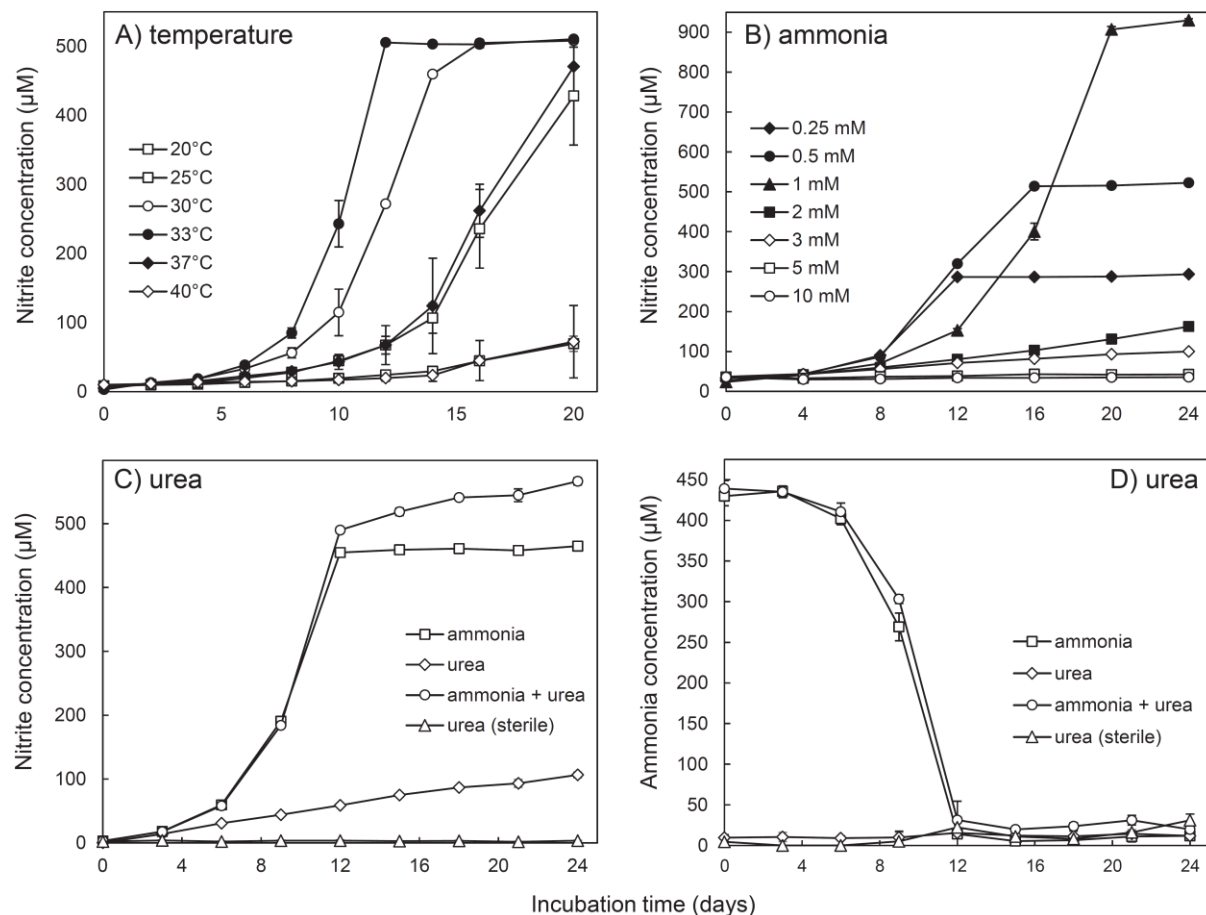
Figure 3.2 Ammonia-oxidizing activity of *Ca.* N. aquariensis under A) various incubation temperatures, B) various initial ammonia concentrations, and C, D) with urea as a substrate. For each panel, experiments were set up with the same inoculum, at the same time, and using the same batch of growth medium. For all panels, error bars represent standard error of the mean for biological triplicates. Error bars not seen are contained within symbols.

3.3.1.2 Microscopy and cell morphology

CARD-FISH images of the *Ca.* N. aquariensis enrichment culture permeabilized with proteinase K showed cells that were thin (~0.5 µm) and relatively long (~1.5-3 µm; Fig. 3.3A), and appeared to comprise a low proportion of the total cells. Counterstaining these samples using general bacterial FISH probes revealed that although some bacterial cells were present, many cells in the enrichment culture were visible with DAPI but were not stained with either bacterial or archaeal probes. Conversely, when the *Ca.* N. aquariensis enrichment culture was

62

permeabilized with HCl, cells were numerous and small (~0.5 µm in diameter), with an apparently coccoid morphology (Fig. 3.3B,C). In addition, cells were predominantly observed in clumped biomass (Fig 3.3B). No elongated archaeal cells were observed by CARD-FISH combined with HCl permeabilization.
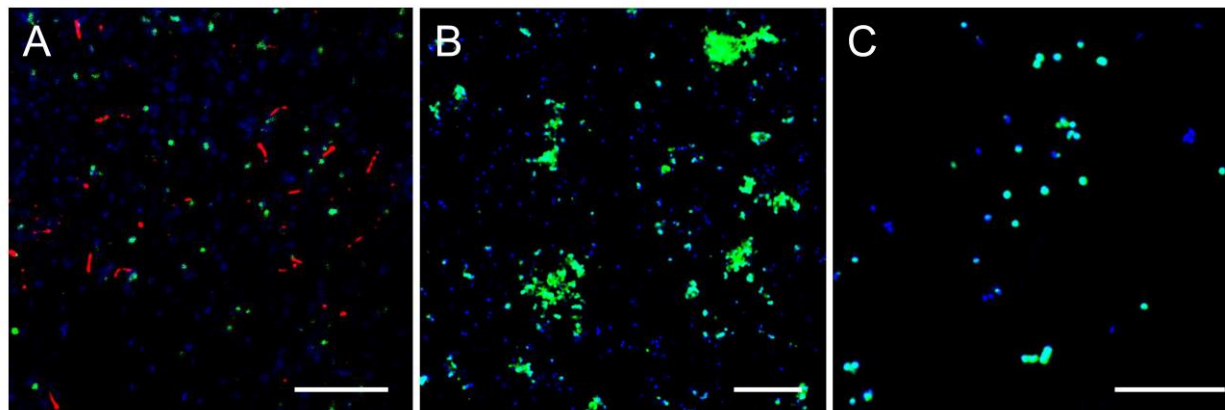
Figure 3.3 Fluorescence *in situ* hybridization micrographs of *Ca.* N. aquariensis. A) CARD-FISH for archaea (probe Arch915, Cy3 tyramides, red) and DOPE-FISH for bacteria (probe EUBmix, double-labelled with fluoroscein, green) in *Ca*. N. exaquare enrichment culture. B, C) CARD-FISH for archaea in *Ca*. N. exaquare enrichment cultures (probe Arch915, FITC tyramides, green). Sample shown in panel A was permeabilized with proteinase K, and samples shown in panels C and C were permeabilized with 0.1 M HCl. All scale bars represent 10 µm. All samples were counterstained with DAPI (blue).

Because of this discrepancy in morphology of *Ca*. N. aquariensis cells observed by FISH, electron microscopy was used to provide more detailed images. *Ca*. N. aquariensis cells imaged by SEM were small and rod-shaped, with a diameter of ~0.3-0.4 µm, and ranged from short rods (~0.5 µm in length) to longer rods (~1.2 µm in length; Fig. 3.4A). However, surface details and cell boundaries were relatively unclear, likely due to poor conductivity of cells. Therefore, TEM was used to provide high resolution details of cell morphology. *Ca*. N. aquariensis cells imaged with TEM displayed crystalline surface layers (S-layers; Fig. 3.4B,C,D) and the majority of cells imaged had a small number of appendages (typically five or fewer; *e.g*., Fig. 3.4B,C). The

location of these appendages varied between cells. In some cases they were polar (*e.g.,* Fig. 3.4B), whereas in other cases they were dispersed around the cell periphery (*e.g.*, Fig. 3.4C). These appendages were very thin and shorter than expected for flagella (*i.e.*, less than the length of the cell itself), although it is possible that they were broken off during processing. When viewed with TEM, *Ca*. N. aquariensis cells were consistently 0.4 ± 0.05 µm in diameter (Fig. 3.4B,C,D), but displayed a broad range of lengths, from very short rods (0.6 µm; Fig. 3.4B) up to 6-fold longer rods (3.6 µm in length; Fig. 3.4D). The apparently coccoid cells observed when permeabilized with HCl were most likely short rods, as fluorescence imaging does not provide highly accurate cell morphologies. The elongated cells visualized with proteinase K permeabilization are consistent with the long rods observed by TEM. It is possible that, as *Ca*. N. aquariensis cells grow, the composition of their cell envelope changes, resulting in differing responses to permabilization techniques.
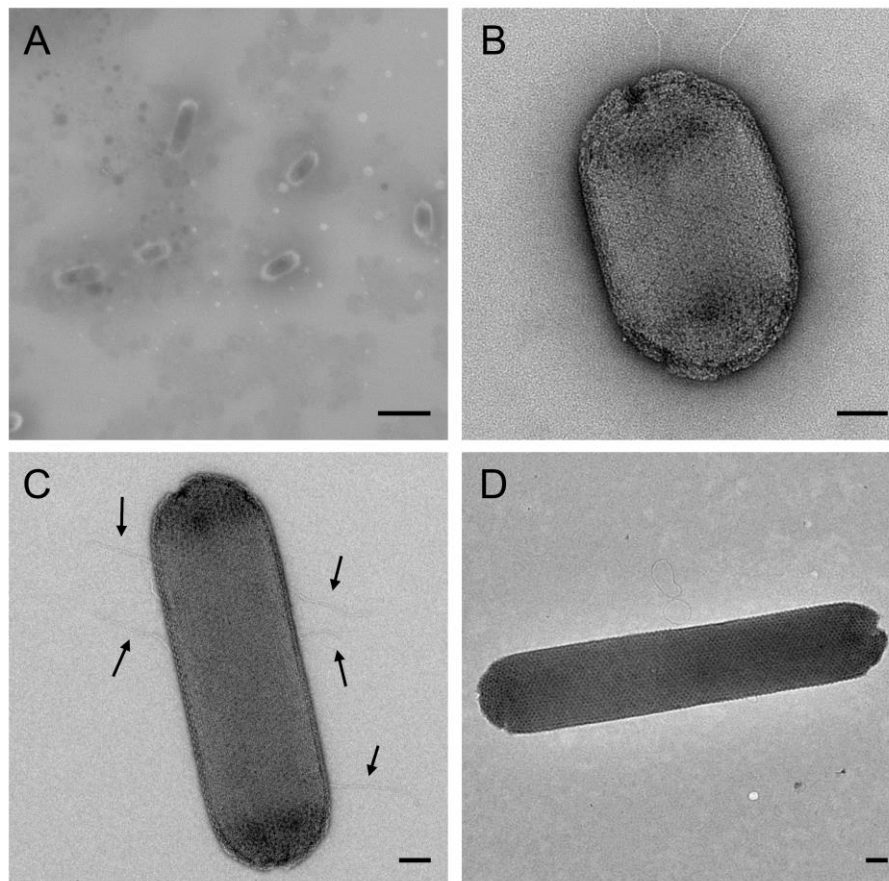
Figure 3.4 Electron micrographs of *Ca*. N. aquariensis. A) Scanning electron micrograph of unstained cells in enrichment culture. Scale bar: 1 µm. B, C, D) transmission electron micrographs of negative stained cells (2% uranyl acetate) in enrichment culture. Arrows in C) indicate cellular appendages. Scale bars in B,C, and D represent 100 nm.

64

Rod-shaped morphologies have been reported for most other Group I.1a *Thaumarchaeota* (Könneke *et al.*, 2005; Lehtovirta-Morley *et al.*, 2011; Jung *et al.*, 2011; Hatzenpichler, 2012; Stieglmeier, Alves, *et al.*, 2014), and cells have been reported to be very small. For example, *N. maritimus* ("the dwarf of the ocean") cells range from 0.17-0.22 µm in width, and 0.5-0.9 µm in length. In particular, the morphology of *Ca*. N. aquariensis shared several similarities with *Ca*. N. uzonensis (Lebedeva *et al.*, 2013) and *Ca*. N. limnia (Mosier *et al.*, 2012). All three cell types demonstrate a rod-shaped morphology with crystalline S-layers and proteinaceous appendages. So far, these appendages have been assumed to be archaeal flagella (Mosier, Lund, *et al.*, 2012; Lebedeva *et al.*, 2013), and in *Ca*. N. limnia and *Ca*. N. uzonensis, one or two long appendages were observed per cell, in polar or subpolar locations. Conversely, several relatively short appendages were observed in *Ca*. N. aquariensis (Fig. 3.4), which may function as flagella, or may be involved in other functions associated with archaeal surface structures, such as motility, attachment to surfaces, biofilm formation, or cell to cell contact (Jarrell *et al.*, 2013). Although the general cellular shape was similar, *Ca*. N. aquariensis cells were larger than other Group I.1a *Thaumarchaeota*. For example, *Ca*. N. limnia cells are 0.19-0.27 µm in diameter and 0.55-1.00 µm in length, and *Ca*. N. uzonensis cells ranges from 0.2-0.3 µm in width and 0.4-1.7 µm in length. At 0.4 µm in width and up to 3.6 µm in length, *Ca*. N. aquariensis can grow up to 2-fold longer *Ca*. N. uzonensis cells and is the longest reported AOA cell to date. Interestingly, despite being closely related to *Ca*. N. aquariensis, *Ca*. N. cloacae exhibits a strikingly different morphology. These latter cells were coccoid with a diameter of 1.1 ± 0.1 µm, and TEM imaging revealed no visible cellular appendages or S-layers (Li *et al.*, 2016).

Although once thought to be rare, S-layers are now known to be relatively common components of the cell envelope in bacteria and nearly universal in archaea (Rachel *et al.*, 1997; Eichler, 2003; Sleytr *et al.*, 2007; Ellen *et al.*, 2010). S-layers are proteinaceous crystalline arrays, often consisting of a single type of protein arranged in a highly ordered regular lattice pattern. The S-layer of *N. viennensis* has been investigated in detail and possesses a protein crystal arrangement with 6-fold p3 symmetry, consisting of a trimer of protein trimers with triangular shaped pores (Stieglmeier, Klingl, *et al.*, 2014). Six-fold p3 symmetry was previously thought to be unique to the order *Sulfolobales*, and all investigated species of this group showed this p3 symmetry in their S-layers (König *et al.*, 2007; Veith *et al.*, 2009). In *N. viennensis*, the S-layer was the only detected outer envelope structure, and was suggested to act as a cell wall,

forming a pseudo-periplasmic space outside of the plasma membrane. S-layers can have a variety of functions, including acting as molecular sieves to keep out large molecules, maintaining or determining cell shape, providing protection from attack, contributing to virulence, or enhancing surface adherence (Sára and Sleytr, 2000). Further research is required to determine the crystalline symmetry of the S-layer in *Ca*. N. aquariensis, but it is likely that this structure acts as a cell wall, maintaining cell shape and structural integrity, and associating closely with the cell membrane to form a pseudoperiplasmic space.

3.3.1.3 Phylogenetic relationship of *Ca*. N. aquariensis

Based on *amoA* gene sequences, *Ca*. N. aquariensis clusters within the Group I.1a *Thaumarchaeota,* and belongs to the *Nitrosotenuis* lineage (Fig. 3.5). This lineage has high bootstrap support (99%), and contains previously described species, including *Ca*. Nitrosotenuis uzonenis (Lebedeva *et al.*, 2013), *Ca*. Nirosotenuis chungbukensis (Jung, Park, *et al.*, 2014), and *Ca*. Nitrosotenuis cloacae (Li, Ding, *et al.*, 2016), as well as two AOA enrichment cultures without formal names, AOA-DW and AOA-AC2 (French *et al.*, 2012). In addition, *Ca*. N. aquariensis is closely related to environmental *amoA* sequences originating from a freshwater aquarium biofilter (JN183461), wastewater treatment plants (JN813561, KJ497142), a recirculating aquaculture filtration tank (KP27128), and Lake Challa, Tanzania (JX990378). Although only one freshwater aquarium biofilter sequence is shown, approximately half of the top 100 hits (based on nucleotide identity) in GenBank originate from freshwater aquarium biofilters, all of which were obtained in a survey of 27 freshwater aquarium biofilters (Chapter 2, Sauder *et al.*, 2011). Interestingly, *Ca*. N. aquariensis-like AOA also originate from other engineered environments, such as an aquaculture systems and municipal WWTPs.
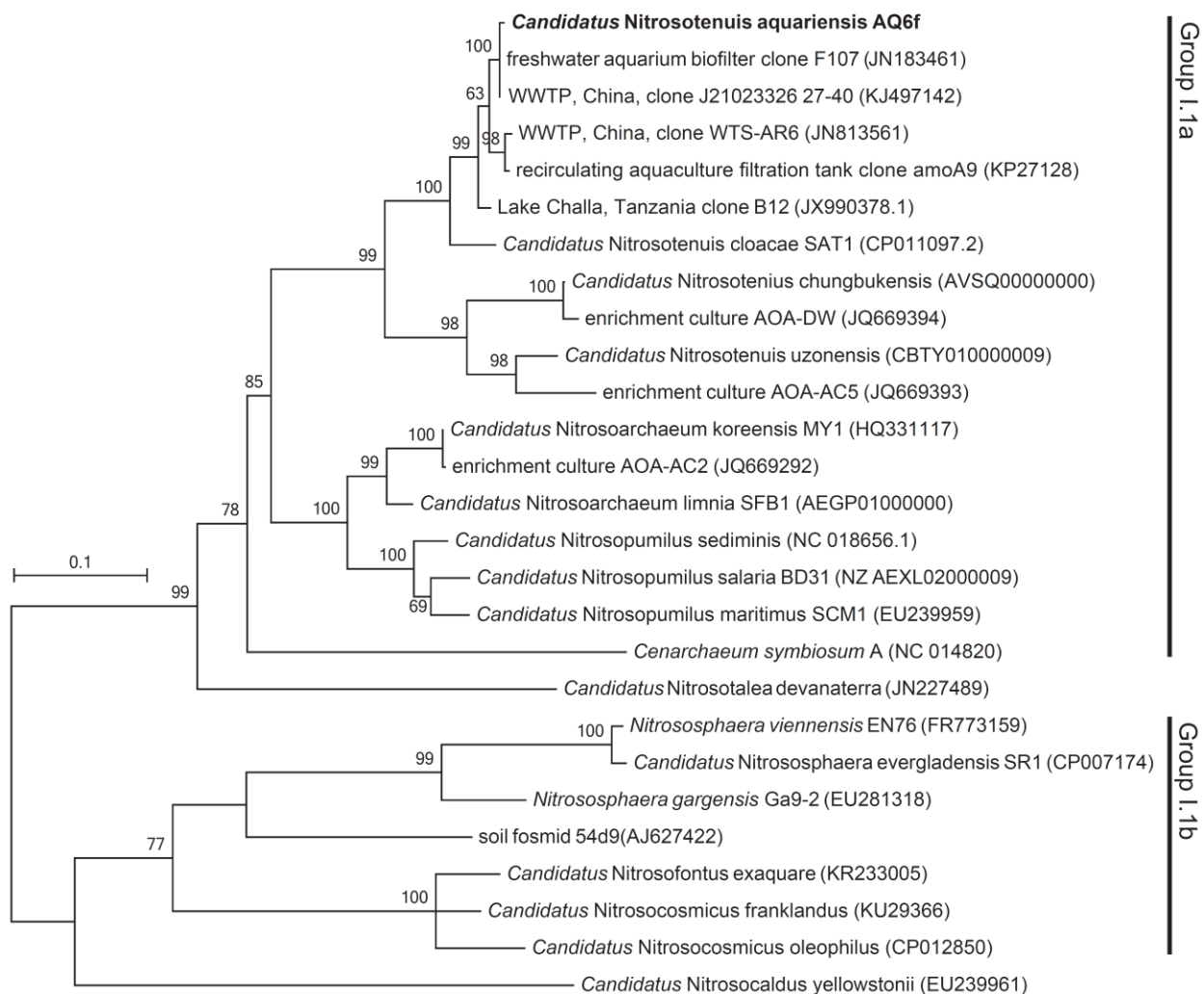
Figure 3.5 Phylogenetic relationship of *Ca*. N. aquariensis and other AOA representatives based on *amoA* gene sequences. GenBank accession numbers for reference sequences are indicated in brackets. Bootstrap values are indicated above branches. Only bootstrap values greater than 50% are shown. Maximum likelihood based on the general time reversible model. The scale bar represents 10% sequence divergence.

The *Nitrosotenuis* clade does not contain any cultured marine AOA representatives, and this lineage appears to be characterized by low salinity AOA. Both *Ca*. N. aquariensis and *Ca*. N. uzonensis (Lebedeva *et al.*, 2013) grow at 0.05% (w/v) salinity, whereas *Ca*. N. cloacae grows optimally at 0.03% salinity (Li, Ding, *et al.*, 2016). Attempts to incubate *Ca*. N. aquariensis in

artificial seawater medium resulted in no growth (data not shown); intermediate salt concentrations were not tested. Members of the *Nitrosoarchaeum* lineage can tolerate at least an order of magnitude higher salinity. For example, *Ca*. N. koreensis originates from soil but tolerates salinity up to 0.4% (Jung *et al.*, 2011). *Ca*. N. limnia is named for the word "freshwater", but originates from an estuary and is also found in higher salinity environments such as salt marshes (Mosier, Lund, *et al.*, 2012). *Ca*. N. limnia grows optimally at 0.88% salinity, and tolerates up to 2.6% salinity, although growth is partially inhibited at this concentration. *Ca*. N. limnia has also been reported to grow in freshwater medium (0.1% salinity), so it appears to demonstrate a broad range of acceptable salt concentrations. For comparison, marine AOA *N. maritimus* tolerates salinity of >3.5% (Könneke *et al.*, 2005; Martens-Habbena and Stahl, 2011). Based on available AOA genomes, the *Nitrosotenuis* lineage is also characterized by higher G+C content than other Group I.1a *Thaumarchaeota* (Table 1.1). Although genomes of the *Nitrosopumilus* and *Nitrosoarchaeum* linages contain <35% G+C content, available *Nitrosotenuis* genomes contain >41% G+C content (Table 1.1). Additional genomes not shown in Table 1.1 also follow this trend, including *Ca*. N. chungbukensis (42%; Jung, Park, *et al.*, 2014), *Ca*. Nitrosopumilus brevis (33%; Santoro *et al.*, 2015), and *Ca*. Nitrosopumilus salaria (34%; Mosier, Lund, *et al.*, 2012), and *Ca*. Nitrosopumilus sediminis (34%; Park, Kim, Jung, Kim, Cha, Ghai, *et al.*, 2012).

3.3.2 Ca. *N. aquariensis genome*

3.3.2.1 *Ca*. N. aquariensis genome characteristics

    The genome of *Ca*. N. aquariensis was assembled into one continuous sequence that was 1,697,207 bases in length (Fig. 3.6). The genome had a G+C content of 42.2%, a protein coding density of 92%, including 2088 genomic objects, 2047 of which were protein-coding genes (Table 3.1). One copy each of 5S, 16S, and 23S rRNA genes were present, as well as 38 tRNA genes. The genome encoded several genes related to chemolithoautotrophic ammonia oxidation, including the *amoA*, *amoB*, and *amoC* subunits of the ammonia monooxygenase, a nitrite reductase (*nirK*) gene, genes encoding ammonium transporters, as well urease subunits (*ureA*, *ureB*, *ureC)* and accessory proteins (*ureD*, *ureE, ureF*). Urease genes and transporters are found in all Group I.1b soil AOA genomes available so far (Spang *et al.*, 2010; Stieglmeier, Klingl, *et*

al., 2014; Zhalnina *et al.*, 2014), and in a few Group I.1a genomes, including *Ca*. Cenarchaeum symbiosum (Hallam *et al.*, 2006), *Ca*. Nitrosopumilus sediminis (Park, Kim, Jung, Kim, Cha, Kwon, *et al.*, 2012), and *Ca*. Nitrosotenuis chungbukensis (Jung, Park, *et al.*, 2014). However, in the *Ca*. N. aquariensis genome, urea transporter genes were not present. Small, uncharged polar molecules such as urea and glycerol can diffuse at low rates across a lipid bilayer (Finkelstein, 1976; Stein, 1986; Lodish *et al.*, 2000), so it is possible that *Ca*. N. aquariensis can utilize small amounts of urea that diffuse across the membrane despite an inability to transport it into the cell. *Ca*. N. aquariensis may be able to degrade urea in times of ammonia depletion, but given that the genome does not contain transporters and that nitrite production activity was much lower on urea than for that observed with ammonia (Fig. 3.1C,D), urea does not appear to be a primary source of energy for *Ca*. N. aquariensis.
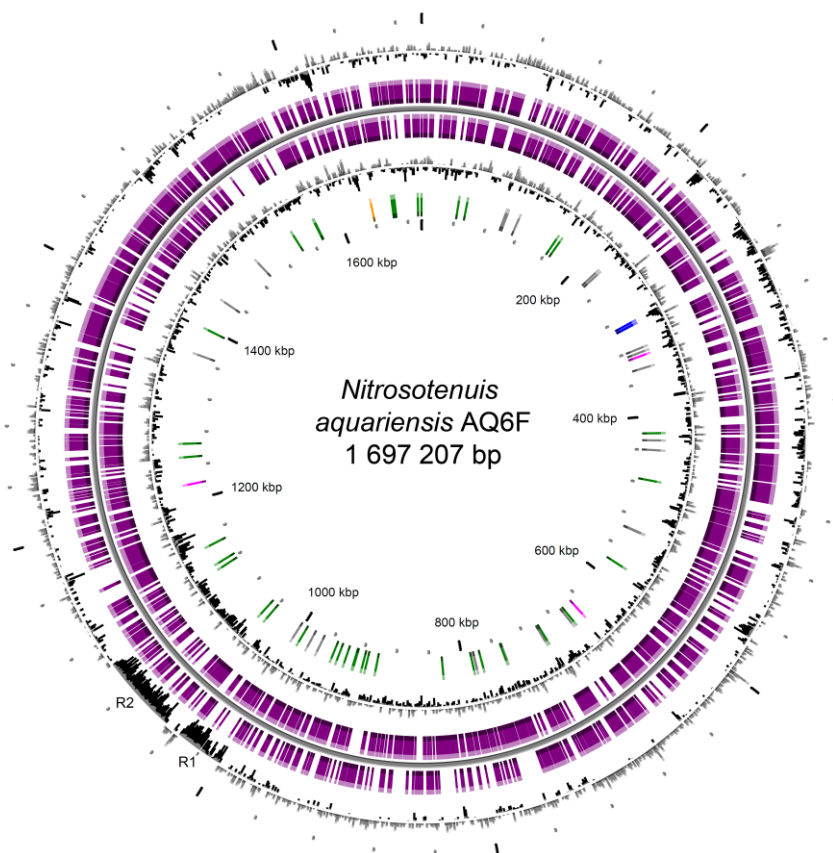
Figure 3.6 Circular plot of the complete *Ca.* N. aquariensis genome. Circles display (from the outside): (1) GC percent deviation (GC window - mean GC) in a 1000-bp window, (2) predicted coding sequences transcribed in the clockwise direction, and (3) predicted coding sequences transcribed in the counterclockwise direction, (4) GC skew (G+C/G-C) in a 1000-bp window, (5) rRNA (blue), tRNA (green), and pseudogenes (grey). The indicated regions R1 and R2 show areas of low G+C content.

Like all known AOA, *Ca*. N. aquariensis encodes the 3-hydroxypropionate/4-

hydroxybutyrate (3HP/4HB) pathway for autotrophic carbon fixation (Table 3.1). In addition to genes for chemolithoautotrophic ammonia oxidation, *Ca*. N. aquariensis encodes genes for several transporters or permeases of organic carbon, including dicarboxylates, citrate, taurine, glycerol, amino acids, oligopeptides, and polyamines (*e.g*., spermidine/putrescine). Similar transporters are found in other Group I.1a *Thaumarchaeota* (e.g. Könneke et al., 2005; Blainey et al., 2011), but so far there is no direct evidence of AOA assimilating or oxidizing any of these compounds.

The *Ca*. N. aquariensis genome contains a gene cluster encoding several flagella-related proteins, including genes encoding archaeal flagellin and flagellar assembly and accessory proteins (Fig. 3.7). Immediately downstream of the flagella gene cluster, there are several genes encoding chemotaxis-related proteins. These genes suggest motility of *Ca*. N. aquariensis driven by chemical signals, and is supported by cellular appendages observed by TEM (Fig. 3.3B,C). Many AOA encode chemotaxis and flagellar proteins, including all available *Nitrososphaera* genomes (Spang *et al.*, 2012; Stieglmeier, Klingl, *et al.*, 2014; Zhalnina *et al.*, 2014), *Ca*. N. devanaterra (Lehtovirta-Morley, Sayavedra-Soto, *et al.*, 2016), and several group I.1a AOA (Blainey *et al.*, 2011; Kim *et al.*, 2011; Park, Kim, Jung, Kim, Cha, Ghai, *et al.*, 2012; Lebedeva *et al.*, 2013; Jung, Park, *et al.*, 2014; Li, Ding, *et al.*, 2016). Interestingly, *Ca*. N. cloacae encodes flagella- and chemotaxis-associated genes, but no appendages were visible through microscopy. Conversely, some AOA lack genes associated with chemotaxis and flagellar synthesis, such as *N. maritimus* (Walker *et al.*, 2010) and *Ca*. Nitrosopumilus brevis (Santoro *et al.*, 2015).
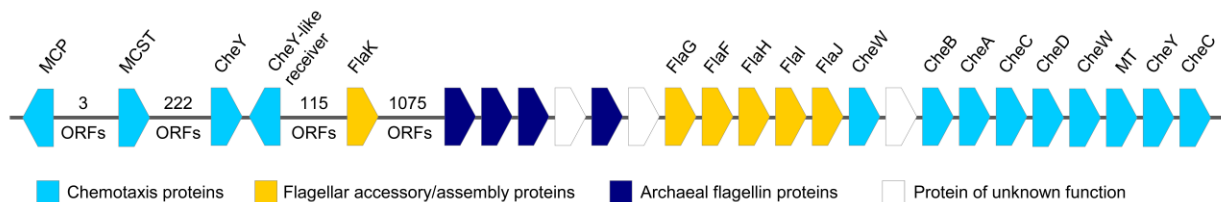
Figure 3.7 Schematic of flagella and chemotaxis proteins in *Ca*. N. aquariensis. Open reading frames (ORFs) on forward and reverse strands are indicated by arrow direction. ORFs are not drawn to scale. MCP: methyl accepting chemotaxis protein. MCST: methyl accepting chemotaxis sensory transducer. Gene locus tags are indicated for each category. See Table B1 for full descriptions of all genes shown.

Table 3.1 Genome features of *Ca.* N. aquariensis and other *Thaumarchaeota*

Genome features	*Nitrosotenuis aquariensis* AQ6F	*Nitrosotenuis uzonensis* N4[1]	*Nitrosotenuis cloacae* SAT1[2]	*Nitrosoarchaeum limnia* BG20[3]	*Nitrosoarchaeum koreensis* MY1[4]	*Nitrosopumilus maritimus* SCM1[5]	*Nitrosotealea devanaterra* Nd1[6]	*Nitrososphaera viennensis* EN76[7]
Cluster	I.1a	I.1a	I.1a	I.1a	I.1a	I.1a	I.1a-associated	I.1b
Habitat	freshwater aquarium	hot spring	WWTP	estuary	soil	marine aquarium	acidic soil	garden soil
Genome size (Mb)	1.70	1.65	1.62	1.86	1.61	1.65	1.81	2.53
GC (%)	42.2	42.3	41.0	32.5	32.7	34.2	37.1	52.7
Total genomic objects	2088	1999	1955	2632	2000	2012	2144	3267
Protein-coding genes	2047	1958	1911	2589	1957	1976	2106	3128
Coding density (%)	92.2	90.4	91.9	87.2	89.9	91.7	90.6	86.4
5S, 16-23S rRNA	1,1	1,1	1,1	1,1	1,1	1,1	1,1	1,1
tRNA	38	38	40	38	38	40	37	39
amoA, *amoB*, *amoC*	1,1,1	1,1,1	1,1,1	1,1,1	1,1,1	1,1,1	1,1,1	1,1,3
nitrite reductase (*nirK*)	+	+	+	+	+	+	+	+
Ammonium transporters	2	2	2	2	2	2	3	3
Urease + accessory proteins	+	-	+	-	-	-	-	+
Urea transporters	-	-	+[a]	-	-	-	-	+
Carbon fixation	3HP/4HB	3HP/4HB	3HP/4HB	3HP/4HB	3HP/4HB	3HP/4HB	3HP/4HB	3HP/4HB
Flagellar proteins	+	+	+	+	-	-	+	+
Chemotaxis proteins	+	+	+	+	-	-	+	+
S-layer associated proteins	+	+	+	+	+	+	+	+
Coenzyme F_{420}	+	+	+	+	+	+	+	+
Cobalamin synthesis	+	+	+	+	+	+	+	+
Short chain PHA synthesis (*phaC*/*phaE*)	+	+	+	+	+	+	+	+
Dicarboxylate transporter (SdcS)	+	+	-	-	-	+	-	-
Citrate transporter	+	-	-	+	+	-	-	-
Amino acid/oligopeptide transport	+	+	+	+	+	+	+	+

[a]truncated
[1]Lebedeva *et al.*, 2013, [2]Li *et al.*, 2016, [3]Blainey *et al.*, 2011, [4]Kim *et al.*, 2011, [5]Walker *et al.*, 2010, [6]Lehtovitra-Morley *et al.*, 2016, [7]Stieglemeir *et al*, 2014

Ca. N. aquariensis encodes both subunits (*phaC*; NAQ_v2_0369, *phaE*; NAQ_v2_0370) of the heterodimeric enzyme poly(R)-hydroxyalkanoic acid synthase (class III), which is a key enzyme for the synthesis of short-chain-length polyhydroxyalkanoates (PHAs). PHAs are aliphatic polyesters produced by many bacteria and some archaea that are used for storage of energy and carbon (Anderson and Dawes, 1990; Lee, 2000). PHA synthase genes are broadly distributed across thaumarchaeotal genomes (Table 3.1; Spang *et al.*, 2012; Zhalnina *et al.*, 2014) and production of PHA has been observed experimentally in *N. gargensis* and *N. viennensis* using Raman spectroscopy (Spang *et al.*, 2012). Although a wide variety of bacteria produce PHAs, only halophilic *Euryarchaeota* (Poli *et al.*, 2011) and *Thaumarchaeota* are known to produce PHAs within the *Archaea*. These compounds could present a useful source of energy and carbon during times of ammonia starvation.

Ca. N. aquariensis encodes genes for synthesis of the polyamines spermine (NAQ_1931) and spermidine (NAQ_0236). Polyamines are positively charged organic polycations containing multiple amine groups, the most common of which are spermidine, spermine, and putrescine (Tabor and Tabor, 1985). Genes encoding for spermine and/or spermidine synthase are also present in some thaumarchaeotal representatives, including *N. gargensis*, *N. viennensis*, *Ca*. N. evergladensis, and *Ca*. N. uzonensis. All available AOA genomes encode putrescine biosynthesis from agmatinase (*speB*; NAQ_0259) and encode deoxyhypusine synthase, which produces the amino acid hyphusine from spermidine, suggesting a widespread role for polyamines in AOA. Polyamines are involved in a wide variety of biological processes in plants, fungi, and bacteria, including nucleic acid and protein synthesis, stabilizing membranes, and stimulating several enzymes, especially those involved in stress response (Abraham, 1968; Tabor and Tabor, 1985; Frydman *et al.*, 1992; Huang *et al.*, 1990; Jantaro *et al.*, 2003; Alcázar *et al.*, 2006). In addition to these biological processes, polyamines can provide a source of carbon, nitrogen, and energy to heterotrophic bacteria (Höfle, 1984), and it has recently been suggested that marine AOA enrichment cultures can oxidize putrescine and other polyamines directly to nitrite (Hollibaugh *et al.*, 2015). In addition to polyamine synthesis genes, *Ca*. N. aquariensis encodes the PotABCD system for import of polyamines (*e.g.*, spermidine/putrescine), a polyamine uptake system that has been identified in *Escherichia coli*, cyanobacteria, yeast, and several marine bacterial groups (Incharoensakdi *et al.*, 2010; Igarashi and Kashiwagi, 1999; Mou *et al.*, 2010).

Interestingly, genes encoding this system were not detected in any other AOA genomes. These genes in *Ca*. N. aquariensis include a *potA* homolog (NAQ_1601), which functions as an ATP binding region, and *potBC* (NEX_1600), which appears to have arisen from the fusion of *potB* and *potC*. In addition, there is an adjacent gene encoding an extracellular solute binding protein (NEX_1599), which is the function of *potD*. Although this gene shares little homology with the bacterial *potD*, it likely performs the same role given its location and predicted function. The ability to import exogenous polyamines could provide an advantage in reducing the energy expenditure needed to synthesize them, or even provide an alternate source of energy, nitrogen, or carbon.

3.3.2.2 *Ca*. N. aquariensis gene clusters of interest

The genome of *Ca*. N. aquariensis contains a region consisting of approximately 34 open reading frames (ORFs) that has a sudden shift in G+C content compared to the rest of the genome (R1; Fig. 3.6A). This observed change in G+C content coincides with a sharp break in synteny with related AOA, and the majority of genes contained within this region have little or no homology to genes in other AOA genomes. This region contains several genes related to restriction-modification systems, including restriction endonucleases, components of Type I restriction-modification systems (M subunit, S subunit), ATPases, and several DNA methyltransferases (Fig. 3.8). One cluster of four ORFs encoding a Type I restriction-modification system is shared by *N. viennensis* and *N. maritimus*, but none of the other genes in this segment share high homology to genes in AOA. In addition to this restriction-modification system, *Ca*. N. aquariensis encodes BseR1, a Type IIS restriction endonuclease discovered in *Bacillus* species (Mushtaq *et al.*, 1993). Given the abrupt change in synteny and nucleotide characteristics, this segment of DNA was identified as one that potentially arose from horizontal gene transfer (HGT; Lawrence and Ochman, 2002; Ravenhall *et al.*, 2015). Many accessory genes acquired by HGT form discrete regions called genomic islands, and acquiring these DNA segments contributes to the diversification and adaption of microorganisms (Juhas *et al.*, 2009). This segment of DNA in *Ca*. N. aquariensis contains several hallmarks of genetic islands: it is flanked by a tRNA gene, contains integrase genes and direct repeats, contains several phage-related genes, and encodes a cluster of genes performing a related function (Fig. 3.8; Juhas *et al.*, 2009). Given these

characteristics and its absence in related AOA this segment of DNA was likely acquired by HGT.
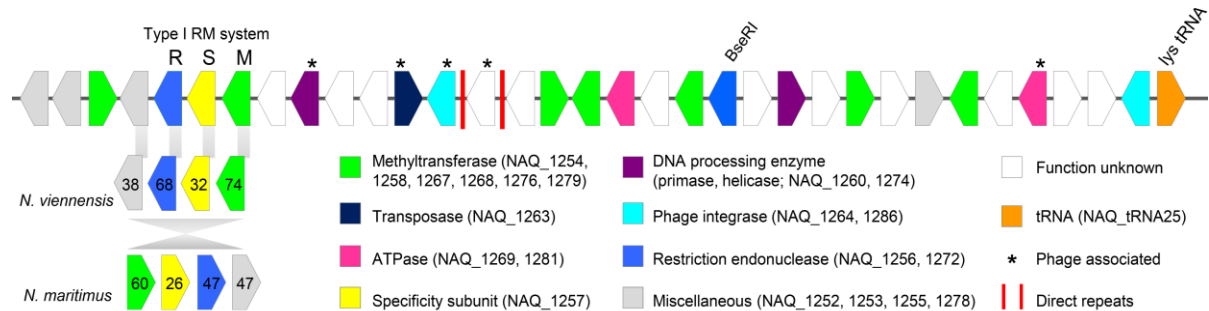
Figure 3.8 Schematic of genetic defense island in *Ca*. N. aquariensis genome. ORFs on forward and reverse strands are indicated by arrow direction. ORFs are not drawn to scale. Numbers inside arrows represent percent (%) amino acid identity to *Ca*. N aquariensis proteins. Gene locus tags are indicated for each category. See Table B2 for full descriptions of all genes shown.

The *Ca*. N. aquariensis genome encodes a second region with an abrupt change in G+C content, which is located relatively close to the genomic island described above (R2, Fig. 3.6). In addition to demonstrating disparate nucleotide frequencies, this region begins with a tRNA and harbours genes of related function, but lacks other signatures of genomic islands (Fig. 3.9). In addition, several genes in this region are homologous to genes found in other AOA, although the overall synteny is very low. This region contains approximately 50 ORFs, many of which encode genes related to glycosylation (Fig. 3.9). For example, this region contains several epimerase, isomerase, and dehydratase enzymes related to nucleotide-sugar metabolism, as well as several glycosyltransferases, methyltransferases, and nucleotidyltransferases. In particular, this genome segment suggests that *Ca*. N. aquariensis synthesizes nonulsonic acids for protein glycosylation, most likely pseudaminic acid (encoded by *pse* genes) or sialic acid (N-acetyl-neuraminic acid, encoded by *neu* genes; Fig. 3.9). Nonulsonic acids are nine-carbon compounds that are widely distributed in biological tissues and often found on glycoproteins. Genes encoding sialic acid synthesis (*neuB*) and *N*-acylneuraminate cytidylyltransferase (*neuA*), two of the key genes in sialic acid synthesis, are

both present in this gene cluster (Fig. 3.9). A nearby phosphoglucose/phosphomannose isomerase could function as *neuC* in the final step of sialic acid synthase. In addition, a polysaccharide biosynthesis protein in this cluster is homologous to *kpsS*, which functions as an export protein for sialic acid.
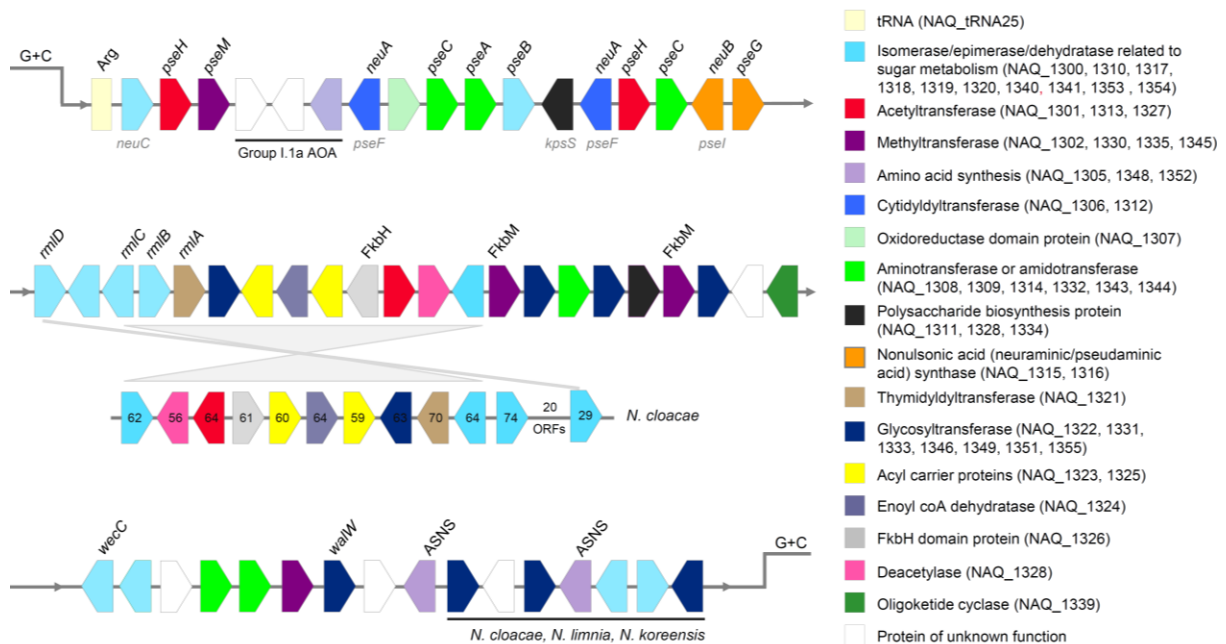
Figure 3.9 Schematic of glycosylation-related genomic segment in *Ca*. N. aquariensis. ORFs on forward and reverse strands are indicated by arrow direction. ORFs are not drawn to scale. Gene groups with lines below are homologs of indicated genes in conserved order in the organisms indicated. Where available, specific gene names are noted above ORFs. Gene names shown in grey below an ORFs indicate a potential alternate role based on predicted function and/or homology. The largest conserved region within this DNA segment was a 12-ORF region in *Ca*. N. cloacae. Numbers in *Ca*. N. cloacae ORFs represent percent amino acid identity to homologues in *Ca*. N. aquariensis. *Pse* genes encode for proteins involved in pseudaminic acid biosynthesis. *Neu* and *kps* genes encode for proteins involved in neuraminic acid synthesis. Fkb proteins are involved in polyketide synthesis. *Rml* genes are involved in rhamnose synthesis. Annotations for all genes shown are available in Table B3.

Biosynthesis of pseudaminic acid has commonalities with sialic acid. For example, the key synthase protein (NeuB or PseI) performs a condensation reaction with phosphoenolpyruvate to create pseudaminic or sialic acid from sugar precursors. In addition to PseI, this genomic region in *Ca*. N. aquariensis encodes all proteins necessary for the biosynthesis of pseudaminic acid from UDP-N-acetylglucosamine. Briefly, these include PseB (a sugar isomerase/dehydratase), PseC (an aminotranferase), PseH (an acetyltransferase), and PseA, (an amidotransferase). PseG is also encoded, but its function is unknown. The role of PseF (a cytidylyltransferase) could be fulfilled by either of the nearby cytidylyltransferases, which are currently annotated as *neuA*. In addition to the genes located in this gene cluster, two trans-sialidase genes are also present in the *Ca*. N. aquariensis genome (NAQ_0881, 0882), which could be involved in transporting synthesized nonulsonic acids to their final destination.

Several bacterial surface proteins and flagellins are modified with various glycan groups, including derivatives of nonulsonic acids (Logan, 2006; Nothaft and Szymanski, 2010). For example, pseudaminic acid is added to the flagella of *Helicobacter pylori* and *Campylobacter jejuni* as a post translational modification (Thibault *et al.*, 2001; Josenhans *et al.*, 2002; Schirm *et al.*, 2003; Schoenhofen *et al.*, 2006; McNally *et al.*, 2006). In addition, the pili of *Pseudomonas aeruginosa* can be glycosylated with derivatives of pseudaminic acid (Castric *et al.*, 2001). In these organisms, glycosylation of flagella or pili is considered a virulence factor and is necessary for successful pathogenesis. In addition, sialic acid is used by some Gram-positive bacteria for glycosylation of outer spore coats (Bliss and Silver, 1996) and for production of polysialic acid capsules (Driks, 1999).

Synthesis of nonulsonic acids for S-layer glycosylation was previously suggested for *Ca*. N. devanaterra (Lehtovirta-Morley, Sayavedra-Soto, *et al.*, 2016). Several genes involved in production of nonulsonic acids were identified, and based on the spatial arrangement of these genes next to the major S-layer protein, it was suggested that their function was S-layer glycosylation. Homology and synteny of nonulsonic acid synthesis genes is low between *Ca*. N. aquariensis and *Ca*. N. devanaterra, but it is plausible that overall functions are similar. In *Ca*. N. aquariensis, genes for glycosylation were not localized with S-layer proteins, and it is possible that either S-layers or observed flagella (or both) are glycosylated with nonulsonic acids. S-layers are present in the majority of archaea

and often possess carbohydrate chains covalently N-linked to asparagine residues (Schneitz *et al.*, 1993). However, glycosylation of S-layers with nonulsonic acids has not previously been observed in the *Euryarchaeota* or *Crenarchaeota* (Albers and Meyer, 2011; Calo *et al.*, 2010).

Glycoproteins have a wide variety of demonstrated functions, such as increasing protein stability and rigidity, acting as virulence factors, cellular signalling, and adhesion to surfaces (Sára and Sleytr, 2000; Larkin and Imperiali, 2011). In *Lactobacillus acidophilus*, the S-layer is responsible for the adhesion of the bacterial cells to the intestinal epithelium (Schneitz *et al.*, 1993). Therefore, it is possible that glycosylation could contribute to the ability of *Ca*. N. aquariensis to adhere to surfaces, an adaptation that would confer an ecological advantage in the biofilm environment from which it originates. Cell envelopes of microorganisms are diverse and strongly reflect adaptations to their environments. Therefore, future research investigating the glycomes of *Ca*. N. aquariensis and other AOA would be useful in further understanding the ecology of these organisms.

Overall, the R2 gene cluster (Fig. 3.9) shares little synteny with available AOA genomes. However, one 11-ORF region within this low G+C region is shared with *Ca*. N. cloacae with a nearly identical gene order. This gene cluster has several hallmarks of polyketide synthesis (Shen, 2003), including acyl carrier proteins (ACPs), acyl transferases, methyltransferases (FkbM domain), an FkbH domain protein (which belongs to polyketide synthases; PKS), an enoyl hydratase, and a polyketide cyclase with a thioester domain (Fig. 3.9, Table B3). Polyketides are secondary metabolites that form the underlying structure of several anticancer agents and antibiotics, particularly macrolides such as streptomycin (Gomes *et al.*, 2013). The FkbH domain homologue was originally identified in the ansamitocin (FK520) biosynthetic cluster of *Streptomyces hydroscopicus*, and has since been found in many PKS enzymes, although its exact function remains unknown (Wu *et al.*, 2000; Carroll *et al.*, 2002). FkbM is required for methylation in the biosynthesis of the immunosuppressant FK506 in *Streptomyces* strain MA6548 (Motamedi *et al.*, 1996). This cluster encoding polyketide biosynthesis-related genes is preceded by *rml* genes, which are associated with the biosynthesis of rhamnose and participate in a variety of biosynthetic pathways. For example, *rml* genes are involved in the production of rhamnolipids, which are glycolipids with glycosyl head groups (rhamnose) and fatty acid tails. Rhamnolipids are

produced by *Pseudomonas aeruginosa* and display antimicrobial activity against Gram-positive organisms (Abdel-Mawgoud *et al.*, 2010). Genes encoding rhamnose production are also involved in general nucleotide sugar metabolism and, interestingly, *rml* genes participate in surface glycosylation in a variety of pathogens, including *Salmonella*, *Shigella*, *Burkholderia*, and *Streptococcus* (Graninger *et al.*, 1999). In addition, *rml* genes are involved in pathways for polyketide sugar unit biosynthesis, and the biosynthesis of antibiotics such as vancomycin and streptomycin. For example, the *rmlABCD* cluster encodes all major proteins needed for the production of the streptose moiety of streptomycin (KEGG map 00521; Kanehisa and Goto, 2000). Given the location of these genes in between those encoding nonulsonic acids and polyketides (Fig. 3.9), it is unclear in which process they participate. However, because these genes belong to the cluster conserved in *Ca*. N. cloacae, it is likely that they function with polyketide synthesis-related genes. The presence of these genes suggests that *Ca*. N. aquariensis may synthesize secondary metabolites that can be used for defense. To date, few antimicrobial compounds produced by archaea ("archaeocins") have been discovered. The vast majority of archaeal antimicrobials are ribosomally synthesized proteins (Besse *et al.*, 2015), although polyketide synthesis pathways have been identified in archaeal genomes (Wang *et al.*, 2014). In addition to ecological benefits for *Ca*. N. aquariensis, archaeal polyketide compounds could represent a source of industrially and medically relevant products.

3.3.2.3 Whole genome comparisons

Overall, the *Ca*. N. aquariensis genome displays a high degree of conserved genome order with other Group I.1a *Thaumarchaeota*, especially the *Nitrosotenuis* representatives *Ca*. N. cloacae and *Ca*. N. uzonensis (Fig. 3.10A, B). Compared to *Ca*. N. cloacae, there is an apparent inversion of a large proportion of the genome (Fig. 3.10A), and compared to marine representative *N. maritimus*, the majority of the genome sequence runs antiparallel (Fig. 3.10C). Conversely, very low genome synteny was observed with Group I.1b representative *Nitrososphaera viennensis* (Fig. 3.10D), which is consistent with a more distant phylogenetic relationship (Fig. 3.4). In addition to conserved gene order, *Ca*. N. aquariensis shares the majority of its genes with other AOA. When compared with other members of the *Nitrosotenuis* genus, the core genome consisted of 1378 gene families and

the pan genome consisted of 2607 gene families (Fig. 3.11A). Among the *Nitrosotenuis* genomes included, *Ca*. N. aquariensis had 323 unique gene families, comprising ~17% of its total genes. When additional *Thaumarchaeota* were included in the analysis that were more distantly related to *Ca*. N. aquariensis (including marine representative *N. maritimus* and soil representative *N. viennensis*), the pan genome increased to 5241 gene families (largely due to unique families in the *N. viennensis* genome), and the core genome was reduced to 736 gene families (Fig. 3.11B).
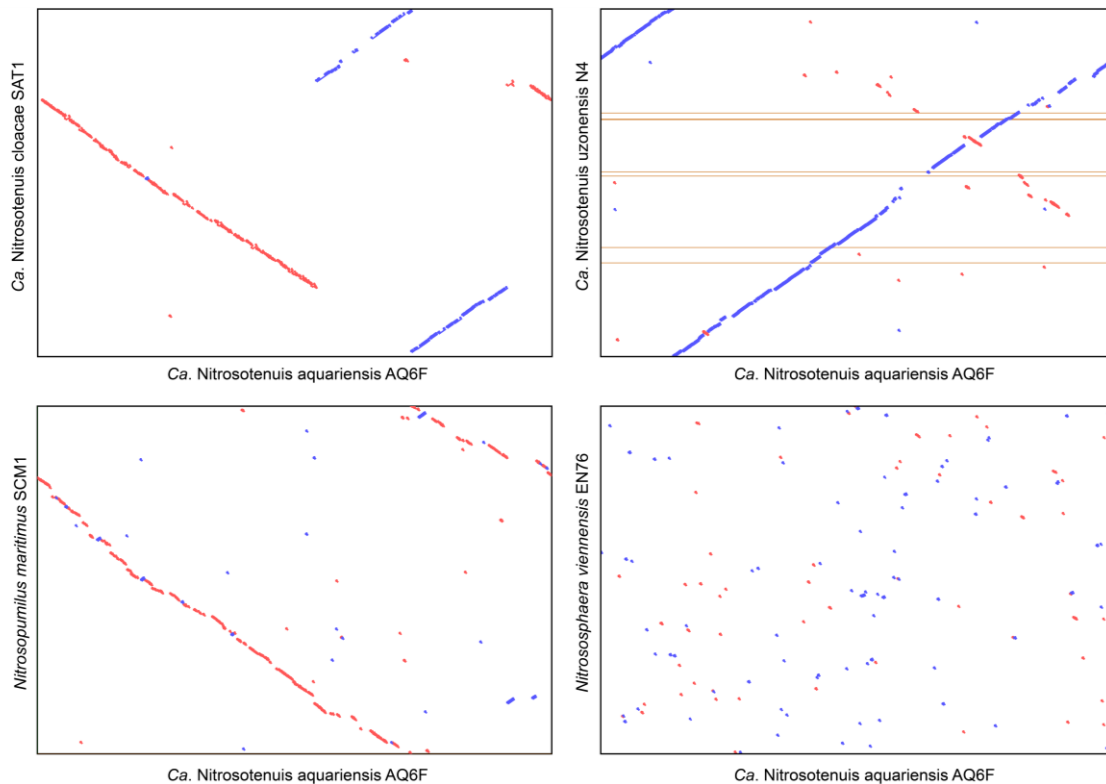
Figure 3.10 Dot plots of pairwise genome alignments of *Ca*. N. aquariensis and selected Group I.1a AOA. Each dot indicates a match between two genome sequences; red and blue dots represent matches on parallel and antiparallel strands, respectively. Horizontal lines indicate contigs of unclosed genomes. Plots were generated using PROmer (within IMG ER), with alignments performed using six frame amino acid translations of the input DNA sequence.
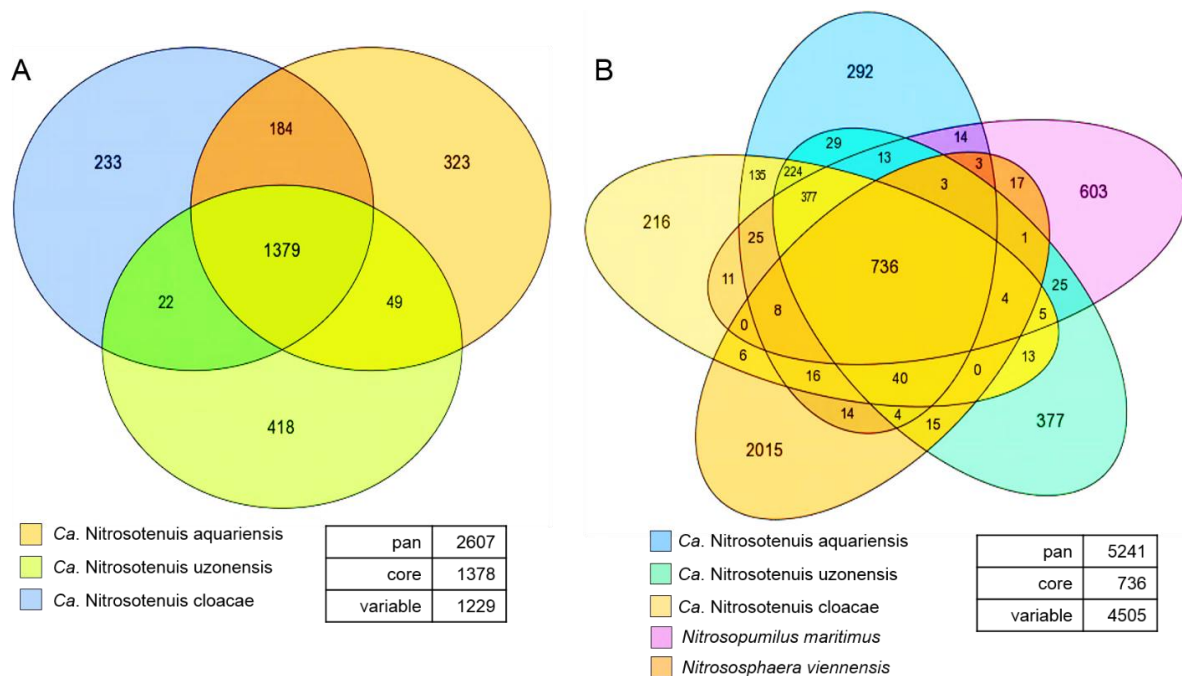
Figure 3.11 Pan-core genome analysis of *Ca*. N. aquariensis and other AOA representatives, including A) *Nitrosotenuis* lineage genomes and B) *Nitrosotenuis* genomes with marine and soil representatives. Circles are not drawn to scale. Core genomes consist of gene families shared by all genomes (centre) whereas variable genomes are either shared by ≥ 2 genomes, or are species-specific (periphery). The pan-genome is the sum of core and variable genomes. Gene family clustering is based on 50% amino acid identity and 80% alignment coverage.

Average nucleotide identity (ANI) and average amino acid identity (AAI) values demonstrated that *Ca*. N. aquariensis is most closely related to *Ca*. N. cloacae with an ANI and AAI of 79.1% and 82.7%, respectively (Table 3.2). The close evolutionary relationship of these organisms is also supported by phylogenetic analyses of *amoA* gene sequences (Fig. 3.4). ANI values below approximately 75% are considered untrustworthy, and when ANI values are in the range of 75-80%, it is recommended that AAI values be used instead (Rodriguez and Konstantinidis, 2014; Rodriguez and Konstantinidis, 2016). Given that all calculated ANI values were below 80%, AAIs were calculated between *Ca*. N. aquariensis and other Group I.1a *Thaumarchaeota*. ANI values offer the best resolution between closely related species, but AAI values are more useful for more distantly related organisms. Next to *Ca*. N. cloacae, *Ca*. N. aquariensis shared the highest AAI with *Ca*. N. uzonensis, at 73.0%, which is also supported by *amoA* phylogenetic relationships (Fig.

3.4). AAI values between *Ca*. N. aquariensis and all other tested Group I.1a *Thaumarchaeota* were all approximately 63%. Both ANI and AAI values offer better resolution than the 16S rRNA gene and show higher correlations with DNA-DNA hybridization values (Konstantinidis and Tiedje, 2005a, 2005b). Microorganisms sharing ANI values above 94-95% are considered to belong to the same species (Konstantinidis and Tiedje, 2005a; Goris *et al.*, 2007). The 70% DNA-DNA reassociation threshold, which has been used as a criterion for species delineation since the 1980s (Moore *et al.*, 1987) corresponds to an AAI of 95-96% (Konstantinidis and Tiedje, 2005b). Based on the species criteria for both ANI and AAI values, *Ca*. N. aquariensis represents a unique species within the genus *Nitrosotenuis*.

Table 3.2 ANI and AAI values for *Ca*. N. aquariensis with selected *Thaumarchaeota*

Organism	ANI (%)	AAI (%)
Ca. Nitrosotenuis cloacae SAT1	79.1	82.7
Ca. Nitrosotenuis uzonensis N4	75.2	73.0
Ca. Nitrosotenuis chungbukensis MY2	75.3	nd
Ca. Nitrosopumilus sediminis AR2	74.6	62.4
Nitrosopumilus maritimus SCM1	74.6	62.8
Ca. Nitrosoarchaeum limnia SFB1	75.0	62.4
Ca. Nitrosoarchaeum limnia BG20	76.3	62.8
Ca. Nitrosoarchaeum koreensis MY1	75.3	62.9

ANI: average nucleotide identity, AAI: average amino acid identity
nd: not determined

3.3.3 Ammonia-oxidizing activity of aquarium filter biomass

Previous studies demonstrated that AOA outnumber AOB in freshwater aquarium biofilters, and that AOB are often below detection limits in these environments (Hovanec and DeLong, 1996; Sauder *et al.*, 2011; Bagchi *et al.*, 2014). However, questions remain regarding the activity of detected AOA in aquarium biofilters. Several studies have linked active nitrification with AOA detected in the environment (Wuchter *et al.*, 2006; Gubry-Rangin *et al.*, 2010; Zhang *et al.*, 2012; Yan *et al.*, 2012; Alves *et al.*, 2013), but others have warned that the presence of AOA, even in high abundance, does not indicate ammonia-

oxidizing activity (Mussman *et al.*, 2011; Sterngren *et al.*, 2015). In the present study, *Ca*. N. aquariensis was enriched from a freshwater aquarium biofilter using ammonia as a sole energy source, and its genome supported chemolithoautotrophy as the primary mode of metabolism, providing support for the suggestion that AOA contribute to nitrification in aquarium biofilters. To assess activity *in situ*, biofilm material from the freshwater aquarium biofilter from which *Ca*. N. aquariensis originated was incubated in aquarium water supplemented with ammonia to assess the effect of differential inhibitors on ammonia-oxidizing activity.

To ensure that nitrification inhibitors worked as expected on *Ca*. N. aquariensis-like AOA, enrichment culture samples were incubated with PTIO and octyne, specific inhibitors of AOA and AOB, respectively. Ammonia-oxidizing activity of *Ca*. N. aquariensis was strongly inhibited by 10 µM PTIO, and completely by 30 µM PTIO (Fig. 3.10A), consistent with previous reports (Shen *et al.*, 2013; Martens-Habbena *et al.*, 2015; Sauder *et al.*, 2016). In contrast, octyne was not inhibitory below 15 µM, and was not strongly inhibitory below 30 µM (Fig. 3.12B), indicating that lower ranges (*e.g.*, <10 µM) are appropriate for specific inhibition of AOB, as reported previously (Taylor *et al.*, 2013, 2015).
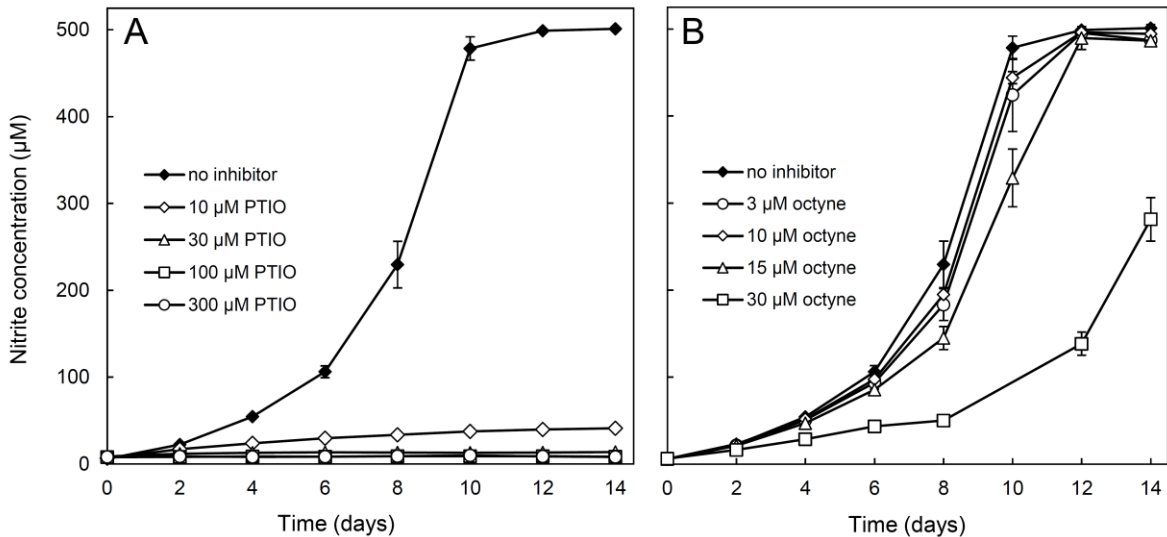
Figure 3.12 Ammonia-oxidizing activity of *Ca*. N. aquariensis with nitrification inhibitors, including A) PTIO and B) octyne. Error bars represent the standard error of the mean from biological triplicates. Error bars not seen are contained within the symbols.

Incubations of biomass from an aquarium were set up at two time points. At the first time point, the aquarium had been established for approximately six years, and a previous study demonstrated that ammonia oxidation and numerical dominance of AOA was stable over time (Sauder *et al.*, 2011). When incubated in aquarium water supplemented with 0.5 mM NH$_4$Cl, aquarium sponge filter biomass depleted all supplied ammonia within approximately two days in the absence of inhibitors (Fig. 3.9A). Conversely, killed biomass controls showed no ammonia depletion during the incubation period, indicating that ammonia depletion was a result of biological activity. Strong inhibition of ammonia oxidation by aquarium filter biomass was observed in conditions containing 200 µM PTIO. At the time point of ammonia depletion (2 days), ~85% of the ammonia remained in the PTIO incubations (compared to initial ammonia concentrations and the killed biomass control). PCR screens of genomic DNA extracted from the biofilm showed strong archaeal *amoA* and 16S rRNA gene signals, and no bacterial *amoA* signal (data not shown). Taken together, these results suggest that AOA are responsible for the majority of ammonia oxidation occurring in this aquarium sponge biofilter. One limitation of these data is that octyne conditions were not tested at this time point and, ideally, demonstration of opposite effects of inhibitors of AOA and AOB would provide the strongest support for contributions to activity. Moreover, the use of acetylene for specific inhibition of prokaryotic nitrification is a preferable control to killed biomass. Therefore, a similar experiment was set up at a later point to include these conditions.

At the second time point, the fish and filter had been transferred to London, Ontario for a period of eight months, then reassembled and some fish were re-introduced. At the time of sampling for this experiment, the aquarium had been fully re-established for approximately six months. Collected filter biomass from this time point was incubated with PTIO, octyne, and acetylene, in addition to a no-inhibitor control. Incubation of biomass in aquarium water supplemented with 0.5 mM NH$_4$Cl resulted in total depletion of ammonia within approximately two days in the absence of inhibitors (Fig. 3.13B), which was similar to the time required to deplete 0.5 mM ammonia by biomass at the first time point (Fig. 3.13A). As expected, acetylene amendment resulted in complete inhibition of ammonia oxidation (Fig. 3.13B). Supplementation with both PTIO and octyne resulted in partial inhibition of

ammonia oxidation (Fig. 3.13B). At the closest time point to ammonia depletion (1.75 days), ~50% of the ammonia remained in the PTIO condition, whereas approximately 40% of the ammonia remained in the octyne condition. PTIO inhibited ammonia oxidation to a lesser extent than in the first time point, but octyne incubations were not available in the first time point for comparison.
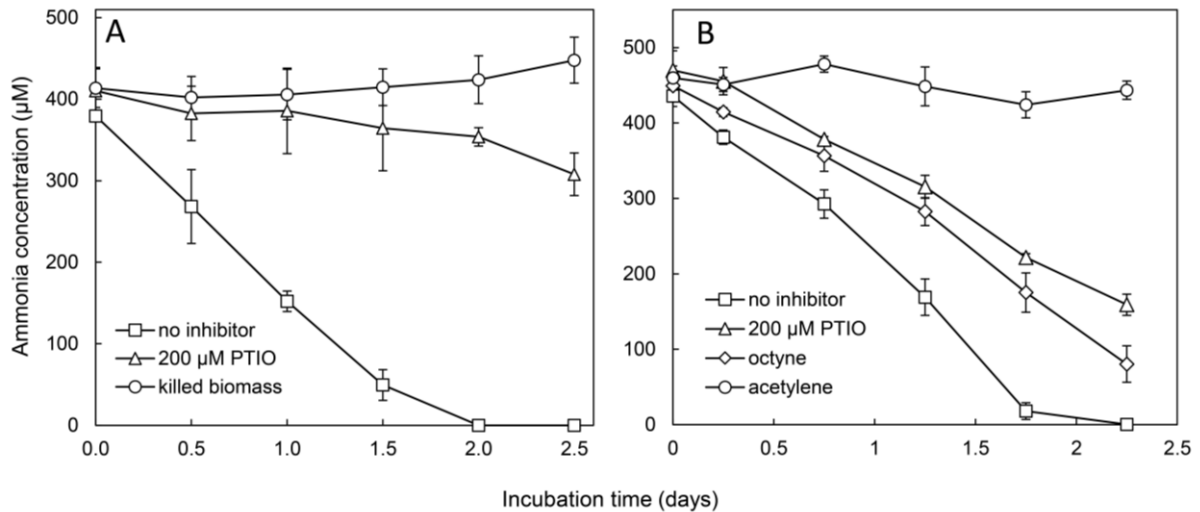
Figure 3.13 Ammonia-oxidizing activity of aquarium sponge filter biomass with nitrification inhibitors A) in an established aquarium biofilter, and B) in the same aquarium biofilter after being decommissioned and re-established. Error bars represent the standard error of the mean from biological triplicates. Error bars not seen are contained within the symbols.

These results provide support for the hypothesis that AOA contribute substantially to ammonia oxidation, but indicate that octyne-sensitive organisms also contribute. PCR screens for genomic DNA extracted from biomass yielded strong signals with archaeal *amoA* primers, indicating that the AOA were present in the newly set up aquarium and supported substantial inhibition by PTIO. Interestingly, no AOB *amoA* genes were detected in the biofilm from this time point, even when the annealing temperature was reduced from 60°C (Rotthauwe *et al.*, 1997) to 55°C (data not shown). It is possible that AOB were present below detection limits, or that AOB representatives with divergent *amoA* genes were not detected by available primers. Alternatively, it is possible that completely nitrifying

84

("comammox") bacteria (van Kessel *et al.*, 2015; Daims *et al.*, 2015) contributed to ammonia oxidation in these experiments. The inhibitor profiles of these recently discovered bacteria are unknown, and molecular tools for detecting comammox in DNA extracts are not yet available. Given that comammox ammonia monooxygenase enzymes are related to those found in AOB (Daims *et al.*, 2015), it is likely that their inhibitor profiles more closely resemble those observed in AOB than those observed in AOA. Although aquarium biofilters are vigorously aerated, the biofilm environment formed on media surfaces would provide zones of low oxygen, which are believed to be preferred by both comammox (van Kessel *et al.*, 2016) and AOA (Park *et al.*, 2006, 2010; Yan *et al.*, 2012). It is therefore plausible that the portion of inhibition resulting from octyne supplementation resulted from commamox organisms of the genus *Nitrospira*.

3.4 Conclusions

This study reports the cultivation and complete genome sequence of *Ca*. N. aquariensis, a mesophilic ammonia-oxidizing archaeon that originates from a freshwater aquarium biofilter and belongs to the *Nitrosotenuis* lineage of the *Thaumarchaeota*. *Ca*. N. aquariensis grows chemolithoautotrophically using ammonia as a sole source of energy and bicarbonate as a sole source of carbon, and its genome encodes genes for ammonia oxidation and bicarbonate fixation, supporting autotrophic ammonia oxidation as a primary lifestyle. Although *Ca*. N. aquariensis cells can become relatively long, they remain consistently thin, which maintains a high surface area to volume ratio. *Ca*. N. aquariensis encodes chemotaxis and flagellar genes, and appendages are present on the cell surface, indicating that the cells are likely motile. The genome encodes several genes for protein glycosylation, which could affect flagella or S-layer proteins, and may promote enhanced adhesion ability. The ability to adhere to surfaces would be ecologically advantageous when living in a biofilm environment that is subject to constant flowing water, such as that of an aquarium biofilter.

Incubations of biofilter sponge biomass from the freshwater aquarium from which *Ca*. N. aquariensis originates demonstrate that AOA contribute to ammonia oxidation *in situ*. Addition of PTIO inhibits at least 50% of ammonia oxidation, and up to 85% in a long-established aquarium biofilter. This study presents first evidence that AOA contribute to

ammonia oxidation in freshwater aquarium biofilters, and supports the previously reported numerical dominance of AOA in freshwater aquarium biofilters (Sauder *et al.*, 2011; Bagchi *et al.*, 2014). This work further suggests that, contrary to common belief in the aquarium industry, AOB are likely not primarily responsible for ammonia oxidation in aquarium biofilters. Laboratory cultures of AOA from freshwater aquaria, such as *Ca*. N. aquariensis, are useful for future investigations of the ecology of freshwater AOA and may have practical applications in aquarium and aquaculture operations, given that all available products are AOB-based supplements.

Chapter 4

Low ammonia niche of ammonia-oxidizing archaea in rotating biological contactors of a municipal WWTP[3]

4.1 Introduction

Ammonia is a waste product in industrial and municipal wastewater that threatens aquatic ecosystems with toxicity, oxygen depletion, and algal blooms. A primary objective of wastewater treatment is to prevent these adverse environmental impacts by removing ammonia from wastewater prior to discharge into receiving waters. Ammonia removal in wastewater treatment is accomplished by promoting nitrification, a microbially mediated process in which ammonia is oxidized to nitrite and subsequently to nitrate. WWTPs may release nitrate-rich effluents, or nitrate may subsequently be anaerobically converted to nitrogen via anaerobic ammonia oxidation (anammox) or denitrification prior to effluent discharge. Both AOA and AOB have been detected in WWTPs based on associated gene sequences (Park *et al.*, 2006; Limpiyakorn *et al.*, 2011, 2013; Mussman *et al.*, 2011; Bai *et al.*, 2012), but factors that determine whether AOA or AOB dominate remain unclear.

Recent studies suggest that ammonia availability influences niche separation of AOA and AOB. Kinetic studies of the AOA isolate *Nitrosopumilus maritimus* demonstrate an exceptionally high substrate affinity for ammonia; *N. maritimus* has a half saturation constant (K_m) of 0.133 µM total ammonia (Martens-Habbena *et al.*, 2009), which is approximately two orders of magnitude lower than that of *Nitrosomonas oligotropha*, for which reported K_m values range from 30 to 75 µM total ammonia (Stehr *et al.*, 1995). As a result of this high substrate affinity and the high relative abundance of AOA in oligotrophic environments, ammonia availability has been suggested to be an important factor in determining niche partitioning of AOA and AOB (Erguder *et al*., 2009; Schleper, 2010). Studies of soil AOA support this observation by demonstrating that AOB are numerically and metabolically

dominant in ammonia-amended soils (Jia and Conrad, 2009; Di *et al*., 2010; Taylor *et al*., 2010; Verhamme *et al*., 2011). However, few studies have examined the role of ammonia availability in determining relative abundances of AOA and AOB in freshwater aquatic environments, especially those in engineered water treatment systems.

This study utilized existing nitrification infrastructure in a municipal WWTP in Guelph, Ontario, Canada to investigate the effect of ammonia concentrations on the abundance and diversity of prokaryotic ammonia-oxidizing communities. The Guelph WWTP features a tertiary treatment system of rotating biological contactors (RBCs), which are nitrification bioreactors comprised of panels of corrugated polymeric medium (Fig. 4.1A) attached to a central rotating shaft and partially submerged in wastewater. Eight individual RBC "stages" are arranged in series (Figs. 4.1B and C), with nitrification at each stage creating an ammonia gradient across the RBC flowpath. Although previous studies have detected AOB in nitrifying RBCs through PCR-based methods and microscopy (Egli *et al.*, 2003; Pynaert *et al.*, 2003; Jang *et al.*, 2005), no study has investigated the occurrence, abundance, or diversity of AOA in nitrifying RBCs. I hypothesized that the abundance of AOA would increase across the RBC flowpath, as wastewater becomes increasingly depleted of ammonia.
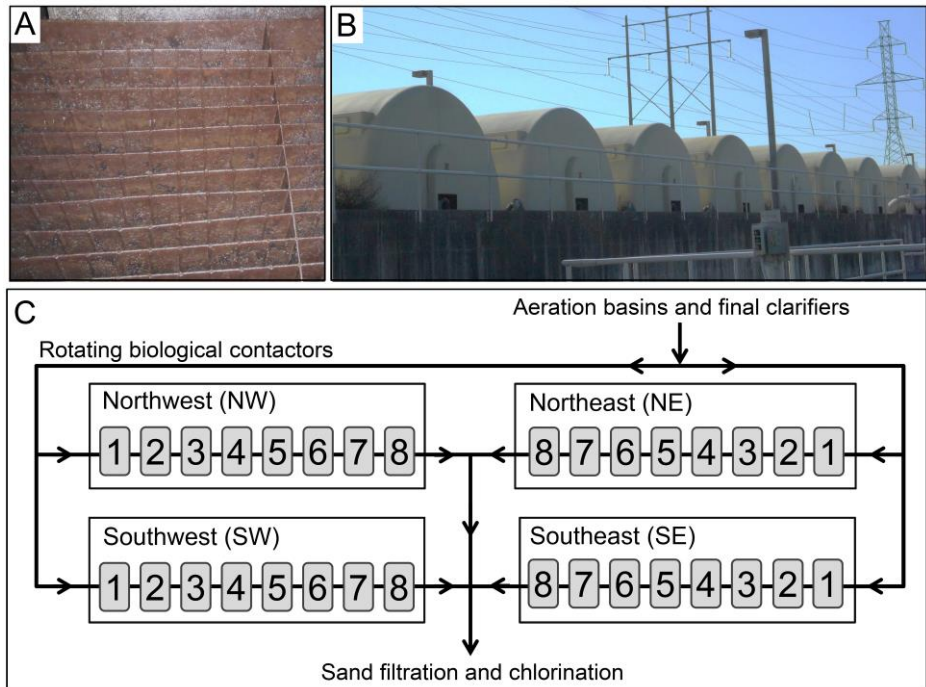
Figure 4.1 Outline of the sampling site in Guelph, Ontario. Internal medium of an RBC stage (A), an external view of a full RBC treatment train (B) and a schematic of the RBC arrangement in the Guelph WWTP (C).

4.2 Materials and methods

4.2.1 Guelph WWTP design, sample collection, and water chemistry analyses

The RBCs in the Guelph WWTP were designed for nitrification and are utilized for tertiary treatment following activated sludge treatment in aeration basins, and prior to sand filtration and chlorination (Fig. 4.1C). The Guelph WWTP features a total of 32 RBC stages arranged in 4 treatment trains, with each train situated in a tank that is 39.5 m in length, 8.0 m in width, and has a water depth of 1.6 m. Each treatment train consists of 8 individual RBC stages which wastewater passes through serially. The total medium surface area per RBC is 13,750 m^2, which results in a combined surface area of 440,000 m^2 (equivalent to >80 football fields). Each RBC is approximately 40% submerged in secondary effluent, and continuous rotation at a velocity of 0.8 to 1.3 rpm is driven by air via centrifugal blowers. The average hydraulic detention time (HDT) across an RBC treatment train is 53 minutes.

Guelph WWTP is a full-scale municipal wastewater treatment plant that serves a population of ~120,000 and treats an average wastewater volume of 42,216 m^3 day^{-1} (based on data from 2010). Samples were collected in February, June, and September 2010. February samples were collected from all stages of the NE treatment train (Fig. 4.1C). In both June and September, all stages of both the NE and SE trains were sampled. Biofilm and RBC-associated wastewater were collected for each RBC stage. Each RBC contains sampling windows, allowing biofilm to be sampled directly from the internal medium surface. Biofilm samples were collected with an ethanol-treated spatula, stored in sterile plastic tubes, and placed on dry ice immediately, where they remained until transferred to -80°C storage. Water samples from each RBC were collected in sterile plastic tubes and stored on ice until return to the laboratory.

Dissolved oxygen (dO_2) and water temperature were measured *in situ* using an HQ30d digital probe (Hach Company, Loveland, Colorado). The pH was measured for all water samples using a DELTA 320 pH meter (Mettler Toledo, Mississauga, Ontario) directly upon return to the laboratory and prior to freezing. All water samples were then stored at -80°C, except samples used for dissolved organic carbon (DOC) measurements, which were filtered (0.22 µm syringe) and stored in the dark at 5°C prior to DOC measurements. DOC was measured using a Dohrman DC-190 High-Temperature TOC Analyzer

(Rosemount Analytical Inc., Santa Clara, CA). Samples were acidified using 20% phosphoric acid and sparged to remove dissolved inorganic carbon (DIC) prior to analysis. Nitrate (NO_3^--N) concentrations were measured by ion chromatography using a Dionex ICS-90 (Dionex Corp., Sunnyvale, CA). Nitrite (NO_2^--N) concentrations were measured by colourimetric analysis using a DU 500 UV/Visible spectrophotometer (Beckman Coulter, Brea, CA). All nitrate, nitrite, and DOC analyses were performed in the Environmental Geochemistry Laboratory, Department of Earth and Environmental Sciences, University of Waterloo. Ammonia (NH_3-N) concentrations were determined fluorometrically, as outlined previously (Holmes *et al.*, 1999), using a TD 700 fluorometer (Turner Designs, Sunnyvale, CA). All ammonia concentrations reported represent total ammonia ($NH_3 + NH_4^+$).

4.2.2 DNA extraction and quantification and quantitative PCR

Genomic DNA was extracted from biofilm samples using the PowerSoil DNA Isolation Kit (Mo Bio Laboratories Inc., Carlsbad, CA) as outlined in the manufacturer's instructions, except beadbeating replaced extended vortexing. Samples were subjected to beadbeating at 5.5 m s^{-1} for 45 s using an FastPrep beadbeater (MP Biomedicals, Santa Ana, CA). Genomic DNA extracts were visualized on a 1% agarose gel by standard gel electrophoresis and quantified spectrophotometrically using a NanoDrop 2000 (Thermo Scientific, Waltham, MA).

Quantification of AOA and AOB *amoA* genes used primers crenamoA23F and a degenerated version of crenamoA616R (Nicol *et al.*, 2008), and amoA-1F and amoA-2R (Rotthauwe *et al*., 1997), respectively. Thaumarchaeotal and general bacterial 16S rRNA genes were quantified using primers 771F and 957R (Ochsenreiter *et al.*, 2003) and 341F and 518R (Muyzer *et al.*, 1993), respectively. All qPCR amplifications were conducted in duplicate on a CFX96 system (Bio-Rad, Hercules, CA). Each reaction volume of 12.6 μl contained 1X iQ SYBR Green Supermix (Bio-Rad), 5 pmol of each primer, 5 μg of bovine serum albumin (BSA) and 1-10 ng of genomic DNA as template. For AOA *amoA* genes, the PCR conditions were 95°C for 3 min followed by 35 cycles of 95°C for 30 s, 53°C for 30 s, and 72°C for 1 min, with a fluorescence reading following each elongation step. For AOB *amoA* genes, PCR conditions were the same, but with an annealing temperature of 58°C. For both thaumarchaeotal and bacterial 16S rRNA genes, PCR conditions were the same but with

an annealing temperature of 55°C and an elongation time of 30 s. Standard curves were constructed using 10-fold serial dilutions of template DNA of known concentration. For all genes, template DNA for standards consisted of PCR amplicons generated from the same primer pair used for qPCR. For AOA and AOB *amoA* and thaumarchaeotal 16S rRNA gene amplicons, the original template source was a freshwater aquarium biofilter (FW27; Sauder *et al.*, 2011). For bacterial 16S rRNA genes, the original template source was *Escherichia coli* genomic DNA.

PCR amplification efficiencies ranged from 80.2% to 98.1% and all R^2 values were greater than 0.99. For all amplification reactions, melt curves were performed from 65°C to 95°C with an incremental increase in temperature of 0.5°C. PCR specificity was verified for all reactions using melt peaks and standard 1% agarose gel electrophoresis.

4.2.3 Lipid extraction and quantification

Biofilm samples were freeze-dried and extracted (3x) using a modified Bligh and Dyer technique (Bligh and Dyer, 1959). A solvent mixture of methanol (MeOH):dichloromethane (DCM):K phosphate buffer at pH 7.4 (2:1:0.8, v/v/v) was added to the sample in a centrifuge tube and placed in an ultrasonic bath for 10 min. The extract was collected after centrifuging the sample at 2500 rpm for 2 min. DCM and phosphate buffer were added to the combined extracts to a new volume ratio of 1:1:0.9 (v/v/v) to achieve phase separation. The organic DCM phase and aqueous MeOH/phosphate buffer phase were separated by centrifuging at 2500 rpm for 2 min. The DCM phase, containing the lipids, was passed over extracted cotton to remove possible remaining particles and collected in a glass tube. The aqueous phase was subsequently rinsed twice with DCM, and all cleaned DCM phases were combined and dried under a N_2 flow and stored at -20°C until analysis.

The extracts were separated into a core lipid (CL) and an intact-polar lipid (IPL) fraction over an activated silica column according to Oba *et al.* (2006) and Pitcher *et al.* (2009), except that hexane:ethyl acetate (1:1, v/v) was used to retrieve the CLs, and MeOH was used to obtain the IPLs. A C_{46} internal glycerol dialkyl glycerol tetraether (GDGT) standard (0.1 µg) was added to the CL fraction and an aliquot of the IPL fraction according to Huguet and coworkers (2006), after which the IPL aliquot was subjected to acid hydrolysis

to cleave all ether-bound and most of the ester-bound headgroups and release their core lipids (IPL-derived GDGTs).

Subsequently, the CL and IPL-derived fractions were dissolved in hexane:isopropanol (99:1, v/v), filtered over a 0.45 µm PTFE filter, and concentrated to ~3 mg mL^{-1} prior to analysis using high performance liquid chromatography (HPLC)/atmospheric pressure chemical ionization (APCI)-MS on an Agilent 1100 series LC/MSD SL according to Schouten et al. (2007), with minor modifications. In short, component separation was achieved with an Alltech Prevail Cyano column (150 mm × 2.1 mm; 3 µm). The GDGTs were eluted isocratically with 90% A and 10% B for 5 min and then with a linear gradient to 16% B for 34 min, where A = hexane and B = hexane:isopropanol (9:1, v/v). The injection volume for all samples was 10 µl. Single ion monitoring of (M+H)$^{+}$-ions was used to detect and quantify the GDGTs. Absolute quantification was performed as described by Huguet et al. (2006), in which a typical analytical standard deviation of 5% was reported.

4.2.4 Denaturing gradient gel electrophoresis (DGGE) and band sequencing

DGGE fingerprinting was performed for AOA and AOB $amoA$ genes, and thaumarchaeotal and general bacterial 16S rRNA genes. DGGE for AOA $amoA$ genes was performed as described previously (Tourna et al., 2008) with minor modifications. The $amoA$ genes were amplified using primers crenamoA23f and a degenerated version of crenamoA616R, and template concentrations ranged from 0.5 ng to 10 ng per reaction. PCR conditions were as described previously, except with an annealing temperature of 53°C. Thaumarchaeotal 16S rRNA genes were amplified using primers 771F and 957R-GC, with amplification and DGGE conditions as outlined previously (Tourna et al., 2008). AOB $amoA$ genes were amplified in a nested PCR approach, using primers amoA-1F and amoA-2R, followed by amoA1F-GC and amoA2R, as outlined by Chu and colleagues (2007). For general bacterial 16S rRNA genes, amplification was performed using primers 341F-GC and 518R, and DGGE was performed as outlined previously (Muyzer et al., 1993; Green et al., 2009).

All gels were run at 60°C and 85 V for 900 minutes, except general bacterial 16S rRNA gels, which were run for 840 minutes. The DGGE system used was a DGGEK-2401 (C.B.S. Scientific Company, Del Mar, CA). Gels were stained with SYBR green (Invitrogen) for 1 h, then scanned using the Typhoon 9400 Variable Mode Imager (GE Healthcare, Piscataway, NJ) or the PharosFX (Bio-Rad). From the original gel images for each gene fragment analyzed, fingerprints were normalized and aligned with GelCompar II (Applied Maths, Austin, TX).

For thaumarchaeotal *amoA* and 16S rRNA genes, DGGE bands were excised, amplified (using the above primers and conditions), and sequenced. Amplified DGGE bands were run on a second gel to ensure that each sequenced band corresponded to the original fingerprint. Because DGGE band sequences arising from thaumarchaeotal 16S rRNA genes were short (<200 bp), a longer thaumarchaeotal 16S rRNA gene sequence was obtained with the archaeal primers 21F (DeLong, 1992) and 957R for the purpose of phylogenetic analysis. The longer sequence encompassed the 158-bp region of the corresponding DGGE band sequence, and the sequences were identical across this span. These DNA sequences have been deposited in GenBank under accession numbers JN695686 and JN695687 for *amoA* and 16S rRNA genes, respectively.

Sequences for thaumarchaeotal *amoA* and 16S rRNA genes were compared to reference sequences (obtained from GenBank) of enriched or isolated AOA representatives as well as environmental representatives. Sequences were aligned using MUSCLE (Edgar, 2004), and the resulting alignments were cropped so that all sequences spanned the same 483-bp and 762-bp regions for *amoA* and 16S rRNA genes, respectively. Evolutionary histories were inferred using the Maximum Likelihood method based on the Tamura-Nei model of sequence evolution (Tamura and Nei, 1993). The trees shown were those with the highest log likelihood. Bootstrap testing was conducted with 500 replicates. All alignments and phylogenetic analyses were conducted in MEGA5 (Tamura *et al.*, 2011).

4.3 Results

4.3.1 Water chemistry

In all sampling seasons and both treatment trains examined (NE and SE, see methods section for sampling details), ammonia decreased along the RBC flowpaths (Fig. 4.2A and Table 4.1). Overall, wastewater ammonia concentrations were highest in February and lowest in September, and were consistently higher in the northeast treatment train than the southeast train. Nitrite decreased across RBC flowpaths in patterns similar to ammonia, and nitrite concentrations were always relatively low (*i.e.*, <400 μg L^{-1}, Table 4.1). In contrast, nitrate concentrations were always relatively high (15-30 mg L^{-1}), and measured nitrate levels did not change in a predictable manner across individual RBC flowpaths. For all RBC stages in all seasons, the pH varied within a narrow range of 7.2 to 7.6. Other parameters, such as temperature and dissolved organic carbon (DOC), varied little across a given RBC flowpath but showed seasonal differences. Dissolved oxygen (dO$_2$) in this aerated system was always greater than 6 mg L^{-1}, and increased by $\leq$ 2 mg L^{-1} across a given RBC flowpath.

4.3.2 Gene abundances

Thaumarchaeotal *amoA* and 16S rRNA gene sequences were detected in all RBC stages from all seasons. In each RBC train sampled, AOA *amoA* gene abundance in genomic DNA extracts obtained from biofilm increased across the RBC flowpath (Fig. 4.2B). In addition, thaumarchaeotal 16S rRNA gene abundance increased across the flowpath, in a pattern congruent with archaeal *amoA* genes (Fig. 4.2B). For both thaumarchaeotal *amoA* and 16S rRNA genes, abundance varied by season; gene abundances were highest in September and lowest in February (Fig. 4.2B). In addition, in both June and September, gene abundances were higher in the SE treatment train than the NE train.

Bacterial *amoA* genes were detected in biofilm extracts from all RBC stages. In contrast to AOA, bacterial *amoA* gene abundance did not show predictable or consistent patterns between or across RBC trains when analyzed independently (Fig. 4.3A). In addition, general bacterial 16S rRNA gene abundances (measured as a control gene) were relatively consistent across all RBC stages, regardless of treatment train or season (Fig. 4.3). When biofilm and associated wastewater from all RBC stages (*i.e.*, from all sampling times and

treatment trains) were considered together, the relative abundance of AOA *amoA* genes (as a proportion of total *amoA* genes) comprised between 10-61% of the total ammonia-oxidizing community (Fig. 2.3). The relative abundance of AOA *amoA* genes demonstrated a negative trend with ammonia concentration (R^2= 0.51; Fig. 3). Furthermore, Spearman's rank correlation coefficients were negative and statistically significant for influent ammonia concentrations with both the relative abundance of AOA *amoA* genes (*i.e.*, as a proportion of total *amoA* genes; $r = -0.69$, $p<0.0001$) as well as independent AOA a*moA* gene abundances ($r=-0.61$, $p<0.0001$).
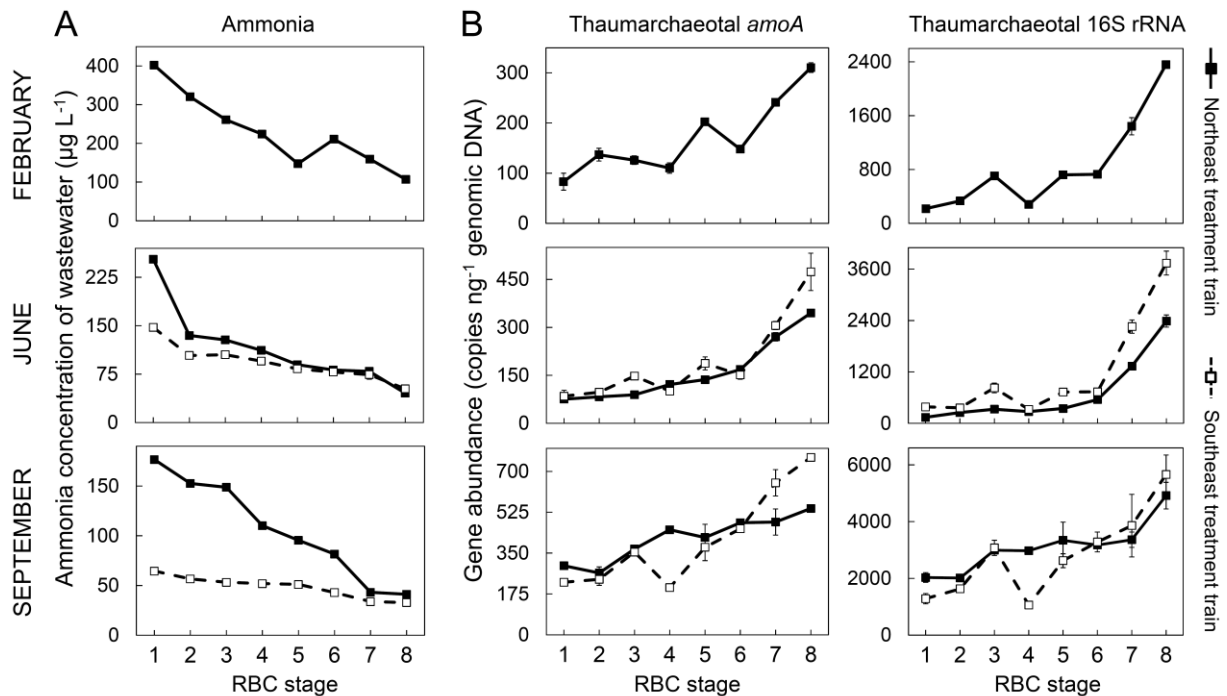
Figure 4.2 Ammonia concentrations and thaumarchaeotal gene abundances across the RBC flowpath. A) Ammonia concentrations of wastewater at each RBC stage. B) thaumarchaeotal *amoA* and 16S rRNA gene abundances in associated biofilm samples. Data from the Northeast and Southeast treatment trains are indicated with solid and dashed lines, respectively. Error bars represent standard deviations based on technical duplicates. Error bars that are not seen are contained within the symbols.

Table 4.1 Water chemistry data for RBC-associated wastewater.

Sample	pH	temperature (°C)	dO$_2$ (mg L^{-1})	DOC (mg L^{-1})	Nitrate (mg L^{-1})	Nitrite (µg L^{-1})	Ammonia (µg L^{-1})
FNER1	7.2	13.1	7.1	ND	29.4	375.8	401.9
FNER2	7.3	12.2	8.0	ND	22.5	294.6	320.3
FNER3	7.4	12.1	8.3	ND	28.1	245.9	260.9
FNER4	7.4	12.6	7.8	ND	28.4	186.4	223.8
FNER5	7.5	12.1	8.9	ND	28.9	148.5	147.5
FNER6	7.4	11.9	8.7	ND	28.2	170.1	210.6
FNER7	7.5	12.5	8.5	ND	29.0	148.5	159.3
FNER8	7.5	12.2	8.7	ND	28.5	102.5	106.8
JNER1	7.4	18.4	5.9	10.4	21.2	327.3	252.9
JNER2	7.4	18.2	6.9	10.1	21.5	190.4	135.0
JNER3	7.4	18.1	7.3	10.2	21.7	155.4	128.1
JNER4	7.5	17.9	7.6	10.6	21.1	111.1	112.0
JNER5	7.5	17.9	7.7	10.3	21.5	116.8	89.7
JNER6	7.5	18.0	7.4	10.6	21.7	103.3	81.5
JNER7	7.5	18.0	7.5	10.6	21.4	100.2	79.3
JNER8	7.6	18.0	7.8	10.6	22.0	63.6	45.5
JSER1	7.4	18.0	5.5	11.2	20.9	220.4	147.4
JSER2	7.4	17.9	6.7	10.3	20.9	152.3	103.9
JSER3	7.4	18.0	6.5	10.6	20.9	159.3	105.2
JSER4	7.4	18.0	6.8	9.5	21.5	144.6	95.2
JSER5	7.4	18.0	7.1	10	20.6	115.7	83.3
JSER6	7.5	17.9	7.2	10.3	21.1	107.6	78.4
JSER7	7.5	18.0	7.3	9.8	21.4	84.6	74.2
JSER8	7.6	18.0	7.5	10.3	20.6	72.8	52.3
SNER1	7.3	21.0	6.0	9.3	12.9	91.7	176.6
SNER2	7.4	21.1	6.1	10.3	13.1	66.5	152.6
SNER3	7.3	21.0	6.4	10.7	14.8	56.8	148.7
SNER4	7.3	21.0	6.6	10.0	20.6	65.7	110.2
SNER5	7.4	20.9	6.8	10.0	15.0	51.9	95.4
SNER6	7.4	20.9	6.9	10.7	17.5	46.8	81.6
SNER7	7.3	21.0	7.0	10.6	15.8	27.6	43.1
SNER8	7.5	21.0	7.1	10.2	22.7	38.4	41.2
SSER1	7.3	21.0	5.9	9.6	15.1	51.4	64.5
SSER2	7.3	21.1	6.5	9.3	15.7	39.7	56.6
SSER3	7.5	21.0	6.6	9.0	15.2	35.1	53.2
SSER4	7.2	21.1	6.6	8.8	22.5	43.5	51.9
SSER5	7.4	21.0	6.7	9.1	11.9	27.0	51.1
SSER6	7.4	21.0	6.9	9.1	17.9	28.9	42.9
SSER7	7.3	21.0	7.1	9.1	19.2	43.0	33.8
SSER8	7.3	21.0	7.0	9.1	15.8	21.9	32.8

DOC: dissolved organic carbon, dO$_2$: dissolved oxygen, ND: not determined
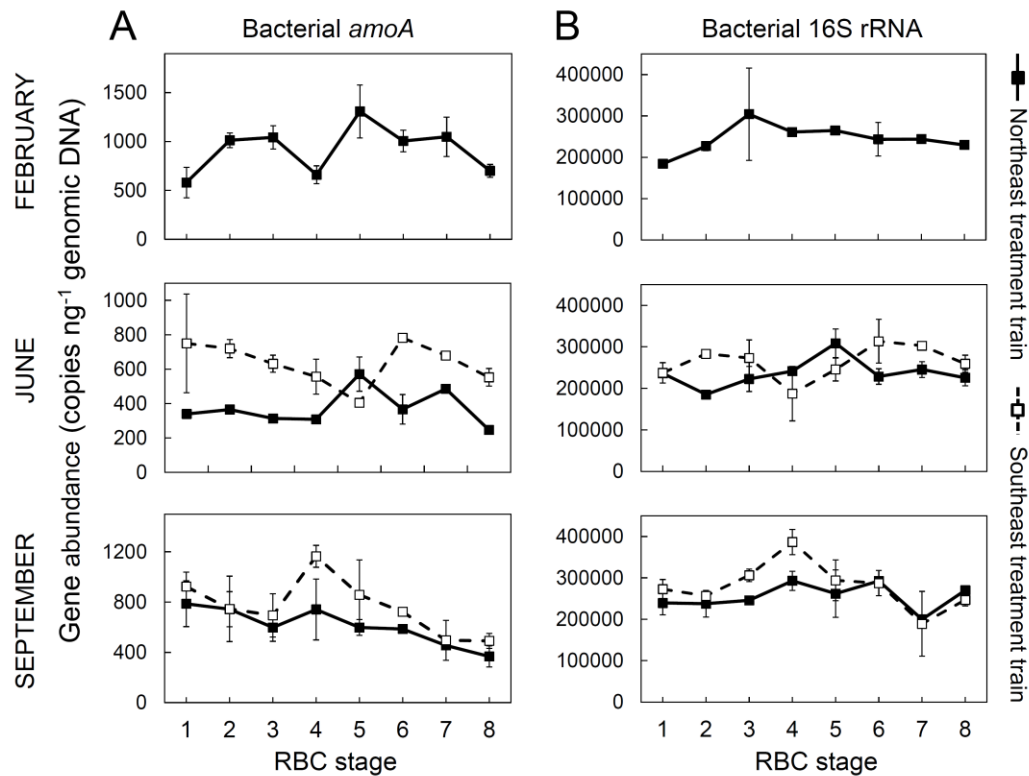
Figure 4.3 Bacterial *amoA* (A) and general bacterial 16S rRNA (B) gene copies in biofilm samples across RBC flowpaths. Error bars represent standard deviations based on technical duplicates; error bars that are not seen are contained within the symbols.
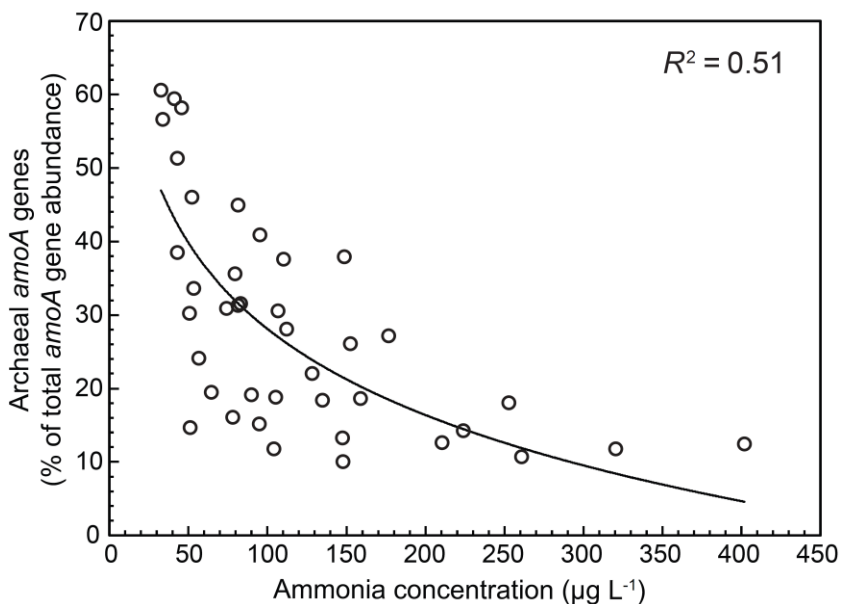
Figure 4.4 Ammonia concentrations of RBC-associated wastewater and relative abundance of archaeal *amoA* genes (as a per cent of total archaeal and bacterial *amoA* genes) in corresponding RBC biofilm.

4.3.3 Lipid abundances

In addition to quantification of key genes, concentrations of thaumarchaeol, the characteristic membrane lipid of ammonia-oxidizing thaumarchaeota (Pitcher, Villanueva, *et al.*, 2011) were determined both as core lipid as well as derived from intact polar lipids. Core lipids are assumed to represent fossilized (*i.e.,* dead) biomass, whereas intact polar lipids are biomarkers indicative of viable microbial cells (Sturt *et al.*, 2004; Biddle *et al.*, 2006; Pitcher *et al.*, 2009; Pitcher, Hopmans, *et al.*, 2011). Thaumarchaeol in biofilm samples from all RBC stages of the June NE treatment train was quantified; both core and IPL-derived thaumarchaeol increased across the RBC flowpath (Fig. 4.5A). For all other RBC trains, lipid analyses were performed for RBCs 1 and 8 only. In all cases, biofilm samples from RBC 8 yielded higher core and IPL-derived thaumarchaeol abundances than RBC 1 (Fig. 4.5B).
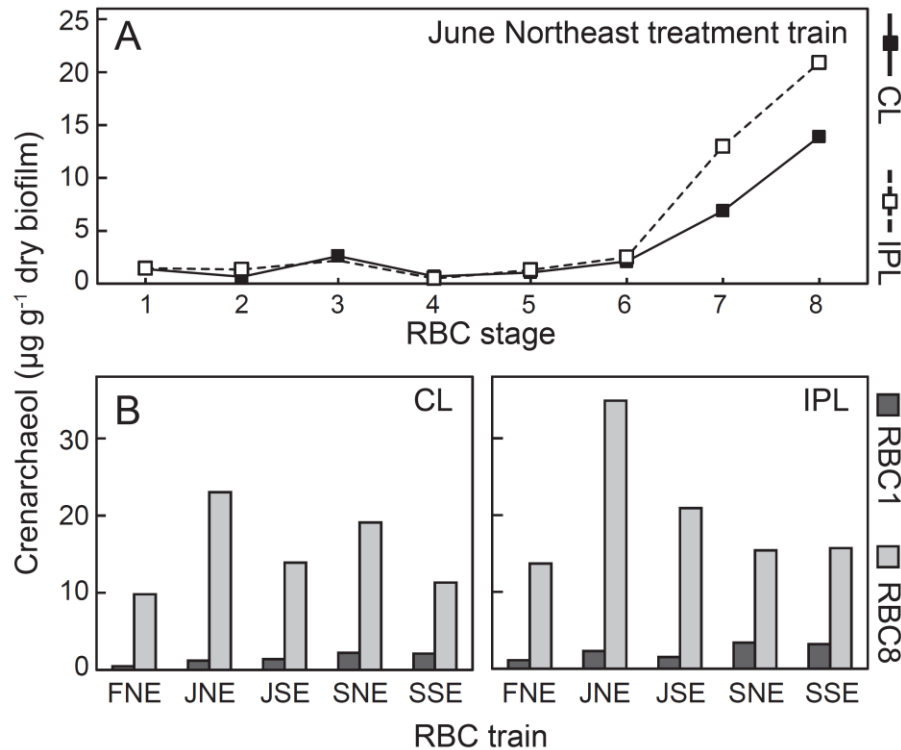
Figure 4.5 GDGT lipid abundances in RBC biofilm samples. A) CL- and IPL-derived thaumarchaeol abundance in biofilm across the June NE RBC flowpath. B) CL- and IPL-derived thaumarchaeol abundances for RBC 1 and 8 biofilm for all seasons and treatment trains. F, J and S denote February, June and September, respectively.

4.3.4 Gene diversity across RBC flowpath

For all genes analyzed, communities were highly similar across all RBC stages of a given flowpath (Figs. 4.6 and 4.7). DGGE profiles for thaumarchaeotal *amoA* and 16S rRNA genes revealed simple patterns and low diversity; one dominant band was observed for both archaeal *amoA* and thaumarchaeotal 16S rRNA genes (Fig. 4.6). For both thaumarchaeotal genes analyzed, diversity and community composition were identical across all RBC stages sampled in all seasons (Figs. 4.6 and 4.7). Bacterial *amoA* DGGE profiles were more complex, and patterns were similar across a given flowpath and between seasons (Figs. 4.6 and 4.7). General bacterial 16S rRNA gene fingerprints were complex and highly similar, both across RBCs of a given treatment train (Fig. 4.6) and between treatment trains and seasons (Fig. 4.7).

As described above, DGGE profiles showed simple patterns for archaeal *amoA* and 16S rRNA genes. Representative bands from both treatment trains (NE and SE) from all seasons were excised from gels and sequenced to confirm that populations were identical across all RBC stages, treatment trains, and seasons. The resulting *amoA* sequence clustered with environmental sequences derived from other engineered environments, including landfills and activated sludge of municipal WWTPs (Fig. 4.8A). The *amoA* sequence retrieved from the Guelph RBCs shared a sequence identity of 94% with its most closely related sequences, which originated from a municipal WWTP (HM589803) and nitrifying activated sludge (GU936642). Similarly, the thaumarchaeotal 16S rRNA gene sequence obtained from Guelph WWTP clustered with genes retrieved from high-nutrient environments such as fertilized soils and WWTPs, and clustered distinctly from isolated or enriched AOA representatives (Fig. 4.8B). This sequence shared 100% sequence identity with sequences retrieved from an industrial WWTP (treating oil refinery waste; HQ316970), activated sludge from a municipal WWTP (HM639792), and with sludge from a nitrous oxide oxidation system (AB619712).
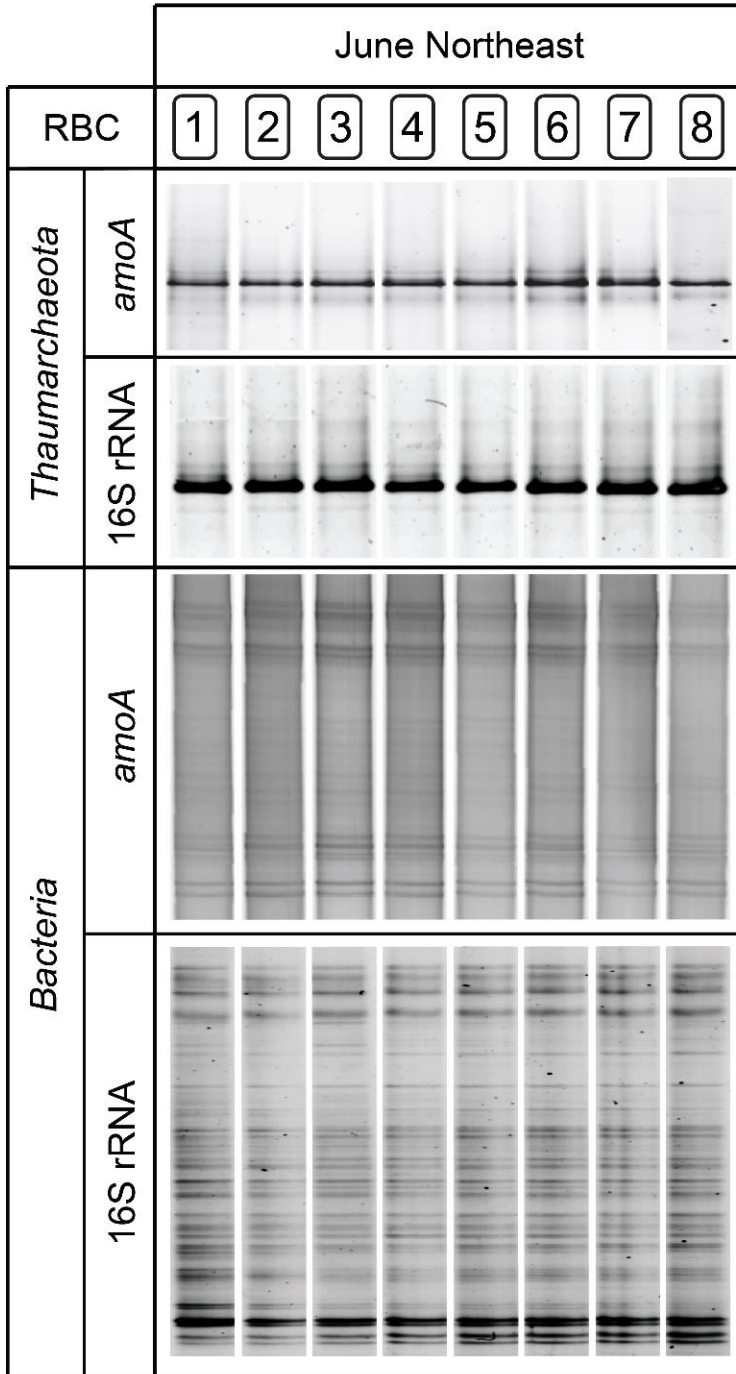
Figure 4.6 DGGE fingerprints for thaumarchaeotal and bacterial *amoA* and 16S rRNA genes in RBC biofilm (June NE). Numbers 1 to 8 represent eight serial RBC stages within one train. Data from all treatment trains are shown in Fig. 4.7.
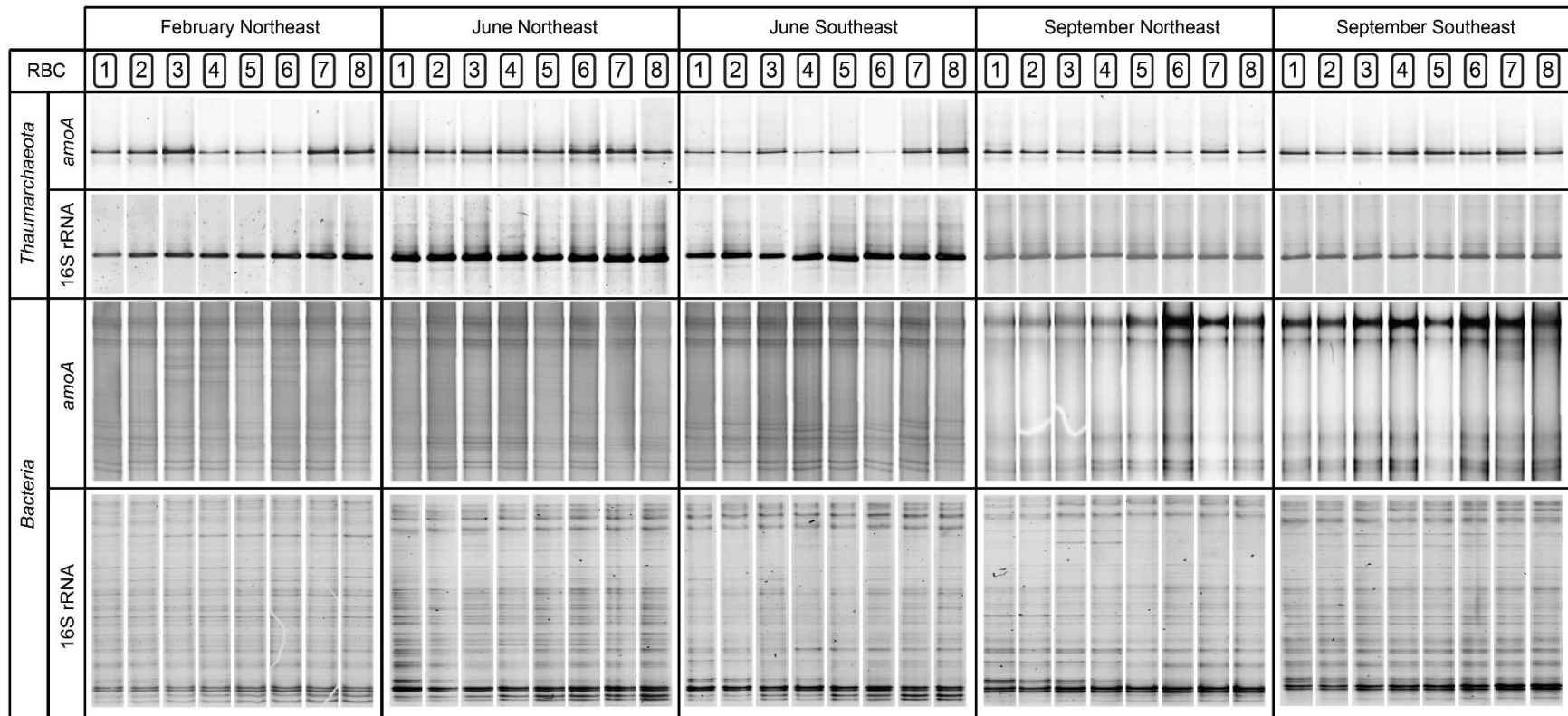
Figure 4.7 DGGE fingerprints for thaumarchaeotal and bacterial *amoA* and 16S rRNA genes (all sampling seasons and RBC treatment trains). Numbers 1 to 8 represent eight serial RBC stages within one train

A

- landfill (HM164885)
- WWTP activated sludge (HM191509) — 100
- municipal WWTP (HM589803)
- nitrifying activated sludge, municipal WWTP (GU936642) — 79
- **Guelph RBCs** — 94
- hot spring microbial mat (GQ226088) — 80
- cattle manure compost (AB542171) — 100
- anoxic granular sludge (EU010404)
- soil under manure pond (HQ407496)
- landfill cover soils (HM467067) — 80
- San Franciso Bay sediment (DQ278583)
- estuary sediments (HM364031) — 93, 99
- soil fosmid clone 54d9 (AJ627422) — 60
- *Candidatus* Nitrososphaera gargensis (EU281321) — 99
- *Candidatus* Nitrososphaera viennensis EN76 (FR773159)
- *Candidatus* Nitrosocaldus yellowstonii (EU239961)
- freshwater aquarium biofilter (JN183811) — 50
- *Nitrosopumilus maritimus* SCM1 (EU239959) — 55
- *Candidatus* Nitrosoarchaeum limnia (AEGP01000066) — 99
- *Candidatus* Cenarchaeum symbiosum A (DP000238)

0.05

B

- WWTP, oil refinery (HQ316970.2)
- activated sludge (HM639792)
- **Guelph RBCs**
- alkaline soil (FJ84303) — 87
- petroleum contaminated soil (AB161340)
- thermophilic digested sludge (AB353209)
- WWTP; tannery waste (HQ316969)
- N$_2$O oxdidation system sludge (AB619712) — 61
- agricultural soil (HQ678244)
- landfill sludge (AJ831160)
- hydrocarbon contaminated saline alkaline soil (HQ400477) — 99
- cattle manure compost (AB541694)
- outfall sediment (JF304141)
- salt marsh sediment (EU284637)
- Horsetooth reservoir, Colorado (AF418935) — 74
- *Candidatus* Nitrososphaera gargensis — 95
- *Candidatus* Nitrososphaera viennensis EN76 (FR773157)
- soil fosmid clone 54d9 (AY278106) — 98
- *Candidatus* Nitrsosocaldus yellowstonii (EU239960)
- *Nitrosopumilus maritimus* SCM1 (DQ085097) — 72
- *Candidatus* Nitrosoarchaeum limnia (NZ_AEGP01000029) — 100
- *Candidatus* Cenarchaeum symbiosum A (NC_014820)

0.02

Figure 4.8 Phylogenetic affiliations of *Thaumarchaeota* in Guelph RBC biofilm. A) *amoA* and B) 16S rRNA gene sequences retrieved from Guelph WWTP RBCs. Trees were inferred using the Maximum Likelihood method based on the Tamura–Nei model of sequence evolution. Bootstrap values are located above branches and are based on 500 replicates. Only bootstrap values greater than 50% are indicated on tree. The scale bars represent 5% and 2% nucleotide divergence for A and B, respectively.

4.4 Discussion

The present study suggests niche adaptation of ammonia-oxidizing archaea to low ammonia conditions, and identifies a wastewater environment in which AOA are abundant. For each RBC treatment train analyzed, AOA populations increased in abundance as ammonia decreased along the flowpath (Fig. 4.2). When all RBCs from all seasons were analyzed together, a negative correlation with high statistical significance (r=-0.69, p<0.0001) was observed between ammonia concentration of wastewater and relative abundance of AOA, implying that ammonia availability is an important factor in determining the relative proportions of ammonia-oxidizing populations.

Ammonia concentrations in the SE treatment train were consistently lower than in the northeast treatment train, presumably because this train is located farther from the influent source (see Fig. 4.1C), and nitrification and volatilization may occur in the wastewater *en route* to the treatment train. Thaumarchaeotal *amoA* and 16S rRNA genes were consistently more abundant in the southeast treatment train (Fig. 4.2B), further supporting the inference of niche adaptation of AOA to low ammonia conditions. Moreover, AOA gene abundances were highest in September, when ammonia concentrations were lowest.

In all RBC stages from all seasons, AOA comprised a substantial proportion of the ammonia-oxidizing community (*i.e.*, always greater than 10%), which is an important finding because studies of activated sludge in municipal wastewater treatment plants typically show that AOB dominate ammonia oxidizing communities, with AOA having low abundance or being absent (Wells *et al.*, 2009; Jin *et al.*, 2010; Zhang *et al.*, 2011). These studies have investigated suspended growth treatment systems used for secondary treatment, where high ammonia concentrations likely preclude the growth of AOA. Although two previous studies have suggested that AOA are abundant in aeration basins of municipal WWTPs (Limpiyakorn *et al.*, 2011; Kayee *et al.*, 2011), both studies used circular plasmids for qPCR standards, a practice that has been shown to cause serious overestimation of absolute gene copy numbers (Hou *et al.*, 2010). Therefore, it remains unclear whether AOA may be abundant in some traditional aeration basin treatment systems.

Although overall abundance patterns between thaumarchaeotal *amoA* and 16S rRNA genes were consistent (Fig. 4.2B), thaumarchaeotal 16S rRNA genes were approximately an

order of magnitude higher than archaeal *amoA* genes. It is currently unclear whether all *Thaumarchaeota* oxidize ammonia, but three lines of evidence suggest that all thaumarchaeotal populations in the Guelph WWTP RBCs possess *amoA* genes. First, the similarity between thamarchaeotal *amoA* and 16S rRNA gene abundances across a given RBC flowpath is readily apparent (Fig. 4.2B), which would be unlikely if these genes did not represent the same population. Moreover, DGGE of both thaumarchaeotal *amoA* and 16S rRNA genes (Figs. 4.6, 4.7, and 4.8) suggest that a single detectable thaumarchaeotal population inhabits this wastewater treatment system. Finally, the thaumarchaeotal *amoA* and 16S rRNA gene sequences both have congruent phylogenies, and both cluster within the Group I.1b *Thaumarchaeota*, of which all known representatives oxidize ammonia (Hatzenpichler *et al.*, 2008). It is also possible that higher thaumarchaeotal 16S rRNA gene copy numbers result from archaeal populations that possess multiple 16S rRNA operons. However, given that all available AOA genomes contain only one 16S rRNA gene (Hallam *et al.*, 2006; Walker *et al.*, 2010; Blainey *et al.*, 2011; Kim *et al.*, 2011), it is more likely that low AOA *amoA* numbers result from poor primer matching with template DNA, consistent with previous findings (Konstantinidis *et al*., 2009). Indeed, although thaumarchaeotal 16S rRNA genes were readily amplified from all samples, *amoA* genes could not be reliably amplified without use of a degenerated reverse primer and a decreased annealing temperature (data not shown). In this study, we considered archaeal *amoA* genes to be markers for AOA in an attempt to be conservative in our conclusions. However, based on thaumarchaeotal 16S rRNA gene abundances, it is likely that this study has underestimated the abundance of AOA based on measured *amoA* gene copies, and perhaps potential archaeal contributions to ammonia oxidation in this RBC treatment system. If thaumarchaeotal 16S rRNA genes were compared to bacterial *amoA* genes, AOA would, in fact, outnumber AOB in the majority of biofilm samples collected, regardless of treatment train or sampling season, in some cases by orders of magnitude.

In addition to qPCR data, this study quantified thaumarchaeol as an independent metric of AOA abundance. Thaumarchaeol is a GDGT lipid that serves as a biomarker for ammonia-oxidizing archaea in ecological studies. Thaumarchaeol has been detected in isolated and enriched AOA, including *N. maritimus* SCM1 (Schouten *et al.*, 2008), *Candidatus* Nitrosocaldus yellowstonii (de la Torre *et al.*, 2008), *Candidatus* Nitrososphaera

gargensis (Pitcher *et al.*, 2010) and *Candidatus* Nitrosoarchaeum limnia (Pitcher, Hopmans, *et al.*, 2011). Intact polar lipids (IPL) are found in cell membranes of living organisms, and are therefore considered as biomarkers for viable cells. Upon cell death, polar head groups are rapidly hydrolyzed, resulting in core lipids, which are indicative of fossilized biomass. Lipid analyses are valuable because they are comparatively unbiased due to the lack of an amplification step. Indeed, Pitcher and colleagues (Pitcher, Villanueva, *et al.*, 2011) found strong congruence between thaumarchaeol IPLs and abundances and expression of thaumarchaeotal 16S rRNA in the Arabian Sea. In a representative full-length treatment train (June, NE train), both core and IPL-derived thaumarchaeol abundances increased across the RBC flowpath (Fig. 4.5A). In addition, both CL- and IPL-derived thaumarchaeol were higher in RBC 8 than RBC 1 for all treatment trains sampled (Fig. 4.5B). These data corroborate quantitative PCR results, and the high proportion of IPL-derived thaumarchaeol suggests that the *Thaumarchaeota* detected in this system represent viable cells, which are most likely contributing to ammonia oxidation. A few seasonal discrepancies were observed between lipid and genetic data. For example, thaumarchaeol abundances were highest in June biofilm samples, whereas thaumarchaeotal gene abundances were highest in September biofilm samples. However, direct comparison of genetic and lipid data can be problematic because measured gene abundances are relative values (*i.e.*, copies per ng genomic DNA), whereas lipid measurements represent absolute abundances (*i.e.*, µg thaumarchaeol per gram of biofilm). Taken together, the same overall trend is supported by both lipid and genetic data.

Although ammonia concentration correlated with AOA abundances, it had no observable effects on AOA diversity or community composition within the ammonia concentrations measured here ($\sim$30-400 µg L^{-1}). Thaumarchaeotal *amoA* and 16S rRNA profiles contained one dominant band regardless of RBC stage, treatment train, or season. Phylogenetic analyses of thaumarchaeotal *amoA* and 16S rRNA genes retrieved from this RBC system demonstrated that archaeal sequences clustered with environmental sequences derived from other relatively high-ammonia environments, and share low homology with sequences from enriched or isolated AOA (Figs. 4.8A,B). This finding may imply that lineages of AOA exist that are adapted to environments with varying nutrient concentrations.

A variety of laboratory studies have identified ammonia as a key environmental parameter for determining relative abundances or activity of AOA and AOB, particularly in

soil environments (Di *et al.*, 2010; Taylor *et al.*, 2010; Verhamme *et al.*, 2011). In addition, laboratory incubations of soils have indicated that AOB are metabolically dominant following ammonia amendment (Jia and Conrad, 2009). The present study has taken advantage of an ammonia gradient created by existing wastewater treatment infrastructure and is unique because it provides a practical example of a phenomenon previously only identified through laboratory experiments.

Four previous studies have documented a relationship between ammonia availability and relative abundances of AOA and AOB in freshwater environments. Herrmann and colleagues (Herrmann *et al.*, 2011) demonstrated an increased ratio of AOB:AOA in simulated creek ecosystems amended with ammonia. In addition, Limpiyakorn and colleagues (2011) suggested ammonia as a potential variable in determining the relative abundances of AOA and AOB in municipal WWTPs, but this study produced no statistically significant correlations. A survey of Bangkok WWTPs reported a negative correlation between AOA *amoA* gene abundance in activated sludge and effluent ammonia concentrations (Kayee *et al.*, 2011), but a similar correlation was not found with influent ammonia concentrations, and this study was later retracted. A correlation was also observed between AOA:AOB ratios and ammonia concentration in freshwater aquarium biofilters (Sauder *et al.*, 2011). Our study complements these initial observations by providing evidence for the role of ammonia in determining the relative abundances of AOA and AOB in engineered freshwater environments.

A recent study of municipal and industrial WWTPs found that AOA genes could rarely be detected in municipal wastewater treatment plants, but that in certain industrial wastewater treatment plants, thaumarchaeotal *amoA* genes outnumbered bacterial *amoA* genes by up to four orders of magnitude (Mussman *et al.*, 2011). In one of these industrial plants, it was shown that the *Thaumarchaeota* were not obligate chemolithoautotrophs, but instead were using organic carbon for mixotrophic or heterotrophic metabolism. Although all currently cultured or enriched *amoA*-encoding *Thaumarcheota* oxidize ammonia (Könneke *et al.*, 2005; de la Torre *et al.*, 2008; Hatzenpichler *et al.*, 2008; Tourna *et al.*, 2011), this study by Mussman and colleagues (2011) calls into question whether all *Thaumarchaeota* possessing *amoA* genes mediate ammonia oxidation. Therefore, it is possible that the *Thaumarchaeota* detected in the Guelph RBCs may be obtaining energy from organic carbon

instead of, or in addition to, ammonia. Indeed, the 16S rRNA gene sequence retrieved from these RBCs clustered with clone sequences derived from industrial WWTPs analyzed by Mussman *et al*. (2011; Fig. 4.8), although these sequences did not originate from the WWTP (Plant D) which the majority of their study was based on. Further activity studies and cultivation attempts will be necessary to confirm the role of *Thaumarchaeota* in tertiary wastewater treatment. Nonetheless, the *Thaumarchaeota* identified in this study demonstrate increased abundance in low ammonia conditions, whether or not they are strict chemolithoautotrophs.

Because the discovery of AOA is a recent phenomenon, most existing nitrification infrastructure has been designed on the premise that it will host populations of AOB. However, this study suggests that AOA may play a role in ammonia oxidation in low ammonia biofiltration systems, such as nitrifying RBCs, aquaculture, aquarium biofilters, and drinking water treatment plants. These systems rely on nitrification for ammonia removal, but low ammonia concentrations may preclude AOB from obtaining sufficient energy for survival and growth. Existing studies support the hypothesis that AOA dominate low-ammonia engineered systems such as groundwater treatment and distribution systems (van der Wielen *et al.*, 2009) and granular activated carbon of drinking water treatment plants (Kasuga *et al.*, 2010). This may be important when designing biofiltration systems, because AOB and AOA likely vary in a variety of additional ecological adaptations. For example, previous studies have suggested that AOA thrive in low oxygen conditions (Park *et al.*, 2006, 2010; Yan *et al.*, 2012). Therefore, the aggressive aeration typically provided in engineered biofilters (that would be beneficial for AOB) may actually interfere with the ability of AOA to oxidize ammonia efficiently.

The results of this study provide evidence for a low-ammonia niche of AOA within the RBC system in Guelph, Ontario, and provides a foundation for future activity, cultivation and genomic analyses for characterizing nitrogen biogeochemistry within engineered freshwater environments.

Chapter 5[4]

Cultivation and characterization of *Candidatus* Nitrosocosmicus exaquare, an ammonia-oxidizing archaeon from a municipal wastewater treatment system

5.1 Introduction

Nitrification is an important process for municipal and industrial wastewater treatment plants (WWTPs) because it prevents the negative impacts of releasing ammonia to receiving waters, including toxicity to fish, eutrophication, and increased oxygen demand. Ammonia-oxidizing bacteria (AOB) were believed traditionally to mediate ammonia oxidation in soils, aquatic habitats, and engineered environments, including WWTPs. The recent discovery of ammonia-oxidizing archaea (AOA; Venter *et al.*, 2004; Könneke *et al.*, 2005) and subsequent activity and abundance studies have implicated AOA as dominant ammonia oxidizers in many environments, including the open ocean (Wuchter *et al.*, 2006), estuarine sediments (Beman and Francis, 2006), soils (Leininger *et al.*, 2006; Stopnisek *et al.*, 2010; Yao *et al.*, 2011; Zhang *et al.*, 2012), and engineered environments such as aquaculture operations and aquarium biofilters (Sauder *et al.*, 2011; Bagchi *et al.*, 2014; Brown *et al.*, 2013). However, there is evidence that AOB are numerically dominant in some environments, and that AOB may mediate ammonia oxidation in several soils, despite a numerical dominance of AOA (Mosier and Francis, 2008; Di *et al.*, 2009; Banning *et al.*, 2015; Sterngren *et al.*, 2015).

The role of AOA in WWTPs remains unclear. Compared to many natural soil and aquatic environments, WWTPs contain relatively high levels of ammonia, which should favour AOB over AOA (Schleper, 2010; Martens-Habbena *et al.*, 2009). Indeed, many studies have reported a numerical dominance of AOB in municipal and industrial WWTPs, often with AOA below detection limits (Gao *et al.*, 2013; Mussman *et al.*, 2011;

---

[4] A version of this chapter has been accepted for publication in ISME J:
Sauder LA, Albertsen M, Engel K, Schwarz J, Nielsen P, Wagner M, Neufeld JD. Cultivation and characterization of *Candidatus* Nitrosocosmicus exaquare, an ammonia-oxidizing archaeon from a municipal wastewater treatment plant. *In press.*

Limpiyakorn *et al.*, 2011; Wells *et al.*, 2009). Nevertheless, AOA have been detected in several WWTPs (Park *et al.*, 2006; Wells *et al.*, 2009; Zhang *et al.*, 2009; Kayee *et al.*, 2011; Mussman *et al.*, 2011; Sauder *et al.*, 2012; Bai *et al.*, 2012; Gao *et al.*, 2014, 2013), and in some cases outnumber AOB (Kayee *et al.*, 2011; Bai *et al.*, 2012). Although the abundance and diversity of AOA and AOB has been assessed in several WWTPs, no previous study has tested the relative contributions of AOA and AOB to nitrification in any municipal WWTP. Intact polar lipids (IPLs) originating from thaumarchaeotal membranes have been identified in WWTP biofilms (Sauder *et al.*, 2012), indicating that the detected AOA were viable in the system, though not necessarily oxidizing ammonia. Mussman and co-workers (2011) were unable to demonstrate bicarbonate assimilation by group I.1b *Thaumarchaeota* in nitrifying sludge and, based on further experimental and modelling data, called into question a strictly chemolithoautotrophic lifestyle of AOA in the examined industrial WWTP.

Currently, only one AOA enrichment culture exists from a wastewater treatment system, belonging to the Group 1.Ia *Thaumarchaeota* (Li, Ding, *et al.*, 2016). This study reports the cultivation and complete genome sequence of a novel group I.1b *Thaumarchoaeta* representative, belonging to the *Nitrososphaera* sister cluster, with the proposed name *Candidatus* Nitrosocosmicus exaquare . This representative was enriched from biofilm of rotating biological contactors (RBCs) of a municipal WWTP in Guelph, Canada, where it was first discovered based on DNA and lipid signatures (Sauder *et al*. 2012).

5.2 Materials and methods

5.2.1 Sampling site

Biofilm for enrichment culture inoculum was collected from the Guelph WWTP (Ontario, Canada) in September 2012 from the 8th RBC ("RBC 8") of the Southeast (SE) treatment train. For a plant schematic and description of wastewater treatment processes, see Sauder *et al*. (2012) and Chapter 4 (Fig. 4.1). In August 2014, the SW portion of the Guelph WWTP RBCs was shut down for cleaning for the first time since their installation in 1978 (leaving the NE, NW, and SE RBC treatment trains intact). During this cleaning, wastewater was diverted away from the treatment process and biofilm was completely removed from the reactors. Upon sampling approximately eight months later (April 2015), biofilm in the SW

train was regenerated and used for comparison to the NE, SE, and NW trains. Following this, all 4 treatment trains were decommissioned (in November 2015) and regenerated biofilm was sampled approximately one month later (December 2015). Biofilm for various experiments presented in this chapter were collected at multiple time points and sampling details are summarized in Table 5.1.

Table 5.1 Guelph WWTP RBC biofilm sampling details

Collection date	RBCs sampled	Experiments/Analyses	Corresponding figures and tables
September 2012	Southeast RBC 8	Inoculum for cultivation	Described in text
April 2013	Southeast RBC 1 and 8	FISH quantitative FISH	Figs. 5.5, 5.6 Described in text
July 2013	Southeast RBC 1 and 8	CARD-MAR-FISH	Fig. 5.15
April 2015	Northeast RBC 1 and 8 Southeast RBC 1 and 8	Incubations with inhibitors Biofilm regeneration	Fig. 5.14 Fig. 5.16
December 2015	Northeast RBC 1 and 8 Southwest RBC 1 and 8	Incubations with inhibitors qPCR	Fig. 5.11 Table 5.3

5.2.2 Cultivation

Biofilm was collected from a rotating biological contactor (RBC) of the Guelph WWTP in September 2012 (Guelph, Ontario, Canada), and was used as starting inoculum for *Ca.* N. exaquare enrichment cultures. Biofilm originated from the 8th RBC ("RBC 8") of the Southeast (SE) quadrant, which had previously shown a high abundance of AOA and an ammonia concentration of approximately 50-60 µg N-NH$_3$ L^{-1} (Sauder *et al.*, 2012). Initial cultivation efforts used a 0.1% (w/v) inoculation of biofilm in HEPES-buffered freshwater medium (Tourna *et al.*, 2011) with 0.5 mM ammonia. Medium was supplemented with kanamycin (50 µg ml^{-1}) and streptomycin (100 µg ml^{-1}) to inhibit growth of Gram-negative bacteria (especially AOB), and later with ampicillin (50 µg ml^{-1}) to inhibit growth of Gram-positive bacteria. Cultures were eventually transitioned to a growth medium containing excess calcium carbonate, which provides inorganic carbon, a substrate for biofilm attachment, and buffering capacity. This growth medium has been used previously for

growth of both AOA and AOB (Krümmel and Harms, 1982; Lebedeva *et al.*, 2005; Hatzenpichler *et al.*, 2008). Briefly, the medium contained per L: 0.05 g KH$_2$PO$_4$, 0.075 g KCl, 0.05 g MgSO$_4$·7H$_2$0, 0.58 g NaCl, and 4 g CaCO$_3$. After autoclaving, the medium was supplemented with filter-sterilized NH$_4$Cl (to 0.5-1 mM), 1 ml selenite-tungstate solution, and 1 ml trace element solution (Widdel and Bak, 1992; Könneke *et al.*, 2005), and the resulting pH of the medium was approximately 8.5 and was not adjusted. Cultures were incubated at 28-30°C in the dark, without shaking. Cultures were grown in acid-washed and autoclaved glass bottles with sealed caps.

5.2.3 Incubations for growth curve, temperature optimum, and ammonia and nitrite tolerance

Growth curve incubations used a 1% inoculum of actively growing culture subcultured into growth medium containing 1 mM NH$_4$Cl and supplemented with 0.5 mM sodium pyruvate. Triplicate cultures were incubated at 30°C in the dark and without shaking. A 2 ml sample of culture was removed at each sampling time point and pelleted by centrifugation for 10 minutes at 15,000 x g. Supernatants were removed for water chemistry measurements and pellets were used for genomic DNA extractions. Both supernatant and pellet samples were stored at -20°C until processing. For temperature incubations, *Ca.* N. exaquare cultures were incubated at varying temperatures, ranging from 21°C (room temperature) to 43°C, and all cultures were incubated with 0.5 mM NH$_4$Cl. For testing ammonia and nitrite tolerance, cultures were set up with varying starting concentrations of NH$_4$Cl and NaNO$_2$, respectively. All assays were set up with a 1% inoculum in the growth medium described above. To achieve 0 mM NaNO$_2$ conditions, the initial inoculum was pelleted for 10 minutes at 10,000 x g, supernatant removed, then washed and re-suspended in fresh growth medium. Washed and suspended biomass served as the 0 mM NaNO$_2$ inoculum for subcultures.

5.2.4 Incubations with organic carbon supplementation

In order to test the ability of pyruvate and other sources of organic carbon to stimulate activity, *Ca.* N. exaquare cells were subcultured (0.1% inoculum) and grown with or without organic carbon in the presence of 0.5 mM NH$_4$Cl. All organic carbon stock solutions were

filter-sterilized and added to the medium after autoclaving. Several compounds related to glycolysis and the tricarboxylic acid (TCA) cycle were tested, including pyruvate, citrate, succinate, malate, acetate, and glucose. These compounds were supplied at 0.25 mM, except glucose, which was supplied at 0.1 mM. Additional tested organic carbon sources included taurine (0.25 mM), glycerol (0.0007%), yeast extract (0.01%), and butyrate (0.1 mM). Concentration ranges were based on those used by Tourna and colleagues (Tourna *et al.*, 2011), and in some cases were adjusted to decrease heterotrophic growth and accompanying ammonia assimilation. All conditions were tested in triplicate, using the same medium and starting inoculum. Flasks were incubated in the dark, without shaking, at 28°C. All samples were stored at -20°C until further analysis.

5.2.5 Cryopreservation and 4°C storage of Ca. N. exaquare

      To test viability of the *Ca.* N. exaquare enrichment culture at 4°C, duplicate cultures were stored refrigerated for 0, 1, 3, and 6 months. For all time points (including 0 months), the culture used for inoculation was cooled to 4°C prior to inoculation to control for the effects of cooling on the cells. After the indicated storage time, cultures were inoculated in fresh medium containing 0.5 mM NH₄Cl (10% transfer) and incubated in the dark at 28°C, without shaking. Samples for water chemistry were stored at -20°C until processing.

      For cryopreservation, 1 ml of actively growing *Ca.* N. exaquare enrichment culture was placed in a 2 ml screw cap cryo-tube and 1 volume of cryoprotectant was added. Cryoprotectants used were 14% DMSO (7% final concentration) or 70% glycerol (35% final concentration). In both cases, cryoprotectants were prepared in ammonia free medium and sterilized with a 0.22 µm filter. Tubes were inverted several times to mix and were then placed in dry ice. When tube contents were completely frozen, they were moved to -80°C for storage. Cells were resuscitated after 2 weeks to assess the impact of freezing and cryopreservation treatment, and after 1 year to assess the impact of long term storage of cells. To resuscitate cells, tubes were thawed at room temperature for 10 minutes, and pelleted during centrifugation at 15,000 x g for 5 minutes. Supernatant was aspirated and discarded, and pellets were washed two times to remove residual DMSO or glycerol. To wash, 1 ml fresh medium was added to tubes, which were then centrifuged as above, and supernatant was removed. After washing, pellets were suspended in 2 ml growth medium, which was

then used as inoculum into fresh media containing 0.5 mM NH$_4$Cl (5% transfer). Flasks were then incubated in the dark at 28°C and without shaking. Samples for water chemistry analysis were collected at 2 day intervals, and stored at -20°C until processing. No-freeze control flasks were included that were treated with cryoprotectant as outlined, but were not frozen and were inoculated directly into fresh medium. Biological duplicates were prepared for all conditions.

5.2.6 Inhibitor assays on WWTP biofilm

Biofilm and wastewater from RBCs 1 and 8 were obtained from the Northeast (NE) and Southeast (SE) trains of the Guelph WWTP in April 2015, and the NE and Southwest (SW) trains in December 2015 (due to limited SE access). Biofilm was stored on ice following collection and incubations were set up immediately upon return to the laboratory (~1 hour following sampling). Incubations were performed in 125 ml glass serum bottles with silicone stoppers. Triplicate incubations were performed in the dark and without shaking. Each flask contained 20 ml incubation volumes, consisting of 2% (w/v) biofilm suspended in 0.22 µm filtered wastewater (composited from influent to the four sampled RBCs), amended with 1 mM ammonia chloride, a concentration suitable for the growth of all known AOA and AOB. Flasks were supplemented with inhibitors as appropriate, including 6 µM acetylene (aqueous), 10 µM allylthiourea (ATU), 8 µM octyne (aqueous), and both 200 and 400 µM PTIO. Ammonia concentrations were monitored over the course of the experiment and flasks were sampled for five days.

5.2.7 Incubation of Ca. *N. exaquare with PTIO, ATU, and octyne*

To assess the sensitivity of the ammonia-oxidizing activity of *Ca.* N exaquare to commonly used differential nitrification inhibitors, actively growing cells were incubated with varying concentrations of PTIO, ATU, and octyne. Incubations were prepared using a 10% inoculum of *Ca.* N. exaquare cells into fresh medium containing 0.5 mM NH$_4$Cl. Incubations containing octyne and the associated control were performed in 120 ml serum bottles sealed with silicone stoppers, and incubations containing PTIO or ATU (and associated controls) were performed in 100 ml Schott bottles with screw caps. Triplicate

113

bottles were incubated in the dark at 28°C without shaking. Samples for water chemistry analyses were stored at -20°C until analysis.

5.2.8 Incubation of Nitrosomonas europaea *with PTIO, ATU, and octyne*

N. europaea was used as a positive control to ensure that inhibitor assays functioned as expected on an AOB representative. For these experiments, *N. europaea* was grown in the calcium carbonate medium described above. Subcultures (10% v/v) were made from actively growing cultures, either with no inhibitor, or supplemented with inhibitors at the concentrations used for the activity experiments (*i.e.*, 10 µM ATU, 8 µM octyne, 200 and 400 µM PTIO). Cultures were set up in 120 ml serum bottles with silicone stoppers, and 25 ml volumes. Cultures were incubated in the dark, at 30°C, and without shaking. All conditions were performed in triplicate.

5.2.9 Water chemistry

Nitrite concentrations were measured colourimetrically using the Griess reagent system in 96-well plates, as described previously (Miranda *et al.*, 2001). Briefly, samples were diluted 1:10 in mineral salts medium (10 µL sample, 90 µL diluent) and 100 µL of Griess reagent was added. Samples were incubated at room temperature for 10 minutes prior to measurement of absorbance at 550 nm using a Filtermax F5 Multi-Mode Microplate Reader (Molecular Devices, Sunnyvale, CA). Ammonia measurements were determined colourimetrically using Nessler's reagent (Meseguer-Lloret *et al.*, 2002). Briefly, 1 volume (80 µl) of both sodium potassium tartrate (35.4 mM) and Nessler's reagent were added to 80 µl of sample in clear 96-well plates. Assay plates were incubated at room temperature for 30 minutes and absorbance measured at 450 nm using a FilterMax F5 Multi-Mode Microplate Reader. Reported ammonia concentrations represent total ammonia ($NH_3 + NH_4^+$) unless otherwise specified. All technical measurements were performed in duplicate. For both nitrite and ammonia readings, sample concentrations were determined by comparison to standards using the software package SoftMax Pro 6.4 (Molecular Devices).

5.2.10 DNA extractions, quantitative PCR, phylogenetic reconstruction, and DGGE

All DNA extractions were performed using the PowerSoil DNA Isolation Kit (for biofilm) or the Ultraclean Microbial DNA Isolation Kit (for laboratory cultures), both according to the manufacturer's instructions (MO BIO, Carlsbad, CA, USA). The protocol was modified to use a FastPrep-24 beadbeater (MP Biomedicals, Santa Ana, CA) at 5.5 m s^{-1} for 45 seconds instead of extended vortexing. Genomic DNA extracts were visualized on a 1% agarose gel by standard gel electrophoresis and quantified fluorometrically using the Qubit dsDNA HS Assay Kit on a Qubit 2.0 fluorometer, according to manufacturer's specifications (Thermo Fisher Scientific, Waltham, MA, USA).

Quantification of thaumarchaeotal and bacterial 16S rRNA genes was performed using primers 771F and 957R (Ochsenreiter *et al.*, 2003) and 341F and 518R (Muyzer *et al.*, 1993), respectively. The *amoA* genes from AOB were quantified using primers amoA1F and amoA2R (Rotthauwe *et al.*, 1997). All qPCR amplifications were conducted using technical duplicates on a CFX96 system (Bio-Rad, Hercules, CA, USA). Each 10 µl reaction contained 5 µl iQ SYBR Green Supermix (Bio-Rad), 3 pmol of each primer, 2.5 µg of bovine serum albumin, and 0.1-5 ng of genomic DNA as template. For thaumarchaeotal and bacterial 16S rRNA genes, the qPCR conditions were 98°C for 2 min, followed by 35 cycles of 98°C for 30 s, 55°C for 30 s, and 72°C for 30 s, with a fluorescence reading following each elongation step. For AOB *amoA* genes, qPCR conditions were the same, except with an elongation time of 1 minute. In all cases, melt curves were performed from 65°C to 95°C, with incremental 2 s temperature increases of 0.5°C. Standard curves were constructed using 10-fold serial dilutions of template DNA of known concentration. For all genes, template DNA consisted of PCR amplicons generated from the same primer pair used for qPCR. For thaumarchaeotal 16S rRNA gene amplicons, the template source was genomic DNA extracted from the *Ca.* N. exaquare enrichment culture. For AOB *amoA*, the template source was genomic DNA that was extracted from Guelph WWTP biofilm, and for bacterial 16S rRNA genes, the template source was genomic DNA from *Escherichia coli*. All qPCR efficiencies were >80% and R^2 values were >0.99.

For the *Ca.* N. exaquare growth curve, cell numbers were estimated based on measured 16S rRNA gene copies. To approximate cell numbers, quantified thaumarchaeotal 16S rRNA genes copy numbers were divided in half to account for two 16S rRNA gene

copies encoded by the *Ca.* N. exaquare genome, with an assumption of one genome per cell. Generation time was estimated from the slope of the natural log-transformed thaumarchaeotal cell numbers (as estimated by 16S rRNA gene copies) during exponential growth.

For phylogenetic analyses, *Ca.* N. exaquare *amoA* and 16S rRNA gene sequences were compared to reference sequences of enriched or isolated AOA representatives, as well as environmental sequences obtained from GenBank. Global alignment of sequences was performed using MUSCLE (Edgar, 2004). Evolutionary histories were inferred using the Maximum Likelihood method based on the General Time Reversible model of sequence evolution, and the trees shown are those with the highest log likelihood. A discrete Gamma distribution was used to model evolutionary rate differences among sites. Bootstrap testing was conducted with 500 replicates. All alignments and phylogenetic analyses were conducted in MEGA6 (Tamura *et al.*, 2013). Full-length *amoA* and 16S rRNA gene sequences from *Ca.* N. exaquare were deposited in GenBank under accession numbers KR233006.1 and KR233005.1, respectively.

DGGE fingerprinting was performed for thaumarchaeotal and general bacterial 16S rRNA genes. Thaumarchaeotal 16S rRNA genes were amplified using primers 771F and 957R-GC, with amplification and DGGE conditions as outlined previously (Tourna *et al.*, 2008). For general bacterial 16S rRNA genes, amplification was performed using primers 341F-GC and 518R, and DGGE was performed as outlined previously (Muyzer *et al.*, 1993). All gels were run at 60°C and 85 V for 900 minutes. The DGGE system used was a DGGEK-2401 (C.B.S. Scientific Company, Del Mar, CA, USA) using previously described technical modifications (Green *et al.*, 2009). Gels were stained with SYBR Green (Invitrogen, Carlsbad, CA, USA) for 1 h, then scanned with the PharosFX Molecular Imager using SYBR Green excitation and emission settings (excitation at 488 nm, emission at 530 nm; Bio-Rad). Fingerprints from gel images were normalized and aligned with GelCompar II (Applied Maths, Austin, TX, USA).

5.2.11 Microscopy (SEM, CARD-FISH, DOPE-FISH)

For scanning electron microscopy (SEM), a sample obtained from actively growing culture was applied to a silicon wafer and attached to an aluminum stub with conductive carbon tape. Cells were imaged unfixed and without any specialized coating. Immediately after drying, cells were imaged using a LEO 1550 field-emission scanning electron microscope (Zeiss, Oberkochen, DE). The InLens SE detector was used for high resolution topographic imaging, with an electron high voltage (EHT) of 7.00 kV, and a working distance of 10.3 mm.

For catalyzed reporter deposition-fluorescence *in situ* microscopy (CARD-FISH), biofilm and enrichment culture samples were fixed with 4% formaldehyde at room temperature for three hours. CARD-FISH samples were processed as described previously (Ishii *et al.*, 2004; Mussman *et al.*, 2011), with modifications. Briefly, fixed samples were applied to a poly-l-lysine coated slide, subjected to a standard ethanol series (50%, 80%, 98%; 3 minutes each), and then embedded in 0.2% agarose. Cells were permeabilized with proteinase K (15 µg ml^{-1} in 0.1 M Tris-0.01 M EDTA or 1X PBS) for 10 minutes at room temperature. Cells were then incubated in 0.01 M HCl for 20 minutes at room temperature to inactivate the proteinase K. To inactivate endogenous peroxidases, slides were treated with 0.3% H_2O_2 in 100% methanol for 30 minutes at room temperature for enrichment cultures, and overnight for biofilm material. Probes Arch915 (Stahl and Amann, 1991) or Thaum726 (Beam, 2015) were used for hybridization, with formamide concentrations of 10% and 25%, respectively. Both thaum726_compA and thaum726_compB were used as competitor probes with thaum726 (Table A1). Probes were applied in hybridization buffer at a final concentration of 0.17 ng µl^{-1}. Probes were hybridized for 2.5 hours at 46°C and washed for 15 minutes at 48°C. FITC tyramides and H_2O_2 (0.15%) were added to the amplification buffer and incubated at 46°C for 30 minutes. All samples were counterstained with 4',6-diamidino-2-phenylindole DAPI (5 µg ml^{-1}) for nonspecific DNA staining. In all cases, no probe controls and HRP-labelled nonsense probes were prepared and imaged to ensure signal specificity.

For FISH and double labelling of oligonucleotide probes (DOPE)-FISH, biofilm samples were fixed with 4% PFA and subjected to an ethanol series as described above. For thaumarchaeota and bacteria, samples were hybridized with double labeled probes, including

thaum726 double labelled with fluorescein and applied with unlabelled competitor probes (Table A1), and EUB 338 mix (Table A1), double labelled with Cy3. For AOB and *Nitrospira*, previously published probe mixes were used (Table S4). Probes were hybridized at 46°C for 90 minutes in a humid chamber containing the same formamide concentration, then washed for 15 minutes at 48°C in corresponding wash buffer (0.15 mM NaCl, 20 mM tris, 5 mM EDTA), rinsed with ice cold distilled water and dried using compressed air.

For all fluorescence microscopy, Citifluor AF1 antifadent mountant solution (Citiflour, London, UK) was applied to samples prior to fluorescence microscopy. Samples were visualized and imaged on an inverted Leica TCS SP8 confocal laser-scanning microscope (CLSM). For imaging FITC/fluorescein signals, excitation and emission wavelengths were 492 nm and 520 nm, respectively. For imaging Cy3, exciation and emission wavelengths were 514 nm and 566 nm, respectively. For imaging DAPI signal, excitation and emission wavelengths were 400 nm and 600 nm, respectively. All images were obtained with a 60X glycerol objective (total magnification of 600X). DAIME image analysis software (Daims *et al.*, 2006) was used for quantitative FISH (AOB and NOB) and quantitative CARD-FISH (AOA) analyses.

5.2.12 Combined FISH and microautoradiography (MAR)

Incubations of *Ca*. N. exaquare cells for MAR-FISH were prepared in 5 ml volumes of active enrichment culture in sterile 50 ml tissue culture flasks. Cells were incubated with 0.5 mM NH_4Cl in HEPES-buffered freshwater medium (FWM; Tourna *et al*., 2011), with calcium carbonate excluded to minimize unlabelled inorganic carbon availability. Each flask was amended with 10 µCi ^{14}C-bicarbonate (Hanke Laboratory Products, Vienna, AT). Flasks were incubated at 28°C for 24 hours in the dark, without shaking. For biofilm incubations, biofilm from SE RBC 1 and RBC 8 was sampled on July 29, 2013 and kept chilled during transport and until experimental set-up. Biofilm suspensions were diluted 1:5 in 0.22 µm-filtered RBC influent, and were pre-incubated for 3 h with 0.05 mM NH_4Cl at ambient temperature. Biofilm suspensions were then aliquoted into 5 ml volumes in 50 ml tissue culture flasks and amended with 0.5 mM NH_4Cl and 10 µCi ^{14}C-bicarbonate. Flasks were incubated at ambient temperature in the dark, without shaking, and biomass was removed and fixed after 6 h and 20 h of incubation. For both enrichment culture and biofilm samples,

incubations were prepared in duplicate. No-ammonia and killed biomass (*i.e.*, 4% formaldehyde fixed) controls were included to check for activity without added substrate, and for physical or chemical interactions of the biofilm with ^{14}C-bicarbonate, respectively. After incubation, biomass was fixed with 4% PFA and CARD-FISH was performed as described above. Microautoradiography (MAR) was performed as described earlier with modifications (Lee *et al.*, 1999; Mussman *et al.*, 2011). MAR was performed on poly-l-lysine coated coverslips. The hybridized samples were dipped in pre-warmed (45°C) LM-1 emulsion (Amersham, Little Chalfont, UK), exposed at 4°C in the dark, and developed in Kodak D19 (40 g L^{-1}) before microscopy using a Leica TCS SP8 CLSM. For many but not all samples, the MAR signals were recorded with a colour-CCD camera (DFC 450, Leica Microsystem, Wetzlar, Germany) attached to the CLSM in order to differentiate between the black silver grains and brown biofilm material included in the samples. Enrichment culture samples were exposed for 12 days, and biofilm culture samples were exposed for 9, 12, and 15 days.

5.2.13 Sequencing, genome assembly, and genome annotation

Genomic DNA for sequencing was extracted from *Ca.* N. exaquare using the Powersoil DNA Isolation Kit (MO BIO Laboratories), according to the manufacturer's instructions. Enrichment cultures containing either no organic carbon or supplemented with 0.5 mM taurine, which demonstrated a high AOA proportion compared to other cultures supplemented with organic carbon sources, were extracted separately in order to obtain two metagenomes suitable for differential abundance binning.

Genomic DNA was prepared for sequencing using the TruSeq PCR-free kit (Illumina, San Diego, CA) according to the manufactures instructions with the alternative nebulizer fragmentation, gel-free size selection and 550 bp target insert size. A mate-pair library was prepared using the Nextera Mate Pair Sample Preparation Kit (Illumina) according to the manufacturer's instructions. The resulting libraries were sequenced (2x301 bases) on a MiSeq (Illumina) using MiSeq Reagent Kit v3. Paired-end reads in FASTQ format were imported to CLC Genomics Workbench version 7.0 (CLC Bio, Qiagen) and trimmed using a minimum phred score of 20, a minimum length of 50 bases, allowing no ambiguous nucleotides and removal of Illumina sequencing adapters if found. All trimmed paired-end

metagenome reads were assembled using the CLC *de novo* assembly algorithm, using a kmer length of 63 and a minimum scaffold length of 1 kb. Mate-pair reads in FASTQ format were trimmed using NextClip (Leggett *et al.*, 2014) and only reads in class A were used for mapping.

Metagenome binning and data generation was conducted as described previously (Albertsen *et al.*, 2013) using the mmgenome R package and scripts (see: http://madsalbertsen.github.io/mmgenome/). Briefly, coverage profiles were generated by mapping reads to the metagenome scaffolds using the CLC Map Reads to Reference algorithm with a minimum similarity of 95% over 90% of the read length. Open reading frames were predicted in the assembled scaffolds using the metagenome version of Prodigal (Hyatt *et al.*, 2010). A set of 107 HMMs of essential single-copy genes (Dupont *et al.*, 2012) was searched against the predicted open reading frames using HMMER3 (http://hmmer.janelia.org/) with default settings, except the trusted cutoff was used (-cut_tc). The identified proteins were classified taxonomically using BLASTP against the RefSeq protein database (version 52) with a maximum e-value cutoff of 1e-5. MEGAN (Huson *et al.*, 2011) was used to extract class level taxonomic assignments from the BLAST .xml output file. The script network.pl was used to extract paired-end and mate-pair read connections between scaffolds using a SAM file of the read mappings to the metagenome. Metagenome binning was conducted using the mmgenome in R and can be fully recreated using the Rmarkdown file available at http://madsalbertsen.github.io/mmgenome/. The genome was manually scaffolded using paired-end and mate-pair connections aided by visualization in Circos (Krzywinski *et al.*, 2009), using the pre-processing scripts available at http://madsalbertsen.github.io/mmgenome/. Gaps were closed using GapFiller (Boetzer and Pirovano, 2012) and manually through inspections of read alignments in the CLC Genomics Workbench.

The assembled *Ca.* N. exaquare genome was annotated using both the Integrated Microbial Genomes Expert Review (IMG ER) system (Markowitz *et al.*, 2009) and the MicroScope platform for microbial genome annotation (MaGe; Vallenet *et al.*, 2009). Dot plots between genomes were constructed with PROmer (PRrotein MUMmer), implemented in IMG ER using six frame amino acid translation of the DNA input sequences. Heat maps showing comparative analysis of MetaCyc degradation, utilization, and assimilation

pathways were generated automatically in MicroScope, and updated manually to remove incorrect assignments made during the automatic heat map generation. Indicated locus tags refer to gene assignments in MicroScope. The full genome sequence of *Ca.* N. exaquare G61 and associated annotations are publicly available no both the IMG ER (IMG ID 2603880166) and MicroScope (#U7DNPY) platforms.

5.3 Results

5.3.1 Ca. *N. exaquare enrichment culture*

Candidatus Nitrosocosmicus exaquare has been growing in laboratory culture for over three years and, based on quantitative PCR of thaumarchaeotal and bacterial 16S rRNA genes, comprises >99% of cells present in the enrichment culture. *Can* N. exaquare depletes supplied ammonia and produces nitrite at near-stoichiometric levels (Fig. 5.1A). Based on thaumarchaeotal 16S rRNA gene copies, the estimated generation time of *Ca.* N. exaquare was 51.7 hours. The total density of *Ca.* N. exaquare after oxidizing 1 mM NH$_4$Cl was approximately 5.6 x 10^7 cells ml^{-1} (assuming 2 copies of 16S rRNA per cell). *Ca.* N. exaquare is able to grow over a broad temperature range, with optimal ammonia-oxidizing activity at 33°C, and total inhibition of activity at 43°C (Fig. 5.1B). Nitrite-free medium resulted in the fastest ammonia-oxidizing activity by *Ca.* N. exaquare, with activity slowing as initial NaNO$_2$ concentrations increased, and 0.5 mM NH$_4$Cl fully oxidized in the presence of up to 15 mM nitrite (Fig. 5.1C). A comparison of growth at varying initial ammonia concentrations demonstrated that *Ca.* N. exaquare had the fastest growth with starting concentrations of 0.5-1 mM NH$_4$Cl (Fig. 5.1D). Although ammonia-oxidizing activity slowed above initial concentrations of 1 mM NH$_4$Cl, initiation of ammonia-oxidizing activity persisted up to 20 mM ammonia. At 15 mM NH$_4$Cl, *Ca.* N. exaquare cells were able to oxidize all supplied ammonia to nitrite, although this required incubation for greater than six months (data not shown).
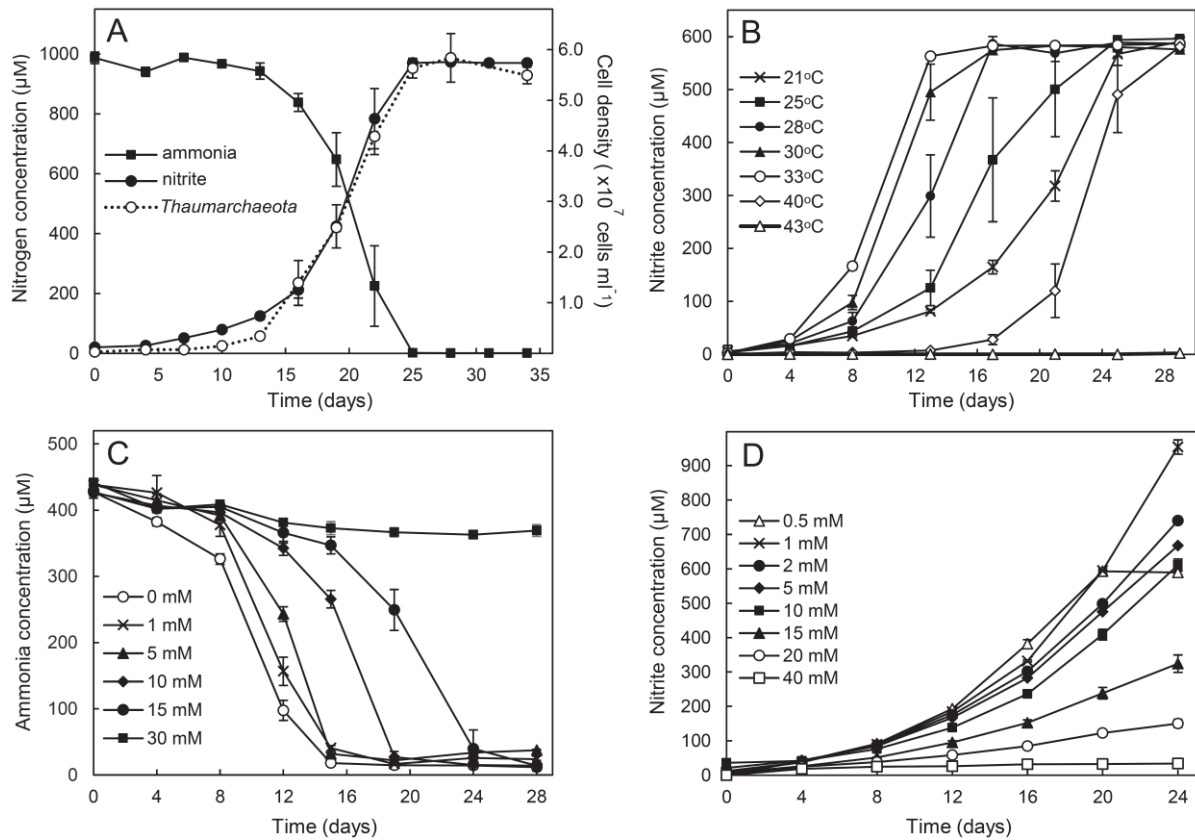
Figure 5.1 Growth of *Ca.* N. exaquare. A) Growth curve, indicating conversion of 1 mM ammonia to nitrite and corresponding increase in thaumarchaeotal cell numbers. Cell numbers were determined by thaumarchaeotal 16S rRNA gene copy numbers, halved to account for two 16S rRNA gene copies per genome. B) *Ca.* N. exaquare growth at varying incubation temperatures. C) Growth at varying initial nitrite concentrations. D) *Ca.* N. exaquare growth at varying starting ammonia concentrations. Nitrite production stopped earlier in the 0.5 mM incubation due to the depletion of available ammonia. All incubations were prepared from a 1% inoculum from an actively growing enrichment culture. All incubations were performed in the dark, without shaking. Unless otherwise indicated, the incubation temperature was 30°C and starting ammonia concentration was 0.5 mM. Error bars indicate standard error of the mean for biological triplicates. Error bars not seen are contained within the symbols.

Ca. N. exaquare cells were revived following storage at 4°C for up to 6 months (the longest time point tested), although ammonia-oxidizing activity slowed in comparison to no storage or short-term storage at the same temperature (Fig. 5.2A). In addition, cells that were cryopreserved at -80°C, using 7% DMSO or 30% glycerol as cryoprotectant, were revived after 2 weeks and 1 year of storage, with no observed loss in ammonia-oxidizing activity (Fig. 5.2B).
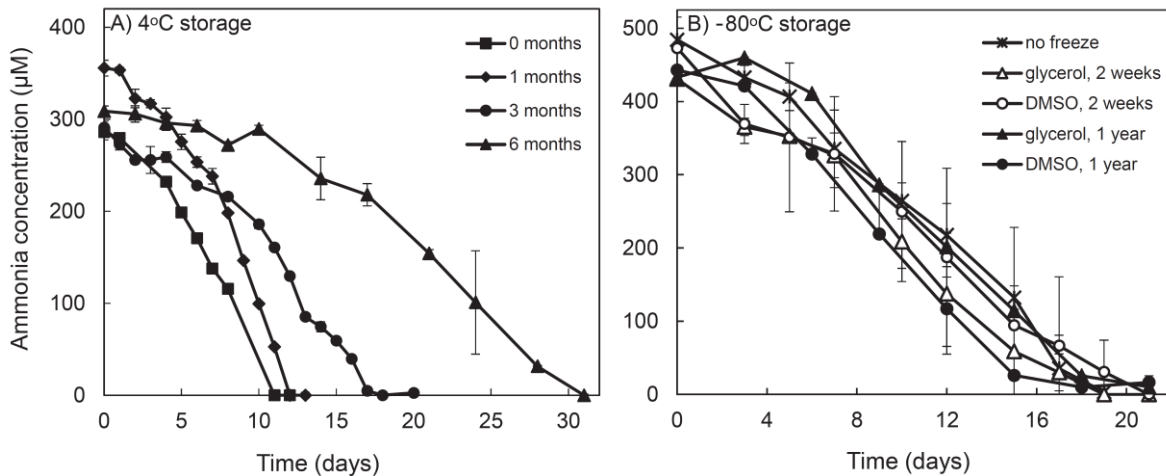
Figure 5.2 Ammonia oxidation by *Ca.* N. exaquare after storage in growth media at A) 4°C, and B) -80°C in 35% glycerol or 7% DMSO. Times indicated in legends represent storage time in a given condition. Upon inoculation of stored cells into fresh media (10% inoculum for A; 5% inoculum for B), all cultures were incubated in the dark at 28°C without shaking. Error bars indicate standard error of the mean for biological duplicates.

Based on *amoA* (Fig. 5.3) and 16S rRNA (Fig. 5.4) gene sequences, *Ca.* N. exaquare belongs to the soil Group I.1b *Thaumarchaeota* cluster, specifically in the *Nitrososphaera* sister cluster, and is related to *Candidatus* Nitrosocosmicus franklandus (Lehtovirta-Morley, Ross, *et al.*, 2016). In addition, *Ca.* N. exaquare gene sequences are closely related to environmental sequences originating from several municipal WWTPs, as well as industrial WWTPs, such as those treating waste from tanneries and oil refineries. *Ca.* N. exaquare has gene sequence identities of >99% and 100% to respective environmental *amoA* and 16S rRNA gene sequences obtained from the RBC biofilm from Guelph municipal WWTP (Canada), the environment from which *Ca.* N. exaquare originated.
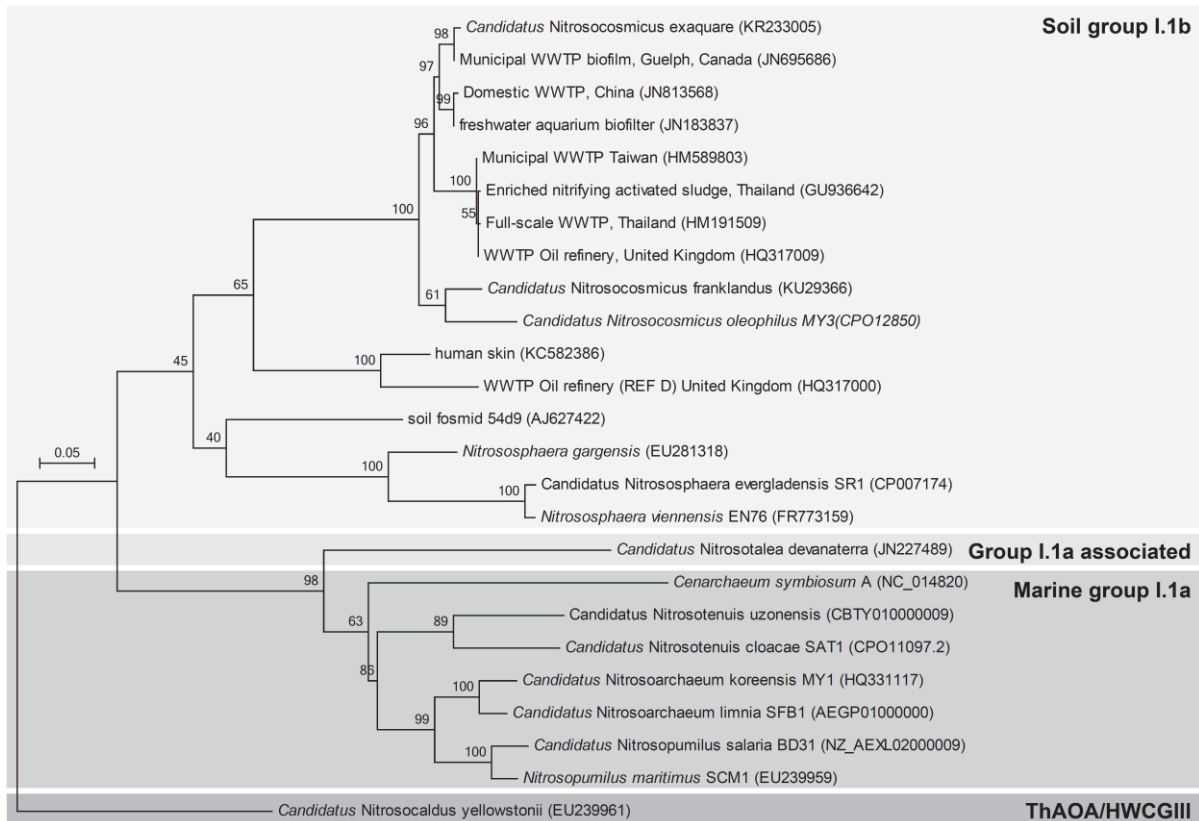
Figure 5.3 Phylogenetic affiliations of *amoA* gene sequences for *Ca.* N. exaquare and other thaumarchaeotal representatives inferred using the Maximum Likelihood method based on the General Time Reversible model. The tree is drawn to scale, with branch lengths measured as the number of substitutions per site. Bootstrap values are located above branches and are based on 500 replicates. The scale bar represents 5% nucleotide divergence.
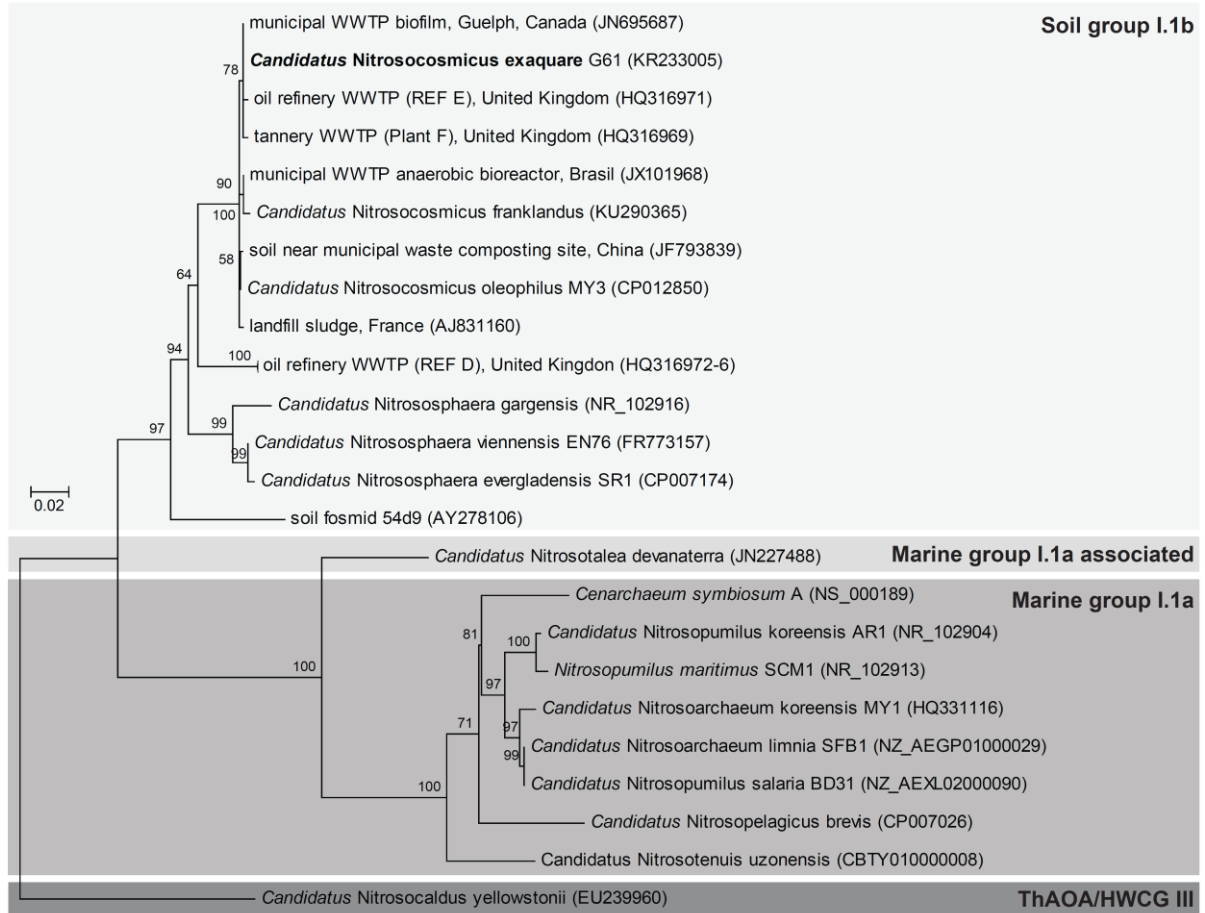
Figure 5.4 Phylogenetic affiliations of *Ca.* N. exaquare 16S rRNA gene sequence and selected *Thaumarchaeota*. The tree was inferred using the Maximum Likelihood method based on the General Time Reversible model. Bootstrap values are located above branches and are based on 500 replicates. The scale bar represents 2% nucleotide divergence.

Ca. N. exaquare cells are coccoid and approximately 1.3 µm in diameter (Fig. 5.5A-D). Cells often appeared in pairs or groups, which appeared to be covered in an extracellular matrix (Fig. 5.5B,C). Cells up to ~2 µm in diameter were observed, with large cells often having two discrete regions of nucleic acid when counterstained with DAPI (Fig. 5.5E). Environmental RBC biofilm samples from Guelph WWTP also possessed coccoid archaeal cells with a diameter of approximately 1-2 µm (Fig. 5.5F,G). *Ca.* N. exaquare cells in enrichment culture assimilated ^{14}C-bicarbonate in association with ammonia-oxidizing activity, as indicated by microautoradiographic signal in association with CARD-FISH labelled thaumarchaeotal cells (Fig. 5.5H).
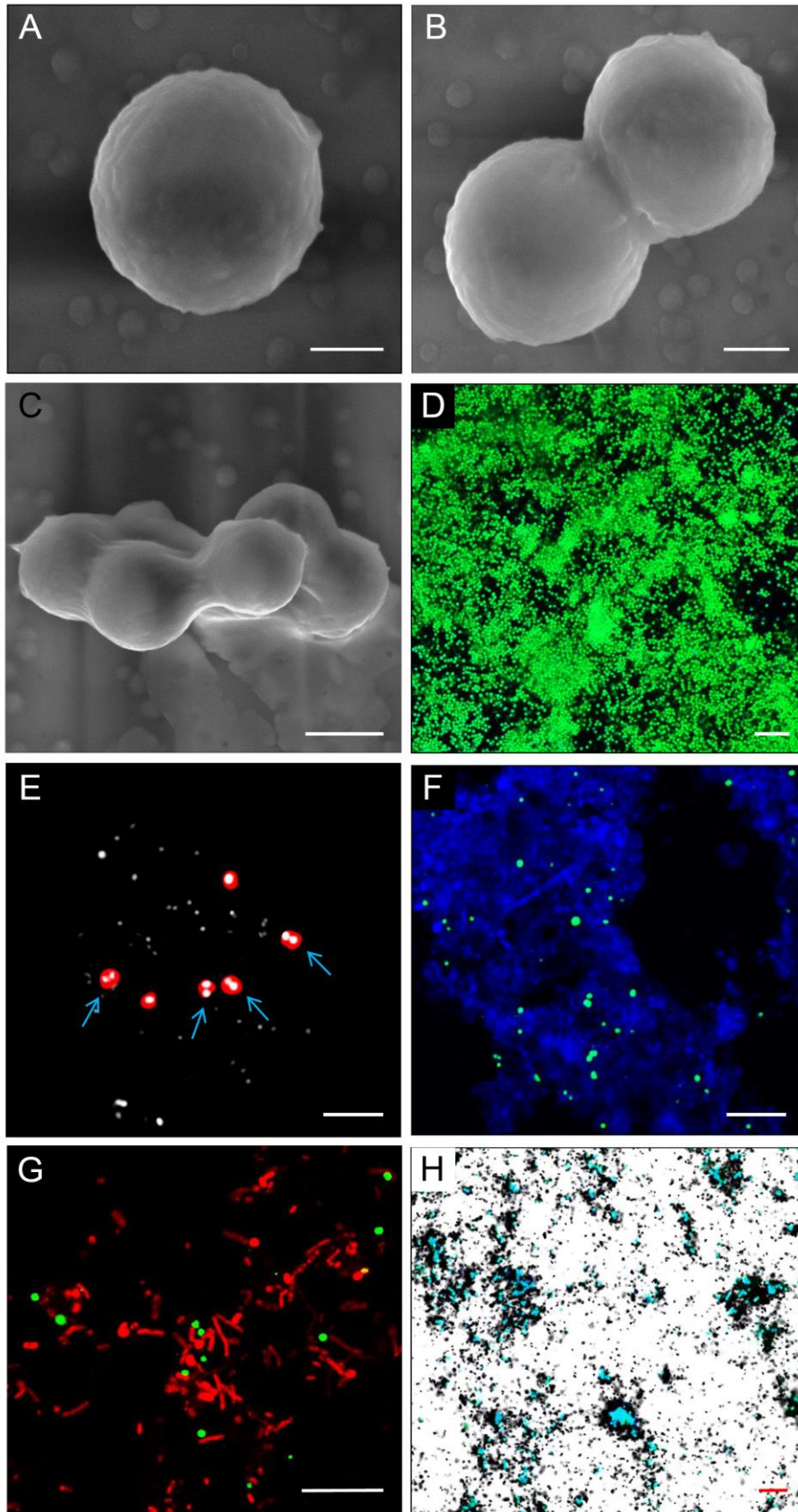
Figure 5.5 Micrographs of *Ca.* N. exaquare. Scanning electron micrographs of A) a single cell, B) cells in pairs (scale bars 400 µm) and C) cells in clusters (scale bar 1 µm). D and E) CARD-FISH images of *Ca*. N. exaquare in enrichment culture. F) CARD-FISH and G) DOPE-FISH images of thaumarchaeotal cells in Guelph RBC biofilm. H) CARD-MAR-FISH of *Ca.* N. exaquare cells labelled with ^{14}C-bicarbonate. (more details on next page). Panels D, F, and H were obtained with probe thaum726 and FITC-labelled tyramides (green) and DAPI (blue). Scale bars are 10 µm. In panel E, archaeal cells were labelled with probe Arch915 (Cy3; red) and DNA was stained with DAPI (white). The scale bar represents 5 µm. In panel G, thaumarchaeotal cells were imaged with probe thaum726 (FITC; green) and bacteria were detected with probe EUB 338 mix (Cy3; red). The scale bar represents 10 µm.

Despite incorporation of inorganic carbon, slowing of growth and ammonia-oxidizing activity of *Ca.* N. exaquare cells was observed as the culture became more highly enriched, which was a pattern reported previously for *N. viennensis* (which was alleviated by addition of 0.25-2 mM pyruvate; Tourna *et al.*, 2011). Amendment of the standard growth medium with various sources of organic carbon resulted in stimulation of growth of *Ca.* N. exaquare in comparison to a no organic carbon control (Fig. 5.6). All tested organic carbon compounds resulted in stimulation of growth, with TCA cycle intermediates malate and succinate providing the most stimulation, followed by pyruvate. Cultures amended with glycerol, butyrate, acetate, and yeast extract had much lower rates of ammonia-oxidation than other organic carbon sources, but still provided stimulation in comparison to no-organic carbon controls.
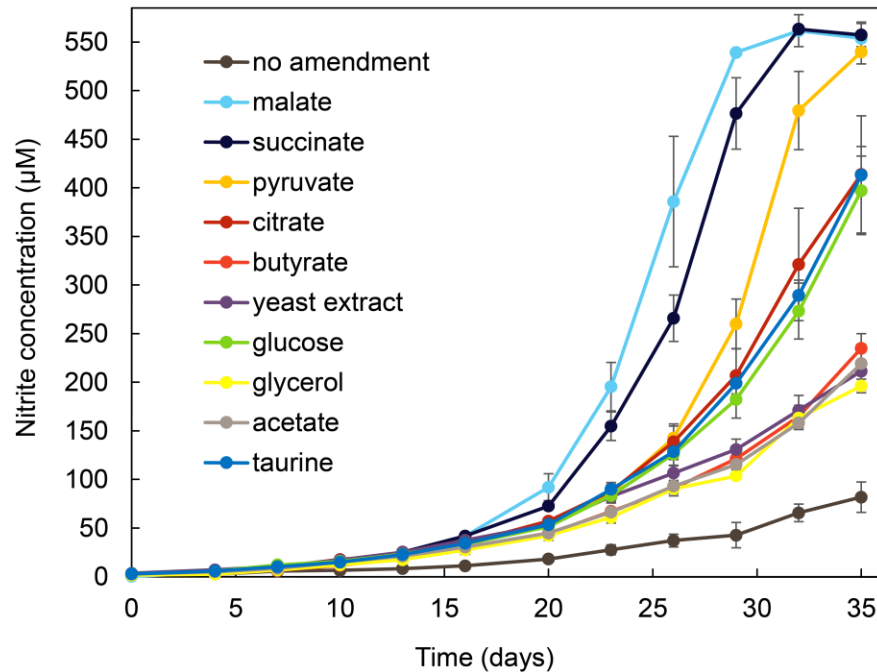
Figure 5.6 Growth of *Ca.* N. exaquare amended with organic carbon and incubated with 0.5 mM NH$_4$Cl. Error bars indicate the standard error of the mean for biological triplicates. Error bars not seen are contained within symbols.

5.3.2 Ca. N. exaquare genome

        The genome of *Ca*. N. exaquare was sequenced and assembled using metagenomic binding, resulting in one circular contiguous sequence of 2.99 megabase pairs (Mbp) in length (Fig. 5.7). This genome has a G+C content of 33.9%, 3206 predicted open reading frames, and 3162 predicted protein-coding sequences, and a coding density of 77.2%. Of the detected protein coding genes, 45.8% had no function prediction based on automated annotation (IMG ER). There were 39 tRNA genes, one 5S rRNA gene, and two copies each of 16S and 23S ribosomal RNA genes (Table 5.2). The duplicated 16S and 23S rRNA gene copies were identical, and in both cases located adjacent to each other with a 703-base intergenic spacer region, but the 5S gene was located in a distant region of the genome. Interestingly, the *Ca*. N. exaquare genome was the only available AOA genome lacking homologues to the S-layer proteins identified in *N. viennensis*. However, this genome did encode proteins involved in the synthesis of several cofactors that have been detected in other *Thaumarchaeota*, including coenzyme F_{420} and cobalamin (vitamin B_{12}). Several genes encoding enzymes associated with detoxification of reactive oxygen species (ROS) were present in the genome, including catalase, peroxidase, superoxide dismutase, alkyl hydroperoxide reductase/peroxiredoxin, and thioredoxin (Table 5.2). The catalase in *Ca*. N. exaquare (NEX_2636) belongs to the Mn-containing family of catalases, with amino acid identities of 67.9% and 57.5% to *Ca*. Nitrososphaera evergladensis and *Cylindrospernum stagnale*, respectively. The catalase gene spans the full length of the homologous Mn-dependent catalase in *Lactobacillus plantarum,* which has a relatively low identity (31.9%) but significant (E=2.81 e-32) homology. As expected, *Ca*. N. exaquare has several genes related to ammonia oxidation, including genes encoding urease and nitrite reductase (Table 5.2), in addition to *amoA*, *amoB*, and three copies of *amoC* (Fig. 5.8). The arrangement of the ammonia monooxygenase associated genes in *Ca.* N. exaquare differs from AOB and from other AOA representatives, with these genes separated by one small (2 ORFs) and three large (>150 ORFs) regions of intervening genetic material. Compared to *N. gargensis*, there is an apparent inversion of *amoB*, and a duplication and inversion of one *amoC* gene. Unlike other I.1b *Thaumarchaeota*, *Ca*. N. exaquare does not encode genes associated with chemotaxis or synthesis of flagella (Table 5.2). When comparing whole translated genomes, there is little shared synteny between *Ca*. N. exaquare and other AOA representatives, including marine

Group I.1a representative *N. maritimus* (Fig. 5.9A), and soil Group I.1b representatives *N. gargensis* (Fig 5.9B) and *N. viennensis* (Fig. 5.9C). In comparison, *N. gargensis* and *N. viennensis* have several regions of conserved gene order (Fig. 5.9D).
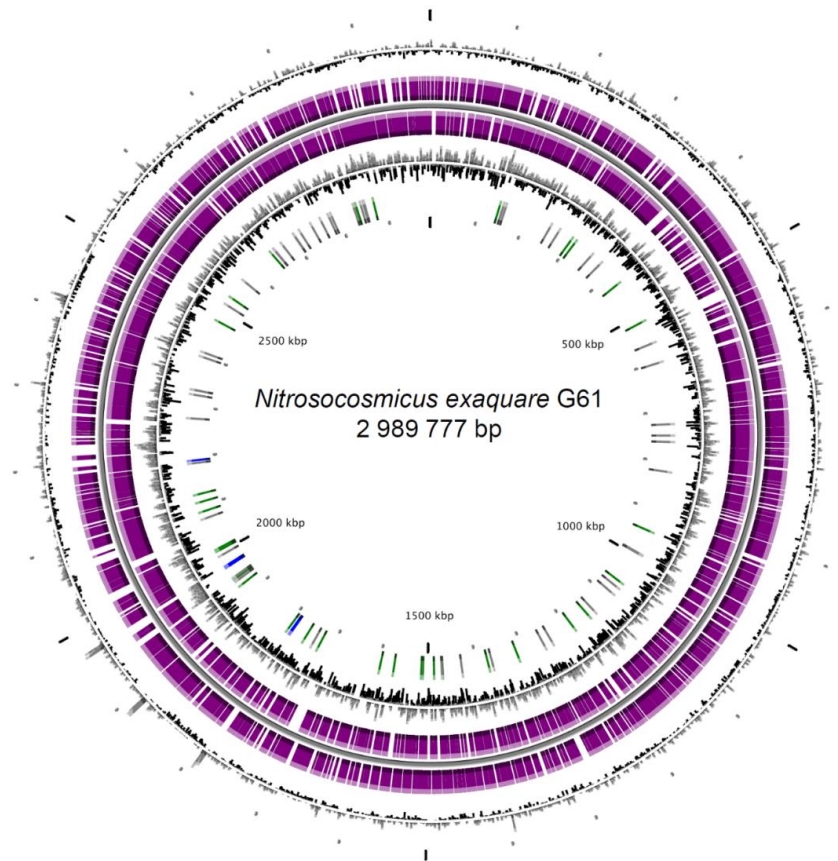
Figure 5.7 Circular genome plot of *Ca.* N. exaquare. Circles display (from the outside): (1) GC percent deviation (GC window - mean GC) in a 1000-bp window, (2) predicted coding sequences transcribed in the clockwise direction, and (3) predicted coding sequences transcribed in the counterclockwise direction, (4) GC skew (G+C/G-C) in a 1000-bp window, (5) rRNA (blue), tRNA (green), and pseudogenes (grey).

Table 5.2 Genome features of *Ca.* N. exaquare and other *Thaumarchaeota*

Genome features	*Nitrosocosmicus exaquare* G61	*Nitrososphaera. gargensis* Ga9-2[1]	*Nitrososphaera viennensis* EN76[2]	*Nitrososphaera. evergladensis* SR1[3]	*Nitrosopumilus maritimus* SCM1[4]
Cluster	I.1b	I.1b	I.1b	I.1b	I.1a
Genome size (Mb)	2.99	2.83	2.53	2.95	1.6
Contigs	1	1	1	1	1
GC (%)	33.9	48.4	52.7	50.14	34.2
Total genes	3206	3609	3167	3548	1847
Protein-coding genes	3162	3566	3027	3505	1796
Coding density (%)	77.2	81.5	87.3	83.6	90.8
16-23S rRNA	2	1	1	1	1
5S rRNA	1	1	1	1	1
tRNA	39	40	39	39	44
CRISPR loci	2	1	2	1	-
Cell division	FtsZ, Cdv	FtsZ, Cdv	FtsZ, Cdv	FtsZ, Cdv	FtsZ, Cdv
Motility/chemotaxis	-	+	+	+	-
Carbon fixation	3HP/4HB	3HP/4HB	3HP/4HB	3HP/4HB	3HP/4HB
Ammonium transporters	1	3	3	3	2
Nitrite reductase (*nirK*)	1	1	1	1	1
Urease/urea transport	+/+	+/+	+/+	+/+	-/-
S-layer proteins	-	+	+	+	+
Coenzyme F_{420}	+	+	+	+	+
Cobalamin synthesis	+	+	+	+	+
Polyhydroxyalkanoate synthesis	+	+	+	+	-
Dicarboxylate transporter (SdcS)	2	-	-	-	-
Amino acid transporters	+	+	+	+	-
Dipeptide/oligopeptide transporters	+	+	+	+	+
Catalase (Mn-containing)	1	1[a]	0	1	0
Peroxidase	1	0	0	0	0
Superoxide dismutase	1	1	1	1	2
Alkyl hydroperoxide reductases	+	+	+	+	+
Thioredoxins	+	+	+	+	+

[1]Spang et al., 2012; [2]Stieglmeier et al., 2014; [3]Zhalnina et al., 2014; [4]Walker et al., 2010
[a]truncated gene
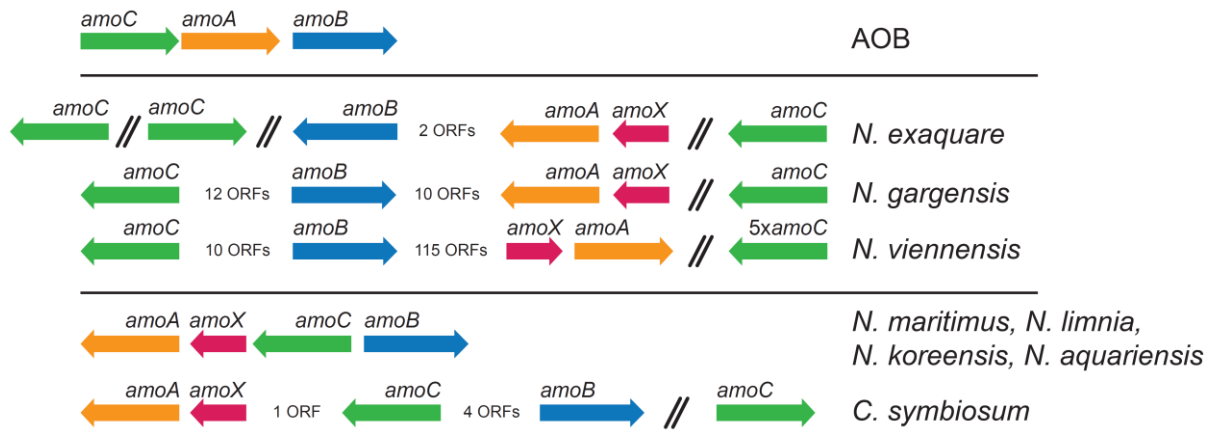
Figure 5.8 Ammonia monooxygenase gene arrangement of *Ca.* N. exaquare, selected group I.1b and I.1a thaumarchaeota, and known ammonia-oxidizing bacteria (AOB). Slashes indicate large spatial separation of genes (>150 ORFs).
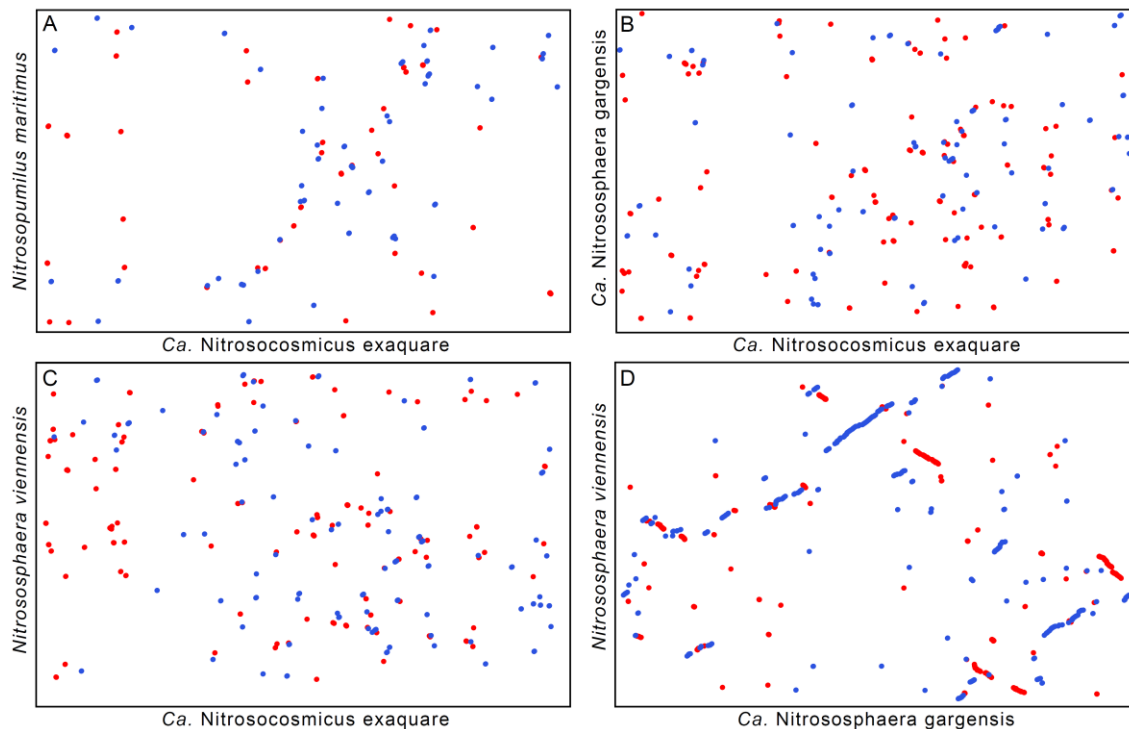
Figure 5.9 Dot plots of pairwise alignments of *Ca.* N. exaquare, *Ca.* N. gargensis, and *N. viennensis* genomes. Plots were generated using MUMmer, with alignments performed using six frame amino acid translations of the DNA input sequence. A dot represents a match between the two genome sequences, with red and blue indicating forward and reverse matches, respectively.

A summary of the MetaCyc pathways associated with the category "degradation, utilization, and assimilation" present in *Ca.* N. exaquare demonstrates overall metabolic similarity with other AOA representatives, especially with Group I.1b *Thaumarchaeota* (Fig. 5.10). For example, all AOA representatives, including *Ca.* N. exaquare, share pathways associated with proteolysis and have pathways for degradation of several amino acids (*e.g.*, arginine and aspartate). Like other thaumarchaeotal cultures, *Ca.* N. exaquare has few pathways involved in carbohydrate metabolism, with the only unique pathway involving the degradation of 2-O-α-mannosyl-D-glycerate. Automated annotation of the *Ca.* N. exaquare genome also suggested pathways associated with one-carbon (C_1) compound utilization, including methanol oxidation to formaldehyde, and formate oxidation to CO_2 (Fig. 5.10). Protein BLAST indicated that the putative methanol dehydrogenase (NEX_1558) shares high identities (>80%) to other PQQ-dependent dehydrogenases from the methanol/ethanol family, primarily from *Actinobacteria*. Protein BLAST of the formate dehydrogenase (NEX_0738) indicated high identity (>55%) to other formate dehydrogenases from microbial eukaryotes (several *Phytophthora* spp.; *Gladieria sulphuraria*) and >54% identity to formate dehydrogenases of two members of the *Firmicutes*, including *Virgibacillus* sp. and *Bacillus simplex*.
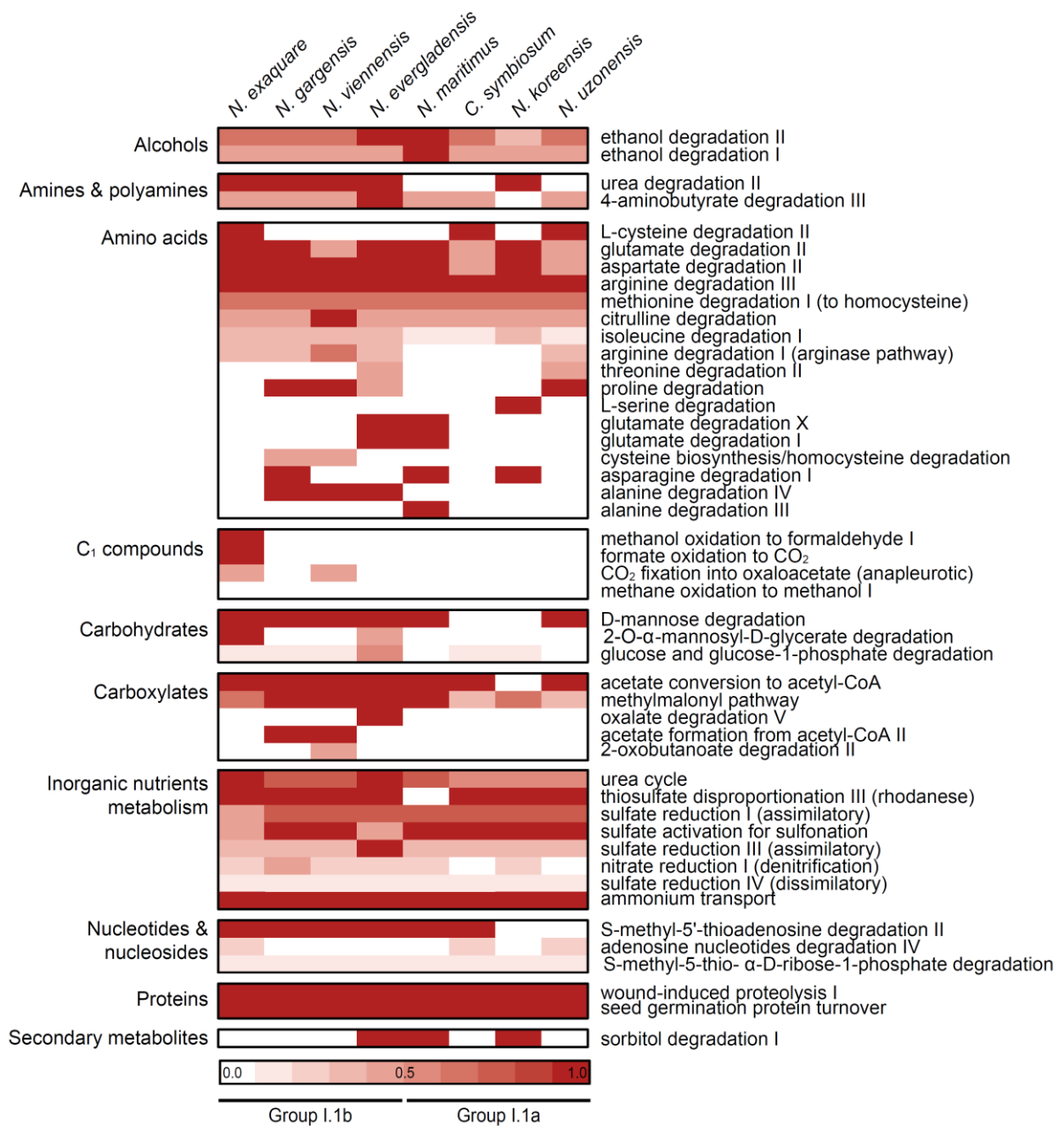
Figure 5.10 Comparative analysis of MetaCyc degradation pathways of *Ca.* N. exaquare and selected *Thaumarchaeota*. The heat map was generated using the MicroScope platform and includes all MetaCyc pathways under the category "Degradation, Utilization, and Assimilation".

5.3.3 Guelph WWTP biofilm

        Incubation of biofilm obtained from Guelph WWTP RBCs in December 2015 indicated that the biofilm actively oxidizes ammonia in the absence of inhibitors (Fig. 5.11 A-D). In all cases, 2% (wet weight) biofilm slurries depleted 1 mM NH_4Cl in four days or fewer. In both the Northeast (NE) and Southwest (SW) trains, RBC 1 samples depleted supplied ammonia faster than those from RBC 8. Consistent with this, biofilm samples from RBC 1 possessed approximately 3-fold higher numbers of ammonia-oxidizing prokaryotes (AOP) per ng of extracted DNA than corresponding RBC 8 biofilm samples (Table 5.3). Control flasks containing acetylene showed no ammonia depletion over the incubation period. In fact, acetylene controls had increasing ammonia concentrations over the incubation period, presumably arising from ammonification. In all cases, biofilm slurries containing 10 µM ATU depleted ammonia slowly compared to control flasks, but still showed complete or near-complete oxidation of 1 mM ammonia over the five-day period. This concentration of ATU did not have an inhibitory effect on actively growing *Ca.* N. exaquare cells in enrichment culture, which only showed inhibited ammonia-oxidizing activity at higher ATU concentrations (≥100 µM; Fig. 5.12A). Octyne did not inhibit *Ca.* N. exaquare at any concentration tested (up to 30 µM; Fig. 5.12B), and PTIO was strongly inhibitory at 30 µM, with total inhibition observed at 100 µM (Fig. 5.12C). As expected, both 10 µM ATU and 8 µM octyne were sufficient for inhibition of laboratory cultures of *Nitrosomonas europaea* (Fig. 5.13). Conversely, no inhibition of *N. europaea* was observed at 200 µM PTIO, and slight inhibition was observed at 400 µM PTIO.

        For NE RBC 1, neither PTIO nor octyne amendment resulted in observable inhibition of ammonia oxidation (Fig. 5.11A). In NE RBC 8, 200 µM PTIO resulted in some inhibition of ammonia oxidation, whereas 400 µM PTIO was strongly inhibitory, similar to ATU (Fig. 5.12C). In SW RBC 1, both PTIO and octyne resulted in similar inhibition of ammonia-oxidizing activity, but depletion of ammonia was only delayed by approximately 1 day (Fig. 5.12B). In SW RBC 8, both octyne and 200 µM PTIO resulted in some inhibition; 400 µM PTIO was strongly inhibitory (Fig. 5.11D). A similar experiment performed in April 2015 demonstrated that ammonia-oxidizing activity in all tested RBCs was partially inhibited by the addition of 200 µM PTIO (Fig. 5.14).

In NE and SW RBC 1, *Thaumarchaeota* comprised 55-60% of the total ammonia-oxidizing prokaryotes (AOA+AOB), as detected by qPCR, whereas the proportion of AOA was higher in NE and SW RBC 8, at 89% and 76%, respectively (Fig. 5.11; Table 5.3). Although the proportion of *Thaumarchaeota* of the total ammonia-oxidizing community was higher in RBC 8, the absolute abundance per ng extracted DNA was approximately 3-fold higher in RBC 1 biofilm samples, resulting in a higher abundance relative to the total community. The abundance of AOB-associated gene copies per ng extracted DNA was also higher in NE and SW RBC 1 biofilm samples compared to the corresponding biofilm samples from NE and SW RBC 8 (Table 5.3).
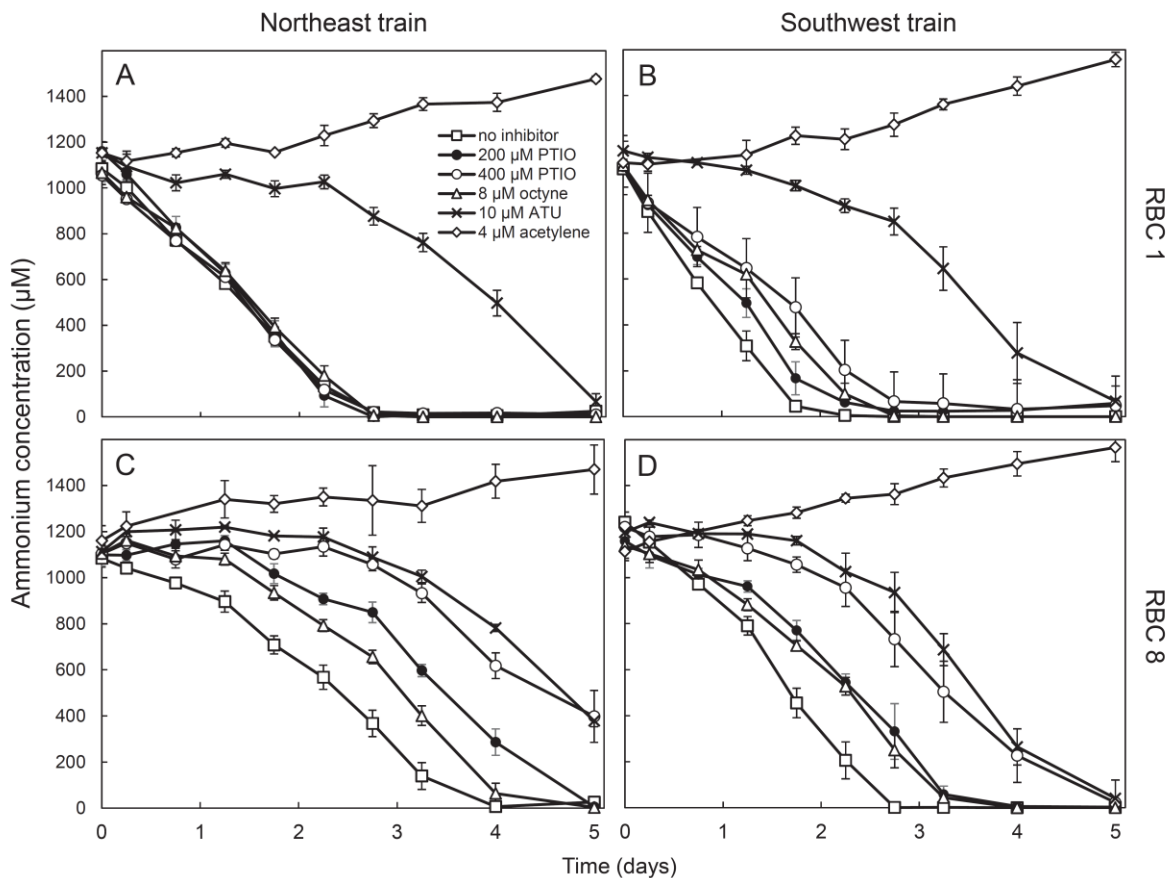
Figure 5.11 Ammonia-oxidizing activity of biofilm incubated with 1 mM NH$_4$Cl-supplemented wastewater. Error bars represent the standard error for biological triplicates. % AOA represents the proportion of AOA 16S rRNA genes compared to AOB *amoA*, as measured by qPCR. % TC represents the relative abundance of AOA in the total community (TC), as measured by qPCR of thaumarchaeotal and bacterial 16S rRNA genes (Table 5.3).

Table 5.3 Quantitative PCR data for Guelph WWTP biofilm samples (December 2015)

Biofilm Sample	AOA 16S rRNA genes*	SD	AOB amoA genes*	SD	Bacterial 16S rRNA genes*	SD	Total AOP (AOA 16S + AOB amoA genes)	% AOA of total AOP	% AOA of TC (total 16S rRNA genes)
NE RBC 1	5689	249	4750	492	144883	12041	10440	54.5	3.78
NE RBC 8	2682	96	335	96	194541	1858	3017	88.9	1.36
SW RBC 1	2789	322	1970	46	190359	1187	4759	58.6	1.44
SW RBC 8	1343	165	421	74	141691	1605	1764	76.2	0.94

*copies ng^{-1} genomic DNA (gene copies not standardized based on 16S copy number)
SD: standard deviation of technical duplicates
AOP: ammonia-oxidizing prokaryotes
TC: total community (total bacterial and thaumarchaeotal 16S rRNA genes)
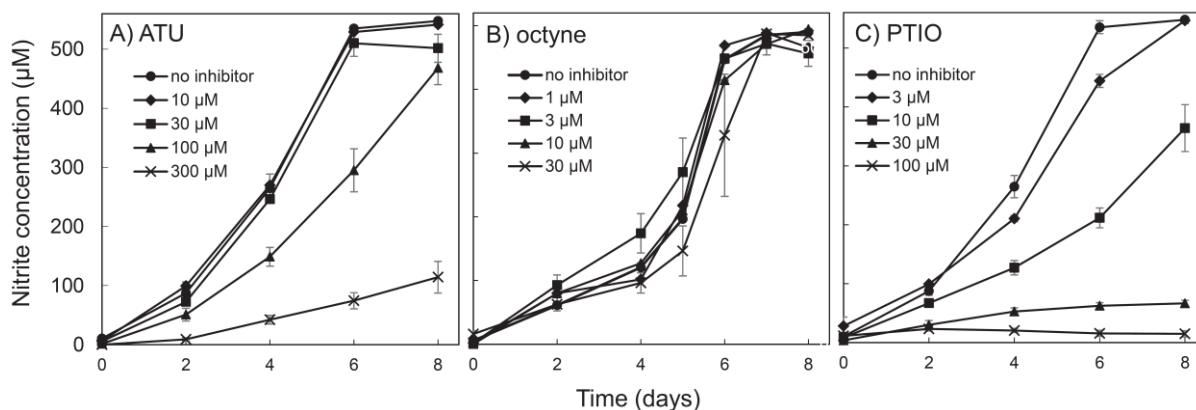
Figure 5.12 Ammonia-oxidizing activity of *Ca.* N. exaquare in the presence of various concentrations of the nitrification inhibitors, including A) ATU, B) octyne, and C) PTIO following a 10% inoculum into fresh media containing 0.5 mM NH$_4$Cl. Error bars represent the standard deviation of biological triplicates.
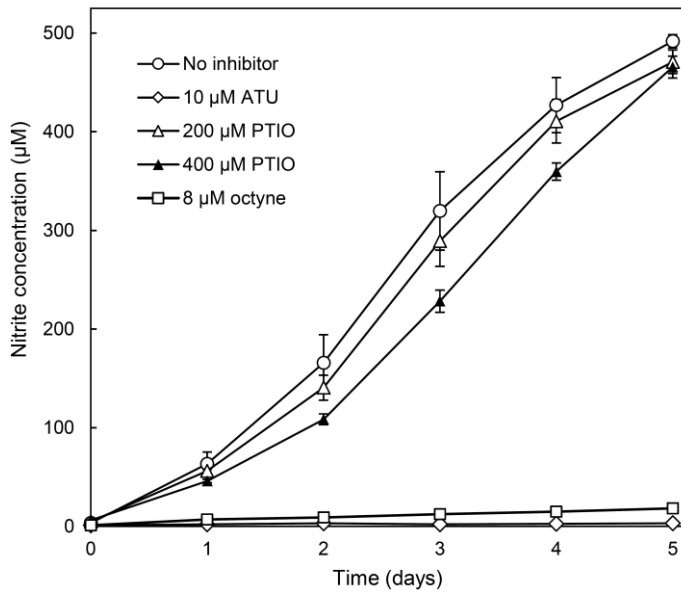
Figure 5.13 *Nitrosomonas europaea* activity with inhibitors used in this study. All incubations were performed at the same time using the same inoculum. Error bars represent the standard error of triplicate incubations. Error bars not seen are contained within symbols.
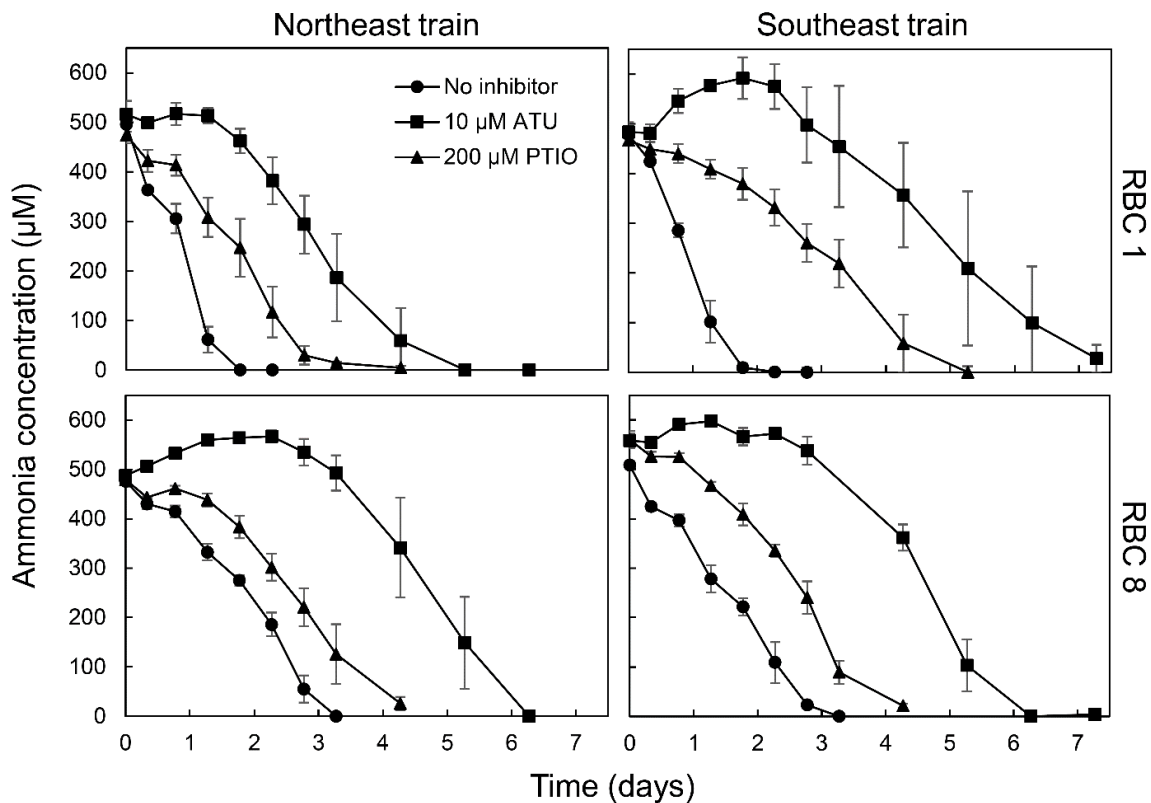
Figure 5.14 Ammonia-oxidizing activity in Guelph RBC biofilm samples (April 2015). Incubations consisted of 1% biofilm (w/v) suspended in 0.22 μm-filtered RBC influent, supplemented with 0.5 mM NH_4Cl. Error bars represent the standard error of triplicate incubations. Error bars not seen are contained within the symbols.

The community composition of nitrifying microbes was analyzed in biofilm (collected April 2013) by quantitative FISH (for AOB and NOB) and CARD-FISH (for AOA). In SE RBC 1, 1% of the biovolume of DAPI stained cells was also detected with an AOB-specific probe set; this number decreased to 0.6% in SE RBC 8. Higher relative abundances were recorded for AOA in these samples with 4.2% for SE RBC 1 and 2.4% for SE RBC 8. Interestingly, comparable amounts of nitrite-oxidizers of the genus *Nitrospira* were present in both biofilm samples. In RBC 1, 5.7% of the biovolume of the DAPI stained biomass was also labelled with the *Nitrospira*-specific probe Ntspa662, whereas the proportion decreased to 2.3% in RBC 8. No nitrite-oxidizers of the genera *Nitrobacter* or *Nitrotoga* were detected by specific FISH probes in the biofilm samples.

In CARD-FISH-MAR experiments, the *Thaumarchaeota* in SE RBC 1 and RBC 8 bilfilm did not show incorporation of ^{14}C-labeled bicarbonate in the presence of 0.5 mM ammonia after incubation for 6 or 20 hours, using MAR exposure times of 9, 12, and 15 days (Fig. 5.15). Although the MAR results were negative for many thaumarchaeotal cells, no statements could be made for other thaumarchaeotal cells that were located in close proximity to larger MAR-positive AOB- or *Nitrospira*-microcolonies. In contrast, FISH-MAR using ^{14}C-labelled bicarbonate in the presence of 0.5 mM ammonia resulted in positive signals for the AOB and *Nitrospira* microcolonies in both RBC 1 and 8 samples (Fig. 5.15). In RBC 1, following 6 h and 20 h of incubation with labeled bicarbonate and ammonia, 59% and 71% of AOB colonies, and 14% and 36% of *Nitrospira* colonies, were MAR-positive, respectively. Approximately 8% (6 hours) and 16% (20 hours) of the *Nitrospira* microcolonies in RBC 8 were MAR positive. In control FISH-MAR experiments, performed in the absence of added ammonia, no MAR positive AOB nor NOB microcolonies could be detected in RBC 8. In RBC 1, up to 10% of the AOB and 7% of the *Nitrospira* microcolonies showed a positive MAR signal, suggesting that autotrophic activity in the absence of added ammonia was most likely increased by the release of ammonia via mineralization of biomass. Control experiments with dead biofilm samples resulted in no detectable MAR-positive cells, excluding chemographic effects.
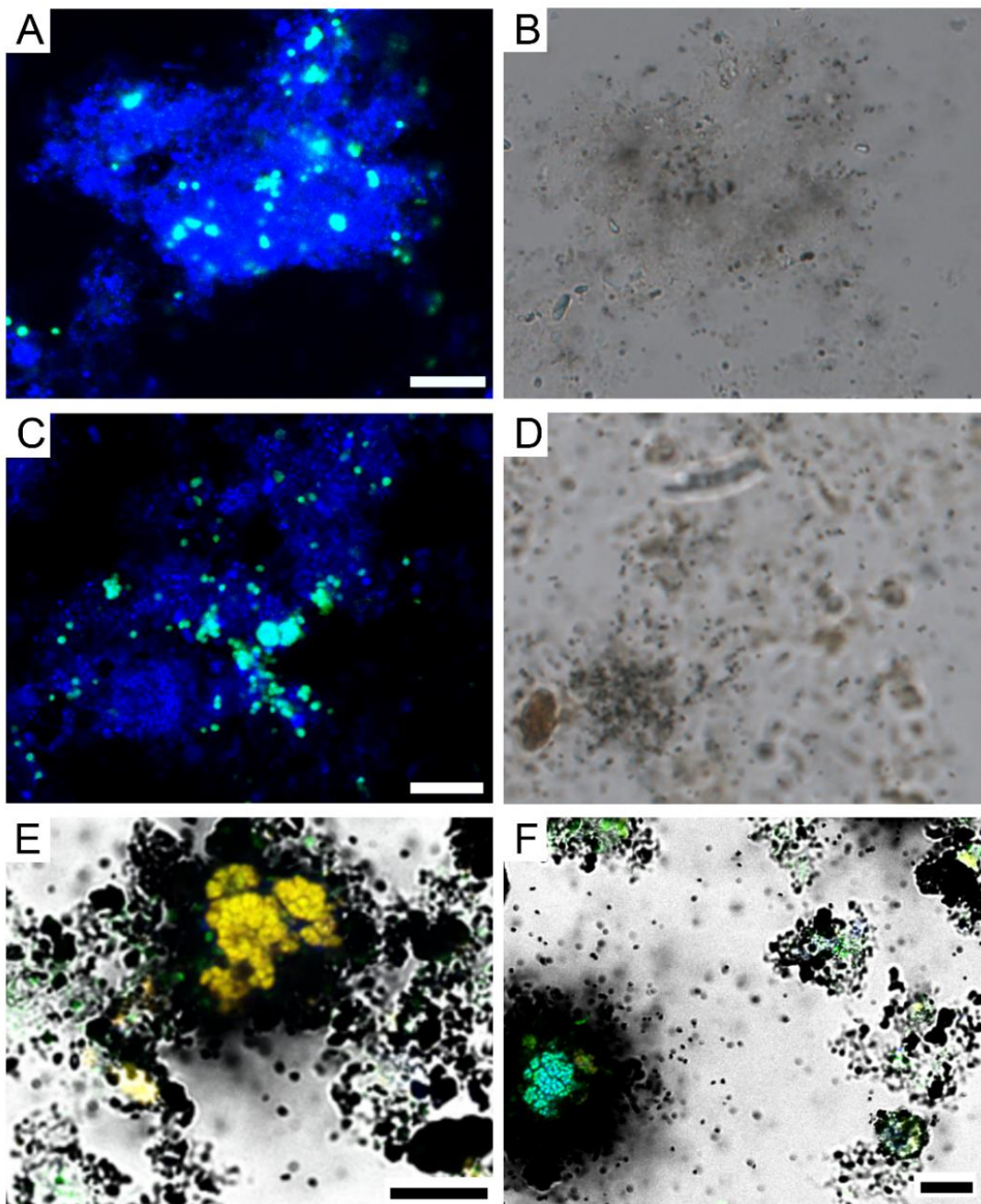
Figure 5.15 CARD-FISH-MAR for *Thaumarchaeota* in RBC 1 (A, B) and RBC 8 (C, D) biofilm. FISH-MAR for AOB (orange/yellow) and *Nitrospira* (blue) (panels E and F; both RBC 8). Green signals in panels E and F originate from the EUB338 probe mix targeting most bacteria. Microautoradiographic images were taken with the CCD black/white camera integrated in the CLSM (panels E, F) or with an external CCD colour camera (panels B and D). All scale bars represent 10 µm.

In August 2014, the SW portion of the Guelph WWTP RBCs was shut down for cleaning for the first time since their installation in 1978 (leaving the NE, NW, and SE RBC treatment trains intact). Upon sampling the regenerated biofilm approximately eight months later (April 2015), one dominant thaumarchaeotal phylotype was detected, which yielded an identical sequence and DGGE band to that detected in the uncleaned RBCs (Fig. 5.16). In addition, the bacterial communities identified post-RBC cleaning were highly similar to those of the RBCs that had never been cleaned (Fig. 5.16). In November 2015, all four treatment trains were closed for cleaning. After approximately 1 month (December 2015), biofilm from RBC 1 and 8 of the NE and SW treatment trains was sampled and used for the described activity incubations and molecular analyses (Fig. 5.11, Table 5.3). The DGGE fingerprints from this time point indicated that both bacterial and archaeal communities had re-established and were similar to pre-cleaning communities (Fig. 5.16).
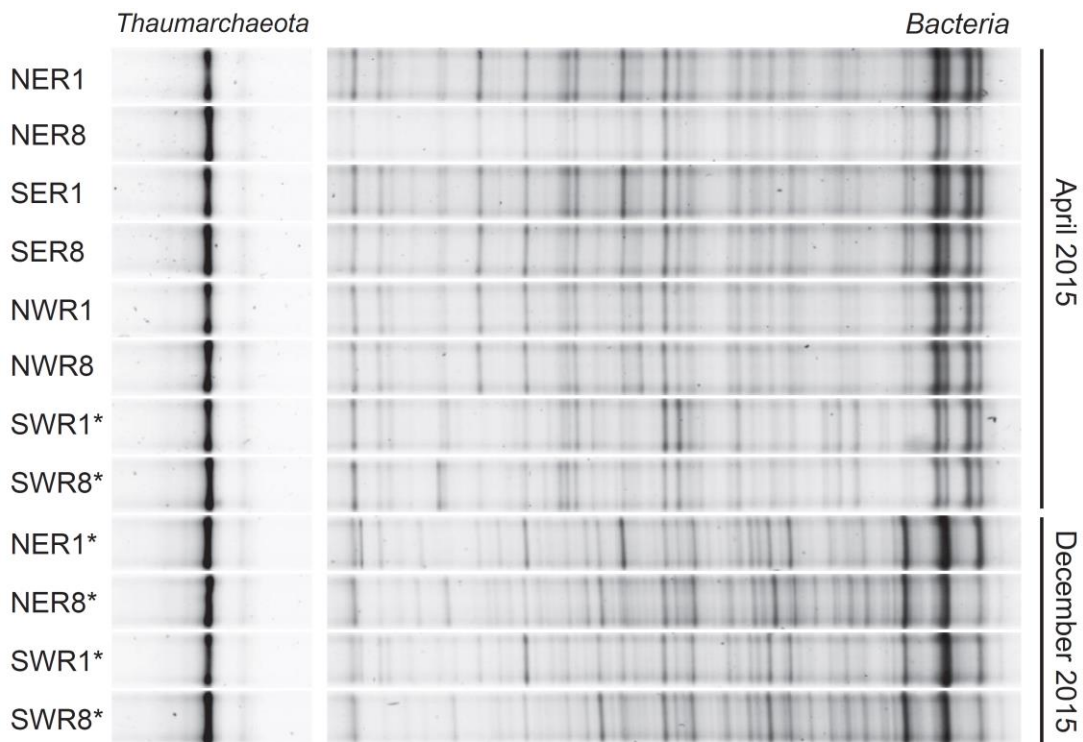
Figure 5.16 DGGE fingerprints for thaumarchaeotal and bacterial 16S rRNA gene fragments in Guelph WWTP RBCs. Cleaned RBCs are indicated with an asterisk. RBCs from April and December 2015 had ~8 months and ~1 month to regenerate, respectively.

5.4 Discussion

Little is known about the metabolism and activity of *Thaumarchaeota* members detected in WWTPs, despite the importance of these environments to human and environmental health. This work describes the cultivation of a *Thaumarchaeota* representative originating from a municipal WWTP, which in laboratory culture oxidizes ammonia, fixes inorganic carbon, and possesses a genomic repertoire consistent with a chemolithoautotrophic growth strategy. The genus name is based on the related organism *Ca.* Nitrosocosmicus franklandus (Lehtovirta-Morley, Ross, *et al.*, 2016). The species name "*exaquare*" is latin for "water running out" or "sewage", which reflects the wastewater origin of this organism.

Ca. N. exaquare produces nitrite from ammonia at near stoichiometric values (Fig. 5.1A), consistent with the activity observed from other cultured members of the phylum *Thaumarchaeota* (Könneke *et al.*, 2005; Tourna *et al.*, 2011). Estimated cell numbers follow nitrite production closely, providing evidence that energy for cell growth is derived from the oxidation of ammonia to nitrite, and that nitrite concentrations can be used as a proxy for cell growth. The calculated generation time of *Ca*. N. exaquare was 51.7 hours, which is approximately 1.5-fold higher than the reported generation time for *N. maritimus* (33 hours; Könneke *et al.*, 2005). However, this generation time is similar to that originally reported for *N. viennensis* (46 hours), although a shorter generation time of 27.5 hours was later reported (Stieglmeier, Klingl, *et al.*, 2014). *Ca.* N. exaquare is mesophilic, with optimal growth observed at 33°C (Fig. 5.1B), which is higher than the optimal temperatures of several reported Group I.1a *Thaumarchaeota* (Könneke *et al.*, 2005; Blainey *et al.*, 2011; Jung *et al.*, 2011), and similar to *N. viennensis*, which has a reported optimal growth temperature of 35°C (Tourna *et al.*, 2011). No growth was observed for *Ca.* N. exaquare above 40°C, in contrast to *N. gargensis*, which grows optimally at 46°C (Hatzenpichler *et al.*, 2008) and *N. viennensis*, which can tolerate temperatures of at least 47°C.

Ca. N. exaquare can withstand relatively high concentrations of both ammonia and nitrite (Fig. 5.1C,D). Ammonia oxidation proceeded in the presence of up to 15 mM $NaNO_2$, with complete inhibition observed at 30 mM. In comparison, *N. viennensis* was shown to oxidize ammonia with little inhibition at 10 mM $NaNO_2$ (the highest concentration tested), but ammonia oxidation ceased if ~3.5 mM nitrification-derived nitrite accumulated (Tourna

et al., 2011). In contrast, *Ca.* N. exaquare is able to fully oxidize at least 15 mM NH_4Cl, indicating that it may be better able to tolerate nitrite or other ammonia oxidation intermediates. Initiation of ammonia oxidation can be achieved with ammonia concentrations of up to 20 mM, with complete inhibition not observed until 30 mM (Fig. 5.1D). For the growth conditions used (*i.e.*, pH 8.0, 30°C), 20 mM NH_4Cl is equivalent to 1.49 mM un-ionized ammonia (NH_3). For comparison, reported inhibitory concentrations of un-ionized ammonia reported for other AOA are 18-27 µM, <9 µM, and 0.51-0.75 µM for *N. maritimus*, *Ca.* N. devanaterra, and *N. viennensis*, respectively (see Hatzenpichler, 2012 for a review). High tolerance to ammonia is perhaps unsurprising given that *Ca.* N. exaquare originates from a municipal WWTP, where ammonia concentrations would be higher than in most naturally occurring soil or aquatic environments. It has been suggested that niche partitioning occurs between AOA and AOB based on ammonia availability (Erguder *et al.*, 2009; Schleper, 2010), and several studies have supported this previously (Martens-Habbena *et al.*, 2009; Jia and Conrad, 2009; Schleper, 2010; Sauder *et al.*, 2012). However, given the global distribution of AOA across diverse environments, it is also possible that niche partitioning based on ammonia concentrations also occurs within the *Thaumarchaeota.* Similarly, nitrite concentration has been suggested as major driver for niche partitioning for nitrite-oxidizers of the genus *Nitrospira* (Maixner *et al.*, 2006).

Ca. N. exaquare is the first reported representative of the *Nitrososphaera* sister cluster within the 1.1b *Thaumarchaeota* for which a genome sequence is available, and the first from this clade originating from a WWTP. Both *amoA* (Fig. 5.3) and 16S rRNA (Fig. 5.4) gene sequences clustered with other *Thaumarchaeota* from WWTPs, both industrial and municipal, as well as other waste-related environments such as landfills and landfill contaminated soils. Studies of WWTPs have predominantly found that most or all detected thaumarchaeotal sequences affiliate with the I.1b soil group, often in the *Nitrososphaera* sister cluster (Mussman *et al.*, 2011; Kayee *et al.*, 2011; Bai *et al.*, 2012; Gao *et al.*, 2013; Limpiyakorn *et al.*, 2013). These engineered environments represent comparatively nutrient-rich environments, characterized by relatively high levels of organic carbon and ammonia. Combined with the observed high tolerance to ammonia and nitrite, this clustering could reflect an adaptation of *Ca.* N. exaquare and related *Thaumarchaeota* to relatively high nutrient environments. In addition, AOA *amoA* gene sequences from human skin (Probst *et*

al., 2013) and skin-related environments (Moissl *et al.*, 2008; Mahnert *et al.*, 2015) cluster within the Group I.1b *Nitrososphaera* sister-taxa, which suggests a common evolutionary origin between skin-associated *Thaumarchaeota* and those from engineered environments for wastewater treatment.

With cell sizes ranging from approximately 1-2 µm in diameter, *Ca.* N. exaquare is the largest reported member of the *Thaumarchaeota*. Most observed cells were ~1.3 µm (Fig.5), which is substantially larger than Group I.1a *Thaumarchaeota*, which have been reported to be very small (*e.g.*, *N. maritimus* cells are approximately 0.2 µm x 0.7 µm; Könneke *et al.*, 2005). Reported Group I.1b *Thaumarchaeota* have larger cell sizes, including *N. gargensis* and *N. viennensis*, which have cell diameters of ~0.9 µm and 0.5-0.8 µm, respectively (Hatzenpichler *et al.*, 2008; Tourna *et al.*, 2011). Known Group I.1a and I.1a-associated AOA have rod morphologies (Könneke *et al.*, 2005; Lehtovirta-Morley *et al.*, 2011; Lebedeva *et al.*, 2013), whereas coccoid morphologies have been reported for Group 1.Ib *Thaumarchaoeta*. Although *Ca.* N. exaquare has a coccoid morphology, it appears smoothly spherical (Fig. 5.5A), whereas *N. viennensis* cells are irregular, with concave areas that appear collapsed into the cell (Tourna *et al.*, 2011). The cell size and morphology of *Ca.* N. exaquare closely represents thaumarchaeotal cells previously detected by CARD-FISH in wastewater sludge samples from industrial WWTPs (Mussman *et al.*, 2011).

Ca. N. exaquare incorporated bicarbonate into biomass in association with ammonia oxidation (Fig. 5.5H) and encodes the 3-hydroxypropionate/4-hydroxybutyrate (3HP/4HB) carbon fixation pathway (Table 5.2), which is used by all known *Thaumarchaeota* (Berg *et al.*, 2007; Hallam *et al.*, 2006; Berg, 2011). In addition, it has grown in enrichment culture for several years without any externally supplied organic carbon. These results indicate that *Ca.* N. exaquare combines ammonia oxidation with autotrophic carbon fixation, as expected for a classical ammonia-oxidizing microorganism. Despite this use of inorganic carbon, *Ca.* N. exaquare is strongly stimulated by the addition of organic carbon (Fig. 5.6), which may indicate a mixotrophic metabolism, or some other indirect benefit. A variety of organic carbon sources stimulated growth in *Ca.* N. exaquare, with malate and succinate resulting in the highest level of stimulation (Fig. 5.6). *Ca.* N. exaquare may be able to incorporate these metabolic intermediates directly into its TCA cycle, which could provide precursors to biomolecules for assimilation into biomass and decrease the burden on carbon fixation

pathways. In addition, uptake of TCA cycle intermediates could provide additional reducing power in the form of NADH and/or $FADH_2$ to improve energy generation through electron transport. Given the wide variety of organic carbon compounds that stimulate the growth of *Ca.* N. exaquare (*e.g.*, glycerol, yeast extract, and butyrate), it is likely that not all organic carbon sources directly stimulate growth of *Ca.* N. exaquare, but are instead metabolized by bacteria present in the mixed culture, and that one or more central metabolites in turn stimulate growth of *Ca.* N. exaquare. A mixotrophic lifestyle for *Ca.* N. exaquare is consistent with observations in other AOA. For example, *N. viennensis* requires pyruvate for optimal growth and ammonia-oxidizing activity and, although pyruvate is assimilated, less than 10% of total biomass is derived from this substrate (Tourna *et al.*, 2011). In addition, two marine thaumarchaeotal isolates demonstrated obligate mixotrophy and incorporated carbon from α-ketoglutaric acid into biomass (Qin *et al.*, 2014). Even *N. maritimus* is stimulated by the addition of pyruvate (Stahl and de la Torre, 2012) and alpha-ketoglutaric acid (Qin *et al*., 2014), despite initial data suggesting inhibition by small amounts of organic carbon (Könneke *et al.*, 2005). In addition, marine archaea have been shown to assimilate amino acids (Ouverney and Fuhrman, 2000) and radiocarbon-based analyses of the membrane lipids demonstrate that pelagic marine *Thaumarchaeota* include a combination of autotrophs and heterotrophs, or consist of a single population with a mixotrophic metabolism (Ingalls *et al.*, 2006). Alternatively, organic compounds could directly detoxify reactive oxygen species (ROS; Kim *et al.*, 2016), or stimulate growth of heterotrophs that in turn detoxify ROS and thereby encourage growth of AOA by diminishing oxidative stress, which would be consistent with previous studies suggesting a preference by AOA for low oxygen conditions (Park *et al.*, 2010; Yan *et al.*, 2012). However, *Ca*. N. exaquare encodes a variety of genes that may confer protection from ROS. In addition to several genes shared among many *Thaumarchaeota* (*e.g.*, superoxide dismutase, alkyl hydroperoxide reductase) *Ca*. N. exaquare encodes a peroxidase, which is unique among sequenced thaumarchaeotal genomes, and a manganese-dependent catalase, which is also present in *Ca*. N. evergladensis.

At 2.99 Mbp, *Ca*. N. exaquare possesses the largest reported AOA genome (Table 5.2), and shares many features with other Group I.1b soil *Thaumarchaeota*. For example, *Ca.* N. exaquare encodes urease genes and urea transporters and has an arrangement of AMO-associated genes that more closely reflects its Group I.1b counterparts than Group I.1a AOA

or members of the AOB (Fig. 5.8). Interestingly, *Ca.* N. exaquare has a G+C content (33.9%), comparable with several Group I.1a *Thaumarchaeota*, and lower than other sequenced soil *Thaumarchaeota*, which have G+C contents of approximately 50%. The genome contains all key components for ammonia oxidation and bicarbonate fixation pathways, supporting its role as a chemolithoautotrophic ammonia oxidizer. In addition, *Ca.* N. exaquare has a similar metabolic profile to other AOA (Fig. 5.10), with few genes associated with heterotrophic pathways, such as those involved in carbohydrate metabolism. The only unique carbohydrate metabolism pathway identified in *Ca.* N. exaquare was that encoding for the degradation of mannosylglycerate, which is used as an osmolyte by hyperthermophilic archaea and bacteria, and can be used by *Escherichia coli* as a carbon and energy source. However, *Ca.* N. exaquare also encodes mannosylglycerate synthesis, as do other Group I.1b *Thaumarchaeta* (Zhalnina *et al.*, 2014; Spang *et al.*, 2012), so it is more likely that its degradation pathway relates to osmotic regulation than energy generation or carbon assimilation.

Interestingly, *Ca.* N. exaquare encodes genes for C_1 metabolism, including formate dehydrogenase, which is used by methylotrophs in the terminal step in the conversion of C_1 compounds to CO_2. Other autotrophs, such as *Nitrobacter hamburgensis, Nitrospira defluvii*, and *Nitrospira moscoviensis* encode formate dehydrogenase genes (Starkenburg *et al.*, 2008; Lücker *et al.*, 2010) and strains of both *Nitrobacter winogradskii* and *Nitrospira moscoviensis* have been shown to oxidize formate (Malavolta *et al.*, 1962; Van Gool and Laudelout, 1966; Koch *et al.*, 2015). In addition, members of *Nitrospira* from activated sludge assimilate formate during nitrite oxidation (Gruber-Dorninger *et al.*, 2015). However, formate dehydrogenase can also be used for detoxification of formate, so its presence does not necessarily indicate an ability to use formate as a source of carbon, and further work is necessary to assess whether use of formate as a source of energy and/or carbon could supplement or replace autotrophic metabolism in *Ca.* N. exaquare metabolism.

The genome of *Ca.* N. exaquare encodes two gene copies of a sodium-dependent dicarboxylate transporter (SdcS; Table 5.2), which transports succinate, malate, and fumarate in *Staphylococcus aureus* (Hall and Pajor, 2005, 2007). Expression of this transporter could provide an explanation for the observed stimulation of *Ca.* N. exaquare by succinate and malate (Fig. 5.6). In addition to being a TCA cycle intermediate, succinate is a central

compound in the 3HB/4HP cycle (Berg, 2011) and could feed directly into this carbon fixation pathway. Labelling studies with *Metallosphaera medulla*, a representative of the *Sulfolobales* that uses the 3HP/4HP cycle (Berg *et al.*, 2007), demonstrated that both supplied succinate and acetate can be incorporated into biomass, but that the majority of anabolic precursors are derived from succinate (Estelmann *et al.*, 2011). Given the presence of this transporter and the strong stimulatory effects of succinate and malate, C_4 compounds may play an important role in supplementing *Ca.* N. exaquare metabolism.

AOA have been detected and quantified in several WWTPs, and associated gene sequences often cluster within Group 1.1b *Thaumarchaeota* (Kayee *et al.*, 2011; Sonthiphand and Limpiyakorn, 2011; Mussman *et al.*, 2011; Bai *et al.*, 2012; Limpiyakorn *et al.*, 2013; Gao *et al.*, 2013, 2014). However, only one study has assessed the relative contributions of ammonia-oxidizing prokaryotes to ammonia oxidation in WWTPs. Mussman and colleagues (2011) detected *Thaumarchaeota* in industrial WWTPs treating oil refinery waste, but showed that these *Archaea* were not fixing CO_2 and were likely not primarily responsible for chemolithoautotrophic ammonia oxidation in the system, despite actively expressing *amoA* genes. This study has important implications for the assumption that contributions of AOA and AOB to ammonia oxidation correspond to detection of thaumarchaeotal *amoA* genes. Although the organisms detected by Mussman and colleagues are phylogenetically related (Fig. 5.3) and morphologically similar to *Ca*. N. exaquare, *Ca.* N. exaquare oxidizes ammonia and assimilates bicarbonate in enrichment culture and encodes a genome that also supports chemolithoautotrophic metabolism. Of course, substrate promiscuity has been reported for the ammonia monooxygenase enzyme (Pester *et al.*, 2011), and different growth conditions can elicit different physiological responses from a single organism, so the role of *Ca.* N. exaquare *in situ* is likely more complex than that observed in the laboratory when supplied solely with ammonia for energy and bicarbonate as a carbon source.

Incubations of Guelph WWTP RBC biofilm with differential inhibitors were performed to investigate the role of *Ca.* N. exaquare-like *Thaumarchaeota* in nitrification in this system. In these experiments, the differential inhibitors octyne, PTIO, and ATU inhibited ammonia oxidation to varying degrees. Octyne has been reported as a specific inhibitor of ammonia oxidation by AOB (Taylor *et al.*, 2013, 2015) and several AOA have been reported to tolerate higher concentrations of the nitrification inhibitor ATU than AOB (Hatzenpichler

et al., 2008; Shen *et al.*, 2013; Jung, Well, *et al.*, 2014; Martens-Habbena *et al.*, 2015). The results obtained from octyne and ATU should be correlated, as has been observed previously (Taylor *et al.*, 2013), but inhibition by ATU and octyne was inconsistent in this study. Several advantages have previously been reported for octyne (Taylor *et al.*, 2013), and octyne did not result in inhibition of *Ca.* N. exaquare cells in enrichment culture at any tested concentration (Fig. 5.12B). However, inhibition of AOB by octyne has not been reported in a WWTP environment, and it is possible that octyne was degraded, and therefore inactivated, by the microorganisms residing in the biofilm. Therefore, in this environment, ATU may provide a better indication of AOB-mediated activity. Two PTIO concentrations were included because lower concentrations may be insufficient in environmental samples due to production of NO from non-nitrification processes (*e.g.*, denitrification) that would use up the supplied PTIO, but higher concentrations might result in inhibition of both AOA and AOB. PTIO concentrations of 400 μM have been reported to be inhibitory to *N. multiformis* (Shen *et al.*, 2013), but this concentration only resulted in slight inhibition of *N. europaea* (Fig. 5.13). The similarity of inhibition by ATU and 400 μM PTIO in some samples (*i.e.*, NE and SW RBC 8; Fig. 5.11C,D) presents some inconsistencies and suggests that either ATU inhibits AOA in these environmental samples, that 400 μM PTIO inhibits AOB present in the biofilm, or that other organisms with unknown inhibitor profiles (*e.g.*, comammox) contribute to ammonia oxidation in this environment.

The NE RBC 1 biofilm showed no inhibition of ammonia oxidation by octyne nor PTIO at any concentration (Fig. 5.11A), although 10 μM ATU resulted in inhibition, making it most likely that AOB dominate ammonia oxidation in this RBC, and suggesting that the *Thaumarchaeota* detected in this RBC may rely on an alternate metabolism. In SW RBC 1, SW RBC 8, and NE RBC 8, PTIO amendment resulted in varying degrees of inhibition. Overall, all biofilm samples except NE RBC 1 demonstrated some inhibition by 200 μM PTIO, with stronger inhibition at 400 μM (Fig. 5.11, Fig. 5.14). In addition, higher levels of inhibition by PTIO were observed for RBC 8 biofilm activity, compared to RBC 1 biofilm of the same treatment train, suggesting that a larger proportion of the ammonia-oxidizing activity arises from AOA, which is supported by quantitative PCR data demonstrating that AOA comprise a higher proportion of the ammonia-oxidizing prokaryotes in RBC 8 compared to RBC 1 (Fig. 5.11, Table 5.2). Although questions remain regarding the efficacy

of octyne at inhibiting AOB in this biofilm and whether AOB were also inhibited using 400 μM PTIO, the observed inhibition of ammonia-oxidizing activity by 200 μM PTIO suggests that *Thaumarchaeota* contribute to ammonia-oxidizing activity of the biofilm. The previously reported relationship (Sauder *et al.*, 2012) between ammonia concentration and thaumarchaeotal abundance in this biofilm further supports the role of *Ca*. N. exaquare-like AOA as ammonia oxidizers *in situ*. However, this work only considers AOA and AOB, but completely nitrifying *Nitrospira* organisms (*i.e.*, comammox bacteria; van Kessel *et al.*, 2015; Daims *et al.*, 2015) with unknown sensitivities to these inhibitors could be contributing to nitrification activity in the biofilm, as they have also been detected in biofilters for drinking water treatment (Pinto *et al.*, 2016). The fact that *Nitrospira* abundance in the system was similar to the abundance of *Thaumarchaeota*, and higher than that of AOB, might indeed indicate the presence of comammox bacteria in this system.

The CARD-MAR-FISH data from the RBC biofilm samples indicated that when supplied with ammonia, both AOB and *Nitrospira* (NOB or comammox bacteria) are clearly MAR positive, whereas there was no evidence for bicarbonate fixation by *Thaumarchaeota* (Fig. 5.15). This implies that the detected *Thaumarchaeota* cells were either predominantly relying on an alternative metabolism, or that they were oxidizing ammonia for energy but assimilating a carbon source other than bicarbonate for growth. Most observed AOB in RBC 1 and RBC 8 showed strong MAR signals, which is consistent with the strongly inhibitory effect of ATU, but not with the weak inhibitory effect of octyne. Although MAR-FISH and inhibitor experiments were conducted at different points in time, the abundances of AOA and AOB were similar in biofilms at these times. Positive MAR signals were observed for some *Nitrospira* microcolonies (Fig. 5.15), which could have arisen from either nitrite-oxidizing or comammox activity. However, several non-CO_2-fixing *Nitrospira* were also observed in RBC 8, which could indicate growth based on other metabolic activities (*e.g.*, hydrogen, formate), as described recently (Koch *et al.*, 2015, 2014).

Ca. N. exaquare is the first Group I.1b *Thaumarchaeota* representative cultivated from a WWTP, and clusters phylogenetically with many other AOA originating from WWTPs. The observed laboratory activity and its genetic complement suggest that *Ca.* N. exaquare is able to thrive as a classic ammonia-oxidizing microorganism, which may be stimulated by organic carbon. In the wastewater treatment system from which it originates,

both qPCR and qFISH indicate that *Thaumarchaeota* consistently outnumber AOB. In addition, the rapid regeneration of the *Ca*. N. exaquare-like *Thaumarchaeota* population following two massive disturbances indicates that these organisms are active, reproducing, and robust within the RBC biofilm environment. However, the metabolic role played *in situ* by *Ca*. N. exaquare appears to be more complex than strictly chemolithoautotrophic nitrification, and it is possible that the relatively high abundance of *Thaumarchaeota* could be explained by growth primarily on other substrates present in the biofilm. Further work is needed to elucidate the contributions of *Ca*. N. exaquare-like *Thaumarchaeota* to ammonia oxidation in this system and to assess the *in situ* potential for mixotrophic or alternative metabolism.

Chapter 6

Nitric oxide scavengers differentially inhibit ammonia oxidation in ammonia-oxidizing archaea and bacteria[5]

6.1 Introduction

Since the discovery of AOA a decade ago (Venter *et al.*, 2004; Könneke *et al.*, 2005), extensive research has focussed on the abundance of AOA and AOB in a wide range of terrestrial and aquatic environments. Although AOA outnumber AOB in a variety of natural and engineered environments (Leininger *et al.*, 2006; Wuchter *et al.*, 2006; Tourna *et al.*, 2008; Sauder *et al.*, 2011), AOB outnumber AOA in other sampled environments, including those obtained from several wastewater treatment plants (WWTPs) and eutrophic estuary sediments (Mosier and Francis, 2008; Wells *et al.*, 2009; Limpiyakorn *et al.*, 2011). In addition to quantifying the abundance of AOA and AOB, methods for investigating ammonia-oxidizing activity are critical for understanding the biogeochemical contributions of detected organisms. Many efforts have been made to assess the relative contributions of AOA and AOB to environmental ammonia oxidation. For example, several studies have compared target gene or transcript abundances with nitrification potential (Wuchter *et al.*, 2006; He *et al.*, 2007; Offre *et al.*, 2009; Yao *et al.*, 2011). Other approaches include use of DNA and RNA stable-isotope probing for assessing incorporation of labelled substrate into AOA or AOB biomass during nitrification (Jia and Conrad, 2009; Zhang *et al.*, 2010, 2012; Pratscher *et al.*, 2011; Xia *et al.*, 2011) and microautoradiography-fluorescence *in situ* hybridization (MAR-FISH) for detecting uptake of ^{14}C-labelled bicarbonate in association with ammonia oxidation (Hatzenpichler *et al.*, 2008; Mussman *et al.*, 2011). Although these methods provide insight into the activity of AOA and AOB, they are typically labour intensive and are limited by sample throughput, the need for specialized equipment, and the high cost of labelled substrates. The use of differential inhibitors provides a simple and rapid

---

method for determining the relative contributions of AOA and AOB to nitrification in an environment of interest, which can be used alone or in conjunction with other methods for determining activity and abundance of target groups.

Both AOA and AOB use ammonia as a substrate for generating energy, but they differ in their proposed pathways for oxidizing ammonia. Importantly, these differences allow for selective inhibition of each group. Although both AOA and AOB produce hydroxylamine from ammonia (Vajrala *et al.*, 2013), the proposed downstream pathway differs for AOA and AOB, with only AOA utilizing nitric oxide (NO) as an intermediate (Walker *et al.*, 2010; Stahl and de la Torre, 2012). Some compounds, such as acetylene, act as suicide substrates and inhibit ammonia oxidation irreversibly in both AOA and AOB (Offre *et al.*, 2009; Taylor *et al.*, 2010). For selectively inhibiting ammonia oxidation in AOB, allylthiourea (ATU) and octyne have been commonly used (Hatzenpichler *et al.*, 2008; Shen *et al.*, 2013; Taylor *et al.*, 2013; Martens-Habbena *et al.*, 2015). Selective inhibition of ammonia oxidation by AOA has been achieved with 2-phenyl-4,4,5,5-tetramethylimidazoline-1-oxyl 3-oxide (PTIO; Yan *et al.*, 2012; Shen *et al.*, 2013; Jung, Well, *et al.*, 2014; Martens-Habbena *et al.*, 2015), a nitric oxide scavenger that catalyzes the conversion of nitric oxide (NO) to nitrite (NO_2^-) or nitrate (NO_3^-), and has been used extensively in medical and physiological studies. PTIO has been shown to inhibit ammonia oxidation in pure cultures of AOA representatives *Nitrosopumilus maritimus* and *Nitrososphaera viennensis* at significantly lower concentrations than for AOB representatives (Shen *et al.*, 2013; Martens-Habbena *et al.*, 2015), presumably through its interaction with nitric oxide. In addition, PTIO has been used to inhibit ammonia oxidation in environmental samples with high AOA abundances, such as marine water samples (Yan *et al.*, 2012; Martens-Habbena *et al.*, 2015).

Despite the utility of PTIO, it is expensive (see Table 6.1), a factor that may render large-scale incubation experiments prohibitive for many laboratories. Moreover, the specificity of PTIO as a nitric oxide scavenger has been questioned, and it has been demonstrated that the effects of PTIO are diverse and include reactions with other nitrogenous compounds (Pfeiffer *et al.*, 1997). However, there are several inexpensive and commercially available compounds that scavenge nitric oxide. In this study, I assessed four

known nitric oxide scavengers, including caffeic acid, curcumin, methylene blue hydrate, and trolox, for their suitability as differential inhibitors of AOA and AOB. The objective of this study was to assess previously untested nitric oxide scavengers, which could represent alternatives to PTIO, for their ability to differentially inhibit AOA and AOB. In addition, this study aimed to provide support for the role of nitric oxide in the thaumarchaeotal ammonia oxidation pathway by demonstrating differential inhibition by a variety of nitric oxide scavengers. These data show that in axenic and enrichment cultures, all nitric oxide scavengers tested demonstrated differential inhibition of AOA and AOB, providing further support for the role of nitric oxide in thaumarchaeotal ammonia oxidation.

Table 6.1 Cost comparison of nitric oxide scavengers (list prices from Sigma)

Compound	Cost per gram ($CDN)	Cost per incubation ($CDN)*	Working concentration (µM)
Carboxy-PTIO	4250.00	2.48	100
Trolox	72.40	0.68	1500
Methylene blue hydrate	33.70	<0.01	3
Caffeic acid	25.70	<0.01	100
Curcumin	8.12	<0.01	100

* Costs per incubation are based on determined working concentrations

6.2 Materials and Methods

6.2.1 Reagents

Five nitric oxide scavengers were tested in this study, including carboxy-PTIO (PTIO), caffeic acid, 6-hydroxy-2,5,7,8-tetramethylchroman-2-carboxylic acid (trolox), curcumin, and methylene blue hydrate (MBH), all of which were obtained from Sigma (St. Louis, MO, USA). Stock solutions were freshly prepared in water (caffeic acid and MBH), directly in the growth medium (trolox), or in dimethyl sulfoxide (DMSO; curcumin), and sterilized using a 0.22 µm filter. PTIO was used at a concentration of 100 µM, which has been reported to be effective against both Group I.1a and I.1b *Thaumarchaeota* (Shen *et al.*, 2013; Martens-Habbena *et al.*, 2015). All other nitric oxide scavengers were tested at a

variety of concentrations, following preliminary experiments to determine appropriate concentration ranges for each chemical.

6.2.2 Incubations of cultures of ammonia-oxidizing archaea and bacteria

Three distinct AOA representatives were tested, including *Nitrosopumilus maritimus* SCM1, *Ca*. N. aquariensis, and *Ca*. N. exaquare. *Nitrosomonas europaea* was included as a betaproteobacterial AOB representative, obtained from the American Type Culture Collection (ATCC 19718). Incubations with *N. europaea*, *Ca*. N. aquariensis, and *Ca*. N. exaquare were performed in a mineral salts medium used previously for growth of both AOA and AOB (Lebedeva *et al.*, 2005; Hatzenpichler *et al.*, 2008). Briefly, the medium contained per L: 0.05 g KH_2PO_4, 0.075 g KCl, 0.05 g $MgSO_4·7H_2O$, 0.58 g NaCl, and 4 g $CaCO_3$. In addition, the medium was supplemented with 1 ml selenite-tungstate solution and 1 ml trace element solution (Widdel and Bak, 1992). The pH of this medium was approximately 8.5, and buffered by added $CaCO_3$. *N. maritimus* was grown in a synthetic crenarchaeote medium (SCM) using a previously published recipe, with a pH of 7.5, buffered with HEPES (Martens-Habbena and Stahl, 2011). All media were supplemented with 0.5 mM NH_4Cl. Cultures were maintained in 125 ml glass serum bottles with aluminum foil caps, with 25 ml culture volumes. Incubations were performed in triplicate at 30°C, in the dark, and without shaking. Biological triplicates were set up on the same day, using the same inoculum and batch of growth medium. Ammonia concentrations were monitored over the course of the experiment, and all incubations were sampled until ammonia was depleted in the no-inhibitor controls of the corresponding organism. Each flask was inoculated using a 10% transfer from an active culture, except for *N. maritimus*, for which a 1% inoculum was necessary to achieve complete oxidation of ammonia. Samples of cultures collected for water chemistry analyses were stored at -20°C until processing.

6.2.3 Incubations of an environmental sample

Biofilm was obtained from a Fluval 404 Canister Filter sponge (Hagen, Baie d'Urfé, QC, Canada) from a freshwater aquarium, which was previously determined to have a high numerical abundance of AOA that was stable over time (sample code FW27; Sauder *et al.*, 2011; Chapters 2 and 3). The biofilm-covered sponge was squeezed into aquarium

water (pH 8.3), and the resulting slurry was amended with 0.5 mM ammonia chloride. All incubations were performed in triplicate and were incubated at room temperature in the dark in 125 ml serum bottles with aluminum foil covers. Nitric oxide scavengers were added to appropriate flasks, including PTIO at 100 µM, caffeic acid at 100 µM, and methylene blue hydrate at 3 µM. Chosen concentrations reflected those that differentially inhibited AOA and AOB in laboratory cultures (see Table 6.2 and Fig. 6.2).

6.2.4 Ammonia and nitrite measurements

Ammonia and nitrite measurements were performed at all time points for all water samples originating from laboratory cultures. Nitrite concentrations are displayed for cultures because nitrite is a direct product of ammonia oxidation and has been shown to follow growth of ammonia oxidizers (*e.g.,* Tourna *et al.*, 2011). For incubations of the aquarium biofilm, ammonia concentrations are displayed because the mixed biofilm community, including nitrite-oxidizing bacteria (NOB), prevents accumulation of nitrite. In addition, high background concentrations of nitrate prevent accurate measurements of total oxidized nitrogen.

Nitrite concentrations were measured colourimetrically using the Greiss reagent system in 96-well plates, as described previously (Miranda *et al.*, 2001). Briefly, samples were diluted 1:10 in NH_4Cl-free mineral salts medium (10 µL sample, 90 µL diluent) and 100 µL of Greiss reagent was then added. Sample absorbances were compared to standard curves prepared from twofold dilutions of sodium nitrite within the linear range of 2.5-250 µM. Samples and standards were incubated at room temperature for 10 minutes prior to measurement at 550 nm using a Filtermax F5 Multi-Mode Microplate Reader (Molecular Techniques, Sunnyvale, CA). All technical measurements were performed in duplicate.

Ammonia concentrations were measured using Nessler's reagent, as described previously (Meseguer-Lloret *et al.*, 2002), and all reported ammonia concentrations represent total ammonia ($NH_3 + NH_4^+$). Briefly, samples were diluted 1:2 in NH_4Cl-free medium, and then 1 volume (50 µL) of each Na^+ K^+ tartrate (35.4 mM) and Nessler's reagent were added to 50 µL of diluted sample. Sample absorbances were compared to standard curves with a range of 5-500 µM, which were prepared from 2-fold dilutions of ammonia chloride. Assay

plates were incubated at room temperature for 30 minutes and measured spectrophotometrically at 450 nm using a FilterMax F5 Multi-Mode Microplate Reader (Molecular Techniques). All technical measurements were performed in duplicate.

6.2.5 Calculation of EC$_{50}$

The half maximal effective concentration (EC$_{50}$), representing the inhibitor concentration that reduces the amount of ammonia oxidized by 50%, was calculated using SigmaPlot 12.5 (Systat Software Inc., Chicago, IL). This value was calculated by plotting the inhibitor concentration against activity inhibition for each inhibitor and test organism. The line of best fit and standard error were determined with the Standard Curves macro in SigmaPlot 12.5. A four parametric logistic equation, y= min+(max-min)/(1+(x/EC50)^(-Hillslope)), was calculated by log transforming the X axis scale and applying a dynamic curve fit with a curve fit tolerance of 1.0e-10 and 1000 maximum fit iterations. The "predict unknowns" feature was used to calculate EC$_{50}$.

6.3 Results and Discussion

This study assessed the inhibitory effects of several known nitric oxide scavengers on three AOA representatives, including two Group I.1a *Thaumarchaeota* representatives (*N. maritimus* and *Ca*. N. aquariensis), and one Group I.1b representative (*Ca.* N. exaquare). We also tested these compounds on *N. europaea*, a model AOB representative that has been extensively studied and has provided much of the current knowledge about AOB ecology, physiology, and biochemistry (Sayavedra-Soto and Arp, 2011). Because all microorganisms tested in this study oxidize ammonia to nitrite, nitrite production was used as an indicator of ammonia-oxidizing activity. Compared to no-inhibitor controls, addition of 100 µM PTIO completely inhibited nitrite production in all tested AOA cultures, and did not result in inhibition in *N. europaea* (Fig. 6.1A-D). These results are consistent with previously calculated EC$_{50}$ values of 18.3 µM for *N. viennensis*, and >400 µM for *N. multiformis* (Shen *et al.*, 2013). In addition, Martens-Habbena and colleagues (2015) showed total inhibition of *N. maritimus* at 100 µM PTIO, and little or no inhibition of a several AOB representatives at this concentration, including *N. europaea*. These results demonstrate that PTIO is effective at

inhibiting ammonia oxidation in two previously untested strains of AOA, thereby providing further support for the efficacy of PTIO as a differential inhibitor.

Caffeic acid is a phenolic intermediate of lignin biosynthesis that can be isolated from a variety of plants, including barley, ferns, and eucalyptus bark (Sueishi *et al.*, 2011). In this study, caffeic acid was tested in the range of 10-300 µM. All tested concentrations resulted in complete inhibition of ammonia oxidation by *N. maritimus* and *Ca*. N. aquariensis (Fig. 6.2A, B). Calculated EC_{50} values for both of these strains were below the lowest tested concentration of this inhibitor (<10 µM; Table 6.2). *Ca*. N. exaquare was strongly inhibited by 100 µM caffeic acid and completely inhibited at 300 µM, with an EC_{50} value of 84.3 µM (Fig. 6.2C, Table 6.2). Conversely, *N. europaea* was not inhibited by any of the tested concentrations, and had an EC_{50} value higher than the highest tested concentration (>300 µM; Fig. 6.2D, Table 6.2). These results suggest that caffeic acid could be an effective alternative to PTIO for differential inhibition of AOA and AOB.
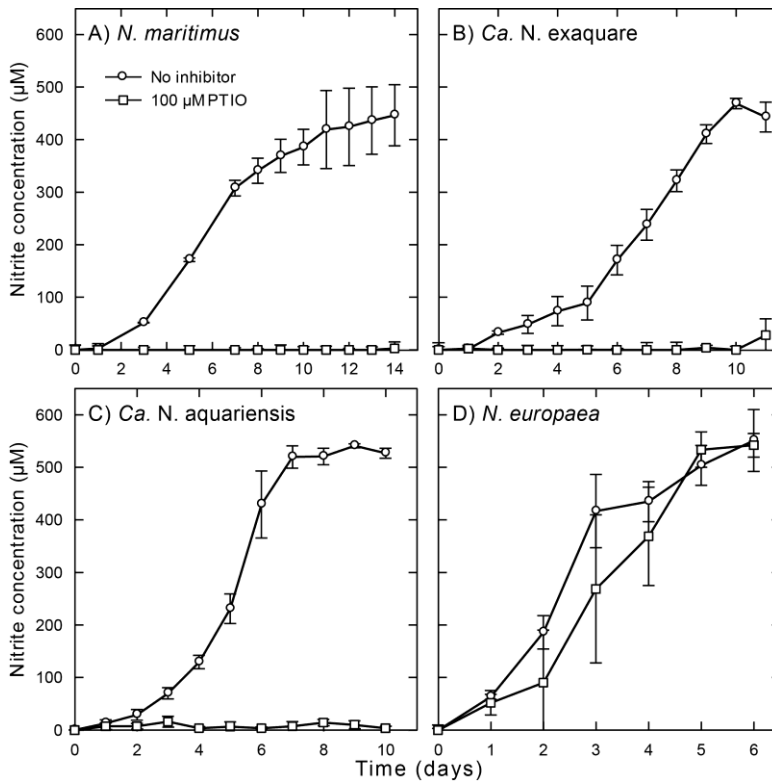
Figure 6.1 Effect of PTIO on ammonia-oxidizing activity of AOA representatives, including A) *N. maritimus*, B) *Ca*. N. exaquare, C) *Ca*. N. aquariensis, and D) *N. europaea*. Error bars indicate standard deviations of biological triplicates.
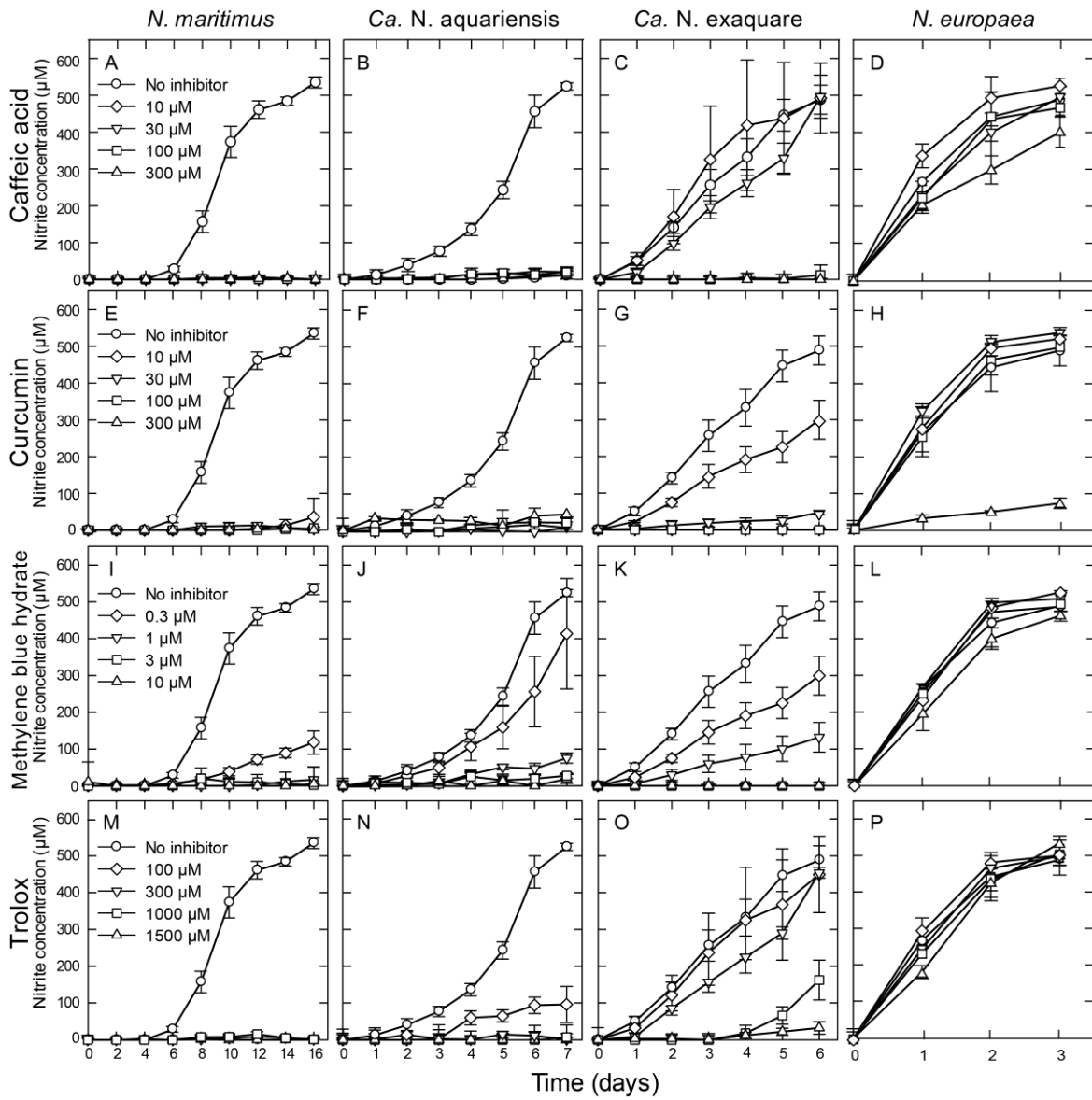
Figure 6.2 Effect of nitrite oxide scavengers on ammonia-oxidizing activity of AOA and AOB representatives, including *N. maritimus*, *Ca.* N. aquariensis, *Ca.* N. exaquare, and *N. europaea*. Error bars indicate standard deviations of biological triplicates.

Table 6.2 Half-maximal effective concentrations (EC_{50}) of nitric oxide scavengers on *N. maritimus, Ca.* N. exaquare, *Ca.* N. aquariensis, and *N. europaea*

Nitric oxide scavengers	*N. maritimus*	*Ca.* N. exaquare	*Ca.* N. aquariensis	*N. europaea*	Concentrations tested (μM)
Caffeic acid	<10[†]	84.3 ± 0.5	<10[†]	>300[‡]	0, 10, 30, 100, 300
Curcumin	<10[†]	13.9 ± 0.1	<10[†]	238.3 ± 0.3	0, 10, 30, 100, 300
MBH	0.15±0.01	0.47 ± 0.10	0.47 ± 0.10	>10[‡]	0, 0.3, 1, 3, 10
Trolox	<100[†]	897.0 ± 162.2	91.6 ± 0.8	>1500[‡]	0, 100, 300, 1000, 1500

[†]Minimal tested concentration
[‡]Maximal tested concentration

Curcumin is derived from *Curcuma longa* (turmeric) rhizomes, and is the principal curcuminoid in curry, providing curry with its orange colour (Sreejayan and Rao, 1997). The effects of curcumin were tested at concentrations of 10-300 µM. Complete inhibition of *N. maritimus* and *Ca.* N. aquariensis was observed at all tested curcumin concentrations (Fig. 6.2E, F), with both strains having EC_{50} values below minimal tested concentrations (<10 µM). *Ca.* N. exaquare was strongly inhibited at 30 µM (Fig. 6.2G) and had an EC_{50} of 13.9 µM (Table 6.2). Conversely, *N. europaea* exhibited a higher tolerance to curcumin and was not strongly inhibited until 300 µM (Fig. 6.2H); the associated EC_{50} of 238 µM was an order of magnitude higher than the highest tested AOA EC_{50} value (Table 6.2). These results demonstrate that curcumin differentially inhibits AOA and AOB. However, because of the low solubility of curcumin in aqueous solutions, this inhibitor was dissolved in DMSO as a carrier, which is known to cause toxicity at high concentrations and has been reported to inhibit nitrification in some soil samples (Taylor *et al.*, 2010; Lehtovirta-Morley *et al.*, 2013). Therefore, DMSO-only controls were included for all tested strains (Fig. 6.3). Control incubations containing DMSO without curcumin (at 0.1%, the concentration needed to deliver 300 µM curcumin), resulted in complete inhibition of nitrite production in *N. maritimus*, but did not inhibit *Ca.* N. aquariensis, *Ca.* N. exaquare, or *N. europaea* (Fig. 6.2B, C, D). Because *N. maritimus* is widely distributed in marine environments (Walker *et al.*, 2010; Vajrala *et al.*, 2013), the inhibitory effect of DMSO makes curcumin undesirable for use as a differential inhibitor in environmental incubations of marine samples. However,

curcumin may be useful for differential inhibition experiments in samples not containing marine *Thaumarchaeota*, such as those originating from soil or biofilm environments.
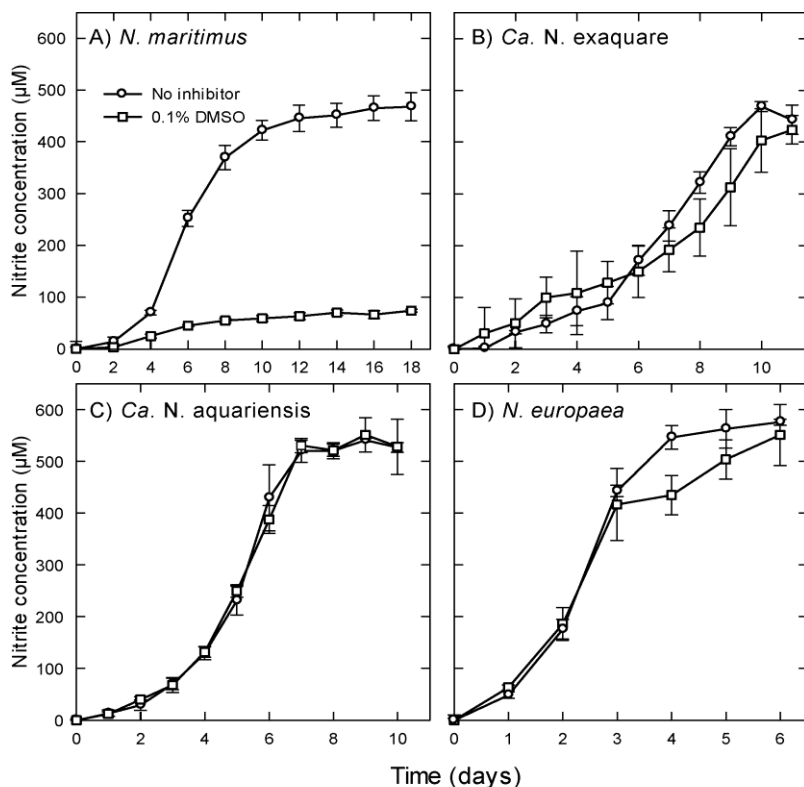

Figure 6.3 Effect of DMSO on ammonia-oxidizing activity of AOA and AOB representatives, including A) *N. maritimus*, B) *Ca.* N. exaquare, C) *Ca.* N. aquariensis, and D) *N. europaea*. The concentration tested is based on that necessary to achieve a final concentration of 300 µM curcumin. Error bars indicate standard deviations of biological triplicates.

Methylene blue hydrate is a heterocyclic aromatic compound that is used commonly in microscopy and as a redox indicator, and has the ability to penetrate cells without causing toxicity in most microorganisms (Barbosa and Peters, 1971). MBH was tested at concentrations of 0.3-10 µM. *N. maritimus* was highly sensitive to this compound, with complete inhibition observed at 1 µM (Fig. 6.2I) and an EC_{50} of 0.15 µM. For both *Ca.* N. aquariensis and *Ca.* N. exaquare, complete inhibition was observed at 3 µM (Fig. 6.2J, K), and both had EC_{50} values of 0.47 µM. Conversely, *N. europaea* had an EC_{50} of >10 µM (Table 6.2), an order of magnitude higher than for *Ca.* N. aquariensis and *Ca.* N. exaquare. Based on these results, MBH was identified as a potentially useful alternative to PTIO for differential inhibition of AOA and AOB.

Trolox is a synthetic vitamin E analogue that is commonly used as a standard in antioxidant assays, where trolox equivalency is used as a benchmark for the antioxidant capacity of a compound or mixture (Miller *et al.*, 1993; Re *et al.*, 1999). Trolox was added to tested cultures in concentrations of 100-1500 µM. *N. maritimus* was the most sensitive to trolox, with complete inhibition observed at all tested concentrations (Fig. 6.2M). *Ca.* N. aquariensis demonstrated strong inhibition at 100 µM (Fig. 6.2N), with an EC_{50} of 91 µM. *Ca.* N. exaquare required 1500 µM for near-complete inhibition of ammonia oxidation (Fig. 6.2O) and had an EC_{50} of 897 µM. *N. europaea* was more resistant to trolox than any of the tested AOA strains; it was not strongly inhibited at any of the tested concentrations (Fig. 6.2P) and had an EC_{50} higher than any tested concentrations (>1500 µM; Table 6.2). Although the EC_{50} of trolox for *Ca*. N. exaquare was substantially lower than for *N. europaea*, some inhibition of *N. europaea* was observed at 1500 µM (~28%; Fig. 6.2P), indicating some overlap in effective concentrations. In addition, the relatively low solubility of trolox precludes further increasing its concentration without the use of solvents. Therefore, despite the differential inhibition observed, trolox does not represent a practical alternative to PTIO for inhibition studies.

Based on these results, all tested nitric oxide scavengers differentially inhibited ammonia-oxidizing activity in AOA and AOB. However, environmental samples vary in parameters such as target population size, community composition, and pH. In order to assess the utility of these selected nitric oxide scavengers for use as a differential inhibitor with environmental samples, we selected caffeic acid and methylene blue as the most suitable candidates for microcosm incubations, with parallel PTIO incubations included for comparison. For these incubations, biomass was obtained from a freshwater aquarium biofilter that was previously found to be dominated by AOA (Sauder *et al.*, 2011). In addition, *Ca.* N. aquariensis was enriched from biomass originating from this particular aquarium biofilter (see Chapter 3 for details). The biomass was incubated in water from the associated aquarium. The incubated aquarium filter biomass without added inhibitors depleted all supplied ammonia within seven days (Fig. 6.3). Samples containing 100 µM PTIO only depleted ~30% of the ammonia present after seven days (*i.e.,* 70% inhibition compared to the control; Fig. 6.4). For incubations containing both caffeic acid (100 µM) and MBH (3 µM), ammonia was depleted in 7 days, which was the same timeframe as the no-

inhibitor control. In order to be useful as an alternative to PTIO, the tested compounds should perform similarly in environmental samples, which was not observed in this study. It is likely that caffeic acid and MBH were rendered ineffective due to biological degradation by microorganisms present in the complex community of the aquarium biofilter, which were not present in laboratory cultures. This is consistent with a previous study demonstrating that incubation of caffeic acid with a sample of active faecal microbiota resulted in rapid disappearance of caffeic acid and its esters (Gonthier *et al.*, 2006). In addition, rapid biodegradation of methylene blue has been demonstrated in an up-flow anaerobic sludge blanket (UASB) reactor, resulting in decolourization (Ong *et al.*, 2005). In the present study, the initially vibrant blue colour of biofilm material incubations with MBH faded over the incubation period, which could suggest biodegradation of the MBH. Alternatively, MBH may have been reduced to a colourless compound upon incubation with the biofilm, given that it is a widely used redox indicator, which changes from blue to colourless upon accepting electrons. Killed biomass MBH controls did not exhibit similar decolourization, indicating that this most likely resulted from biological activity rather than a physical or chemical process. In contrast, no published reports have yet demonstrated the biological decomposition of PTIO.
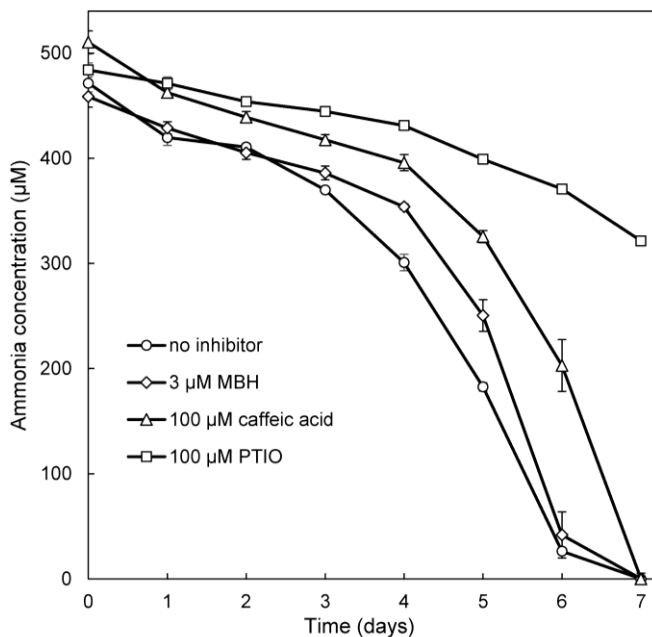
Figure 6.4 Effect of PTIO, caffeic acid, and MBH on ammonia-oxidizing activity of aquarium biofilter biomass. Error bars indicate standard deviations of biological triplicates. Error bars not seen are contained within the symbols.

161

Given that neither caffeic acid nor MBH was effective at inhibiting ammonia oxidation in an AOA-dominated environmental sample, this study cautions against the use of these compounds as differential inhibitors without prior assessment against PTIO. Because additional untested nitric oxide scavengers exist, an alternative recalcitrant nitric oxide scavenger could prove useful as a differential inhibitor. However, many nitric oxide scavengers are naturally occurring organic compounds (*e.g*., hemoglobin, uric acid, N-acetylcysteine), which are also likely to be metabolized by microorganisms in environmental samples. The nitric oxide scavengers tested in this study, including curcumin, caffeic acid, and MBH present effective low-cost alternatives to PTIO for applications in pure cultures, but further development would be required for use on mixed cultures or environmental samples. Therefore, despite its relatively high cost, our results demonstrate that PTIO remains the optimal differential inhibitor for AOA and AOB in environmental samples given its apparent resistance to degradation. However, a drawback to the use nitric oxide scavengers in general is that non-nitrification processes in the environment (*e.g*., denitrification) produce nitric oxide, which could consume added nitric oxide scavengers and limit the ability of these compounds to inhibit thaumarchaeotal ammonia oxidation.

PTIO has been used in laboratory cultures and environmental studies to selectively inhibit ammonia oxidation by AOA (Yan *et al.*, 2012; Jung, Well, *et al.*, 2014; Shen *et al.*, 2013; Sonthiphand and Neufeld, 2014; Martens-Habbena *et al.*, 2015). The differential inhibition of AOA and AOB by PTIO has contributed to the proposal of nitric oxide as an intermediate to the thaumarchaeotal ammonia oxidation pathway. Given the reported substrate promiscuity of PTIO for nitrogenous compounds (Pfeiffer *et al.*, 1997), inhibition of thaumarchaeotal ammonia oxidation by different nitric oxide scavenging compounds provides additional support to the role of nitric oxide in thaumarchaeotal ammonia oxidation. In the present study, we present the first evidence that alternative nitric oxide scavengers, including caffeic acid, methylene blue hydrate, and curcumin, resulted in differential inhibition of AOA and AOB. In addition to increasing the range of known differential inhibitors of AOA and AOB, and providing low cost alternatives for AOA inhibition in laboratory cultures, these results suggest differences in ammonia oxidation pathways of AOA and AOB, and support the proposed role of nitric oxide as a key intermediate in the thaumarchaeotal ammonia oxidation pathway.

Chapter 7

Conclusions, applications, and future directions

7.1 Summary and concluding remarks

In recent years, there have been several major advances in our understanding of global nitrogen cycling and the microorganisms that mediate these biogeochemical processes (for reviews, see Francis *et al.*, 2007; Thamdrup, 2012; Stein and Klotz, 2016). For example, the discovery that members of the domain *Archaea* can mediate aerobic ammonia oxidation challenged longstanding views about nitrification in natural and engineered environments. Given the ubiquity and abundance of ammonia-oxidizing archaea (AOA) in most sampled environments (*e.g.*, Francis *et al.*, 2005; Wuchter *et al.*, 2006; Leininger *et al.*, 2006; Herrmann *et al.*, 2008; Zhang *et al.*, 2010), *Thaumarchaeota* are likely important contributors to global nitrogen and carbon cycling. However, current knowledge of the metabolism and physiology of AOA is limited because the majority of studies are based primarily on molecular surveys using marker genes. Although marker genes are valuable for generating baseline data and correlating with environmental parameters, additional approaches are necessary to assess the activity and metabolism of AOA, such as measurements of ammonia-oxidizing activity in environmental samples, cultivation, and genome sequencing of novel representatives.

When this thesis research project began, no AOA representatives had been cultivated from any freshwater environment. Moreover, only two studies had detected AOA in wastewater treatment plants (WWTPs; Park *et al.*, 2006; Wells *et al.*, 2009) and no studies had assessed the abundance of AOA and ammonia-oxidizing bacteria (AOB) in aquarium biofilters. The overarching objective of this work was to advance the understanding of AOA in engineered freshwater environments by assessing their abundance and diversity in two model environments, including freshwater aquarium biofilters (Chapter 2) and rotating biological contactors (RBCs) of a municipal WWTP (Chapter 4), and to further characterize the identified AOA through laboratory cultivation and genome sequencing (Chapters 4 and 5). Finally, using these cultured representatives, this work aimed to identify rapid and

163

affordable differential inhibitors of AOA and AOB, and provide support for the hypothesis that nitric oxide (NO) is an intermediate in archaeal ammonia oxidation (Chapter 6). The major contributions and conclusions arising from this thesis are summarized below.

7.1.1 AOA abundance and activity in engineered environments

The research reported here demonstrated that AOA outnumbered AOB in freshwater aquarium biofilters, and in some cases were the only ammonia-oxidizing prokaryotes detected by PCR (Figs. 2.1, 2.3). This suggested that AOA are important in aquarium nitrification, and in some cases, may act alone in catalyzing ammonia oxidation in these environments. In Guelph WWTP RBCs, AOA were detected by qPCR for thaumarchaeotal *amoA* and 16S rRNA genes (Figs. 4.2, 5.12), analysis of tetraether lipids (Fig. 4.5), and fluorescence *in situ* hybridization (Figs. 5.5, 5.6, 5.16). Quantitative measurements of AOA and AOB by qPCR (Figs. 4.2, 4.3, 5.12; Table 5.2) and qFISH indicated that AOA always comprised a substantial proportion of the ammonia-oxidizing community, and in most cases outnumbered AOB in this wastewater treatment system. The AOA inhabiting these biofiltration systems were robust; in both aquarium filter FW27 and RBC biofilm, the presence of AOA was detected at several time points over approximately five years, and temporal stability of relative AOA abundance and community composition was observed (Fig. 2.3, Fig. 4.7, Fig. 5.16). During this thesis work, both aquarium FW27 and the Guelph RBCs experienced massive unplanned disturbances; in both cases, AOA rapidly recolonized the biofilters, indicating that they are actively growing in these systems. In Guelph WWTP, after completely removing all biofilm material from the RBCs, *Ca*. N. exaquare-like AOA had recolonized the biofilm within one month (Fig. 5.16). Moreover, the high proportion of intact polar lipid (IPL)- derived thaumarchaeol detected in the RBC biofilm (Fig. 4.5) provides further evidence that detected AOA cells are alive and active.

Incubation of aquarium and RBC biofilm material with PTIO resulted in at least partial inhibition of ammonia-oxidizing activity (Figs. 3.13, 5.11, 5.14, 6.4). The results ranged from little observed inhibition (*e.g.*, Fig. 5.11B), to nearly complete inhibition (*e.g.*, Fig. 3.12A), but in all cases, suggested that AOA participate in ammonia oxidation *in situ*. This work was the first to demonstrate ammonia-oxidizing activity by AOA in any engineered environment. Although an important step forward, more research is needed to

determine the extent of AOA contributions to ammonia-oxidizing activity in additional engineered environments.

7.1.2 Niche differentiation of AOA and AOB

The research presented in this thesis suggests that AOA are adapted to low ammonia conditions, whereas AOB dominate in environments where ammonia concentrations are high. For example, in sampled aquarium biofilters, there was a significant negative correlation between the ammonia concentration of an aquarium and the proportion of AOA (relative to AOB) in the associated biofilter (Fig. 2.2). In addition, in the Guelph WWTP RBCs, AOA increased in abundance (as measured by *amoA* and 16S rRNA genes) as ammonia decreased across the flowpath (Fig. 4.2), and the relative proportions of AOA were negatively correlated with ammonia concentration of corresponding wastewater samples (Fig. 4.4). These findings have implications for the types of biofilters that are likely to be dominated by AOA or AOB. For example, AOA are expected to be dominant in low-ammonia systems, such as aquarium biofilters, tertiary wastewater treatment processes, groundwater treatment systems, drinking water treatment plants, and aquaculture biofilters, where ammonia concentrations must be maintained at concentrations low enough to allow growth of aquatic animals. Indeed, AOA have been identified in all of these environments (van der Wielen *et al.*, 2009; de Vet *et al.*, 2009; Kasuga *et al.*, 2010; Sauder *et al.*, 2011; Brown *et al.*, 2013; Bagchi *et al.*, 2014). However, more research is needed to elucidate the contributions of nitrifying microorganisms to these environments, particularly in aquaculture operations, which have been examined by very few studies, despite their importance to industry and human nutrition. In comparison to these low-ammonia systems, AOB are likely to dominate in biofilters with high concentrations of ammonia, such as activated sludge systems of WWTPs, which has been reported by several studies (*e.g.*, Wells *et al.*, 2009; Mussman *et al.*, 2011; Jin *et al*., Gao *et al.*, 2014).

The abundance and activity of *Ca*. N. exaquare-like AOA in RBC biofilm suggests that AOA are likely to play a role in tertiary WWTP systems designed to produce high quality effluent. Tertiary treatment systems are expected to become increasingly common as human population growth and climate change increase pressure on freshwater resources (WWAP, 2012). For example, in some major rivers (*e.g.*, the Tiber River, Rome, Italy),

flows are so low that they are sustained almost entirely by wastewater during the summer months. In these low flow conditions, extremely high quality effluent becomes critical due to the low assimilative capacity of the receiving water. AOA are likely to thrive in fixed-film low ammonia treatment systems, similar to the Guelph RBCs.

Interestingly, despite being most abundant in low-ammonia RBCs, in enrichment culture, *Ca*. N. exaquare demonstrated tolerance to relatively high ammonia concentrations (Fig. 5.1). For reference, raw influent to Guelph WWTP contains approximately 40 mg L^{-1} N-NH$_4^+$ (Nancy Evans, personal communication). In comparison, *Ca*. N. exaquare actively oxidized ammonia at 10 mM NH$_4$Cl, which is equivalent to 140 mg L^{-1} N-NH$_4^+$. This suggests that AOB are likely better able to outcompete AOA at high ammonia concentrations but that ammonia toxicity to *Ca*. N. exaquare-like AOA is unlikely to be a contributing factor to the observed differential abundance at varying environmental ammonia concentrations. The high ammonia tolerance of *Ca*. N. exaquare suggests that these organisms could contribute to ammonia oxidation in some ammonia-rich environments that are otherwise unsuitable for AOB. For example, AOA dominate in environments that are acidic (Nicol *et al*., 2008; Gubry-Rangin *et al*., 2010; Lehtovirta-Morley *et al*., 2011), hot (Reigstad *et al*., 2008; de la Torre *et al*., 2008; Wang *et al*., 2009; Dodsworth *et al*., 2011), or have low oxygen concentrations (Park *et al*., 2006, 2010; Lam *et al*., 2007; Jung *et al*., 2011). One such environment where AOA could play a role is anammox bioreactors, which require partial nitrification to produce nitrite. Anammox reactors operate at high temperatures and very low oxygen concentrations, which may favour the activity and growth of AOA over AOB, despite their relatively high ammonia concentrations.

7.1.3 AOA cultures and genomes

This thesis reports the cultivation of two novel AOA representatives, both of which are enriched to ~99% purity, and demonstrate growth by chemolithoautotrophic ammonia oxidation. *Ca*. N. aquariensis is a Group I.1a freshwater representative that is mesophilic (Fig. 3.2A), belongs to the *Nitrosotenuis* lineage (Fig. 3.5), and has a generation time of approximately 34 hours. *Ca*. N. aquariensis cells are slender rods (0.4 µm) that vary from 0.6-3.6 µm long and have paracrystalline surface layers and proteinaceous appendages (Fig. 3.4). *Ca*. N. exaquare is a Group I.1b representative that is mesophilic (Fig. 5.1A), tolerant to

relatively high concentrations of ammonia and nitrite (Fig. 5.1C,D) and is greatly stimulated by addition of organic carbon (Fig. 5.6). *Ca*. N. exaquare cells are coccoid and smooth, range in diameter from 1-2 µm, and do not have any apparent appendages (Figs. 5.5, 5.6).

Without cultivation efforts, it would not be possible to describe many of the basic characteristics above, even with complete genome sequences. Nevertheless, the genome sequences of *Ca*. N. aquariensis and *Ca*. N. exaquare have been valuable for comparisons with other AOA, and for providing confirmatory and predictive functions. For example, the presence of genes encoding SdcS-type dicarboxylate transporters (Table 5.2) in the *Ca*. N. exaquare genome was determined after laboratory experiments had demonstrated that this organism was strongly stimulated by the C_4 compounds malate and succinate (Fig. 5.6). The genome therefore provided additional support for activity results, and revealed a potential mechanism for entry of C_4 compounds. On the other hand, genome analyses have also been useful for generating hypotheses. For example, in *Ca* N. exaquare, the genome has suggested the ability to metabolize C_1 compounds (Fig. 5.10), and in *Ca*. N. aquariensis, the genome suggests the ability to utilize polyamines (Table 3.1) or produce polyketides (Fig. 3.9).

Marker gene survey studies have been invaluable for studying uncultured microorganisms in a wide variety of environments. However, the ability of marker genes to infer functional characteristics is relatively poor. As metagenomic sequencing and analyses become increasingly common, functional information for uncultured microorganisms also becomes more readily available, and advances in binning and assembly techniques have made obtaining closed genomes from metagenomic data relatively straightforward (*e.g.*, Albertsen *et al.*, 2013). However, even with complete genome sequences, high proportions of detected genes (typically $\geq 40\%$) encode for proteins with no predicted function. Therefore, cultivation remains the gold standard for characterizing the morphology, metabolism, and physiology of a microorganism of interest (Nichols, 2007), but is most effective when paired with cultivation-independent methods.

7.1.4 AOA carbon metabolism

Both *Ca*. N. aquariensis and *Ca*. N. exaquare have demonstrated long-term growth in media containing ammonia as a sole source of energy and calcium carbonate as a sole source

of carbon, indicating that both grow chemolithoautotrophically. This is supported by their genomes, which encode genes for ammonia oxidation and bicarbonate fixation (Fig. 5.8; Table 3.1, Table 5.2). For *Ca*. N. exaquare, these findings are of particular importance because it has been demonstrated that closely related AOA do not mediate ammonia oxidation in a nitrifying WWTP, regardless of high cell numbers and of active transcription of *amoA* genes (Mussman *et al.*, 2011).

MAR-FISH for cultures of *Ca*. N. exaquare demonstrated the incorporation of ^{14}C labelled bicarbonate into biomass (Fig. 5.5H), supporting an autotrophic lifestyle. Nevertheless, *Ca*. N. exaquare was greatly stimulated by addition of organic carbon, especially the C_4 compounds malate and succinate (Fig. 5.6). Although it has recently been reported that addition of organic carbon improves AOA growth by decreasing oxidative stress from hydrogen peroxide (Kim *et al.*, 2016), *Ca*. N. exaquare encodes genes for peroxidase and catalase (Table 5.2) so it is likely able to detoxify reactive oxygen species without organic carbon supplementation. Although incubations of RBC biofilm with PTIO suggested that AOA contribute to ammonia oxidation (Figs. 3.13, 5.12, 5.15), MAR-FISH for biofilm samples showed incorporation of inorganic carbon for AOB only following biofilm incubation with ammonia (Fig. 5.15). This may imply that in a biofilm environment, AOA preferentially incorporate alternate sources of carbon in association with ammonia oxidation.

Ca. N. aquariensis did not require input of organic carbon to achieve growth rates comparable to those observed in pure cultures of other AOA. Nevertheless, the genome of *Ca* N. aquariensis encodes several transporters for organic carbon compounds, such as dicarboxylates, sulfonates (*e.g.*, taurine), glycerol, citrate, amino acids, oligopeptides, and polyamines (Table 3.1). Given that marine archaea have been shown to incorporate amino acids (Ouverney and Fuhrman, 2000) and transporters for amino acids are conserved across all reported AOA genomes (Table 3.1, Table 5.2), it seems likely that AOA have the ability to use amino acids, either as supplemental energy sources, or for direct assimilation into biomass. Overall, the carbon metabolism of AOA is likely more complex than strict autotrophy.

7.2 Future outlook

Since the recent discovery of AOA (Venter *et al.*, 2004; Könneke *et al.*, 2005), intensive research has focused on the abundance, diversity, ecology, metabolism, and physiology of these organisms, and it seems likely that AOA will remain a fascinating topic of investigation for years to come. As outlined above, the research presented in this thesis (and associated publications) adds to the growing body of knowledge regarding AOA and nitrogen cycling, with a focus on engineered environments. In addition, this work has generated several interesting research questions and has laid the foundation for follow-up experiments. In particular, possessing laboratory cultures of AOA representatives enables testing hypotheses regarding the physiology and ecology of these organisms in a way that would otherwise not be possible. Moreover, the complete genome sequences generated during this project provide an invaluable resource for generating hypotheses regarding AOA metabolism. Specific research questions for future investigation are outlined below.

7.2.1 Ca. N. exaquare future prospects

A major outstanding question is the mechanism by which *Ca*. N. exaquare is stimulated by supplemented organic carbon sources (Fig. 5.6). Future research will assess whether these carbon sources are directly assimilated by *Ca*. N. exaquare, or whether they provide indirect benefits, for example by decreasing oxidative stress (Kim *et al.*, 2016) or providing a nutrient manufactured by remaining heterotrophic bacteria. To assess these questions, activity experiments can be used to assess the relative stimulation provided by catalase in comparison to (and in combination with) organic carbon sources. In addition, labelling approaches such as DNA or lipid stable-isotope probing can assess whether supplied organic compounds are incorporated into cellular biomass.

Given that *Ca*. N. exaquare is most strongly stimulated by C_4 compounds, the two encoded dicarboxylate transporters (Table 5.2) are of particular interest. Assessing whether these genes encode functional transporters that bring in C_4 compounds can be assessed using heterologous expression experiments with a mutant host lacking its own functional transporter. Expression of this transporter would provide strong evidence that *Ca*. N. exaquare is indeed able to utilize C_4 compounds. Additional support for functionality of these

transporters could be obtained using activity experiments. The SdcS-type transporters encoded by *Ca*. N. exaquare import malate, succinate, and fumarate with high efficiency, but have a poor efficiency for oxaloacetate (Hall and Pajor, 2007; Strickler *et al.*, 2009). Therefore, activity studies would be predicted to demonstrate that fumarate provides stimulation approximately equivalent to succinate and malate, whereas addition of oxaloacetate would result in substantially less stimulation of growth and ammonia-oxidizing activity.

Metabolic pathways for C_1 utilization are suggested by the genome of *Ca*. N. exaquare, (Fig. 5.10), and this organism contains a gene encoding formate dehydrogenase. To date, no AOA have been reported to oxidize or assimilate C_1 compounds, although formate can be used by other nitrifying microorganisms (Van Gool and Laudelout, 1966; Koch *et al.*, 2015; Gruber-Dorninger *et al.*, 2015). Future experiments could use activity and growth measurements to determine whether *Ca*. N. exaquare is able to utilize C_1 compounds, (*e.g.*, methanol, formaldehyde, and formate) in addition to, or instead of, chemolithoautotrophic ammonia oxidation.

Finally, the composition of the cell envelope of *Ca*. N. exaquare is currently enigmatic and represents an interesting research question. No crystalline S-layer was observed on *Ca*. N. exaquare cells imaged by SEM (Fig. 5.5A) or TEM (data not shown), and its genome does not encode for any homologues to the S-layer proteins found in *N. viennensis* (Table 5.2). Conversely, all other available AOA genomes encode homologues to these S-layer proteins (Tables 3.1, 5.2). Given that *Ca*. N. exaquare also lacks known genes associated with the production of peptidoglycan or pseudopeptidoglycan, it remains unclear how these cells maintain structural integrity or handle osmostic stress.

7.2.2 Ca. N. aquariensis future prospects

Ongoing efforts to isolate *Ca*. N. aquariensis in pure culture are important for simplifying conclusions drawn from activity experiments. Future purification attempts are likely to be greatly aided by the addition of catalase, which has been shown to be useful for isolation of Group I.1a AOA (Kim *et al.*, 2016). If purification is possible, it creates opportunities for several additional experiments. For example, C*a*. N. aquariensis encodes a

polyamine import system (Table 3.1), and it has been suggested that some *Thaumarchaeota* may have the ability to directly oxidize polyamines (Hollibaugh *et al.*, 2015). Therefore, attempts to grow *Ca*. N. aquariensis on polyamines such as spermine, spermidine, and putrescine may provide insight into additional metabolic processes mediated by this organism. Polyamines are produced and used by a wide variety of prokaryotes and eukaryotes, are released upon cell death, and represent a potential source of carbon, nitrogen, and energy (Igarashi and Kashiwagi, 1999; Nishibori *et al.*, 2001; Kusano *et al.*, 2007). In addition to polyamines, future research could assess whether *Ca*. N. aquariensis is able to utilize other organic carbon compounds for which it encodes potential transporters, such as amino acids, taurine, or glycerol.

Finally, *Ca*. N. aquariensis has an intriguing cell surface structure with an S-layer and several small appendages (Fig. 3.4). In addition, the genome suggests that surface protein glycosylation is a characteristic of *Ca*. N. aquariensis (Fig. 3.9). Future work could determine the lattice symmetry of the S-layer, and assess the associated glycome, including localization, glycosylation patterns, and identities of the glycan units.

7.2.3 Ammonia-oxidizing prokaryotes in engineered environments

The research presented in this thesis considers the abundance and contributions of AOA and AOB in two environments. However, interpretations of presented data are complicated by the recent discovery of comammox bacteria (van Kessel *et al.*, 2015; Daims *et al.*, 2015), which may participate in ammonia (and nitrite) oxidation in engineered freshwater environments. To address questions regarding the abundance and activity of comammox in biological filters, it is necessary to develop molecular tools for specific detection of comammox, such as primers targeting comammox *amoA* genes. In addition, establishing comammox inhibitor profiles will be valuable for determining relative contributions of these organisms to ammonia oxidation, but this is complicated by the requirement for laboratory cultures. In the meantime, comammox *amoA* genes can be detected in metagenomics datasets from environments of interest. Indeed, metagenomic libraries obtained from both aquarium FW27 and Guelph WWTP RBC biofilm indicate the presence of comammox genes (unpublished data). Future research efforts using these datasets could provide insight into the abundance and diversity of comammox bacteria in these

171

engineered biofilter environments, which would contribute to the overarching goal of this thesis, understanding ammonia-oxidizing microorganisms in these biofilter environments.

7.2.4 Practical applications of research

Many species of fish are of ornamental, economic, and nutritional value to humans. Recent estimates suggest that 12 million households in the United States maintain freshwater aquaria (American Pet Products Association, 2016). In fish culture systems, ammonia toxicity is a major issue, and elevated ammonia concentrations interfere with several biochemical processes, resulting in stress and disease (Ip *et al.*, 2001; Ip and Chew, 2010). Acute ammonia toxicity is most likely related to the ability of NH_4^+ to displace K^+ in ion transporters (Binstock and Lecar, 1969) and disrupt electrochemical gradients in the central nervous systems (Cooper and Plum, 1987). Overstocking of tanks can result in chronically elevated ammonia concentrations, but even in tanks with few fish, start-up aquaria are prone to ammonia spikes that can result in fish disease and death. As a result, the use of aquarium supplements for promoting aquarium nitrification and preventing the negative effects of ammonia on fish is commonplace. Aquarium nitrifying supplements advertise that they contain AOB, and indeed, available analyses of aquarium supplements confirm that AOB are present in these supplements whereas AOA are absent (Chapter 2; Sauder *et al.*, 2011; Bagchi *et al.*, 2014).

Traditionally, AOB, such as *Nitrosomonas* spp., were thought to be solely responsible for the first step of nitrification in aquaria, and AOB have been enriched from freshwater aquarium biofilters (Burrell *et al.*, 2001). However, this thesis establishes that AOA are numerically dominant in freshwater aquarium biofilters and are likely the major contributors to ammonia-oxidizing activity in established aquaria. Therefore, development of commercial supplements containing *Ca*. N. aquariensis-like AOA could prove valuable for promoting nitrification in aquarium biofilters, resulting in reduced lag times in aquarium set up and improved fish health. In addition, given that *Ca*. N. aquariensis is closely related to AOA from aquaculture environments (Fig. 3.5), it is likely that AOA-based supplements could also be valuable in aquaculture systems to promote nitrification, reduce tank cycling times, and reduce fish stress.

7.3 Research significance and concluding remarks

The combination of cultivation-independent and cultivation-dependent techniques used in this research has addressed an important gap in the understanding of nitrogen cycling in engineered water treatment systems. These results have established baseline data for AOA and AOB diversity and abundance, and are the first to report contributions of AOA to ammonia-oxidizing activity in wastewater treatment systems and aquarium biofilters. In addition, two new AOA species have been identified and characterized, contributing to AOA cultures and genomes available for further study. Taken together, this research advances current understanding of abundance, diversity, ecology, physiology, and activity of AOA associated with engineered biofiltration systems.

The importance of water treatment to the environment and to human civilization cannot be overstated. Pollution of freshwater resources has been cited as one of the major factors in the downfall of the ancient civilizations of Rome, Easter Island, Sumer, and Maya (Wright, 2004). Pressure on freshwater resources is expected to increase dramatically within the next 50 years, as climate change reduces precipitation in most parts of the world, and population growth accelerates both the demand for freshwater and the production of waste (WWAP, 2012). As a result, water recycling will become increasingly important, and tertiary treatment systems are likely to play an integral role in future water management. Tertiary systems can produce effluent of sufficient quality for discharge into sensitive environments, and for use in irrigation, industrial cooling, aquifer recharge, recreation, and augmentation of drinking water supplies. Given this, identifying and understanding the ecology and metabolism of microorganisms associated with tertiary wastewater treatment processes is critical, and may contribute to improvements in bioreactor performance and development of new infrastructure for water treatment. Because of the damaging effects of ammonia on aquatic animals and environments, nitrification is one of the most important processes for effective water treatment. AOA in engineered biofilter systems may contribute to the ability of these bioreactors to provide high effluent quality that can be safely recycled, which in turn reduces stress on freshwater ecosystems. Therefore, AOA adapted to low-ammonia biofilter environments may be important global contributors to freshwater recycling, and may play a continued role in maintaining freshwater resources.

173

References

Abdel-Mawgoud AM, Lépine F, Déziel E. (2010). Rhamnolipids: diversity of structures, microbial origins and roles. *Appl Microbiol Biotechnol* **86**:1323–1336.

Abraham KA. (1968). Studies on DNA-dependent RNA polymerase from *Escherichia coli*. The mechanism of polyamine induced stimulation of enzyme activity. *Eur J Biochem* **5**:143–146.

Adamczyk J, Hesselsoe M, Iversen N, Horn M, Lehner A, Nielsen PH, *et al.* (2003). The isotope array, a new tool that employs substrate-mediated labeling of rRNA for determination of microbial community structure and function. *Appl Environ Microbiol* **69**:6875–6887.

Agogué H, Brink M, Dinasquet J, Herndl GJ. (2008). Major gradients in putatively nitrifying and non-nitrifying Archaea in the deep North Atlantic. *Nature* **456**:788–791.

Albers S-V, Meyer BH. (2011). The archaeal cell envelope. *Nat Rev Microbiol* **9**:414–426.

Albertsen M, Hugenholtz P, Skarshewski A, Nielsen KL, Tyson GW, Nielsen PH. (2013). Genome sequences of rare, uncultured bacteria obtained by differential coverage binning of multiple metagenomes. *Nat Biotechnol* **31**:533–538.

Alcázar R, Marco F, Cuevas JC, Patron M, Ferrando A, Carrasco P, *et al.* (2006). Involvement of polyamines in plant response to abiotic stress. *Biotechnol Lett* **28**:1867–1876.

Allison SM, Prosser JI. (1991). Urease activity in neutrophilic autotrophic ammonia-oxidizing bacteria isolated from acid soils. *Soil Biol Biochem* **23**:45–51.

Alves RJE, Wanek W, Zappe A, Richter A, Svenning MM, Schleper C, *et al.* (2013). Nitrification rates in Arctic soils are associated with functionally distinct populations of ammonia-oxidizing archaea. *ISME J* **7**:1620–1631.

Amann RI, Binder BJ, Olson RJ, Chisholm SW, Devereux R, Stahl DA. (1990). Combination of 16S rRNA-targeted oligonucleotide probes with flow cytometry for analyzing mixed microbial populations. *Appl Environ Microbiol* **56**:1919–1925.

American Pet Products Association. (2016). APPA National Pet Owners Survey. Greenwich, CT. http://www.americanpetproducts.org/pubs_survey.asp.

Anderson AJ, Dawes EA. (1990). Occurrence, metabolism, metabolic role, and industrial uses of bacterial polyhydroxyalkanoates. *Microbiol Rev* **54**:450–472.

Andrews C, Exell A, Carrington N. (1988). The Manual of Fish Health. Tetra Press: Morris Plains, NJ.

Arp DJ, Sayavedra-Soto LA, Hommes NG. (2002). Molecular biology and biochemistry of ammonia oxidation by *Nitrosomonas europaea*. *Arch Microbiol* **178**:250–255.

Bagchi S, Vlaeminck SE, Sauder LA, Mosquera M, Neufeld JD, Boon N. (2014). Temporal and spatial stability of ammonia-oxidizing archaea and bacteria in aquarium biofilters. *PLoS One* **9**:e113515.

Bai Y, Liu R, Liang J, Qu J. (2013). Integrated metagenomic and physiochemical analyses to evaluate the potential role of microbes in the sand filter of a drinking water treatment system. *PLoS One* **8**:e61011.

Bai Y, Sun Q, Wen D, Tang X. (2012). Abundance of ammonia-oxidizing bacteria and archaea in industrial and domestic wastewater treatment systems. *FEMS Microbiol Ecol* **80**:323–330.

Baker BJ, Lesniewski RA, Dick GJ. (2012). Genome-enabled transcriptomics reveals archaeal populations that drive nitrification in a deep-sea hydrothermal plume. *ISME J* **6**:2269–2279.

Bang C, Schmitz RA. (2015). Archaea associated with human surfaces: not to be underestimated. *FEMS Microbiol Rev* **39**:631–648.

Bankevich A, Nurk S, Antipov D, Gurevich AA, Dvorkin M, Kulikov AS, *et al.* (2012). SPAdes: A new genome assembly algorithm and its applications to single-cell sequencing. *J Comput Biol* **19**:455–477.

Banning NC, Maccarone LD, Fisk LM, Murphy DV. (2015). Ammonia-oxidising bacteria not archaea dominate nitrification activity in semi-arid agricultural soil. *Sci Rep* **5**:11146.

Barbosa P, Peters TM. (1971). The effects of vital dyes on living organisms with special reference to methylene blue and neutral red. *Histochem J* **3**:71–93.

Bartossek R, Nicol GW, Lanzen A, Klenk H-P, Schleper C. (2010). Homologues of nitrite reductases in ammonia-oxidizing archaea: diversity and genomic context. *Environ Microbiol* **12**:1075–1088.

Bartram A, Poon C, Neufeld JD. (2009). Nucleic acid contamination of glycogen used in nucleic acid precipitation and assessment of linear polyacrylamide as an alternative co-precipitant. *Biotechniques* **47**:1019–1022.

Beam JP. (2015). Geobiological interactions of archaeal populations in acidic and alkaline geothermal springs of Yellowstone National Park, WY, USA. Montana State University.

Beam JP, Jay ZJ, Kozubal MA, Inskeep WP. (2014). Niche specialization of novel *Thaumarchaeota* to oxic and hypoxic acidic geothermal springs of Yellowstone National Park. *ISME J* **8**:938–951.

Beman JM, Francis CA. (2006). Diversity of ammonia-oxidizing archaea and bacteria in the sediments of a hypernutrified subtropical estuary: Bahía del Tóbari, Mexico. *Appl Environ Microbiol* **72**:7767–7777.

Beman MJ, Popp BN, Francis CA. (2008). Molecular and biogeochemical evidence for ammonia oxidation by marine Crenarchaeota in the Gulf of California. *ISME J* **2**:453–453.

Bennett S. (2004). Solexa Ltd. *Pharmacogenomics* **5**:433–438.

Berg IA. (2011). Ecological aspects of the distribution of different autotrophic CO_2 fixation pathways. *Appl Environ Microbiol* **77**:1925–1936.

Berg IA, Kockelkorn D, Buckel W, Fuchs G. (2007). A 3-hydroxypropionate/4-hydroxybutyrate autotrophic carbon dioxide assimilation pathway in *Archaea*. *Science* **318**:1782–1786.

Besse A, Peduzzi J, Rebuffat S, Carré-Mlouka A. (2015). Antimicrobial peptides and proteins in the face of extremes: Lessons from archaeocins. *Biochimie* **118**:344–355.

Biddle JF, Lipp JS, Lever M, Lloyd KG, Sorensen KB, Anderson R, *et al.* (2006). Heterotrophic Archaea dominate sedimentary subsurface ecosystems off Peru. *Proc Natl Acad Sci U S A* **103**:3846–3851.

Binstock L, Lecar H. (1969). Ammonium ion currents in the squid giant axon. *J Gen Physiol* **53**:342–361.

Blainey PC, Mosier AC, Potanina A, Francis CA, Quake SR. (2011). Genome of a low-salinity ammonia-oxidizing archaeon determined by single-cell and metagenomic analysis. *PLoS One* **6**:e16626.

Bligh EG, Dyer WJ. (1959). A rapid method of total lipid extraction and purification. *Can J Biochem Physiol* **37**:911–917.

Bliss JM, Silver RP. (1996). Coating the surface: a model for expression of capsular polysialic acid in *Escherichia coli* K1. *Mol Microbiol* **21**:221–231.

Boetzer M, Pirovano W. (2012). Toward almost closed genomes with GapFiller. *Genome Biol* **13**:R56.

Bouskill NJ, Eveillard D, Chien D, Jayakumar A, Ward BB. (2012). Environmental factors determining ammonia-oxidizing organism distribution and diversity in marine environments. *Environ Microbiol* **14**:714–729.

Brochier-Armanet C, Boussau B, Gribaldo S, Forterre P. (2008). Mesophilic crenarchaeota: proposal for a third archaeal phylum, the Thaumarchaeota. *Nat Rev Microbiol* **6**:245–252.

Brochier-Armanet C, Forterre P, Gribaldo S. (2011). Phylogeny and evolution of the Archaea: one hundred genomes later. *Curr Opin Microbiol* **14**:274–281.

Brown MN, Briones A, Diana J, Raskin L. (2013). Ammonia-oxidizing archaea and nitrite-oxidizing nitrospiras in the biofilter of a shrimp recirculating aquaculture system. *FEMS Microbiol Ecol* **83**:17–25.

Buckley DH, Graber JR, Schmidt TM. (1998). Phylogenetic analysis of nonthermophilic members of the kingdom *Crenarchaeota* and their diversity and abundance in soils. *Appl Environ Microbiol* **64**:4333–4339.

Burrell PC, Phalen CM, Hovanec TA. (2001). Identification of bacteria responsible for ammonia oxidation in freshwater aquaria. *Appl Environ Microbiol* **67**:5791–5800.

Busiek KK, Margolin W. (2011). Split decision: a thaumarchaeon encoding both FtsZ and Cdv cell division proteins chooses Cdv for cytokinesis. *Mol Microbiol* **82**:535–538.

Calo D, Kaminski L, Eichler J. (2010). Protein glycosylation in Archaea: Sweet and extreme. *Glycobiology* **20**:1065–1076.

Capone DG, Popa R, Flood B, Nealson KH. (2006). Follow the nitrogen. *Science* **312**:708–709.

Carroll BJ, Moss SJ, Bai L, Kato Y, Toelzer S, Yu TW, *et al.* (2002). Identification of a set of genes involved in the formation of the substrate for the incorporation of the unusual 'glycolate' chain extension unit in ansamitocin biosynthesis. *J Am Chem Soc* **124**:4176–4177.

Castric P, Cassels FJ, Carlson RW. (2001). Structural characterization of the *Pseudomonas aeruginosa* 1244 pilin glycan. *J Biol Chem* **276**:26479–26485.

Chu H, Fujii T, Morimoto S, Lin X, Yagi K, Hu J, *et al.* (2007). Community structure of ammonia-oxidizing bacteria under long-term application of mineral fertilizer and organic manure in a sandy loam soil. *Appl Environ Microbiol* **73**:485–491.

Church MJ, DeLong EF, Ducklow HW, Karner MB, Preston CM, Karl DM. (2003). Abundance and distribution of planktonic *Archaea* and *Bacteria* in the waters west of the Antarctic Peninsula. *Limnol Oceanogr* **48**:1893–1902.

Clark C, Schmidt EL. (1966). Effect of mixed culture on *Nitrosomonas europaea* simulated by uptake and utilization of pyruvate. *J Bacteriol* **91**:367–373.

Clark C, Schmidt EL. (1967). Growth response of *Nitrosomonas europaea* to amino acids. *J Bacteriol* **93**:1302–1308.

Cooper AJ, Plum F. (1987). Biochemistry and physiology of brain ammonia. *Physiol Rev* **67**:440–519.

De Corte D, Yokokawa T, Varela MM, Agogué H, Herndl GJ. (2009). Spatial distribution of Bacteria and Archaea and *amoA* gene copy numbers throughout the water column of the Eastern Mediterranean Sea. *ISME J* **3**:147–158.

Cruz-Ramos H, Glaser P, Wray L V, Fisher SH. (1997). The *Bacillus subtilis ureABC* operon. *J Bacteriol* **179**:3371–3373.

Cussac V, Ferrero RL, Labigne A. (1992). Expression of *Helicobacter pylori* urease genes in *Escherichia coli* grown under nitrogen-limiting conditions. *J Bacteriol* **174**:2466–2473.

Daims H, Brühl A, Amann R, Schleifer KH, Wagner M. (1999). The domain-specific probe EUB338 is insufficient for the detection of all Bacteria: development and evaluation of a more comprehensive probe set. *Syst Appl Microbiol* **22**:434–444.

Daims H, Lebedeva EV, Pjevac P, Han P, Herbold C, Albertsen M, *et al.* (2015). Complete nitrification by *Nitrospira* bacteria. *Nature* **528**:504–509.

Daims H, Lücker S, Wagner M. (2006). daime, a novel image analysis program for microbial ecology and biofilm research. *Environ Microbiol* **8**:200–213.

Daims H, Nielsen JL, Nielsen PH, Schleifer KH, Wagner M. (2001). *In situ* characterization of *Nitrospira*-like nitrite-oxidizing bacteria active in wastewater treatment plants. *Appl Environ Microbiol* **67**:5273–5284.

Davis AA. (1992). Novel major archaebacterial group from marine plankton. *Nature* **356**:148–149.

DeLong EF. (1992). Archaea in coastal marine environments. *Proc Natl Acad Sci U S A* **89**:5685–5689.

DeLong EF. (1998). Everything in moderation: Archaea as 'non-extremophiles'. *Curr Opin Genet Dev* **8**:649–654.

DeLong EF, Wu KY, Prézelin BB, Jovine R V. (1994). High abundance of Archaea in Antarctic marine picoplankton. *Nature* **371**:695–697.

Di HJ, Cameron KC, Shen JP, Winefield CS, O'Callaghan M, Bowatte S, *et al.* (2009). Nitrification driven by bacteria and not archaea in nitrogen-rich grassland soils. *Nat Geosci* **2**:621–624.

Di HJ, Cameron KC, Shen J-P, Winefield CS, O'Callaghan M, Bowatte S, *et al.* (2010). Ammonia-oxidizing bacteria and archaea grow under contrasting soil nitrogen conditions. *FEMS Microbiol Ecol* **72**:386–394.

Ding K, Wen X, Li Y, Shen B, Zhang B. (2015). Ammonia-oxidizing archaea versus bacteria in two soil aquifer treatment systems. *Appl Microbiol Biotechnol* **99**:1337–1347.

Dodsworth JA, Hungate BA, Hedlund BP. (2011). Ammonia oxidation, denitrification and dissimilatory nitrate reduction to ammonium in two US Great Basin hot springs with abundant ammonia-oxidizing archaea. *Environ Microbiol* **13**:2371–2386.

Dong B, Tan J, Yang Y, Pang Z, Li Z, Dai X. (2016). Linking nitrification characteristic and microbial community structures in integrated fixed film activated sludge reactor by high-throughput sequencing. *Water Sci Technol.* In press.

Driks A. (1999). *Bacillus subtilis* spore coat. *Microbiol Mol Biol Rev* **63**:1–20.

Dupont CL, Rusch DB, Yooseph S, Lombardo M-J, Richter RA, Valas R, *et al.* (2012). Genomic insights to SAR86, an abundant and uncultivated marine bacterial lineage. *ISME J* **6**:1186–1199.

Edgar RC. (2004). MUSCLE: multiple sequence alignment with high accuracy and high throughput. *Nucleic Acids Res* **32**:1792–1797.

Egli K, Bosshard F, Werlen C, Lais P, Siegrist H, Zehnder JB, *et al.* (2003). Microbial composition and structure of a rotating biological contactor biofilm treating ammonium-rich wastewater without organic carbon. *Microb Ecol* **45**:419–432.

Eichler J. (2003). Facing extremes: Archaeal surface-layer (glyco)proteins. *Microbiology* **149**:3347–3351.

Ellen AF, Zolghadr B, Driessen AMJ, Albers S-V. (2010). Shaping the archaeal cell envelope. *Archaea* **2010**:608243.

Erguder TH, Boon N, Wittebolle L, Marzorati M, Verstraete W. (2009). Environmental factors shaping the ecological niches of ammonia-oxidizing archaea. *FEMS Microbiol Rev* **33**:855–869.

Estelmann S, Hügler M, Eisenreich W, Werner K, Berg IA, Ramos-Vera WH, *et al.* (2011). Labeling and enzyme studies of the central carbon metabolism in *Metallosphaera sedula*. *J Bacteriol* **193**:1191–1200.

Felenstein J. (1989). PHYLIP-phylogeny inference package (version 3.2). *Cladistics* **5**:163–166.

Finkelstein A. (1976). Water and nonelectrolyte permeability of lipid bilayer membranes. *J Gen Physiol* **68**:127–135.

Foesel BU, Gieseke A, Schwermer C, Stief P, Koch L, Cytryn E, *et al.* (2008). *Nitrosomonas* Nm143-like ammonia oxidizers and *Nitrospira marina*-like nitrite oxidizers dominate the nitrifier community in a marine aquaculture biofilm. *FEMS Microbiol Ecol* **63**:192–204.

Frame CH, Casciotti KL. (2010). Biogeochemical controls and isotopic signatures of nitrous oxide production by a marine ammonia-oxidizing bacterium. *Biogeosciences* **7**:2695–2709.

Francis CA, Beman JM, Kuypers MMM. (2007). New processes and players in the nitrogen cycle: the microbial ecology of anaerobic and archaeal ammonia oxidation. *ISME J* **1**:19–27.

Francis CA, Roberts KJ, Beman MJ, Santoro AE, Oakley BB, Beman JM, *et al.* (2005). Ubiquity and diversity of ammonia-oxidizing archaea in water columns and sediments of the ocean. *Proc Natl Acad Sci U S A* **102**:14683–14688.

French E, Kozlowski JA, Mukherjee M, Bullerjahn G, Bollmann A. (2012). Ecophysiological characterization of ammonia-oxidizing archaea and bacteria from freshwater. *Appl Environ Microbiol* **78**:5773–5780.

Frydman L, Rossomando PC, Frydman V, Fernandez C, Frydman B, Samejimat K. (1992). Interactions between natural polyamines and tRNA: an 15N NMR analysis. *Proc Natl Acad Sci U S A* **89**:9186–9190.

Fukushima T, Wu YJ, Whang LM. (2012). The influence of salinity and ammonium levels on *amoA* mRNA expression of ammonia-oxidizing prokaryotes. *Water Sci Technol* **65**:2228–2235.

de Gannes V, Eudoxie G, Dyer DH, Hickey WJ. (2012). Diversity and abundance of ammonia oxidizing archaea in tropical compost systems. *Front Microbiol* **3**:244.

Gao J-F, Luo X, Wu G-X, Li T, Peng Y-Z. (2013). Quantitative analyses of the composition and abundance of ammonia-oxidizing archaea and ammonia-oxidizing bacteria in eight full-scale biological wastewater treatment plants. *Bioresour Technol* **138**:285–296.

Gao J-F, Luo X, Wu G, Li T, Peng Y-ZY. (2014). Abundance and diversity based on *amoA* genes of ammonia-oxidizing archaea and bacteria in ten wastewater treatment systems. *Appl Microbiol Biotechnol* **98**:3339–3354.

Gomes ES, Schuch V, Lemos EG. (2013). Biotechnology of polyketides: New breath of life for the novel antibiotic genetic pathways discovery through metagenomics. *Brazilian J Microbiol* **44**:1007–1034.

Gonthier M-P, Remesy C, Scalbert A, Cheynier V, Souquet J-M, Poutanen K, *et al.* (2006). Microbial metabolism of caffeic acid and its esters chlorogenic and caftaric acids by human faecal microbiota in vitro. *Biomed Pharmacother* **60**:536–540.

van Gool A, Laudelout H. (1966). Formate utilization by *Nitrobacter winogradskyi*. *Biochim Biophys Acta* **127**:295–301.

Goreau TJ, Kaplan WA, Wofsy SC. (1980). Production of NO_2^- and N_2O by nitrifying bacteria at reduced concentrations of oxygen. *Appl Environ Microbiol* **40**:526–532.

Goris J, Konstantinidis KT, Klappenbach JA, Coenye T, Vandamme P, Tiedje JM. (2007). DNA-DNA hybridization values and their relationship to whole-genome sequence similarities. *Int J Syst Evol Microbiol* **57**:81–91.

van de Graaf AA, Mulder A, de Bruijn P, Jetten MS, Robertson LA, Kuenen JG. (1995). Anaerobic oxidation of ammonium is a biologically mediated process. *Appl Environ Microbiol* **61**:1246–1251.

Graninger M, Nidetzky B, Heinrichs DE, Whitfield C, Messner P. (1999). Characterization of dTDP-4-dehydrorhamnose 3,5-epimerase and dTDP-4-dehydrorhamnose reductase, required for dTDP-L-rhamnose biosynthesis in *Salmonella enterica* serovar typhimurium LT2. *J Biol Chem* **274**:25069–25077.

Green SJ, Leigh MB, Neufeld JD. (2009). Denaturing gradient gel electrophoresis (DGGE) for microbial community analysis. In:*Microbiology of Hydrocarbons, Oils, Lipids, and Derived Compounds*, Vol. 1, Springer: Heidelberg, Germany, pp. 4137–4158.

Griffiths RI, Whiteley AS, O'Donnell AG, Bailey MJ. (2000). Rapid method for coextraction of DNA and RNA from natural environments for analysis of ribosomal DNA- and rRNA-based microbial community composition. *Appl Environ Microbiol* **66**:5488–5491.

Gruber-Dorninger C, Pester M, Kitzinger K, Savio DF, Loy A, Rattei T, *et al.* (2015). Functionally relevant diversity of closely related *Nitrospira* in activated sludge. *ISME J* **9**:643–655.

Gubry-Rangin C, Nicol GW, Prosser JI. (2010). Archaea rather than bacteria control nitrification in two agricultural acidic soils. *FEMS Microbiol Ecol* **74**:566–574.

Hall JA, Pajor AM. (2005). Functional characterization of a Na^+-coupled dicarboxylate carrier protein from *Staphylococcus aureus*. *J Bacteriol* **187**:5189–5194.

Hall JA, Pajor AM. (2007). Functional reconstitution of SdcS, a Na^+-coupled dicarboxylate carrier protein from *Staphylococcus aureus*. *J Bacteriol* **189**:880–885.

Hallam SJ, Mincer TJ, Schleper C, Preston CM, Roberts K, Richardson PM, *et al.* (2006). Pathways of carbon assimilation and ammonia oxidation suggested by environmental genomic analyses of marine *Crenarchaeota*. *PLoS Biol* **4**:e95.

Hatzenpichler R. (2012). Diversity, physiology, and niche differentiation of ammonia-oxidizing archaea. *Appl Environ Microbiol* **78**:7501–7510.

Hatzenpichler R, Lebedeva EV, Spieck E, Stoecker K, Richter A, Daims H, *et al.* (2008). A moderately thermophilic ammonia-oxidizing crenarchaeote from a hot spring. *Proc Natl Acad Sci U S A* **105**:2134–2139.

He J-Z, Shen J-P, Zhang L-M, Zhu Y-G, Zheng Y-M, Xu M-G, *et al.* (2007). Quantitative analyses of the abundance and composition of ammonia-oxidizing bacteria and ammonia-oxidizing archaea of a Chinese upland red soil under long-term fertilization practices. *Environ Microbiol* **9**:2364–2374.

Herndl GJ, Reinthaler T, Teira E, Aken H, Veth C, Pernthaler A, *et al.* (2005). Contribution of *Archaea* to total prokaryotic production in the deep atlantic ocean. *Appl Environ Microbiol* **71**:2303–2309.

Herrmann M, Saunders AM, Schramm A. (2008). Archaea dominate the ammonia-oxidizing community in the rhizosphere of the freshwater macrophyte *Littorella uniflora*. *Appl Environ Microbiol* **74**:3279–3283.

Herrmann M, Saunders AM, Schramm A. (2009). Effect of lake trophic status and rooted macrophytes on community composition and abundance of ammonia-oxidizing prokaryotes in freshwater sediments. *Appl Environ Microbiol* **75**:3127–3136.

Herrmann M, Scheibe A, Avrahami S, Küsel K. (2011). Ammonium availability affects the ratio of ammonia-oxidizing bacteria to ammonia-oxidizing archaea in simulated creek ecosystems. *Appl Environ Microbiol* **77**:1896–1899.

Höfle MG. (1984). Degradation of putrescine and cadaverine in seawater cultures by marine bacteria. *Appl Environ Microbiol* **47**:843–849.

Hollibaugh JT, Tolar BB, Popp BB, Wallsgrove NJ. (2015). Evidence for the direct oxidation of polyamine nitrogen by *Thaumarchaeota*-dominated marine nitrifying comunities. In:*2015 Aquatic Sciences Meeting*. Granada, Spain. http://www.sgmeet.com/aslo/granada2015/viewabstract.asp?AbstractID=26435

Holmes RM, Aminot A, Kerouel R, Hooker BA, Peterson BJ. (1999). A simple and precise method for measuring ammonium in marine and freshwater ecosystems. *Can J Fish Aquat Sci* **56**:1801–1808.

Hommes NG, Sayavedra-Soto LA, Arp DJ. (2003). Chemolithoorganotrophic growth of *Nitrosomonas europaea* on fructose. *J Bacteriol* **185**:6809–6814.

Hou Y, Zhang H, Miranda L, Lin S. (2010). Serious overestimation in quantitative PCR by circular (supercoiled) plasmid standard: microalgal *pcna* as the model gene. *PLoS One* **5**:e9545.

Hovanec TA, DeLong EF. (1996). Comparative analysis of nitrifying bacteria associated with freshwater and marine aquaria. *Appl Environ Microbiol* **62**:2888–2896.

Hovanec TA, Taylor LT, Blakis A, Delong F. (1998). *Nitrospira*-like bacteria associated with nitrite oxidation in freshwater aquaria. *Appl Environ Microbiol* **64**:258–264.

Huang S-C, Panagiotidis CA, Canellakis ES. (1990). Transcriptional effects of polyamines on ribosomal proteins and on polyamine-synthesizing enzymes in *Escherichia coli*. *Biochemistry* **87**:3464–3468.

Huguet C, Hopmans E, Feboayala W, Thompson D, Sinninghedamste J, Schouten S. (2006). An improved method to determine the absolute abundance of glycerol dibiphytanyl glycerol tetraether lipids. *Org Geochem* **37**:1036–1041.

Huson DH, Mitra S, Ruscheweyh H-J, Weber N, Schuster SC. (2011). Integrative analysis of environmental sequences using MEGAN4. *Genome Res* **21**:1552–1560.

Hyatt D, Chen G-L, Locascio PF, Land ML, Larimer FW, Hauser LJ. (2010). Prodigal: prokaryotic gene recognition and translation initiation site identification. *BMC Bioinformatics* **11**:119.

Igarashi K, Kashiwagi K. (1999). Polyamine transport in bacteria and yeast. *Biochem J* **344**:633–642.

Im J, Lee S-W, Bodrossy L, Barcelona MJ, Semrau JD. (2011). Field application of nitrogen and phenylacetylene to mitigate greenhouse gas emissions from landfill cover soils: effects on microbial community structure. *Appl Microbiol Biotechnol* **89**:189–200.

Incharoensakdi A, Jantaro S, Raksajit W, Mäenpää P. (2010). Polyamines in cyanobacteria: biosynthesis, transport and abiotic stress response. In: *Current research, technology and education topics in applied microbiology and microbial biotechnology*, Mendez-Vilas, A (ed), Formatex: Badajoz, pp. 23–32.

Ingalls AE, Shah SR, Hansman RL, Aluwihare LI, Santos GM, Druffel ERM, *et al.* (2006). Quantifying archaeal community autotrophy in the mesopelagic ocean using natural radiocarbon. *Proc Natl Acad Sci U S A* **103**:6442–6447.

Ip YK, Chew SF. (2010). Ammonia production, excretion, toxicity, and defense in fish: A review. *Front Physiol* **1**:134.

Ip YK, Chew SF, Randall DJ. (2001). Ammonia toxicity, tolerance, and excretion. *Fish Physiol* **20**:109–148.

Ishii K, Mussman M, MacGregor BJ, Amann R. (2004). An improved fluorescence in situ hybridization protocol for the identification of bacteria and archaea in marine sediments. *FEMS Microbiol Ecol* **50**:203–213.

Jang A, Okabe S, Watanabe Y, Kim IS, Bishop PL. (2005). Measurement of growth rate of ammonia oxidizing bacteria in partially submerged rotating biological contactor by fluorescent *in situ* hybridization (FISH). *J Environ Eng Sci* **4**:413–420.

Jantaro S, Mäenpää P, Mulo P, Incharoensakdi A, Epstein E, Norlyn JD, *et al.* (2003). Content and biosynthesis of polyamines in salt and osmotically stressed cells of *Synechocystis* sp. PCC 6803. *FEMS Microbiol Lett* **228**:129–35.

Jarrell KF, Ding Y, Nair DB, Siu S. (2013). Surface appendages of archaea: structure, function, genetics and assembly. *Life* **3**:86–117.

Jeong S, Cho K, Bae H, Keshvardoust P, Rice SA, Vigneswaran S, *et al.* (2016). Effect of microbial community structure on organic removal and biofouling in membrane adsorption bioreactor used in seawater pretreatment. *Chem Eng J* **294**:30–39.

Jia Z, Conrad R. (2009). *Bacteria* rather than *Archaea* dominate microbial ammonia oxidation in an agricultural soil. *Environ Microbiol* **11**:1658–1671.

Jin T, Zhang T, Yan Q, Jin T, Yan Q, Zhang T, *et al.* (2010). Characterization and quantification of ammonia-oxidizing archaea (AOA) and bacteria (AOB) in a nitrogen-removing reactor using T-RFLP and qPCR. *Appl Microbiol Biotechnol* **87**:1167–1176.

Jones LC, Peters B, Lezama Pacheco JS, Casciotti KL, Fendorf S. (2015). Stable Isotopes and Iron Oxide Mineral Products as Markers of Chemodenitrification. *Environ Sci Technol* **49**:3444–3452.

Josenhans C, Vossebein L, Friedrich S, Suerbaum S. (2002). The *neuA*/*flmD* gene cluster of *Helicobacter pylori* is involved in flagellar biosynthesis and flagellin glycosylation. *FEMS Microbiol Lett* **210**:165–172.

Juhas M, Van Der Meer JR, Gaillard M, Harding RM, Hood DW, Crook DW. (2009). Genomic islands: Tools of bacterial horizontal gene transfer and evolution. *FEMS Microbiol Rev* **33**:376–393.

Jung M-Y, Park S-J, Kim S-J, Kim J-G, Sinninghe Damsté JS, Jeon CO, *et al.* (2014). A mesophilic, autotrophic, ammonia-oxidizing archaeon of thaumarchaeal group I.1a cultivated from a deep oligotrophic soil horizon. *Appl Environ Microbiol* **80**:3645–3655.

Jung M-Y, Park S-J, Min D, Kim J-S, Rijpstra WIC, Sinninghe Damste JS, *et al.* (2011). Enrichment and characterization of an autotrophic ammonia-oxidizing archaeon of mesophilic crenarchaeal Group I.1a from an agricultural soil. *Appl Environ Microbiol* **77**:8635–8647.

Jung M-Y, Well R, Min D, Giesemann A, Park S-J, Kim J-G, *et al.* (2014). Isotopic signatures of N_2O produced by ammonia-oxidizing archaea from soils. *ISME J* **8**:1115–1125.

Jurgens G, Lindström K, Saano A. (1997). Novel group within the kingdom *Crenarchaeota* from boreal forest soil. *Appl Environ Microbiol* **63**:803–805.

Kampschreur MJ, Kleerebezem R, de Vet WWJM, van Loosdrecht MCM. (2011). Reduced iron induced nitric oxide and nitrous oxide emission. *Water Res* **45**:5945–5952.

Kanehisa M, Goto S. (2000). KEGG: Kyoto Encyclopedia of Genes and Genomes. *Nucleic Acids Res* **28**:27–30.

Karner MB, DeLong EF, Karl DM. (2001). Archaeal dominance in the mesopelagic zone of the Pacific Ocean. *Nature* **409**:507–510.

Kasuga I, Nakagaki H, Kurisu F, Furumai H. (2010). Predominance of ammonia-oxidizing archaea on granular activated carbon used in a full-scale advanced drinking water treatment plant. *Water Res* **44**:5039–5049.

Kayee P, Sonthiphand P, Rongsayamanont C, Limpiyakorn T. (2011). Archaeal *amoA* genes outnumber bacterial *amoA* genes in municipal wastewater treatment plants in Bangkok. *Microb Ecol* **62**:776–788.

van Kessel MAHJ, Speth DR, Albertsen M, Nielsen PH, Op den Camp HJM, Kartal B, *et al.* (2015). Complete nitrification by a single microorganism. *Nature* **528**:555–559.

Kim BK, Jung M, Yu DS, Park S, Oh TK, Rhee S, *et al.* (2011). Genome sequence of an ammonia-oxidizing soil archaeon, 'Candidatus Nitrosoarchaeum koreensis ' MY1. *Appl Environ Micobiol* **193**:5539–5540.

Kim J-G, Park S-J, Sinninghe Damsté JS, Schouten S, Rijpstra WIC, Jung M-Y, *et al.* (2016). Hydrogen peroxide detoxification is a key mechanism for growth of ammonia-oxidizing archaea. *Proc Natl Acad Sci U S A* **113**:7888–7893.

Koch H, Galushko A, Albertsen M, Schintlmeister A, Gruber-Dorninger C, Lücker S, *et al.* (2014). Growth of nitrite-oxidizing bacteria by aerobic hydrogen oxidation. *Science* **345**:1052–1054.

Koch H, Lücker S, Albertsen M, Kitzinger K, Herbold C, Spieck E, *et al.* (2015). Expanded metabolic versatility of ubiquitous nitrite-oxidizing bacteria from the genus *Nitrospira*. *Proc Natl Acad Sci U S A* **112**:11371–11376.

König H, Rachel R, Claus H. (2007). Proteinaceous surface layers of *Archaea*: ultrastructure and biochemistry. In: *Archaea: molecular and cellular biology*, American Society of Microbiology, pp. 315–340.

Könneke M, Bernhard AE, de la Torre JR, Walker CB, Waterbury JB, Stahl DA. (2005). Isolation of an autotrophic ammonia-oxidizing marine archaeon. *Nature* **437**:543–546.

Könneke M, Schubert DM, Brown PC, Hügler M, Standfest S, Schwander T, *et al.* (2014). Ammonia-oxidizing archaea use the most energy-efficient aerobic pathway for CO_2 fixation. *Proc Natl Acad Sci U S A* **111**:8239–8244.

Konstantinidis KT, Braff J, Karl DM, DeLong EF. (2009). Comparative metagenomic analysis of a microbial community residing at a depth of 4,000 meters at station ALOHA in the North Pacific subtropical gyre. *Appl Environ Microbiol* **75**:5345–5355.

Konstantinidis KT, Tiedje JM. (2005a). Genomic insights that advance the species definition for prokaryotes. *Proc Natl Acad Sci U S A* **102**:2567–2572.

Konstantinidis KT, Tiedje JM. (2005b). Towards a genome-based taxonomy for prokaryotes. *J Bacteriol* **187**:6258–6264.

Koops HP, Bottcher B, Moller UC, Pommerening-Roser A, Stehr G. (1991). Classification of eight new species of ammonia-oxidizing bacteria: *Nitrosomonas communis* sp. nov., *Nitrosomonas ureae* sp. nov., *Nitrosomonas aestuarii* sp. nov., *Nitrosomonas marina* sp. nov., *Nitrosomonas nitrosa* sp. nov. *Microbiology* **137**:1689–1699.

Koops HP, Pommerening-Röser A. (2001). Distribution and ecophysiology of the nitrifying bacteria emphasizing cultured species. *FEMS Microbiol Ecol* **37**:1–9.

Koops HP, Purkhold U, Pommerening-Röser A, Timmermann G, Wagner M. (2006). The lithoautotrophic ammonia-oxidizing bacteria. In:*Prokaryotes*, Dworkin, M, Falkow, S, Rosenberg, E, Schleifer, K-H, & Stackebrandt, E (eds), Springer New York: New York, pp. 778–811.

Koper TE, El-Sheikh AF, Norton JM, Klotz MG. (2004). Urease-encoding genes in ammonia-oxidizing bacteria. *Appl Environ Microbiol* **70**:2342–2348.

Kowalchuk GA, Stephen JR. (2001). Ammonia-oxidizing bacteria: a model for molecular microbial ecology. *Annu Rev Microbiol* **55**:485–529.

Kozlowski JA, Stieglmeier M, Schleper C, Klotz MG, Stein LY. (2016). Pathways and key intermediates required for obligate aerobic ammonia-dependent chemolithotrophy in bacteria and Thaumarchaeota. *ISME J* **10**:1836–1845.

Krümmel A, Harms H. (1982). Effect of organic matter on growth and cell yield of ammonia-oxidizing bacteria. *Arch Microbiol* **133**:50–54.

Krzywinski M, Schein J, Birol I, Connors J, Gascoyne R, Horsman D, *et al.* (2009). Circos: an information aesthetic for comparative genomics. *Genome Res* **19**:1639–1645.

Kurtz S, Phillippy A, Delcher AL, Smoot M, Shumway M, Antonescu C, *et al.* (2004). Versatile and open software for comparing large genomes. *Genome Biol* **5**:R12.

Kusano T, Yamaguchi K, Berberich T, Takahashi Y. (2007). Advances in polyamine research in 2007. *J Plant Res* **120**:345–350.

Lam P, Jensen MM, Lavik G, McGinnis DF, Muller B, Schubert CJ, *et al.* (2007). Linking crenarchaeal and bacterial nitrification to anammox in the Black Sea. *Proc Natl Acad Sci U S A* **104**:7104–7109.

Lam P, Kuypers MMM. (2011). Microbial nitrogen cycling processes in oxygen minimum zones. *Ann Rev Mar Sci* **3**:317–345.

Larkin A, Imperiali B. (2011). The expanding horizons of asparagine-linked glycosylation. *Biochemistry* **50**:4411–4426.

Lawrence JG, Ochman H. (2002). Reconciling the many faces of lateral gene transfer. *Trends Microbiol* **10**:1–4.

Lebedeva E V, Hatzenpichler R, Pelletier E, Schuster N, Hauzmayer S, Bulaev A, *et al.* (2013). Enrichment and genome sequence of the group I.1a ammonia-oxidizing archaeon 'Ca. Nitrosotenuis uzonensis' representing a clade globally distributed in thermal habitats. *PLoS One* **8**:e80835.

Lebedeva E V., Alawi M, Fiencke C, Namsaraev B, Bock E, Spieck E. (2005). Moderately thermophilic nitrifying bacteria from a hot spring of the Baikal rift zone. *FEMS Microbiol Ecol* **54**:297–306.

Lee N, Nielsen PH, Andreasen KH, Juretschko S, Nielsen JL, Schleifer K-H, *et al.* (1999). Combination of fluorescent *in situ* hybridization and microautoradiography-a new tool for structure-function analyses in microbial ecology. *Appl Environ Microbiol* **65**:1289–1297.

Lee SY. (2000). Bacterial polyhydroxyalkanoates. *Biotechnol Bioeng* **49**:1–14.

Leggett RM, Clavijo BJ, Clissold L, Clark MD, Caccamo M. (2014). NextClip: an analysis and read preparation tool for Nextera Long Mate Pair libraries. *Bioinformatics* **30**:566–568.

Lehtovirta-Morley LE, Ross J, Hink L, Weber EB, Gubry-Rangin C, Thion C, *et al.* (2016). Isolation of 'Candidatus Nitrosocosmicus franklandus', a novel ureolytic soil archaeal ammonia oxidiser with tolerance to high ammonia concentration. *FEMS Microbiol Ecol* **92**:fiw057.

Lehtovirta-Morley LE, Sayavedra-Soto LA, Gallois N, Schouten S, Stein LY, Prosser JI, *et al.* (2016). Identifying potential mechanisms enabling acidophily in the ammonia-oxidising archaeon '*Candidatus* Nitrosotalea devanaterra'. *Appl Environ Microbiol* **82**:2608–2619.

Lehtovirta-Morley LE, Stoecker K, Vilcinskas A, Prosser JI, Nicol GW. (2011). Cultivation of an obligate acidophilic ammonia oxidizer from a nitrifying acid soil. *Proc Natl Acad Sci U S A* **108**:15892–15897.

Lehtovirta-Morley LE, Verhamme DT, Nicol GW, Prosser JI. (2013). Effect of nitrification inhibitors on the growth and activity of *Nitrosotalea devanaterra* in culture and soil. *Soil Biol Biochem* **62**:129–133.

Leininger S, Urich T, Schloter M, Schwark L, Qi J, Nicol GW, *et al.* (2006). Archaea predominate among ammonia-oxidizing prokaryotes in soils. *Nature* **442**:806–809.

Li P-E, Lo C-C, Anderson JJ, Davenport KW, Bishop-Lilly KA, Xu Y, *et al.* (2016). Enabling the democratization of the genomics revolution with a fully integrated web-based bioinformatics platform. *bioRxiv* 040477.

Li Y, Ding K, Wen X, Zhang B, Shen B, Yang Y. (2016). A novel ammonia-oxidizing archaeon from wastewater treatment plant: Its enrichment, physiological and genomic characteristics. *Sci Rep* **6**:23747.

Limpiyakorn T, Fürhacker M, Haberl R, Chodanon T, Srithep P, Sonthiphand P. (2013). *amoA*-encoding archaea in wastewater treatment plants: a review. *Appl Microbiol Biotechnol* **97**:1425–1439.

Limpiyakorn T, Sonthiphand P, Rongsayamanont C, Polprasert C. (2011). Abundance of *amoA* genes of ammonia-oxidizing archaea and bacteria in activated sludge of full-scale wastewater treatment plants. *Bioresour Technol* **102**:3694–3701.

Lo C-C, Chain PSG. (2014). Rapid evaluation and quality control of next generation sequencing data with FaQCs. *BMC Bioinformatics* **15**:366.

Lodish H, Berk A, Zipursky SL, Matsudaira P, Baltimore D, Darnell J. (2000). Diffusion of small molecules across phospholipid bilayers. 4th ed. W. H. Freeman: New York.

Logan SM. (2006). Flagellar glycosylation - A new component of the motility repertoire? *Microbiology* **152**:1249–1262.

Löscher CR, Kock A, Könneke M, LaRoche J, Bange HW, Schmitz RA. (2012). Production of oceanic nitrous oxide by ammonia-oxidizing archaea. *Biogeosciences* **9**:2419–2429.

Lücker S, Schwarz J, Gruber-Dorninger C, Spieck E, Wagner M, Daims H. (2015). *Nitrotoga*-like bacteria are previously unrecognized key nitrite oxidizers in full-scale wastewater treatment plants. *ISME J* **9**:708–720.

Lücker S, Wagner M, Maixner F, Pelletier E, Koch H, Vacherie B, *et al.* (2010). A *Nitrospira* metagenome illuminates the physiology and evolution of globally important nitrite-oxidizing bacteria. *Proc Natl Acad Sci U S A* **107**:13479–13484.

Macgregor BJ, Moser DP, Alm EW, Nealson KH, Stahl DA. (1997). *Crenarchaeota* in Lake Michigan Sediment. *Appl Environ Microbiol* **63**:1178–1181.

Mahnert A, Vaishampayan P, Probst AJ, Auerbach A, Moissl-Eichinger C, Venkateswaran K, *et al.* (2015). Cleanroom maintenance significantly reduces abundance but not diversity of indoor microbiomes. *PLoS One* **10**:e0134848.

Maixner F, Noguera DR, Anneser B, Stoecker K, Wegl G, Wagner M, *et al.* (2006). Nitrite concentration influences the population structure of *Nitrospira*-like bacteria. *Environ Microbiol* **8**:1487–1495.

Malavolta E, Delwiche CC, Burge WD. (1962). Formate oxidation by cell-free preparations from *Nitrobacter agilis*. *Biochim Biophys Acta* **57**:347–351.

Malovanyy A, Trela J, Plaza E. (2015). Mainstream wastewater treatment in integrated fixed film activated sludge (IFAS) reactor by partial nitritation/anammox process. *Bioresour Technol* **198**:478–487.

Markowitz VM, Mavromatis K, Ivanova NN, Chen I-MA, Chu K, Kyrpides NC. (2009). IMG ER: a system for microbial genome annotation expert review and curation. *Bioinformatics* **25**:2271–2278.

Martens-Habbena W, Berube PM, Urakawa H, de la Torre JR, Stahl DA. (2009). Ammonia oxidation kinetics determine niche separation of nitrifying Archaea and Bacteria. *Nature* **461**:976–979.

Martens-Habbena W, Qin W, Horak REA, Urakawa H, Schauer AJ, Moffett JW, *et al.* (2015). The production of nitric oxide by marine ammonia-oxidizing archaea and inhibition of archaeal ammonia oxidation by a nitric oxide scavenger. *Environ Microbiol* **17**:2261–2274.

Martens-Habbena W, Stahl DA. (2011). Nitrogen metabolism and kinetics of ammonia-oxidizing archaea. *Methods Enzymol* **496**:4654–4687.

Martiny H, Koops HP. (1982). Incorporation of organic compounds into cell protein by lithotrophic, ammonia-oxidizing bacteria. *Antonie Van Leeuwenhoek* **48**:327–336.

Massana R, Murray AE, Preston CM, DeLong EF. (1997). Vertical distribution and phylogenetic characterization of marine planktonic Archaea in the Santa Barbara Channel. *Appl Environ Microbiol* **63**:50–56.

McInerney JO, Mullarkey M, Wernecke ME, Powel R. (1997). Phylogenetic analysis of Group I marine archaeal rRNA sequences emphasizes the hidden diversity within the primary group Archaea. *Proc R Soc B Biol Sci* **264**:1663–1669.

McNally DJ, Hui JPM, Aubry AJ, Mui KKK, Guerry P, Brisson JR, *et al.* (2006). Functional characterization of the flagellar glycosylation locus in *Campylobacter jejuni* 81-176 using a focused metabolomics approach. *J Biol Chem* **281**:18489–18498.

Men Y, Han P, Helbling DE, Jehmlich N, Herbold C, Gulde R, *et al.* (2016). Biotransformation of two pharmaceuticals by the ammonia-oxidizing archaeon *Nitrososphaera gargensis*. *Environ Sci Technol* **50**:4682–4692.

Merbt SN, Stahl DA, Casamayor EO, Martí E, Nicol GW, Prosser JI. (2012). Differential photoinhibition of bacterial and archaeal ammonia oxidation. *FEMS Microbiol Lett* **327**:41–46.

Meseguer-Lloret S, Molins-Legua C, Campins-Falco P. (2002). Ammonium determination in water samples by using OPA-NAC reagent: a comparative study with nessler and ammonium selective electrode methods. *Int J Environ Anal Chem* **82**:475–489.

Miele V, Penel S, Duret L. (2011). Ultra-fast sequence clustering from similarity networks with SiLiX. *BMC Bioinformatics* **12**:116.

Miller NJ, Rice-Evans C, Davies MJ, Gopinathan V, Milner A. (1993). A novel method for measuring antioxidant capacity and its application to monitoring the antioxidant status in premature neonates. *Clin Sci* **84**:407–412.

Miranda KM, Espey MG, Wink DA. (2001). A rapid, simple spectrophotometric method for simultaneous detection of nitrate and nitrite. *Nitric Oxide* **5**:62–71.

Mobarry B, Wagner M, Urbain V, Rittmann B, Stahl D. (1996). Phylogenetic probes for analyzing abundance and spatial organization of nitrifying bacteria. *Appl Environ Microbiol* **62**:2156–2162.

Mobley HL, Island MD, Hausinger RP. (1995). Molecular biology of microbial ureases. *Microbiol Rev* **59**:451–480.

Moissl C, Bruckner JC, Venkateswaran K. (2008). Archaeal diversity analysis of spacecraft assembly clean rooms. *ISME J* **2**:115–119.

Moissl-Eichinger C. (2011). Archaea in artificial environments: their presence in global spacecraft clean rooms and impact on planetary protection. *ISME J* **5**:209–219.

Moore WEC, Stackebrandt E, Kandler O, Colwell RR, Krichevsky MI, Truper HG, *et al.* (1987). Report of the *ad hoc* committee on reconciliation of approaches to bacterial systematics. *Int J Syst Evol Microbiol* **37**:463–464.

Morou-Bermudez E, Burne RA. (2000). Analysis of urease expression in *Actinomyces naeslundii* WVU45. *Infect Immun* **68**:6670–6676.

Mosier AC, Allen EE, Kim M, Ferriera S, Francis CA. (2012). Genome sequence of '*Candidatus* Nitrosopumilus salaria' BD31, an ammonia-oxidizing archaeon from the San Francisco Bay estuary. *J Bacteriol* **194**:2121–2122.

Mosier AC, Francis CA. (2008). Relative abundance and diversity of ammonia-oxidizing archaea and bacteria in the San Francisco Bay estuary. *Environ Microbiol* **10**:3002–3016.

Mosier AC, Lund MB, Francis CA. (2012). Ecophysiology of an ammonia-oxidizing archaeon adapted to low-salinity habitats. *Microb Ecol* **64**:955–963.

Motamedi H, Shafiee A, Cai SJ, Streicher SL, Arison BH, Miller RR. (1996). Characterization of methyltransferase and hydroxylase genes involved in the biosynthesis of the immunosuppressants FK506 and FK520. *J Bacteriol* **178**:5243–5248.

Mou X, Sun S, Rayapati P, Moran M. (2010). Genes for transport and metabolism of spermidine in *Ruegeria pomeroyi* DSS-3 and other marine bacteria. *Aquat Microb Ecol* **58**:311–321.

Mulder A, Graaf AA, Robertson LA, Kuenen JG. (1995). Anaerobic ammonium oxidation discovered in a denitrifying fluidized bed reactor. *FEMS Microbiol Ecol* **16**:177–184.

Murphy TF, Brauer AL, Murphy T, Faden H, Bakaletz L, Kyd J, *et al.* (2011). Expression of urease by *Haemophilus influenzae* during human respiratory tract infection and role in survival in an acid environment. *BMC Microbiol* **11**:183.

Murray AE, Preston CM, Massana R, Taylor LT, Blakis A, Wu K, *et al.* (1998). Seasonal and spatial variability of bacterial and archaeal assemblages in the coastal waters near Anvers Island, Antarctica. *Appl Environ Microbiol* **64**:2585–2595.

Mushtaq R, Naeem S, Sohail A, Riazuddin S. (1993). BseRI a novel restriction endonuclease from a Bacillus species which recognizes the sequence 5'...GAGGAG...3'. *Nucleic Acids Res* **21**:3585.

Mussman M, Brito I, Pitcher A, Sinninghe Damste JS, Hatzenpichler R, Richter A, *et al.* (2011). Thaumarchaeotes abundant in refinery nitrifying sludges express *amoA* but are not obligate autotrophic ammonia oxidizers. *Proc Natl Acad Sci U S A* **108**:16771–16776.

Muyzer G, de Waal EC, Uitterlinden AG. (1993). Profiling of complex microbial populations by denaturing gradient gel electrophoresis analysis of polymerase chain reaction-amplified genes coding for 16S rRNA. *Appl Environ Microbiol* **59**:695–700.

Neufeld JD, Mohn WW, de Lorenzo V. (2006). Composition of microbial communities in hexachlorocyclohexane (HCH) contaminated soils from Spain revealed with a habitat-specific microarray. *Environ Microbiol* **8**:126–140.

Ng K-H, Srinivas V, Srinivasan R, Balasubramanian M. (2013). The *Nitrosopumilus maritimus* CdvB, but not FtsZ, assembles into polymers. *Archaea* **2013**:104147.

Nichols D. (2007). Cultivation gives context to the microbial ecologist. *FEMS Microbiol Ecol* **60**:351–357.

Nicol GW, Leininger S, Schleper C. (2011). Distribution and activity of ammonia-oxidizing archaea in natural environments. In:*Nitrification*, Ward, BB, Arp, DJ, & Klotz, MG (eds), American Society of Microbiology, pp. 157–178.

Nicol GW, Leininger S, Schleper C, Prosser JI. (2008). The influence of soil pH on the diversity, abundance and transcriptional activity of ammonia oxidizing archaea and bacteria. *Environ Microbiol* **10**:2966–2978.

Nishibori N, Nishii A, Takayama, H. (2001). Detection of free polyamine in coastal seawater using ion exchange chromatography. *ICES J Mar Sci* **58**:1201–1207.

Nothaft H, Szymanski CM. (2010). Protein glycosylation in bacteria: sweeter than ever. *Nat Rev Microbiol* **8**:765–78.

Oba M, Sakata S, Tsunogai U. (2006). Polar and neutral isopranyl glycerol ether lipids as biomarkers of archaea in near-surface sediments from the Nankai Trough. *Org Geochem* **37**:1643–1654.

Ochsenreiter T, Selezi D, Quaiser A, Bonch-Osmolovskaya L, Schleper C. (2003). Diversity and abundance of Crenarchaeota in terrestrial habitats studied by 16S RNA surveys and real time PCR. *Environ Microbiol* **5**:787–797.

Offre P, Prosser JI, Nicol GW. (2009). Growth of ammonia-oxidizing archaea in soil microcosms is inhibited by acetylene. *FEMS Microbiol Ecol* **70**:99–108.

Oishi R, Hirooka K, Otawa K, Tada C, Nakai Y. (2012). Ammonia-oxidizing archaea in laboratory-scale activated sludge systems for wastewater of low- or high-ammonium concentration. *Anim Sci J* **83**:571–576.

Oishi R, Tada C, Asano R, Yamamoto N, Suyama Y, Nakai Y. (2012). Growth of ammonia-oxidizing archaea and bacteria in cattle manure compost under various temperatures and ammonia concentrations. *Microb Ecol* **63**:787–793.

Ong S, Toorisaka E, Hirata M, Hano T. (2005). Biodegradation of redox dye methylene blue by up-flow anaerobic sludge blanket reactor. *J Hazard Mater* **124**:88–94.

Ouverney CC, Fuhrman JA. (2000). Marine planktonic archaea take up amino acids. *Appl Environ Microbiol* **66**:4829–4833.

Palatinszky M, Herbold C, Jehmlich N, Pogoda M, Han P, von Bergen M, *et al.* (2015). Cyanate as an energy source for nitrifiers. *Nature* **524**:105–108.

Park B-J, Park S-J, Yoon D-N, Schouten S, Sinninghe Damste JS, Rhee S-K. (2010). Cultivation of autotrophic ammonia-oxidizing archaea from marine sediments in coculture with sulfur-oxidizing bacteria. *Appl Environ Microbiol* **76**:7575–7587.

Park H-D, Wells GF, Bae H, Criddle CS, Francis CA. (2006). Occurrence of ammonia-oxidizing archaea in wastewater treatment plant bioreactors. *Appl Environ Microbiol* **72**:5643–5647.

Park S-J, Kim J-G, Jung M-Y, Kim S-J, Cha I-T, Ghai R, *et al.* (2012). Draft genome sequence of an ammonia-oxidizing archaeon, '*Candidatus* Nitrosopumilus sediminis' AR2, from Svalbard in the Arctic Circle. *J Bacteriol* **194**:6948–6949.

Park S-J, Kim J-G, Jung M-Y, Kim S-J, Cha I-T, Kwon K, *et al.* (2012). Draft genome sequence of an ammonia-oxidizing archaeon, '*Candidatus* Nitrosopumilus koreensis' AR1, from marine sediment. *J Bacteriol* **194**:6940–1941.

Parker R. (2002). Aquaculture science. 2nd ed. Delmar/Thomson Learning: Albany, NY.

Pedersen H, Lomstein BA, Henry BT. (1993). Evidence for bacterial urea production in marine sediments. *FEMS Microbiol Ecol* **12**:51–59.

Pelve EA, Lindås A-C, Martens-Habbena W, de la Torre JR, Stahl DA, Bernander R. (2011). Cdv-based cell division and cell cycle organization in the thaumarchaeon *Nitrosopumilus maritimus*. *Mol Microbiol* **82**:555–566.

Pester M, Rattei T, Flechl S, Gröngröft A, Richter A, Overmann J, *et al.* (2012). *amoA*-based consensus phylogeny of ammonia-oxidizing archaea and deep sequencing of *amoA* genes from soils of four different geographic regions. *Environ Microbiol* **14**:525–539.

Pester M, Schleper C, Wagner M. (2011). The *Thaumarchaeota*: an emerging view of their phylogeny and ecophysiology. *Curr Opin Microbiol* **14**:300–306.

Pfeiffer S, Leopold E, Hemmens B, Schmidt K, Werner ER, Mayer B. (1997). Interference of carboxy-PTIO with nitric oxide- and peroxynitrite-mediated reactions. *Free Radic Biol Med* **22**:787–794.

Pinto AJ, Marcus DN, Ijaz UZ, Bautista-de lose Santos QM, Dick GJ, Raskin L. (2016). Metagenomic evidence for the presence of comammox *Nitrospira*-like bacteria in a drinking water system. *mSphere* **1**:e00054–15.

Pitcher A, Hopmans EC, Mosier AC, Park S-J, Rhee S-K, Francis CA, *et al.* (2011). Core and intact polar glycerol dibiphytanyl glycerol tetraether lipids of ammonia-oxidizing archaea enriched from marine and estuarine sediments. *Appl Environ Microbiol* **77**:3468–3477.

Pitcher A, Hopmans EC, Schouten S, Sinninghe Damsté JS. (2009). Separation of core and intact polar archaeal tetraether lipids using silica columns: Insights into living and fossil biomass contributions. *Org Geochem* **40**:12–19.

Pitcher A, Rychlik N, Hopmans EC, Spieck E, Rijpstra WIC, Ossebaar J, *et al.* (2010). Crenarchaeol dominates the membrane lipids of *Candidatus* Nitrososphaera gargensis, a thermophilic Group I.1b Archaeon. *ISME J* **4**:542–552.

Pitcher A, Villanueva L, Hopmans EC, Schouten S, Reichart G-J, Sinninghe Damsté JS. (2011). Niche segregation of ammonia-oxidizing archaea and anammox bacteria in the Arabian Sea oxygen minimum zone. *ISME J* **5**:1896–1904.

Poli A, Di Donato P, Abbamondi GR, Nicolaus B. (2011). Synthesis, production, and biotechnological applications of exopolysaccharides and polyhydroxyalkanoates by Archaea. *Archaea* **2011**:693253.

Pratscher J, Dumont MG, Conrad R. (2011). Ammonia oxidation coupled to CO_2 fixation by archaea and bacteria in an agricultural soil. *Proc Natl Acad Sci U S A* **108**:4170–4175.

Preston CM, Wu KY, Molinski TF, DeLong EF. (1996). A psychrophilic crenarchaeon inhabits a marine sponge: *Cenarchaeum symbiosum* gen. nov., sp. nov. *Proc Natl Acad Sci U S A* **93**:6241–6246.

Probst AJ, Auerbach AK, Moissl-Eichinger C. (2013). Archaea on human skin. *PLoS One* **8**:e65388.

Pynaert K, Smets BFBF, Wyffels S, Beheydt D, Siciliano SD, Verstraete W. (2003). Characterization of an autotrophic nitrogen-removing biofilm from a highly loaded lab-scale rotating biological contactor. *Appl Environ Microbiol* **69**:3626–3635.

Qin W, Amin SA, Martens-Habbena W, Walker CB, Urakawa H, Devol AH, *et al.* (2014). Marine ammonia-oxidizing archaeal isolates display obligate mixotrophy and wide ecotypic variation. *Proc Natl Acad Sci U S A* **111**:12504–12509.

Rachel R, Pum D, Smarda J, Smajs D, Komrska J, Krzyzanek V, *et al.* (1997). Fine structure of S-layers. *FEMS Microbiol Rev* **20**:13–23.

Randall D. J, Tsui TK. KN. (2002). Ammonia toxicity in fish. *Mar Pollut Bull* **45**:17–23.

Ravenhall M, Škunca N, Lassalle F, Dessimoz C. (2015). Inferring horizontal gene transfer. *PLoS Comput Biol* **11**:e1004095.

Re R, Pellegrini N, Proteggente A, Pannala A, Yang M, Rice-Evans C. (1999). Antioxidant activity applying an improved ABTS radical cation decolorization assay. *Free Radic Biol Med* **26**:1231–1237.

Reddy DA, Subrahmanyam G, Shivani Kallappa G, Karunasagar I. (2014). Detection of ammonia-oxidizing archaea in fish processing effluent treatment plants. *Indian J Microbiol* **54**:434–438.

Reigstad LJ, Richter A, Daims H, Urich T, Schwark L, Schleper C. (2008). Nitrification in terrestrial hot springs of Iceland and Kamchatka. *FEMS Microbiol Ecol* **64**:167–174.

Reinthaler T, Winter C, Herndl GJ. (2005). Relationship between bacterioplankton richness, respiration, and production in the southern North Sea. *Appl Environ Microbiol* **71**:2260–2266.

Rodriguez LM, Konstantinidis KT. (2014). Bypassing cultivation to identify bacterial species. *Microbe* **9**:111–118.

Rodriguez LM, Konstantinidis KT. (2016). The enveomics collection: a toolbox for specialized analyses of microbial genomes and metagenomes. *Peer J Prepr* **4**:e1900v1.

Ross AA, Neufeld JD. (2015). Microbial biogeography of a university campus. *Microbiome* **3**:66.

Rosso D, Lothman SE, Jeung MK, Pitt P, Gellner WJ, Stone AL, *et al.* (2011). Oxygen transfer and uptake, nutrient removal, and energy footprint of parallel full-scale IFAS and activated sludge processes. *Water Res* **45**:5987–5996.

Rotthauwe JH, Witzel KP, Liesack W. (1997). The ammonia monooxygenase structural gene *amoA* as a functional marker: molecular fine-scale analysis of natural ammonia-oxidizing populations. *Appl Environ Microbiol* **63**:4704–4712.

Ruby JG, Bellare P, DeRisi JL. (2013). PRICE: software for the targeted assembly of components of (meta)genomic sequence data. *G3* **3**:865–880.

Sakami T, Andoh T, Morita T, Yamamoto Y. (2012). Phylogenetic diversity of ammonia-oxidizing archaea and bacteria in biofilters of recirculating aquaculture systems. *Mar Genomics* **7**:27–31.

Samarkin VA, Madigan MT, Bowles MW, Casciotti KL, Priscu JC, McKay CP, et al. (2010). Abiotic nitrous oxide emission from the hypersaline Don Juan Pond in Antarctica. *Nat Geosci* **3**:341–344.

Sánchez O, Ferrera I, González JM, Mas J. (2013). Assessing bacterial diversity in a seawater-processing wastewater treatment plant by 454-pyrosequencing of the 16S rRNA and amoA genes. *Microb Biotechnol* **6**:435–442.

Santillana GE, Smith HJ, Burr M, Camper AK. (2016). Archaeal ammonium oxidation coupled with bacterial nitrite oxidation in a simulated drinking water premise plumbing system. *Environ Sci Water Res Technol* **85**:95–103.

Santoro AE, Buchwald C, McIlvin MR, Casciotti KL. (2011). Isotopic signature of N_2O produced by marine ammonia-oxidizing archaea. *Science* **333**:1282–1285.

Santoro AE, Casciotti KL. (2011). Enrichment and characterization of ammonia-oxidizing archaea from the open ocean: phylogeny, physiology and stable isotope fractionation. *ISME J* **5**:1796–1808.

Santoro AE, Dupont CL, Richter RA, Craig MT, Carini P, McIlvin MR, *et al.* (2015). Genomic and proteomic characterization of 'Candidatus Nitrosopelagicus brevis': An ammonia-oxidizing archaeon from the open ocean. *Proc Natl Acad Sci U S A* **112**:1173–1178.

Sára M, Sleytr UB. (2000). S-Layer proteins. *J Bacteriol* **182**:859–868.

Satoh Y. (1980). Production of urea by bacterial decomposition of organic matter including phytoplankton. *Int Rev der gesamten Hydrobiol und Hydrogr* **65**:295–301.

Sauder LA, Engel K, Stearns JC, Masella AP, Pawliszyn R, Neufeld JD. (2011). Aquarium nitrification revisited: Thaumarchaeota are the dominant ammonia oxidizers in freshwater aquarium biofilters. *PLoS One* **6**:e23281.

Sauder LA, Peterse F, Schouten S, Neufeld JD. (2012). Low-ammonia niche of ammonia-oxidizing archaea in rotating biological contactors of a municipal wastewater treatment plant. *Environ Microbiol* **14**:2589–2600.

Sauder LA, Ross AA, Neufeld JD. (2016). Nitric oxide scavengers differentially inhibit ammonia oxidation in ammonia-oxidizing archaea and bacteria. *FEMS Microbiol Lett* **363**:fnw052.

Sayavedra-Soto LA, Arp DJ. (2011). Ammonia-oxidizing bacteria: their biochemistry and molecular biology. In:*Nitrification*, Ward, BB, Arp, DJ, & Klotz, MG (eds), American Society for Microbiology Press, pp. 11–38.

Schirm M, Soo EC, Aubry AJ, Austin J, Thibault P, Logan SM. (2003). Structural, genetic and functional characterization of the flagellin glycosylation process in *Helicobacter pylori*. *Mol Microbiol* **48**:1579–1592.

Schleper C. (2010). Ammonia oxidation: different niches for bacteria and archaea? *ISME J* **4**:1092–1094.

Schleper C, Holben W, Klenk H-P. (1997). Recovery of crenarchaeotal rDNA sequences from freshwater lake sediments. *Appl Environ Microbiol* **63**:321–323.

Schleper C, Jurgens G, Jonuscheit M. (2005). Genomic studies of uncultivated archaea. *Nat Rev Microbiol* **3**:479–488.

Schleper C, Nicol GW. (2010). Ammonia-oxidising archaea – physiology, ecology and evolution. In:*Advances in Microbial Physiology*, Vol. 57, Elsevier, pp. 1–41.

Schmidt I. (2009). Chemoorganoheterotrophic growth of *Nitrosomonas europaea* and *Nitrosomonas eutropha*. *Curr Microbiol* **59**:130–138.

Schneitz C, Nuotio L, Lounatma K. (1993). Adhesion of *Lactobacillus acidophilus* to avian intestinal epithelial cells mediated by the crystalline bacterial cell surface layer (S-layer). *J Appl Bacteriol* **74**:290–294.

Schoenhofen IC, McNally DJ, Vinogradov E, Whitfield D, Young NM, Dick S, *et al.* (2006). Functional characterization of dehydratase/aminotransferase pairs from *Helicobacter* and *Campylobacter*: Enzymes distinguishing the pseudaminic acid and bacillosamine biosynthetic pathways. *J Biol Chem* **281**:723–732.

Schouten S, Hopmans EC, Baas M, Boumann H, Standfest S, Konneke M, *et al.* (2008). Intact membrane lipids of 'Candidatus Nitrosopumilus maritimus,' a cultivated representative of the cosmopolitan mesophilic Group I Crenarchaeota. *Appl Environ Microbiol* **74**:2433–2440.

Schouten S, Huguet C, Hopmans EC, Kienhuis MVM, Damste JSS. (2007). Analytical methodology for TEX$_{86}$ paleothermometry by high-performance liquid chromatography/atmospheric pressure chemical ionization-mass spectrometry. *Anal Chem* **79**:2940–2944.

Scott DB, Van Dyke MI, Anderson WB, Huck PM. (2015). Influence of water quality on nitrifier regrowth in two full-scale drinking water distribution systems. *Can J Microbiol* **61**:965–976.

Shen B. (2003). Polyketide biosynthesis beyond the type I, II and III polyketide synthase paradigms. *Curr Opin Chem Biol* **7**:285–295.

Shen T, Stieglmeier M, Dai J, Urich T, Schleper C. (2013). Responses of the terrestrial ammonia-oxidizing archaeon *Ca.* Nitrososphaera viennensis and the ammonia-oxidizing bacterium *Nitrosospira multiformis* to nitrification inhibitors. *FEMS Microbiol Lett* **344**:121–129.

Short MD, Abell GCJ, Bodrossy L, van den Akker B. (2013). Application of a novel functional gene microarray to probe the functional ecology of ammonia oxidation in nitrifying activated sludge. *PLoS One* **8**:e77139.

Sleytr UB, Huber C, Ilk N, Pum D, Schuster B, Egelseer EM. (2007). S-layers as a tool kit for nanobiotechnological applications. *FEMS Microbiol Lett* **267**:131–144.

Sonthiphand P, Limpiyakorn T. (2011). Change in ammonia-oxidizing microorganisms in enriched nitrifying activated sludge. *Appl Microbiol Biotechnol* **89**:843–853.

Sonthiphand P, Neufeld J. (2014). Nitrifying bacteria mediate aerobic ammonia oxidation and urea hydrolysis within the Grand River. *Aquat Microb Ecol* **73**:151–162.

Spang A, Hatzenpichler R, Brochier-Armanet C, Rattei T, Tischler P, Spieck E, *et al.* (2010). Distinct gene set in two different lineages of ammonia-oxidizing archaea supports the phylum *Thaumarchaeota*. *Trends Microbiol* **18**:331–340.

Spang A, Poehlein A, Offre P, Zumbrägel S, Haider S, Rychlik N, *et al.* (2012). The genome of the ammonia-oxidizing *Candidatus* Nitrososphaera gargensis: insights into metabolic versatility and environmental adaptations. *Environ Microbiol* **14**:3122–3145.

Sreejayan, RMN. (1997). Nitric oxide scavenging by curcuminoids. *J Pharm Pharmacol* **49**:105–107.

Srithep P, Khinthong B, Chodanon T, Powtongsook S, Pungrasmi W, Limpiyakorn T. (2015). Communities of ammonia-oxidizing bacteria, ammonia-oxidizing archaea and nitrite-oxidizing bacteria in shrimp ponds. *Ann Microbiol* **65**:267–278.

Stahl D. A., Amann R. (1991). Development and application of nucleic acid probes in bacterial systematics. In:*Nucleic Acid Techniques in Bacterial Systematics*, Stackebrandt, E & Goodfellow, M (eds), John Wiley & Sons Ltd.: Chichester, England, pp. 205–248.

Stahl DA, de la Torre JR. (2012). Physiology and diversity of ammonia-oxidizing archaea. *Annu Rev Microbiol* **66**:83–101.

Starkenburg SR, Larimer FW, Stein LY, Klotz MG, Chain PSG, Sayavedra-Soto LA, *et al.* (2008). Complete genome sequence of *Nitrobacter hamburgensis* X14 and comparative genomic analysis of species within the genus *Nitrobacter*. *Appl Environ Microbiol* **74**:2852–2863.

Stehr G, Böttcher B, Dittberner P, Rath G, Koops H-P. (1995). The ammonia-oxidizing nitrifying population of the River Elbe estuary. *FEMS Microbiol Ecol* **17**:177–186.

Stein LY, Klotz MG. (2016). The nitrogen cycle. *Curr Biol* **26**:R94–R98.

Stein WD. (1986). Transport and diffusion across cell membranes. Academic Press Inc.: Cambridge, MA.

Sterngren AE, Hallin S, Bengtson P. (2015). Archaeal ammonia oxidizers dominate in numbers, but bacteria drive gross nitrification in *N*-amended grassland soil. *Front Microbiol* **6**:1350.

Stieglmeier M, Alves RJE, Schleper C. (2014). The phylum *Thaumarchaeota*. In:*The Prokaryotes: Other Major Lineages of Bacteria and The Archaea*, Rosenberg, E (ed), Springer-Verlag Berlin Heidelberg, pp. 545–577.

Stieglmeier M, Klingl A, Alves RJE, Rittmann SK-MR, Melcher M, Leisch N, *et al.* (2014). *Nitrososphaera viennensis* gen. nov., sp. nov., an aerobic and mesophilic, ammonia-

oxidizing archaeon from soil and a member of the archaeal phylum *Thaumarchaeota*. *Int J Syst Evol Microbiol* **64**:2738–2752.

Stieglmeier M, Mooshammer M, Kitzler B, Wanek W, Zechmeister-Boltenstern S, Richter A, *et al.* (2014). Aerobic nitrous oxide production through N-nitrosating hybrid formation in ammonia-oxidizing archaea. *ISME J* **8**:1135–1146.

Stopnisek N, Gubry-Rangin C, Höfferle S, Nicol GW, Mandic-Mulec I, Prosser JI. (2010). Thaumarchaeal ammonia oxidation in an acidic forest peat soil is not influenced by ammonium amendment. *Appl Environ Microbiol* **76**:7626–7634.

Strickler, Hall, Gaiko, Pajor. 2009. Functional characterization of a Na+-coupled dicarboxylate transporter from *Bacillus licheniformis*. *Biochim Biophys Acta* **12**: 2489–2496.

Sturt HF, Summons RE, Smith K, Elvert M, Hinrichs K-U. (2004). Intact polar membrane lipids in prokaryotes and sediments deciphered by high-performance liquid chromatography/electrospray ionization multistage mass spectrometry-new biomarkers for biogeochemistry and microbial ecology. *Rapid Commun Mass Spectrom* **18**:617–28.

Sueishi Y, Hori M, Kita M, Kotake Y. (2011). Nitric oxide (NO) scavenging capacity of natural antioxidants. *Food Chem* **129**:866–870.

Tabor CW, Tabor H. (1985). Polyamines in microorganisms. *Microbiol Rev* **49**:81–99.

Tamura K, Nei M. (1993). Estimation of the number of nucleotide substitutions in the control region of mitochondrial DNA in humans and chimpanzees. *Mol Biol Evol* **10**:512–526.

Tamura K, Peterson D, Peterson N, Stecher G, Nei M, Kumar S. (2011). MEGA2: molecular evolutionary genetics analysis using maximum likelihood, evolutionary distance, and maximum parsimony methods. *Mol Biol Evol* **28**:2731–2739.

Tamura K, Stecher G, Peterson D, Filipski A, Kumar S. (2013). MEGA6: molecular evolutionary genetics analysis version 6.0. *Mol Biol Evol* **30**:2725–2729.

Taylor AE, Taylor K, Tennigkeit B, Palatinszky M, Stieglmeier M, Myrold DD, *et al.* (2015). Inhibitory effects of C_2 to C_{10} 1-alkynes on ammonia oxidation in two *Nitrososphaera* species. *Appl Environ Microbiol* **81**:1942–1948.

Taylor AE, Vajrala N, Giguere AT, Gitelman AI, Arp DJ, Myrold DD, *et al.* (2013). Use of aliphatic *n*-alkynes to discriminate soil nitrification activities of ammonia-oxidizing thaumarchaea and bacteria. *Appl Environ Microbiol* **79**:6544–6551.

Taylor AE, Zeglin LH, Dooley S, Myrold DD, Bottomley PJ. (2010). Evidence for different contributions of archaea and bacteria to the ammonia-oxidizing potential of diverse Oregon soils. *Appl Environ Microbiol* **76**:7691–7698.

Teira E, Reinthaler T, Pernthaler A, Pernthaler J, Herndl GJ. (2004). Combining catalyzed reporter deposition-fluorescence *in situ* hybridization and microautoradiography to detect substrate utilization by Bacteria and Archaea in the deep ocean. *Appl Environ Microbiol* **70**:4411–4414.

Thamdrup B. (2012). New Pathways and Processes in the Global Nitrogen Cycle. *Annu Rev Ecol Evol Syst* **43**:407–428.

Thibault P, Logan SM, Kelly JF, Brisson JR, Ewing CP, Trust TJ, *et al.* (2001). Identification of the carbohydrate moieties and glycosylation motifs in *Campylobacter jejuni* flagellin. *J Biol Chem* **276**:34862–34870.

Tourna M, Freitag TE, Nicol GW, Prosser JI. (2008). Growth, activity and temperature responses of ammonia-oxidizing archaea and bacteria in soil microcosms. *Environ Microbiol* **10**:1357–1364.

de la Torre JR, Walker CB, Ingalls AE, Könneke M, Stahl DA. (2008). Cultivation of a thermophilic ammonia oxidizing archaeon synthesizing crenarchaeol. *Environ Microbiol* **10**:810–818.

Tourna M, Stieglmeier M, Spang A, Könneke M, Schintlmeister A, Urich T, *et al.* (2011). *Nitrososphaera viennensis*, an ammonia oxidizing archaeon from soil. *Proc Natl Acad Sci U S A* **108**:8420–8425.

Treusch AH, Kletzin A, Raddatz G, Ochsenreiter T, Quaiser A, Meurer G, *et al.* (2004). Characterization of large-insert DNA libraries from soil for environmental genomic studies of Archaea. *Environ Microbiol* **6**:970–980.

Treusch AH, Leininger S, Kletzin A, Schuster SC, Klenk H-P, Schleper C. (2005). Novel genes for nitrite reductase and Amo-related proteins indicate a role of uncultivated mesophilic crenarchaeota in nitrogen cycling. *Environ Microbiol* **7**:1985–1995.

Urakawa H, Tajima Y, Numata Y, Tsuneda S. (2008). Low temperature decreases the phylogenetic diversity of ammonia-oxidizing archaea and bacteria in aquarium biofiltration systems. *Appl Environ Microbiol* **74**:894–900.

Vajrala N, Martens-Habbena W, Sayavedra-Soto LA, Schauer A, Bottomley PJ, Stahl DA, *et al.* (2013). Hydroxylamine as an intermediate in ammonia oxidation by globally abundant marine archaea. *Proc Natl Acad Sci U S A* **110**:1006–1011.

Vallenet D, Engelen S, Mornico D, Cruveiller S, Fleury L, Lajus A, *et al.* (2009). MicroScope: a platform for microbial genome annotation and comparative genomics. *Database* **2009**:bap021.

Veith A, Klingl A, Zolghadr B, Lauber K, Mentele R, Lottspeich F, *et al.* (2009). *Acidianus*, *Sulfolobus* and *Metallosphaera* surface layers: structure, composition and gene expression. *Mol Microbiol* **73**:58–72.

Venables WN, Ripley BD. (2002). Modern Applied Statistics with S. 4th ed. Springer: New York.

Venter JC, Remington K, Heidelberg JF, Halpern AL, Rusch D, Eisen JA, *et al.* (2004). Environmental genome shotgun sequencing of the Sargasso Sea. *Science* **304**:66–74.

Verhamme DT, Prosser JI, Nicol GW. (2011). Ammonia concentration determines differential growth of ammonia-oxidising archaea and bacteria in soil microcosms. *ISME J* **5**:1067–1071.

de Vet WWJM, Dinkla IJT, Muyzer G, Rietveld LC, van Loosdrecht MCM. (2009). Molecular characterization of microbial populations in groundwater sources and sand filters for drinking water production. *Water Res* **43**:182–194.

de Vet WWJM, Kleerebezem R, van der Wielen PWJJ, Rietveld LC, van Loosdrecht MCM. (2011). Assessment of nitrification in groundwater filters for drinking water production by qPCR and activity measurement. *Water Res* **45**:4008–4018.

Veuillet F, Lacroix S, Bausseron A, Gonidec E, Ochoa J, Christensson M, *et al.* (2014). Integrated fixed-film activated sludge ANITA^TM Mox process - A new perspective for advanced nitrogen removal. *Water Sci Technol* **69**:915–922.

Wagner M, Rath G, Amann R, Koops H-P, Schleifer K-H. (1995). *In situ* identification of ammonia-oxidizing bacteria. *Syst Appl Microbiol* **18**:251–264.

Walker CB, de la Torre JR, Klotz MG, Urakawa H, Pinel N, Arp DJ, *et al.* (2010). *Nitrosopumilus maritimus* genome reveals unique mechanisms for nitrification and autotrophy in globally distributed marine crenarchaea. *Proc Natl Acad Sci U S A* **107**:8818–8823.

Wallace W, Knowles SE, Nicholas DJD. (1970). Intermediary metabolism of carbon compounds by nitrifying bacteria. *Arch Mikrobiol* **70**:26–42.

Walsh P, Milligan C. (1995). Effects of feeding and confinement on nitrogen metabolism and excretion in the gulf toadfish *Opsanus beta*. *J Exp Biol* **198**:1559–66.

Wang H, Fewer DP, Holm L, Rouhiainen L, Sivonen K. (2014). Atlas of nonribosomal peptide and polyketide biosynthetic pathways reveals common occurrence of nonmodular enzymes. *Proc Natl Acad Sci U S A* **111**:9259–9264.

Wang S, Xiao X, Jiang L, Peng X, Zhou H, Meng J, *et al.* (2009). Diversity and abundance of ammonia-oxidizing archaea in hydrothermal vent chimneys of the Juan de Fuca Ridge. *Appl Environ Microbiol* **75**:4216–4220.

Weerapperuma D, Silva V De, Seeta VK. (2005). Achieving advanced wastewater treatment standards with IFAS. In:Proceedings of the Water Environment Federation, Water Environment Federation, pp. 1945–1958.

Wells GF, Park H-D, Yeung C-H, Eggleston B, Francis CA, Criddle CS. (2009). Ammonia-oxidizing communities in a highly aerated full-scale activated sludge bioreactor: betaproteobacterial dynamics and low relative abundance of Crenarchaea. *Environ Microbiol* **11**:2310–2328.

Wernersson R. (2006). Virtual Ribosome-a comprehensive DNA translation tool with support for integration of sequence feature annotation. *Nucleic Acids Res* **34**:W385–388.

Widdel F, Bak F. (1992). Gram-negative mesophilic sulfate-reducing bacteria. In:*The Prokaryotes. 2nd ed.*, Balows, A, Trüper, HG, Dworkin, M, Harder, W, & Schleifer, K-H (eds) Vol. IV, Springer, pp. 3352–3378.

van der Wielen PWJJ, Voost S, van der Kooij D. (2009). Ammonia-oxidizing bacteria and archaea in groundwater treatment and drinking water distribution systems. *Appl Environ Microbiol* **75**:4687–4695.

Wilkie MP. (2002). Ammonia excretion and urea handling by fish gills: present understanding and future research challenges. *J Exp Zool* **293**:284–301.

Woese CR, Kandler O, Wheelis ML. (1990). Towards a natural system of organisms: proposal for the domains Archaea, Bacteria, and Eucarya. *Proc Natl Acad Sci U S A* **87**:4576–4579.

Woese CR, Magrum LJ, Fox GE. (1978). Archaebacteria. *J Mol Evol* **11**:245–252.

Wood CM. (1993). Ammonia and urea metabolism and excretion. In:*The Physiology of Fishes*, Evans, DH (ed), CRC press: Boca Raton, Florida, pp. 381–425.

Wright R. (2004). A Short History of Progress. House of Anansi Press: Toronto.

Wu K, Chung L, Revill WP, Katz L, Reeves CD. (2000). The FK520 gene cluster of *Streptomyces hygroscopicus* var. *ascomyceticus* (ATCC 14891) contains genes for biosynthesis of unusual polyketide extender units. *Gene* **251**:81–90.

Wu Y-J, Whang L-M, Fukushima T, Chang S-H. (2013). Responses of ammonia-oxidizing archaeal and betaproteobacterial populations to wastewater salinity in a full-scale municipal wastewater treatment plant. *J Biosci Bioeng* **115**:424–432.

Wu Y-W, Tang Y-H, Tringe SG, Simmons BA, Singer SW. (2014). MaxBin: an automated binning method to recover individual genomes from metagenomes using an expectation-maximization algorithm. *Microbiome* **2**:26.

Wuchter C, Abbas B, Coolen MJL, Herfort L, van Bleijswijk J, Timmers P, *et al.* (2006). Archaeal nitrification in the ocean. *Proc Natl Acad Sci U S A* **103**:12317–12322.

Wuchter C, Schouten S, Boschker HTS, Sinninghe Damsté JS. (2003). Bicarbonate uptake by marine Crenarchaeota. *FEMS Microbiol Lett* **219**:203–207.

WWAP (World Water Assessment Programme). (2012). The United Nations World Water Development Report 4: Managing Water Under Uncertainty and Risk. UNESCO: Paris.

Xia W, Zhang C, Zeng X, Feng Y, Weng J, Lin X, *et al.* (2011). Autotrophic growth of nitrifying community in an agricultural soil. *ISME J* **5**:1226–1236.

Yamamoto N, Otawa K, Nakai Y. (2010). Diversity and abundance of ammonia-oxidizing bacteria and ammonia-oxidizing archaea during cattle manure composting. *Microb Ecol* **60**:807–815.

Yan J, Haaijer SCM, Op den Camp HJM, van Niftrik L, Stahl DA, Könneke M, *et al.* (2012). Mimicking the oxygen minimum zones: stimulating interaction of aerobic archaeal and anaerobic bacterial ammonia oxidizers in a laboratory-scale model system. *Environ Microbiol* **14**:3146–3158.

Yao H, Gao Y, Nicol GW, Campbell CD, Prosser JI, Zhang L, *et al.* (2011). Links between ammonia oxidizer community structure, abundance and nitrification potential in acidic soils. *Appl Environ Microbiol* **77**:4618–4625.

Yapsakli K, Aliyazicioglu C, Mertoglu B. (2011). Identification and quantitative evaluation of nitrogen-converting organisms in a full-scale leachate treatment plant. *J Environ Manage* **92**:714–723.

Ye L, Zhang T. (2011). Ammonia-oxidizing bacteria dominates over ammonia-oxidizing archaea in a saline nitrification reactor under low DO and high nitrogen loading. *Biotechnol Bioeng* **108**:2544–2552.

Zhalnina K, Dias R, Leonard MT, Dorr de Quadros P, Camargo FAO, Drew JC, *et al.* (2014). Genome sequence of *Candidatus* Nitrososphaera evergladensis from Group I.1b enriched from everglades soil reveals novel genomic features of the ammonia-oxidizing archaea. *PLoS One* **9**:e101648.

Zhalnina K, de Quadros PD, Camargo FAO, Triplett EW. (2012). Drivers of archaeal ammonia-oxidizing communities in soil. *Front Microbiol* **3**:210.

Zhang CL, Ye Q, Huang Z, Li W, Chen J, Song Z, *et al.* (2008). Global occurrence of archaeal *amoA* genes in terrestrial hot springs. *Appl Environ Microbiol* **74**:6417–6426.

Zhang L-M, Hu H-W, Shen J-P, He J-Z. (2012). Ammonia-oxidizing archaea have more important role than ammonia-oxidizing bacteria in ammonia oxidation of strongly acidic soils. *ISME J* **6**:1032–1045.

Zhang L-M, Offre PR, He J-Z, Verhamme DT, Nicol GW, Prosser JI. (2010). Autotrophic ammonia oxidation by soil thaumarchaea. *Proc Natl Acad Sci U S A* **107**:17240–17245.

Zhang T, Jin T, Yan Q, Shao M, Wells G, Criddle C, *et al.* (2009). Occurrence of ammonia-oxidizing archaea in activated sludges of a laboratory scale reactor and two wastewater treatment plants. *J Appl Microbiol* **107**:970–977.

Zhang T, Ye L, Tong AHY, Shao M-F, Lok S. (2011). Ammonia-oxidizing archaea and ammonia-oxidizing bacteria in six full-scale wastewater treatment bioreactors. *Appl Microbiol Biotechnol* **91**:1215–1225.

Appendix A

Primer and probe sequences

Table A1 Sequences for FISH probes used in this thesis

Probe	Target	Sequence (5' to 3')	Reference
Thaum726	most *Thaumarchaeota*	GCT TTC ATC CCT CAC CGT C	Beam, 2015
Comp_thaum726A	competitor for thaum726	GCT TTC GTC CCT CAC CGT C	Beam, 2015
Comp_thaum726B	competitor for thaum726	GCT TTC ATC CCT CAC TGT C	Beam, 2015
Arch915	most *Archaea*	GTG CTC CCC CGC CAA TTC CT	Stahl and Amann, 1991
EUB338 mix*	most *Bacteria*	GCT GCC TCC CGT AGG AGT GCA GCC ACC CGT AGG TGT GCT GCC ACC CGT AGG TGT	Amann *et al.*, 1990; Daims *et al.*, 1999
Ntspa662	Genus *Nitrospira*	GGA ATT CCG CGC TCC TCT	Daims *et al.*, 2001
Comp_Ntspa662	Competitor for Ntspa662	GGA ATT CCG CTC TCC TCT	Daims *et al.*, 2001
Nit3	Genus *Nitrobacter*	CCT GTG CTC CAT GCT CCG	Wagner *et al.*, 1995
cNit3	Competitor for NitC	CCT GTG CTC CAG GCT CCG	Wagner *et al.*, 1995
Ntoga122	Genus *Nitrotoga*	TCC GGG TAC GTT CCG ATA T	Lücker *et al.*, 2015
c1Ntoga122	Competitor for Ntoga122	TCW GGG TAC GTT CCG ATA T	Lücker *et al.*, 2015
c2Ntoga122	Competitor for Ntoga122	TCY GGG TAC GTT CCG ATG T	Lücker *et al.*, 2015
NEU**	*N. europaea* & *N. eutropha*	CCC CTC TGC TGC ACT CTA	Wagner *et al.*, 1995
CTE**	Competitor for NEU	TTC CAT CCC CCT CTG CCG	Wagner *et al.*, 1995
Nso192**	*Nitrosomonas oligotropha*	CTT TCG ATC CCC TAC TTT CC	Adamczyk *et al.*, 2003
Comp_Nso192**	Competitor for Nso192	CTT TCG ATC CCC TGC TTC C	Adamczyk *et al.*, 2003
Nso 1225**	Most beta-proteobacterial AOB	CGC CAT TGT ATT ACG TGT GA	Mobarry *et al.*, 1996
nonsense	nonsense (negative control) probe	AGA GAG AGA GAG AGA GAG	Hatzenpichler *et al.*, 2008

*equimolar concentrations of EUB338, EUB338-II, and EUB338-III
**equimolar concentrations of these probes were used together to target AOB

Table A2 Primers used to determine order and orientation of *Ca*. N. aquariensis contigs

Primer	Sequence (5'→3')	Primer	Sequence (5'→3')	Gap
C2R1	GGAATTTCTGTGTGTATTTGTT	C1F1	CAAGTTGGATCACAAATTTTCA	G1
C2R2	TGGATCACTGTGTCTTTCATAA	C1F2	CACGTGGCGTGAAAA	
C2F1	CCAAACTCGATGAGCCTAAG	C3F1	CGGCATATGTGTTCGAAGTC	G2
C2F2	TCAGAACAAGCTTTACGAAAATA	C3F2	GGATGAGATTTTGAGCTTTAATT	
C3R1	GCCGTAAACTCCATTGTTAAA	C1R1	TTCCCAATCCGATTGTCTA	G3
C3R2	GCCTATCGGGTTTACGTTA	C1R2	GCATCAAATGCGTTTTACAG	

C1: contig 1, C2: contig 2, C3: contig 3

Note: Primers shown were all used for pairwise PCRs: successful primer combinations are indicated in the same block and are connected by lines. 1 and 2 indicate two different primers on the same end of the same contig.

Table A3 Primers for *Ca*. N. aquariensis primer walking

Primer	Sequence (5'→3')
G1PF	AGGCGTCAAAATAATCCCAGT
G1PR	CACGTAGAATGTCTGCTGCC
G2PF	AATTCGCAGACAGTTTCGGT
G2P2F	GCCCAGCCATCATATAGG
G2P4F	AGCATTCTGTTGTTTCACATCC
G2P6F	AAAAAACCTCAAAGTCGAGTGC
G2P8F	AGTTCAAGGGCGACACTAC
G2P10F	ACAATCTACCGCAGCTTTTTC
G2P12F	CCCGTCTCTACGAATCTCAG
G2PF	AATTCGCAGACAGTTTCGGT
G2P2F	GCCCAGCCATCATATAGG
G2P4F	AGCATTCTGTTGTTTCACATCC
G2P6F	AAAAAACCTCAAAGTCGAGTGC
G2P8F	AGTTCAAGGGCGACACTAC
G2P10F	ACAATCTACCGCAGCTTTTTC
G2P12F	CCCGTCTCTACGAATCTCAG
G2PR	AAATGAAGAAATCGACGGCG
G2P1R	GACCTATTTCGCTTTCATACTCT
G2P3R	CTACTGCTCGCACTCTGATATG
G2P5R	TTCTTTAGCAAAATACCCAGGC
G2P7R	GACAAGTGTTTTGTCGTGCAG
G2P9R	GTTCTGTACCAAATTTTGCG
G2P11R	GTGATCAGTACAGCATGATCC
G3PF	ATCGATGGAAAAATCTGTCA
G3P4F	GCACTACCAGAGTAGAGCCTG
G3P6F	CGAATTATTCCATCAGAGACG
G3P8F	ATCAAAATCGGCTACACGC
G3P10F	TTTTGGGACTGGAGAAAAAG
G3PRF	ATGCCAAACGACATTGCTTG
G3P3RF	AAACCTGCTCCAAATAGACCAG
G3P5F	CCAATAGAATATGCACTGACTG
G3P7F	CATCTCCGACAGCTTTACACTG
G3P9F	ATTATGCGATGATCGAGGAAC
G3P11F	CATTGAAGTTTGATGTCGC
G3P13F	TTCACTTTAGGGGAGAATACTG

Appendix B

Gene annotations

Table B1 *Ca*. N. aquariensis chemotaxis and flagella-related gene annotations

Locus tag	Gene	Gene product
NAQ_0214		putative methyl-accepting chemotaxis protein (MCP)
NAQ_0218		methyl-accepting chemotaxis sensory transducer
NAQ_0323	*cheY*	chemotaxis protein CheY
NAQ_0324		cheY-like receiver
NAQ_0555	*flaK*	putative archaeal preflagellin peptidase
NAQ_1630		archaeal flagellin N-terminal-like domain protein
NAQ_1631		archaeal flagellin
NAQ_1632		archaeal flagellin
NAQ_1633		conserved exported protein of unknown function
NAQ_1634		archaeal flagellin
NAQ_1635		conserved protein of unknown function
NAQ_1636	*flaG*	putative flagellar protein FlaG
NAQ_1637	*flaF*	putative flagella assembly protein FlaF
NAQ_1638	*flaH*	flagellar accessory protein FlaH
NAQ_1639	*flaI*	putative flagellar protein homolog (FlaI)
NAQ_1640	*flaJ*	putative flagella accessory protein J (FlaJ)
NAQ_1641	*cheW*	chemotaxis protein CheW (Modular protein)
NAQ_1642		conserved protein of unknown function
NAQ_1643	*cheB*	chemotaxis response regulator protein-glutamate methylesterase
NAQ_1644	*cheA*	putative chemotaxis histidine kinase related protein
NAQ_1645	*cheC*	putative CheC protein, inhibitor of MCP methylation (fragment)
NAQ_1646	*cheD*	putative chemoreceptor glutamine deamidase
NAQ_1647		putative chemotaxis protein methyltransferase
NAQ_1648	*cheW*	chemotaxis protein CheW
NAQ_1649	*cheY*	chemotaxis protein CheY
NAQ_1650	*cheC*	putative chemotaxis protein CheC (phosphatase)

Table B2 *Ca*. N. aquariensis defense cluster genes annotations

Locus tag	Gene product
NAQ_1252	signal transduction response regulator, receiver domain
NAQ_1253	putative Histidine kinase
NAQ_1254	DNA methylase N-4/N-6 (fragment)
NAQ_1255	putative metal-dependent hydrolase
NAQ_1256	type I site-specific deoxyribonuclease, HsdR family
NAQ_1257	putative Type I restriction-modification system2C specificity subunit S
NAQ_1258	type I restriction-modification system, M subunit
NAQ_1259	protein of unknown function
NAQ_1260	putative phage associated DNA primase
NAQ_1261	protein of unknown function
NAQ_1262	protein of unknown function
NAQ_1263	putative transposase A
NAQ_1264	putative Phage integrase family protein
NAQ_1265	putative phage Gp37Gp68 family protein
NAQ_1266	protein of unknown function
NAQ_1267	putative Modification methylase BbvI
NAQ_1268	McrBC 5-methylcytosine restriction system component-like protein
NAQ_1269	ATPase
NAQ_1270	protein of unknown function
NAQ_1271	putative RNA methyltransferase fusion protein
NAQ_1272	putative BseRI endonuclease
NAQ_1273	protein of unknown function
NAQ_1274	superfamily II DNA/RNA helicases, SNF2 family
NAQ_1275	protein of unknown function
NAQ_1276	similar to DNA-methyltransferase (Cytosine-specific)
NAQ_1277	putative cytoplasmic protein
NAQ_1278	hydrolase of the metallo-beta-lactamase superfamily
NAQ_1279	putative DNA modification methylase, putative
NAQ_1280	protein of unknown function
NAQ_1281	putative prophage MuMc02, terminase, ATPase subunit
NAQ_1282	conserved protein of unknown function
NAQ_1283	putative ATPase
NAQ_1284	protein of unknown function
NAQ_1285	protein of unknown function
NAQ_1286	putative phage integrase family protein

Table B3 *Ca*. N. aquariensis glycosylation cluster genes annotations

Locus tag	Gene	Gene product
NAQ_1300		putative bifunctional phosphoglucose/phosphomannose isomerase
NAQ_1301	*pseH*	N-acetyltransferase (GNAT family)
NAQ_1302	*pseM*	SAM-dependent methyltransferase
NAQ_1303		conserved protein of unknown function
NAQ_1304		conserved protein of unknown function
NAQ_1305	*mtnA*	methylthioribose-1-phosphate isomerase
NAQ_1306	*neuA*	acylneuraminate cytidylyltransferase
NAQ_1307		oxidoreductase domain protein
NAQ_1308	*pseC*	aminotransferase
NAQ_1309	*pseA*	N-acetyl sugar amidotransferase
NAQ_1310	*pseB*	UDP-N-acetylglucosamine 4,6-dehydratase (inverting)
NAQ_1311		capsule polysaccharide biosynthesis protein
NAQ_1312		cytidylyltransferase
NAQ_1313		histone acetyltransferase HPA2 and related acetyltransferases
NAQ_1314		glutamine--scyllo-inositol transaminase
NAQ_1315	*neuB*	NeuB family protein
NAQ_1316		pseudaminic acid biosynthesis-associated protein PseG
NAQ_1317		NAD-dependent epimerase/dehydratase
NAQ_1318		epimerase 2 domain containing protein
NAQ_1319		putative dTDP-4-dehydrorhamnose 3,5-epimerase
NAQ_1320	*rmlB*	dTDP-glucose 4,6 dehydratase, NAD(P)-binding
NAQ_1321		glucose-1-phosphate thymidylyltransferase
NAQ_1322		glycosyltransferase, group 2 family protein
NAQ_1323		putative holo-[acyl-carrier-protein] synthase
NAQ_1324	*phaJ*	(R)-specific enoyl-CoA hydratase
NAQ_1325		putative acyl carrier protein
NAQ_1326		FkbH domain protein
NAQ_1327		transferase hexapeptide repeat protein
NAQ_1328		Polysaccharide deactylase family protein, PEP-CTERM locus family protein
NAQ_1329		NAD-binding protein
NAQ_1330		methyltransferase, FkbM family
NAQ_1331		glycosyl transferase group 1
NAQ_1332		glutamine--scyllo-inositol transaminase
NAQ_1333		glycosyltransferase
NAQ_1334		polysaccharide biosynthesis protein
NAQ_1335		methyltransferase FkbM family
NAQ_1336		protein of unknown function
NAQ_1337		putative membrane protein
NAQ_1338		protein of unknown function
NAQ_1339		protein of unknown function
NAQ_1340		UDP-glucose/GDP-mannose dehydrogenase
NAQ_1341		NDP-sugar dehydratase or epimerase
NAQ_1342		protein of unknown function
NAQ_1343		DegT/DnrJ/EryC1/StrS aminotransferase family protein
NAQ_1344		aspartate aminotransferase

NAQ_1345		SAM-dependent methyltransferases
NAQ_1346		protein of unknown function
NAQ_1347		conserved protein of unknown function
NAQ_1348	ASNS	asparagine synthase (Glutamine-hydrolyzing)
NAQ_1349		putative glycosyl transferases group 1
NAQ_1350		conserved protein of unknown function
NAQ_1351		putative glycosyl transferases group 1
NAQ_1352	ASNS	asparagine synthase
NAQ_1353		nucleotide sugar dehydrogenase
NAQ_1354		putative NAD dependent epimerase/dehydratase family protein
NAQ_1355		glycosyltransferase